Development of waterborne polymeric dispersions based on biobased monomers for their application as PSAs and coatings

Adrián Badía Rodrigo

Supervised by: Prof. Jose Ramon Leiza

Chemical Engineering Group

University of the Basque Country UPV/EHU

Donostia-San Sebastián

(2020)

Acknowledgements

En primer lugar, me gustaría expresar mi gratitud a mis directores de tesis, Joserra y Mariaje, por brindarme la oportunidad de realizar este doctorado y contribuir de forma crucial en mi desarrollo profesional. Nunca olvidaré vuestra paciencia, comprensión y apoyo en los duros inicios burocráticos que supuso esta tesis. Así mismo, siempre agradeceré esa libertad que me disteis para proponer y ejecutar nuevas ideas, pero, en mayor medida aun si cabe, vuestro conocimiento y experiencia para encauzarme hacia el camino correcto.

Un agradecimiento muy especial al resto de profesores de POLYMAT, Txema, María, Radmila, David, Nick, Miren, porque de alguna forma u otra han contribuido a mi desarrollo científico. Nunca olvidaré aquellos meetings de los lunes a las 12:00 h, el intercambio cuasi obligatorio de opiniones, vuestros consejos en cada charla y la motivación que transmitíais por seguir aprendiendo. Estoy seguro que mi amor hacia la ciencia y hacia la investigación es, en parte, también vuestra culpa. Inés, eres la columna vertebral de POLYMAT, me quedaría sin palabras si tuviera que agradecer todo lo que haces por nosotros en materia burocrática y administrativa. Siempre que necesitamos tu ayuda estas ahí.

Muchas gracias a DSM Coating resins por ofrecerme la oportunidad de realizar mi estancia predoctoral en Paises Bajos, Waalwijk. pero en especial a Jurgen Scheerder y Maud Kastelijn por su supervisión, atención y positivismo en todo momento. He de decir que aprendí de forma abundante con vosotros y con todos los trabajadores de los diferentes departamentos en lo que tuve la ocasión de interactuar. Sin duda alguna, una etapa de desarrollo profesional muy enriquecedora.

Quiero agradecer también toda la ayuda recibida por parte de Amaia en la caracterización por GPC, AF4 y CHDF, así como sus innumerables consejos y reuniones.

Estoy seguro de que vas a ser una directora de tesis formidable. No me olvido de la colaboración, las charlas, las risas y la sidra de Iñaki “El patillas”, gracias a ti logramos desarrollar la investigación del piperonyl methacrylate, uno de nuestros ases. Da gusto ver como una persona siente tanta dedicación hacia su trabajo. Tampoco olvido los consejos de J.I y Mariano, sus bromas y su ayuda prestada. Maite, eres el alma de la planta -1, muchas gracias por estar siempre dispuesta a realizar cualquier corte y preparación de muestra, por tu paciencia, tu risa y otras muchas conversaciones divertidas en el comedor. Si me acuerdo de Maite, no me podría olvidar de Ana, muchas gracias por realizar las medidas de TEM y por dejarme estar contigo durante la captura de imágenes, algo que siempre ha sido ameno y enriquecedor.

Ahora quiero agradecer a todos esos compañeros de POLYMAT que me han ofrecido su mano a lo largo de este camino. No me olvido de los orígenes y, por tanto, de la ayuda, apoyo y enseñanzas de Julie Movellan. Leticia Pardo y Antonio Veloso, siempre estaréis en mi corazón. Habéis sido de las personas más importantes y fundamentales en esta tesis. No tengo palabras para expresar todos aquellos buenos momentos que hemos pasado juntos, todo lo que me habéis aguantado, vuestros consejos y cariño. Leti, tampoco me olvido de toda la química orgánica que me has enseñado, de tu paciencia y de tu motivación en el laboratorio. Sin duda alguna, fuiste un pilar clave para el grupo. Recalcar que esta tesis no habría sido posible sin el apoyo incondicional, los cafés, breaks, las sonrisas, bromas y abrazos de gente como Nikos, Estitxu, Ziortza, Alex, Boris, Fabian, Justine, Sebastian, Aitor, Iñaki, Massimo, Sayrung, Stefano, Vero, Giulia, Irantzu, Nerea, Maialen, Adri, Oihane y muchas otras personas que seguro me dejo en el tintero y que han sido engranajes clave para el transcurso de esta carrera. No me olvido de las tardes de escalada con Fermín, Álvaro o Javi, muchas gracias por contagiarme ese amor a este fantástico deporte. También quiero desear el mejor futuro posible a los nuevos fichajes de

POLYMAT, a Mehdi, Elvis, Sumi, Diulia, Hesham, Sheraz, Thibault, Sara y Ainara. Estoy seguro de que vais a dar lo mejor de vosotros.

Gracias a vosotros Kuadrilla, o mejor dicho a mi familia en San Sebastián. Si tuviera que dar un motivo por el cual tuviera que volver a empezar esta tesis, sería por volver a conoceros. Habéis sido, sin duda, una de las piezas fundamentales en mi vida que deseo seguir manteniendo. Hablo de Juan, Dani, Imanol, Jorge, Marcos, Cristian (A.K.A El pesetas), Barrio, Edu y Plou. Jamas olvidaré todos los momentos que hemos vivido juntos, nuestras salidas nocturnas, las excursiones, el monte, las sidrerías y todos aquellos recuerdos de felicidad que me habéis otorgado. De corazón, mil gracias, os quiero mucho.

Marcos e Iñigo, mis compañeros de piso durante este viaje, gracias por aguantarme en las buenas y en las malas, por esas cenas comunales de los miércoles, nuestros entrenamientos en la playa y esas locas partidas al Catan. Iñigo te deseo lo mejor en tu futuro, además estoy segurísimo de que vas a ser un papá de 10, espero que nos podamos reencontrar pronto. Marcos, empezaste conmigo en la carrera, y a lo largo del doctorado te has convertido en más que un amigo, en un hermano. Mil gracias por todo, porque contigo la cuarentena no llega a decena.

También me gustaría romper una lanza a favor de mi grupo de química de Zaragoza porque, sin duda alguna, siempre os llevo y os llevaré en mi memoria. Os quiero agradecer de corazón todo el apoyo recibido, la comprensión y esa felicidad contagiosa que emana en mí al veros. No tengo duda alguna de que sois y seréis parte de mi vida. Un abrazo enorme para Jorge, Fernando, Anamar, Regina, Alba, Lorena, Javi, Diego, Llorens, Juan, Amaya, Ainhoa, Rebeca, Marcos, Pablo, Aitor y José Antonio. Fer, mil gracias por tu ayuda con el diseño y formato de la portada, estoy seguro de que te vas a convertir en un diseñador de renombre.

Si hablo de Zaragoza, no me puedo olvidar de todas aquellas magníficas personas que, de alguna forma u otra, han formado y forman parte de mi vida. Quiero dar las gracias en especial a Javi, Marta, Gloria, David, Martin, Ester y Dani, porque cada vez que vuelvo a mi ciudad, y tengo la ocasión de veros, conseguís dibujar en mí una sonrisa permanente.

Por último, esta tesis no habría sido posible sin el apoyo incondicional de mi familia. Mamá y papá, este trabajo también es en parte vuestro porque siempre habéis hecho todo lo que ha estado en vuestras manos por ofrecerme la mejor educación posible. Gracias por vuestro amor y cariño cada vez que regresaba a Zaragoza y gracias por preocuparos por mí en todo momento. A mi hermano David, porque eres, sin duda, el mejor hermano que alguien podría tener. Gracias por tu afecto y curiosidad en mi trabajo, por preguntarme periódicamente y por tu alegría en cada una de nuestras conversaciones. Gracias también a mi tío Pablo, mi tía Ana y mi prima Laura por todo su apoyo durante esta etapa. A mi tío Raúl y mi abuelo Félix porque siempre os tengo presentes en mi día a día. Yayo, creo que tú has influido en mi educación de forma determinante, de hecho, creo que mi carácter es, en parte, gracias a ti. Siempre has honrado el trabajo y castigado la vagancia. Nunca me olvidaré de cuando era pequeño y veíamos los documentales de animales de Felix Rodriguez de la Fuente junto con la abuela. Está claro que mi amor hacia la ciencia empezó gracias a ti, en ese cuarto de estar, cuando yo solo tenía 5 o 6 años.

Raquel, sin ti no estaría donde estoy ahora y no sería quien soy. Siempre has estado ahí, en las buenas y en las malas, preparada con una sonrisa. Gracias por esa comprensión, ese cariño y ese amor que siempre han logrado impulsarme hacia delante en cualquier momento de mi carrera. Si pudiese ser una parte de tí, elegiría ser tus lágrimas. Porque tus lagrimas son concebidas en tu corazón, nacen en tus ojos, viven en tus mejillas, y se mueren en tus labios.

“La naturaleza ama el ocultarse”

Heráclito

Contents

Chapter 1. Introduction

Chapter 2. High bio-content waterborne PSAs containing 2-Octyl acrylate and isobornyl (meth)acrylate

Chapter 3. UV-tunable biobased PSAs containing piperonyl methacrylate

Chapter 4. Removable biobased waterborne PSAs containing mixtures of isosorbide methacrylate monomers

Chapter 5. Synthesis of electrosterically stabilized latexes using biobased ASRs for PSAs: High performance and removability

Chapter 6. Development of biobased waterborne coatings containing Ecomer® monomer

Chapter 1

Introduction

1.1 Main motivation and objectives

In recent years, instability of petroleum prices, consumer demands, environmental concerns and strict regulations about greenhouse gas emissions (particularly CO_2) have pushed up our society towards the development of sustainable and environmentally friendly materials. The raw material sources together with "green technologies" and the end-of-life management of the final product have become in main objects of attention. In this context, there is an interest for replacing current petroleum-based materials by renewable feedstocks aiming to reduce the carbon footprint but also to ensure a circular economy[1]. This strategy is being implemented more and more in daily consumer goods such as adhesives and coatings, this is, polymers having a prominent area of interest for industry and academia, which look for new renewable building blocks for their formulations[2].

Small molecules coming from biomass can be easily collected from fermentation of carbohydrates, chemical transformation of natural polymers (*e.g.* starch, lignin) and extraction from natural resources, attaining mostly plant oils and terpenes[3]. Thereafter, these molecules may be functionalized to obtain suitable monomers for the polymerization process. Since the petroleum price is still low and the market value of sectors such as packaging and paints is large, renewable monomers must guarantee not only the bio-economy concept, but also offer additional functionalities. Thus, it is hoped that the performance of the biobased material overcomes or competes with the ones coming from petroleum-based counterparts by providing extra benefits[4]. Among the most demanded features are: UV-tunability, thermo-responsive behavior, degradability and recyclability.

Since emulsion polymerization allows the large production of high-quality materials in a consistent, safe and environmentally way, it is forecast that the global market for waterborne dispersions will increase its value from US$ 7.6 billion (2019) to US$ 11.8 billion

(2027)[5]. In addition, paints & coatings and adhesives & sealants represent more than 60% of the total amount of polymeric dispersions[5]. In this scenario, monomers coming from renewable sources begin to gain importance in the manufacturing of environmentally-friendly materials. Regarding this, monomers derived from vegetable oils, terpenes, lignin and carbohydrates are the main precursors in the development of such kind of products[6]. Figure 1.1 shows the main precursor molecules used for the preparation of biobased monomers suitable for emulsion polymerization and related techniques (usually miniemulsion).

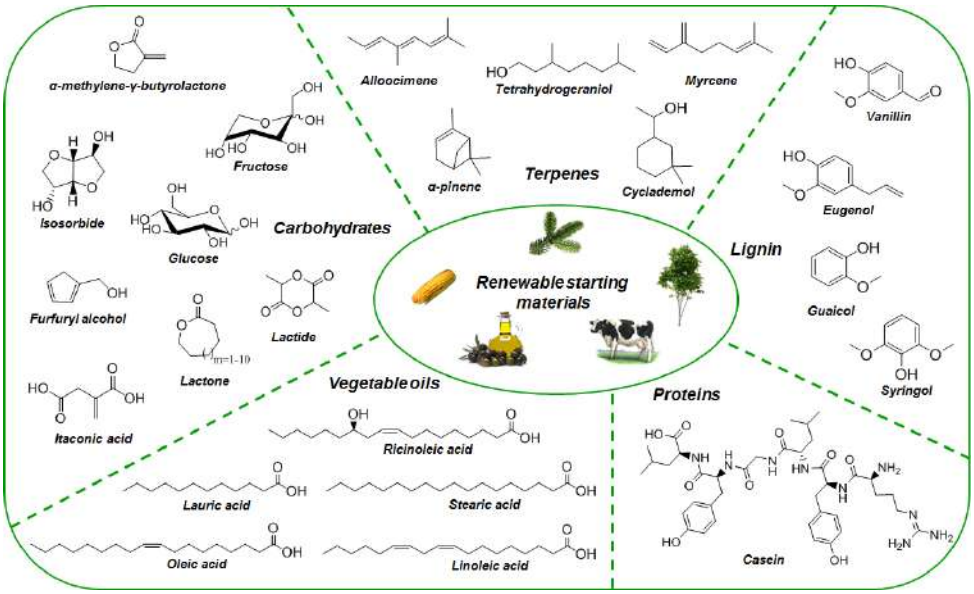

Figure 1.1. Chemical structures of precursor molecules used in the preparation of renewable monomers suitable for emulsion polymerization and related techniques. Starting materials coming from nature are categorized by their type or origin, including terpenes, carbohydrates, vegetable oils, proteins and lignin (modified and upgraded from reference 3).

This work has been focused in the combination of both functional and non-functional biobased monomers together with emulsion polymerization as “green technology” for obtaining high bio-content waterborne pressure sensitive adhesives (PSAs) and coatings

with competitive performance. For this purpose, both commercial and non-commercial biobased monomers have been employed. Therefore, the main objective has been the replacement of petroleum-based monomers by commercial renewable ones, achieving high solids content stable copolymer latexes for adhesive and coating applications. A parallel, but not less important objective, has been the synthesis of new biobased functional monomers and their incorporation into adhesive and coating formulations pursuing the synthesis of valuable materials with special features. Following this line, potential industrial applications have been evaluated and improved, giving an overview of the performance of the obtained environmentally friendly PSAs and coatings.

In what follows, a brief review about waterborne polymeric dispersions and two of the main application fields, pressure sensitive adhesives (PSAs) and coatings will be presented.

1.2 Waterborne polymeric dispersions

Waterborne polymeric dispersions (or latexes) are colloidal dispersions of polymer particles with sizes ranging from 50 nm to 1000 nm in an aqueous medium (*i.e.,* the continuous phase). They are defined as environmentally friendly polymeric materials due to the use of water as solvent and the presence of low to zero volatile organic compounds (VOCs) and hazardous air pollutants (HAP) emissions. In most applications, the water is evaporated from the dispersions giving rise to the formation of a polymer film or powder depending on the composition and/or processing temperature. Thus, the properties of the final material are influenced by the chemical composition of the copolymers, the molar mass and its distribution, particle size distribution, the particle morphology and the morphology of the polymer film[7–9].

Among the different types of polymer dispersions, acrylic dispersions represent the most versatile family with regards to large number of applications. The large variety of both

methacrylic and acrylic esters allows fine tuning the hydrophobicity/hydrophilicity of the final material, as well as the glass transition temperature (Tg). The molar mass and crosslinking degree can be easily adjusted by the use of chain transfer agents (CTA) as well as by the incorporation of di(meth)acrylate units into the formulation (crosslinkers). In addition, acrylic monomers tend to form branched and crosslinked polymer structures since the α-hydrogen atom is susceptible to be abstracted and termination of growing radical chains is mainly by combination. In contrast, methacrylic monomers yield in not crosslinked polymer chains, which usually terminate by disproportionation reactions. As main advantages, acrylic compositions are resistant against water, air oxidation and degradation by light. These remarkable features make possible that acrylic dispersions are widely used in the adhesives & sealants and paints & coatings industrial sector.

It is worth pointing out that polymer dispersions containing elevated amounts of (meth)acrylic acid can be used as thickeners, but also as polymeric stabilizers when pH is increased (conventionally called alkali soluble resins). They provide electrosteric stabilization, minimizing the use of conventional emulsifiers and increasing mechanical properties among others.

1.2.1 Waterborne Pressure Sensitive Adhesives

Pressure sensitive adhesives (PSAs) are viscoelastic materials that can firmly adhere to a wide range of surfaces by the application of a light pressure for a short contact time[10,11]. The global demand of pressure sensitive adhesives was estimated to be 1.6 million metric tons in 2019 and its market size was valued at US$ 11.11 billion in 2018. Moreover, it is expected to register a CAGR (Compound Annual Growth Rate) of 4.3% from 2019 to 2025, reaching 2.1 million metric tons by 2025[12].

PSAs must be permanently tacky at room temperature[13–15]; that is why a perfect balance between viscous and elastic properties is needed and, for that, the final material has to present a low glass transition temperature (typically lower than -15ºC). Viscous behavior is required to generate tack (adhesion), which is mostly related with the polymer chain mobility (e.g., molar mass) and their capability to dissipate energy for the (de)bonding process, whereas elasticity is needed to enable clean removal from the surface. Moreover, strong intermolecular forces (cohesion) are necessary to sustain loads[10,11,15]. The degree of crosslinking controls the balance between cohesive and adhesion forces. Insoluble fractions (related to the degree of crosslinking) in the 50-70% range have been reported as optimal for a good performance in waterborne adhesives[16–21].

Tack, peel strength and shear strength are the three general adhesive properties that determine PSA performance. Tack is related to the bond formed when another surface (e.g. the thumb) is pressed against the adhesive surface for a brief period of time. Peel strength is measured as a force required to remove a standard PSA strip from a specified test surface (substrate) under a standard test angle (e.g., 90º or 180º) and standard conditions. Lastly, shear strength is the internal or cohesive strength of the adhesive mass. Usually, it is determined as the time it takes for a standard strip of PSA to fall from a test panel after application of a load. A PSA is the result of a fine balance between these three major, interrelated properties. The balance is usually tailored according to the end use of the PSA[22].

One of the most advantageous measuring methods in comparison to the standard adhesive test (peel, shear and loop tack) is the probe tack test. This technique provides information about the separation of the deformation mechanism during the debonding process as a function of time[23]. A disc or hemisphere of a standard material (a stainless steel ball probe was used in this work) is brought into contact with the adhesive surface. As a

consequence, the raw data obtained, i.e., a force-displacement curve can be converted into a stress-strain curve, which is nothing more than the force normalized by the initial contact area plotted against the increase in the thickness of the film normalized by its initial thickness. In such a test, it is important to accurately control the following variables: probe material, probe diameter and shape, load, thickness of the adhesive, dwell time, rate of debonding of the probe from adhesive and test temperature.

Figure 1.2 presents a typical stress vs. strain curve where different stages can be clearly appreciated. First, the adhesive layer is homogeneously deformed, and then some cavities nucleate at the interface between the probe and the adhesive layer (cavitation process). They grow until the stress reaches a well-defined maximum (σ_{max}). This peak is followed either by a sharp decrease or by a stabilization of the stress at a nearly constant value. In the case of the sharp decrease, the adhesive layer debonds rapidly from the probe and the adhesion energy (W_{adh}) is low. On the contrary, a stabilization of the stress (plateau) is a signature of the creation of a fibrillating structure where the fibrils are the walls of the preexisting cavities (fibrillation process). In that case, adhesion energy can reach very high values especially when the material is highly deformable.

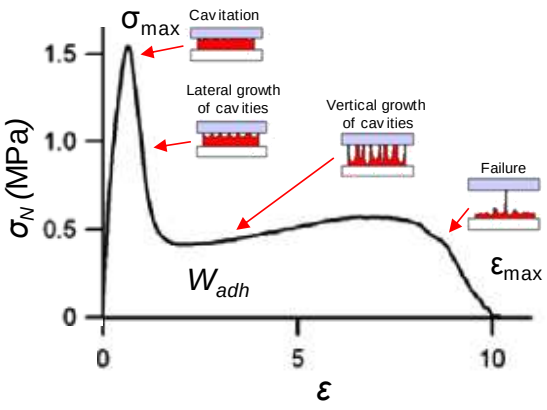

Figure 1.2. Typical probe tack curve (modified from reference 26).

Since the microstructure of the PSA play an important role during the (de)bonding process, different types of strain-stress curves have been observed (Figure 1.3) [24–26].

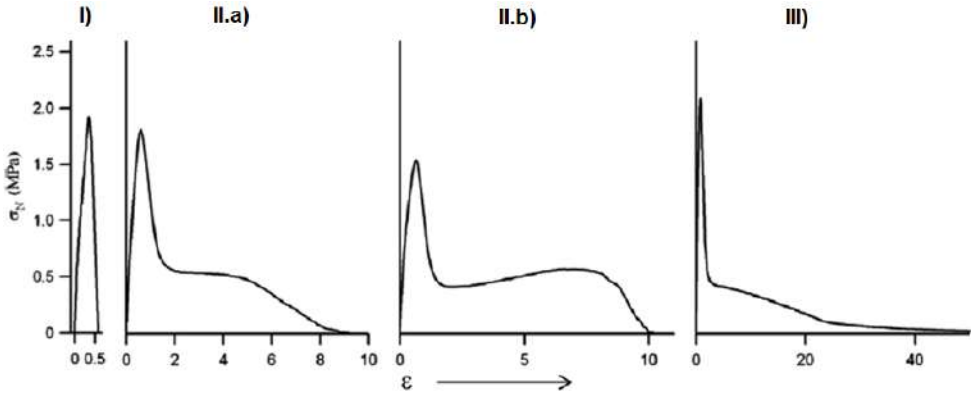

Figure 1.3. Different stress-strain curves. I) Brittle failure, II.a) adhesive debonding, II.b) adhesive debonding with hardening, III) cohesive debonding liquid-like behavior (modified from reference 26).

I) Brittle or interfacial failure. This type of failure is characterized by a sharp maximum at quite low strains and a very small area under the curve. Cavities nucleate at the probe-adhesive interface and expand in the bulk of the adhesive layer. Then, the cavities expand laterally at the interface with very small deformation and finally the adhesive detaches from the probe without leaving any residue on the surface. This performance is typical for PSAs with a remarkable solid-like behavior, which is favored at high glass transition temperatures and high crosslinking degrees and/or molar masses.

II) Adhesive debonding. After cavitation, walls of the cavities deform vertically until the final detachment from the probe. In the case of II.b) the material strain hardens just before the final detachment. At the end, there is no adhesive residue in the probe. This kind of curves belong to PSAs with a well-balanced viscoelastic properties, namely, adhesive fibrils elastic enough to be elongated and dissipate energy.

III) Liquid-like or cohesive failure. The adhesive joint breaks by cohesive fracture within the adhesive and the debonding process is dictated by the viscous flow. At the beginning of the test the structure is made of more or less round cavities. Then the air penetrates to the center due to the movement of the fingers at the edges. At the end there are no cavities, only fingers. These fibrils may finally break (cohesive failure) or to stay attached to the probe. This behavior occurs in PSAs with a high viscous component and lack of cohesion, usually because of the low Tg of the system and/or the low crosslinking degree.

An important family of polymers for PSA applications belongs to acrylic copolymers, which are mainly composed by a low Tg acrylate (e.g. n-butyl acrylate or 2-ethylhexyl acrylate), which provides softness and tackiness, and a low percentage of a hard monomer (e.g. methyl methacrylate) in order to improve cohesiveness of the system, together with an unsaturated carboxylic acid that imparts wettability and enhances both peel and shear strength[11,27,28]. Those commercial PSAs are mostly based on petroleum resources and traditionally have been synthesized by solution polymerization[29]. Acrylic PSAs are generally used on paper and polar surfaces like steel, glass, aluminum, zinc, polycarbonate, tin, and polyvinyl chloride (PVC). Figure 1.4 shows the global adhesives market share, by adhesive chemistry, in 2008[12]. As it can be appreciated acrylics dominate the sector followed by rubber-based PSAs (extensively utilized on non-polar, low-energy surfaces) and silicone-based PSAs (characterized by extreme weather resistance and long durability).

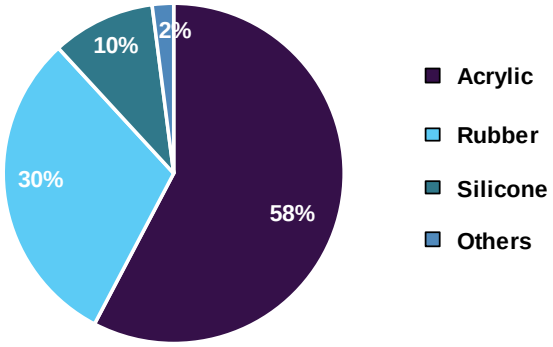

Figure 1.4. Global adhesives market share, by adhesive chemistry, in 2008 (%)[12].

While solvent-based adhesives have been in use since the 19th century, emulsion-based PSAs only started to be widely employed since the 1970s as a result of increased health and environmental concerns. From then, several studies have been carried out aiming to improve the final adhesive performance. Monomers such as butadiene, styrene, acrylonitrile, ethylene, vinyl chloride, vinyl acetate, vinylidene chloride, (meth)acrylic acid and its alkyl esters have been extensively used in the manufacturing of waterborne PSAs[30]. Concerning this, Brooks identified the key factors influencing the properties and PSA performance of acrylic emulsion polymers by working with a butyl acrylate/vinyl acetate/methacrylic acid model terpolymer system[31]. Mohsen et al. investigated the optimal comonomer ratio in the production of latexes containing butyl acrylate (BA) and styrene (St) for wood applications[32], whereas the company Wacker developed waterborne PSAs incorporating vinyl acetate and ethylene in their composition[33]. Moreover, the influence of the acid comonomer level, the crosslinking and chain transfer agent, as well as the type of stabilizer on the adhesive properties has been deeply analyzed. In this context, Garrett and coworkers[34] studied the impact of the amount of acrylic acid (AA) on the shell of two types of core-shell PSA dispersions, one with a soft core composed by poly(butyl acrylate) (PBA) and another with a hard core composed by poly(methyl methacrylate-*co*-allyl methacrylate)

(PMMA/ALMA). They found a counteracting effect between peel strength and shear resistance depending on the nature of the core, as well as a reduction of these properties as the amount of acrylic acid increased (32-49 mol%) on the PBA/AA shell. Czech[35] investigated cross-linking agents from seven different commercially available groups and their influence on the adhesive properties of 2-EHA/BA/VAc/Sty/AA emulsion-based PSAs. On the other hand, Plessis et al.[36] explored the effect of dodecane-1-thiol, as chain transfer agent, on the kinetics, gel fraction, level of branching, and sol molecular weight distribution in seeded semibatch emulsion polymerization of BA. In regards to surfactants, it was shown that sodium dodecyl sulfate (SDS) forms a relatively thick stabilizer layer at the adhesive-substrate interface where the rupture of the adhesive bond will easily propagate[37–40]. The thicker the layer, the easier the propagation. Aguirreurreta and coworkers[19,41,42] deeply explored the use of polymerizable surfactants for improving adhesion properties and water sensibility in high solids content waterborne PSAs. Among other stabilizers, hydroxyethyl cellulose and poly(vinyl alcohol) (PVOH) are common polymeric stabilizers used in PSA formulations for paper industry[43]. It is worth to mention that PVOH stabilized latexes exhibit Newtonian flow even at high shear rates, which makes them suitable for the high speed applicators used in the adhesive industry[44].

As it was discussed above, the adhesive industry has been affected by the increase on environmental constraints and, consequently, several efforts in this area have been carried out aiming to reduce the carbon footprint. The global bioadhesives market size is expected to grow from US$ 5.6 billion in 2019 to US$ 9.1 billion by 2024 at a CAGR of 10.0%, where paper & packaging, woodworking, personal care, and medical are the major applications[45]. One of the main factors driving this growth is the stringent regulations for conventional adhesives in the United States. On the other hand, Europe dominates such market and is expected to witness the highest market share during the forecast period, in

which companies such as Henkel AG & Co. KGaA, Arkema Group (Bostik SA), H.B. Fuller, Ashland and 3M are the key players. Among the different raw materials, rosin, starch, lignin, soy and vegetable oils are considered the most promising candidates for the development of environmentally-friendly adhesives.

Over the past few years, extensive research in the field of biobased pressure sensitive adhesives has been carried out. Concerning this, Vendamme and coworkers provided a nice overview of the recent developments in the field of PSAs derived from renewable building blocks[46]. However, it is worth noting that the number of studies combining both polymerization in dispersed media and biobased monomers as building blocks for PSA applications are scarcely reported in the open literature. Among them, Bunker et al.[47,48] designed waterborne PSA copolymers with biobased acrylated methyl oleate together with oil-based methyl methacrylate (MMA) and ethylene glycol dimethacrylate (EGDMA). Pu et al.[49] reported the synthesis of a biobased macromonomer coming from HEMA, lactide and ε-caprolactone and its copolymerization together *n*-butyl acrylate to produce PSAs with 34% biomass content. Moreno et al.[50,51] carried out the polymerization of the methacrylated oleic acid (MOA) monomer and its copolymerization with α-methylen-γ-butyrolactone to produce waterborne dispersions with potential uses in the PSAs field. More recently, Noppalit et al.[52] synthesized and copolymerized tetrahydrogeraniol acrylate (THGA) and cyclademol acrylate (CDMA), but not optimal adhesive performance was reached. In those cases, miniemulsion polymerization was used to incorporate the hydrophobic monomers into the polymer particles. Miniemulsion polymerization is an energy intensive polymerization technique. Roberge and Dubé[53] incorporated up to 30% of renewable conjugated linoleic acid into terpolymer PSA formulation by batch emulsion polymerization. Sugar-based acrylate macromonomers have been also copolymerized with conventional acrylates in emulsion process to obtain repulpable PSAs[54]. Waterborne PSAs in which more sustainable

components such as surfactants[55] or chain transfer agents based on renewable resources[56] have been added to the formulation have also been described.

Despite the efforts that have been devoted in academia and industry to incorporate renewable resource building blocks in adhesives there is still plenty of room to improve the incorporation by emulsion polymerization and by enhancing performance of the adhesives by providing special features. The fine tuning of the adhesive microstructure by physical stimuli (temperature, electricity or UV-light) or the easy debonding/degradation under mild conditions are key factors for the industrial applications.

1.2.2 Waterborne Coatings

Coatings (such as paints, varnishes and inks) are essential daily consumer goods in modern society, as nearly every surface needs to be coated for several reasons. In this context, the main purpose of applying a coating may be a decorative finish, a protection of the surface or both[57]. The global paints and coatings market was valued at US$ 178.9 billion in 2019 and it is hoped a CAGR of 4.1% over the next five years, reaching US$ 218.3 billion in 2025[58]. Nonetheless, from the economic point of view, protective coatings are the most important ones, since they extend the lifetime of the products and machinery (generally employed on wood and steel surfaces). On the other hand, decorative coatings improve the appeal of products to customers, being decorative paints the most relevant group in this category.

The basic formulation of a coating mainly consists on a binder, fillers, pigments and additives. The binder is the polymer that forms the matrix of the coating and provides mechanical and barrier properties (the gloss of the coating). Whereas fillers (or extenders) are inorganic particles which improve the mechanical strength and reduce the cost, pigments (organic or inorganic particles) are the most expensive components and ensure opacity and

color of the coating. Finally, additives are added in small quantities to modify the properties of the coating (e.g. biocides and corrosion inhibitors).

As PSAs, coatings have been traditionally synthesized in organic solvent solution[59]. However, waterborne coatings present additional advantages such as faster drying times, easy application, minimal odor, easier clean-up and higher economy viability in comparison with the solventborne ones[60,61]. As result, the global demand for waterborne coatings was estimated to be more than 25 million tonnes in 2018 and its market size was valued at US$ 53.32 billion in 2017. In addition, a CAGR of 5.7 % from 2017 to 2025 is estimated[62]. Figure 1.5 shows the expected evolution of the U.S. paints & coatings market by product, during the period 2014-2025[63].

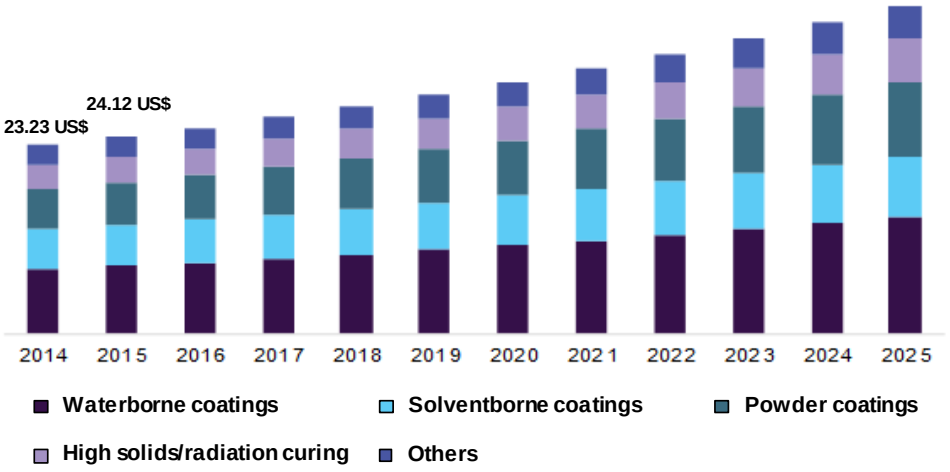

Figure 1.5. Expected evolution of the U.S. paints & coatings market during the period 2014-2025. Note that US$ makes reference to billions.

Most of the waterborne coating compositions involve the use of copolymers based on vinyl acetate with acrylate esters, acrylate-methacrylate, and styrene-acrylate/butadiene copolymers[64]. Regarding this, about 20% of the total production of emulsion polymers are vinyl acetate (VAc) homo and copolymers. Its copolymerization together with hydrophobic

and soft comonomers such as n-butyl acrylate (BA), ethylene or VeoVa10 (a vinyl ester of versatic acid) improves film forming ability and resistance to water, making it a cheap alternative as decorative coating (paints)[65]. Styrene (S) containing copolymers offer a higher hydrophobicity (thus higher water resistance) that the vinyl acetate based coatings. As vinyl acetate, styrene homopolymer is too hard to allow film formation and, consequently, its copolymerization with butadiene provides softer coatings, which are widely used in paper coating industry. For decorative indoor paint applications styrene-acrylate (typically butyl acrylate in a 50-50 weight ratio) copolymers are more common. Styrene copolymers are not useful for exterior paint applications, since the aromatic rings of styrene units absorb UV-light leading to the degradation of the coating by the sunlight. The last important polymer family are the fully acrylic copolymers. The great variety of acrylic esters, as well as the combinations among them, allows the fine tuning of the glass transition temperature and the hydrophobicity of the copolymer. Acrylic copolymers have excellent UV-light and water resistance, making them a better alternative for exterior applications, but at the cost of the price of the raw materials (MMA is more expensive than VAc or S). Thus, among the most demanded applications are their use as protective and industrial coatings (e.g. coatings for industrial structures, machinery, metal containers, wood furniture, marine coatings or traffic marking coatings).

It is worth pointing out that, in last years, the demand of biobased paints and coating systems has constantly increased, finding its own market niche[66]. In this scenario, high bio-content formulations represent a total volume of around 10 %, being the equivalent in value to a EUR 14.2 billion[67]. Recent approaches in polymerization dispersion media include monomers coming from vegetable oils and terpenes as well as modified cellulose esters, biobased polyols and isocyanates and the extended use of itaconic acid[60,61,68]. As a commercial example, Decovery®, which is a family of waterborne paint resins having a bio-

content above 30%, has been developed by DSM for indoor and outdoor coating applications[69]

Among the most relevant research, Moreno et al.[70,71] synthesized latexes by miniemulsion polymerization from methacrylated oleic acid (MOA), methacrylate linoleic acid (MLA) and α-methylene-γ-butyrolactone (MBL). Copolymers of MOA, MLA, MBL and MMA were reported and used in paint formulations. Properties such as hardness, gloss, rheological behaviour and open time were measured and compared with those of commercial samples. Sainz et al.[72] reported a two-step modification of terpenes to form acrylate and methacrylate, followed by free radical polymerization to prepare the final polymer, suitable for coating application. Another approach has been the synthesis of methacrylated monomers using galactose and fructose-protected molecules and their copolymerization with butyl acrylate to produce 45 wt% solids content latexes, which could be used for paint applications[73,74].

Möller and Glittenberg reported the emulsion copolymerization of styrene–butadiene in the presence of corn starches[75]. The final hybrid latexes contained 50 pphm (parts per hundred monomer) of starch exhibiting improved performances in paper coating applications. More recently, De Bruin et al. synthesized polymer latexes stabilized with amylopectin and having a high proportion of high molecular weight starch grafted to the latex particles[76,77]. On the other hand, it was reported the use of carboxymethylcellulose acetate butyrate for improving flow and levelling, reducing cratering, picture framing and other defects in water-based automotive paints[78].

Poussard et al.[79] developed biobased waterborne polyurethanes coming from fully renewable polyols for coating applications. They observed that the nature of the polyols strongly affected the final properties of the materials, reaching values of strain at break

superior to 600%. Itaconic acid (IA) has been incorporated in styrene-based copolymers, providing an improvement of the resistance to wear, corrosion and thermal degradation[80]. Furthermore, paints prepared with latexes containing low proportion of IA resulted to be more resistant to abrasion than those ones having (meth)acrylic acid[81]. Lastly, Picchio et al. have deeply investigated the emulsion polymerization of acrylic monomers in presence of casein, and in absence of emulsifier[82–84]. The use of the obtained hybrid latexes as coatings resulted in an improvement of anti-blocking property, film hardness, resistance to organic solvent and degradability.

1.3 Emulsion polymerization

The most industrially employed polymerization process for the development of waterborne polymeric dispersions is emulsion polymerization. This technique accounts more than 25 million tones/year of the waterborne dispersions worldwide production[8]. Furthermore emulsion polymerization presents several advantages in comparison with processes carried out in bulk or in organic solvents. First of all, the use of water, as continuous phase, not only ensure the environmental friendliness, but also the safety because the high heat capacity and low viscosity of water. Free radical polymerizations are very exothermic reactions and heat removal is one of the key points for the safety and control during the process. Secondly, due to its compartmentalization nature, emulsion polymerization enables to reach high molar masses (with high monomer conversions) and high polymerization rates at the same time. This aspect makes unique this technique, being one of the responsible for its industrial implementation and extensive development. Moreover, the viscosity of the final latex does not depend on the molar mass of the polymer so very high molar masses can be obtained (>10^6 g/mol). Finally, the final product, a latex, is easier to handle than products coming from bulk or solution polymerization.

It is important to mention that the continuous addition of monomers during the reaction allow to control the microstructure of the polymer and the dispersion characteristics of the latex (e.g., copolymer composition, molar mass distribution and particle size) in an efficient way. This remarkable asset promotes the production of high quality materials that are adapted to consumer demands.

Since the understanding of the emulsion polymerization process is a mandatory requisite for the design of new polymer microstructures, a brief description of a batch emulsion polymerization process is presented in the following section.

1.3.1 Description of the batch emulsion polymerization process

A batch emulsion polymerization process consist, mainly, in three different stages, typically called intervals[9,85–88].

System before initiation

At the initial stage, the reaction medium in a batch reactor contains water (forming the continuous phase), monomer and surfactant (emulsifier). The monomer is distributed between 3 phases: As monomer droplets, having a diameter above 1μm, stabilized by the surfactant molecules absorbed at the droplet/water interphase; in the aqueous phase, small amounts of monomer and free surfactant molecules are dissolved at saturation conditions; in micelles (diameter ≈ 1-10 nm), swollen by monomer, formed by self-assembly of surfactant molecules if the surfactant concentration exceeds the critical micellar concentration (CMC). This is the concentration above which is possible to cover the droplets and saturate the aqueous phase. Figure 1.6 shows a representative view of the emulsion polymerization system before the initiation.

Note that surfactants (or polymeric stabilizers) are needed in order to suppress coagulation and phase separation of colloidal dispersions, which are thermodynamically unstable.

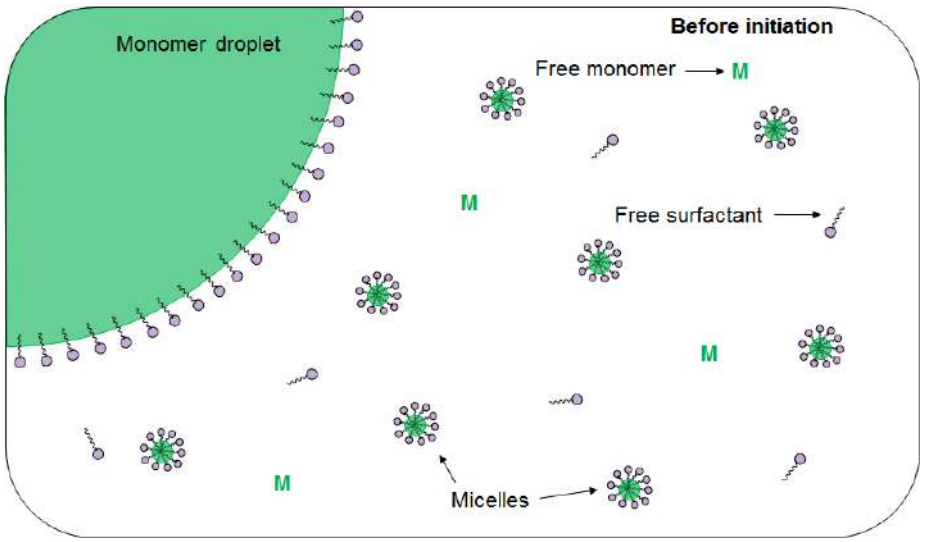

Figure 1.6. Representative view of the emulsion polymerization system before the initiation.

Interval I. Particle nucleation

The first interval of the emulsion polymerization process starts when the initiator is added to the reaction media. Figure 1.7 shows a schematic representation of interval I. Normally, water-soluble initiators are employed in emulsion polymerization generating radicals by thermal dissociation. These radicals are usually too hydrophilic to be able to enter into the micelles so they propagate in the aqueous phase by adding monomer units to form oligoradicals, which become more a more hydrophobic as they grow.

When the oligoradicals reach a certain chain-length (by the continuous addition of monomer units), they are hydrophobic enough to be surface active and, hence, to enter in the micelles producing polymer particles. It is admitted that particle nucleation occurs when

the surfactant concentration is much higher than the CMC. In addition, because the surface area of the micelles is about 3 orders of magnitude larger than the monomer droplets one, the entry into the droplets is negligible. Once the oligoradical enters into the micelle, it immediately propagates forming a polymer particle. This mechanism to form new particles is known as micellar or *heterogeneous nucleation* and takes place for monomers having a low solubility in water (e.g. 2-Ethylhexyl acrylate or styrene).

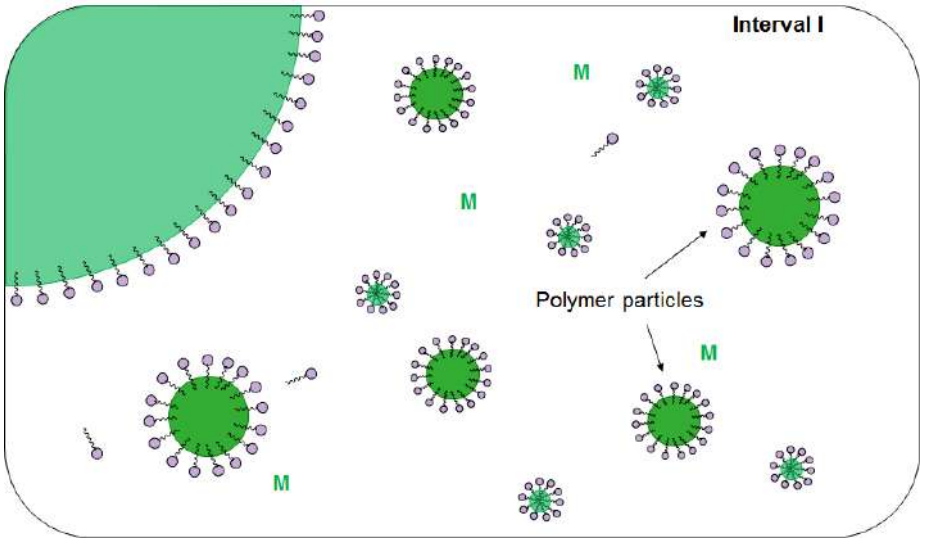

Figure 1.7. Representative view of interval I of the emulsion polymerization process.

Nevertheless, if the monomer is relatively water-soluble (such as 2-Hydroxyehyl methacrylate or methyl methacrylate) its concentration in water will be higher and, thereby, the polymerization rate in the aqueous phase will be higher too. Thus, if the oligoradical reaches a certain critical size, it might become insoluble in water before entering to the micelle. When this happens, the growing chain precipitates and the emulsifier in the water phase will be adsorbed stabilizing the new surface, creating a particle. This mechanism, called *homogeneous nucleation*, takes place not only when the solubility of the monomers in water is relatively high but also when the surfactant concentration is below the CMC.

Independently of the nucleation mechanism, since the growth rate of the surface area of the particles is higher than the absorption rate of the surfactant molecules, the new particles are very small and unstable. Therefore, species formed by both *heterogeneous* and *homogeneous nucleation* may be regarded as unstable precursor particles which are susceptible to coagulate, forming “mature” particles. These larger particles are stable and will become the main locus of the polymerization. This combined process is called *coagulative nucleation*.

To sum up, during the first interval of an emulsion polymerization process particle nucleation takes place. This step is featured by an increase of the number of particles and an increase of the polymerization rate and ends once the number of particles reaches a plateau (disappearance of micelles).

Interval II. Particle growth

During the second interval, consisting in the polymer particles growth, the system is composed of monomer droplets and polymer particles, as represented in Figure 1.8. Monomer droplets behave as reservoirs, constantly replacing the monomer consumed in the polymer particles by monomer that diffuses from the monomer droplets through the aqueous phase. In the presence of monomer droplets, the concentration of monomer in the polymer particles remains relatively constant. For this reason, the polymerization rate (Rp, as defined in equation 1.1) is constant during this interval.

$$R_P = k_P [M]_P \bar{n} \frac{N_P}{N_A} \qquad \textbf{(Eq.1.1)}$$

Where R_P is the polymerization rate, k_P is the propagation rate coefficient, $[M]_P$ is the monomer concentration in polymer particles, $\bar{n}$ is the average number of radicals per particle

(which is equal to 0.5 for the ideal emulsion polymerization), N_P is the number of particles per unit volume and N_A is Avogadro's number.

Morton et al. established the following equation to calculate the equilibrium concentration of monomer in the particles during that stage:

$$2V_m\gamma/RTr_P = -[\ln(1-\Phi_P) + (1-1/X_n)\,\Phi_P + \mu\Phi_P^2 \qquad \textbf{(Eq. 1.2)}$$

Where V_m is the partial molar volume of the monomer, Φ_P the volume fraction of polymer in the particle, γ the polymer/water interfacial tension at swelling equilibrium, R the ideal gas constant, T the absolute temperature, X_n the number average degree of polymerization and μ the Flory-Huggins interaction parameter.

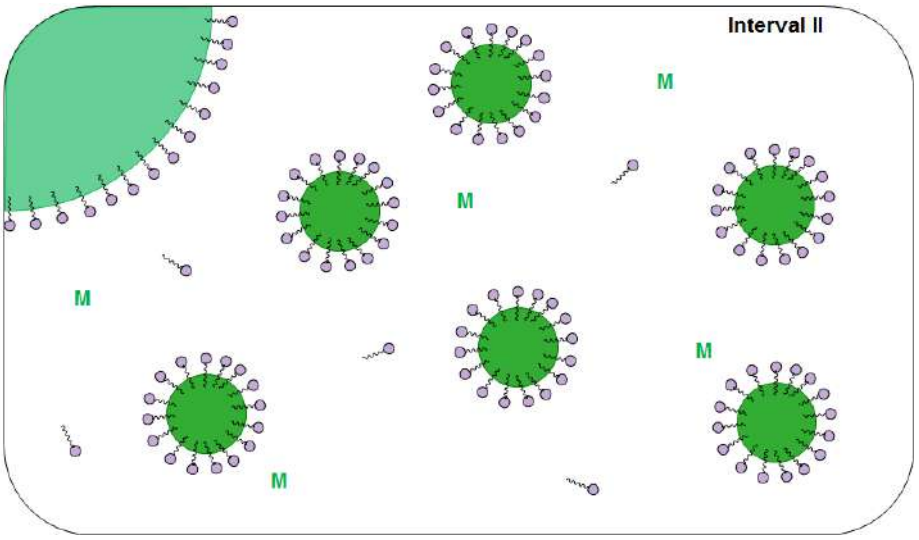

Figure 1.8. Representative view of interval II of the emulsion polymerization process.

As the number of polymer particles and the monomer concentration in polymer particles are constant (assuming complete colloidal stability), the polymerization rate is roughly constant (some variation of the average number of radicals per particle may occur)

along the particles growth until the complete consumption of monomer droplets that marks the end of this stage. The transition from interval II to interval III occurs about 15-40% conversion depending on the monomer nature. In general, the higher the water solubility of the monomer the higher the maximum swelling of the polymer particles and the lower the conversion at which interval II ends.

Interval III. End of polymerization

The final stage of an emulsion polymerization process is characterized by a reduction of the polymerization rate due to a progressive decrease of the monomer concentration inside the polymer particles. On one hand, the polymerization rate is reduced if the monomer concentration in the particles decreases (see Equation 1.1). On the other hand, if the polymer concentration inside the particles increases the viscosity do as well, decreasing the effective termination rate and accelerating the polymerization rate (gel effect). Interval III is represented in Figure 1.9.

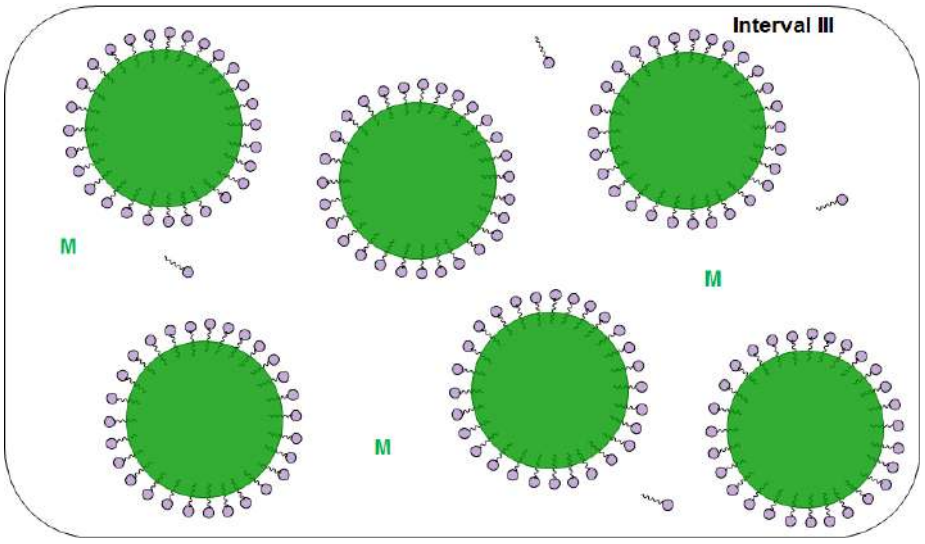

Figure 1.9. Representative view of interval III of the emulsion polymerization process.

1.3.2 Semibatch emulsion polymerization process

Contrary to batch process, semibatch (also known as semi-continuous) emulsion polymerization process is industrially more relevant and is the tool to produce high quality materials with a controlled microstructure. In this context, a semibatch process provides a higher process-flexibility which can be controlled by the feeding streams of the reactants (generally monomers, surfactant, initiator and water). In addition, it is a safer process since monomers are continuously fed under starved conditions, namely, at high instantaneous conversions avoiding potential undesired thermal runaway scenarios.

In a typical semibatch emulsion process the reactor contains a "seed" as initial charge, this is a waterborne dispersion with small particle size and low solids content. During the process, monomers, surfactant, initiator and water are fed into the reactor. Under these circumstances (interval III), newly fed monomer droplets are present in the reactor, and their life-time is short because the monomers diffuse to the polymer particles where they are consumed. In this context and, in order to avoid the accumulation of unreacted monomer and ensure the safety of the process, the feeding rate must not exceed the polymerization rate (starved conditions requisite). In addition, slow monomer addition in systems containing monomers with different reactivity ratios can avoid the composition drift in the copolymer structure that happens in the batch processes.

The feeding control of the surfactant is also important and it has a remarkable effect in the particle size distribution. Regarding this, monomodal particle size distributions are obtained if the surfactant feeding rate is low enough to avoid secondary nucleation. On the contrary, the excess of surfactant leads to the formation of micelles and, hence, to new particle nucleation (*heterogeneous* nucleation). Nonetheless, for some high solids content

applications multimodal particle size distributions are desired since the viscosity of the latex decreases.

1.4 Thesis outline

The content of this thesis is divided in seven chapters, whose description is given below.

Chapter 1 provides a general introduction, motivation and main objectives about this work. The current necessity of replacing petroleum-based components by renewable counterparts in daily consumer goods is overviewed. State of the art and market situation of waterborne PSAs and coatings, and the recent approaches in biobased formulations are presented together with general aspects of emulsion polymerization, which is the main polymerization technique used to produce waterborne polymer dispersions.

In **Chapter 2**, the incorporation of the commercial biobased monomers 2-Octyl acrylate (2OA) and isobornyl methacrylate (IBOMA), via emulsion polymerization, to produce high bio-content waterborne PSAs is explored. The effect of the polymer microstructure in the adhesive properties is investigated, and the performance compared to traditional oil-based counterparts.

Chapter 3 is focused on the synthesis and incorporation of the biobased monomer, with dual functionality, piperonyl methacrylate (PIPEMA) aiming to fulfill the conflict between bio-content degree and adhesive performance. The effect of the UV-light irradiation time on the evolution of the crosslinking degree as well as on the adhesive properties is assessed.

In **Chapter 4** the synthesis of a new functional isosorbide methacrylate derivatives (ISOMAraw and ISOMA) is deeply investigated and their incorporation in emulsion polymerization to produce easily-removable waterborne PSAs is evaluated. The effect of low

percentages of these isosorbide derivative monomers on polymer microstructure, adhesive performance and water removability is explored.

In **chapter 5**, biobased alkali soluble resins are synthesized and used as electrosterically stabilizers for the production of high performance PSAs with the ability to be removable in basic media. The effect of the nature of the resin on the polymer microstructure is studied and the role of supramolecular interactions on the adhesive performance deeply investigated from the rheological point of view.

Chapter 6, focuses on the characterization of the commercial sugar based vinyl monomer Ecomer® and its incorporation in emulsion polymerization for the development of partially biodegradable waterborne coatings. The impact of the caramelization process on the free Ecomer® incorporation, as well as on the coating properties and on the biodegradability of the films is assessed. This chapter was carried out at DSM Coating resins (R&D acrylics team) in The Netherlands as part of the internship of this thesis.

Finally, in **Chapter 7** the most relevant conclusions of this thesis are summarized.

1.5 References

(1) Harris, S.; Staffas, L.; Rydberg, T.; Eriksson, E. *Renewable Materials in the Circular Economy*; 2018.

(2) Harmsen, P.; Hackmann, M. *Green Building Blocks for Biobased Plastics: Biobased Processes and Market Development*; Wageningen, 2012.

(3) Hatton, F. L. Recent Advances in RAFT Polymerization of Monomers Derived from Renewable Resources. *Polym. Chem.* **2020**, *11*, 220–229.

(4) Llevot, A.; Dannecker, P. K.; von Czapiewski, M.; Over, L. C.; Söyler, Z.; Meier, M.

A. R. Renewability Is Not Enough: Recent Advances in the Sustainable Synthesis of Biomass-Derived Monomers and Polymers. *Chem. - A Eur. J.* **2016**, *22*, 11510–11521.

(5) Transparency Market Research. *Polymer Dispersion Market- Global Industry Analysis, Size, Share, Growth, Trends, and Forecast, 2019 - 2027*; New York, 2020.

(6) Molina-Gutiérrez, S.; Ladmiral, V.; Bongiovanni, R.; Caillol, S.; Lacroix-Desmazes, P. Radical Polymerization of Biobased Monomers in Aqueous Dispersed Media. *Green Chem.* **2019**, *21*, 36–53.

(7) Jean-Claude, D.; Pichot, C. *Les Latex Synthétiques Élaboration Propriétés - Applications*; Lavoisier, Ed.; 2006.

(8) Urban, D.; Takamura, K. *Polymer Dispersions and Their Industrial Applications*; Wiley-VCH Verlag GmbH & Co: Charlotte, 2002.

(9) Asua, J. M. Emulsion Polymerization : From Fundamental Mechanisms to Process Development. *J. Polym. Sci.* **2004**, *42*, 1025–1041.

(10) Benedek, I. *Pressure-Sensitive Adhesives and Applications - Second Edition , Revised and Expanded*; CRC Press, Ed.; Marcel Dekker: New York, 2004.

(11) D.Satas. *Handbook of Pressure Sensitive Adhesive Technology.*, 2nd ed.; 1989.

(12) Grand View Research. *Pressure Sensitive Adhesives Market Size, Share & Trends Analysis Report By Product (Films), By Technology (Water-Based, Radiation-Cured), By Adhesive Chemistry, By End Use (Automotive, Packaging), And Segment Forecasts, 2019 - 2025*; 2019.

(13) Pocius, A. V. *Adhesives and Sealants*; Elsevier B.V.: St. Paul, MN, USA, 2012; Vol.

8.

(14) Agirre, A.; Nase, J.; Degrandi, E.; Creton, C.; Asua, J. M. Improving Adhesion of Acrylic Waterborne PSAs to Low Surface Energy Materials: Introduction of Stearyl Acrylate. *J. Polym. Sci. Part A Polym. Chem.* **2010**, *48* (22), 5030–5039.

(15) Creton, C. Pressure-Sensitive Adhesives: An Introductory Course. *MRS Bull.* **2003**, *28* (6), 434–439.

(16) Lee, J. H.; Lee, T. H.; Shim, K. S.; Park, J. W.; Kim, H. J.; Kim, Y.; Jung, S. Effect of Crosslinking Density on Adhesion Performance and Flexibility Properties of Acrylic Pressure Sensitive Adhesives for Flexible Display Applications. *Int. J. Adhes. Adhes.* **2017**, *74*, 137–143.

(17) Lopez, A.; Reyes, Y.; Degrandi-Contraires, E.; Canetta, E.; Creton, C.; Keddie, J. L.; Asua, J. M. Simultaneous Free-Radical and Addition Miniemulsion Polymerization: Effect of the Chain Transfer Agent on the Microstructure of Polyurethane-Acrylic Pressure-Sensitive Adhesives. *Macromol. Mater. Eng.* **2013**, *298* (1), 53–66.

(18) Tobing, S. D.; Klein, A.; Sperling, L. H.; Petrasko, B. Effect of Network Morphology on Adhesive Performance. *J. Appl. Polym. Sci.* **2001**, *81*, 2109–2117.

(19) Aguirreurreta, Z.; Dimmer, J. A.; Willerich, I.; Leiza, J. R.; de la Cal, J. C. Improving the Properties of Water-Borne Pressure Sensitive Adhesives by Using Non-Migratory Surfactants. *Int. J. Adhes. Adhes.* **2016**, *70*, 287–296.

(20) Alarcia, F.; de la Cal, J. C.; Asua, J. M. Continuous Production of Specialty Waterborne Adhesives: Tuning the Adhesive Performance. *Chem. Eng. J.* **2006**, *122* (3), 117–126.

(21) Chauvet, J.; Asua, J. M.; Leiza, J. R. Independent Control of Sol Molar Mass and

Gel Content in Acrylate Polymer/Latexes. *Polymer (Guildf).* **2005**, *46* (23), 9555–9561.

(22) Benedek, I. *Development and Manufacture of Pressure-Sensitive Products*; Marcel Dekker Inc: New York, 1999.

(23) Lakrout, H.; Sergot, P.; Creton, C. Direct Observation of Cavitation and Fibrillation in a Probe Tack Experiment on Model Acrylic Pressure- Sensitive-Adhesives. *J. Adhes.* **1999**, *66*, 307–359.

(24) Shull, K. R.; Creton, C. Deformation Behavior of Thin, Compliant Layers Under Tensile Loading Conditions. *J. Polym. Sci. Part B Polym. Phys.* **2004**, *42*, 4023–4043.

(25) Zosel, A. The Effect of Fibrilation on the Tack of Pressure Sensitive Adhesives. *Int. J. Adhes. Adhes.* **1998**, *18* (4), 265–271.

(26) Deplace, F.; Carelli, C.; Mariot, S.; Retsos, H.; Chateauminois, A.; Ouzineb, K.; Creton, C. Fine Tuning the Adhesive Properties of a Soft Nanostructured Adhesive with Rheological Measurements. *J. Adhes.* **2009**, *85* (1), 18–54.

(27) Zosel, A. Shear Strength of Pressure Sensitive Adhesives and Its Correlation to Mechanical Properties. *J. Adhes.* **1994**, *44* (1–2), 1–16.

(28) Zosel, A. Effect of Cross-Linking on Tack and Peel Strength of Polymers. *J. Adhes.* **1991**, *34* (1–4), 201–209.

(29) Jovanović, R.; Dubé, M. A. Screening Experiments for Butyl Acrylate/Vinyl Acetate Pressure-Sensitive Adhesives. *Ind. Eng. Chem. Res.* **2005**, *44* (17), 6668–6675.

(30) Jovanović, R.; Dubé, M. A. Emulsion - Based Pressure - Sensitive Adhesives : A

Review. *J. Macromol. Sci. Part C Polym. Rev.* **2004**, *44*, 1–55.

(31) Brooks, T. W. . *Tappi J.* **1984**, *29* (9).

(32) Mohsen, R. M.; Nasr, H. E.; Badran, A. S. Some Water-Borne Adhesives Based on Styrene Butyl Acrylate Copolymer Latices. *Pigment Resin Technol.* **1995**, *24* (3), 4–9.

(33) Daniels, C. L.; Mao, C.-L.; Bott, R. H.; Vratsanos, M. S. Water Borne Pressure Sensitive Vinyl Acetate/Ethylene Adhesive Compositions. E.P 0990688A1, 1999.

(34) Garrett, J.; Lovell, P. A.; Shea, A. J.; Viney, R. D. Water-Borne Pressure Sensitive Adhesives: Effects of Acrylic Acid and Particle Structure. *Macromol. Symp.* **2000**, *151*, 487–496.

(35) Czech, Z. Crosslinking of Pressure Sensitive Adhesive Based on Water-Borne Acrylate. *Polym. Int.* **2003**, *52*, 347–357.

(36) Plessis, C.; Arzamendi, G.; Leiza, J. R.; Alberdi, J. M.; Schoonbrood, H. A. S.; Charmot, D.; Asua, J. M. Seeded Semibatch Emulsion Polymerization of Butyl Acrylate: Effect of the Chain-Transfer Agent on the Kinetics and Structural Properties. *J. Polym. Sci. Part A Polym. Chem.* **2001**, *39* (7), 1106–1119.

(37) Charmeau, J. Y.; Berthet, C.; Gringeau, C.; Holl, Y.; Kientz, E. Effects of Film Structure on Mechanical and Adhesion Properties of Latex Films. *Int. J. Adhes. Adhes.* **1997**, *17*, 169–176.

(38) Charmeau, J. Y.; Sartre, A.; Vovelle, L.; Holl, Y. Adhesion of Latex Films. Part II. Loci of Failure. *J. Adhes. Sci. Technol.* **1999**, *13* (5), 593–614.

(39) Charmeau, J. Y.; Gerin, P. A.; Vovelle, L.; Schirrer, R.; Holl, Y. Adhesion of Latex

Films. Part III. Surfactant Effects at Various Peel Rates. *J. Adhes. Sci. Technol.* **1999**, *13* (2), 203–215.

(40) Gerin, P. A.; Grohens, Y.; Schirrer, R.; Holl, Y. Adhesion of Latex Films. Part IV. Dominating Interfacial Effect of the Surfactant. *J. Adhes. Sci. Technol.* **1999**, *13* (2), 217–236.

(41) Aguirreurreta, Z.; Willerich, I.; de la Cal, J. C.; Leiza, J. R. Water Whitening Reduction in Waterborne Pressure-Sensitive Adhesives Produced with Polymerizable Surfactants. *Macromol. Mater. Eng.* **2015**, *9*, 925–936.

(42) Aguirreurreta, Z.; de la Cal, J. C.; Leiza, J. R. Preparation of High Solids Content Waterborne Acrylic Coatings Using Polymerizable Surfactants to Improve Water Sensitivity. *Prog. Org. Coatings* **2017**, *112*, 200–209.

(43) *Handbook of Adhesion Technology*, 2nd ed.; Pizzi, A., Mittal, K. L., Eds.; Marcel Dekker: New York, 1994.

(44) Yuki, K.; Nakamae, M.; Sato, T.; Maruyama, H.; Okaya, T. Physical Properties of Acrylic Copolymer Emulsions Using Poly (Vinyl Alcohol) as a Protective Colloid in Comparison with Those Using Surfactants. *Polym. Int.* **2000**, *49*, 1629–1635.

(45) MarketsandMarkets. *Bioadhesives Market by Type (Plant Based, Animal Based), Application (Paper & Packaging, Construction, Woodworking, Personal Care, Medical), Region (APAC, North America, Europe, Middle East & Africa, South America) - Global Forecasts to 2024*; 2019.

(46) Vendamme, R.; Schüwer, N.; Eevers, W. Recent Synthetic Approaches and Emerging Bio-Inspired Strategies for the Development of Sustainable Pressure-Sensitive Adhesives Derived from Renewable Building Blocks. *J. Appl. Polym. Sci.*

2014, *131* (17), 8379–8394.

(47) Bunker, S. P.; Wool, R. P. Synthesis and Characterization of Monomers and Polymers for Adhesives from Methyl Oleate. *J. Polym. Sci. Part A Polym. Chem.* **2002**, *40* (4), 451–458.

(48) Bunker, S.; Staller, C.; Willenbacher, N.; Wool, R. Miniemulsion Polymerization of Acrylated Methyl Oleate for Pressure Sensitive Adhesives. *Int. J. Adhes. Adhes.* **2003**, *23* (1), 29–38.

(49) Pu, G.; Dubay, M. R.; Zhang, J.; Severtson, S. J.; Houtman, C. J. Polyacrylates with High Biomass Contents for Pressure-Sensitive Adhesives Prepared via Mini-Emulsion Polymerization. *Ind. Eng. Chem. Res.* **2012**, *51* (37), 12145–12149.

(50) Moreno, M.; Goikoetxea, M.; Barandiaran, M. J. Biobased-Waterborne Homopolymers from Oleic Acid Derivatives. *J. Polym. Sci. Part A Polym. Chem.* **2012**, *50* (22), 4628–4637.

(51) Moreno, M.; Goikoetxea, M.; De La Cal, J. C.; Barandiaran, M. J. From Fatty Acid and Lactone Biobased Monomers toward Fully Renewable Polymer Latexes. *J. Polym. Sci. Part A Polym. Chem.* **2014**, *52* (24), 3543–3549.

(52) Noppalit, S.; Simula, A.; Billon, L.; Asua, J. M. Paving the Way to Sustainable Waterborne Pressure-Sensitive Adhesives Using Terpene-Based Triblock Copolymers. *ACS Sustain. Chem. Eng.* **2019**, *7*, 17990–17998.

(53) Roberge, S.; Dubé, M. A. Emulsion-Based Pressure Sensitive Adhesives from Conjugated Linoleic Acid/Styrene/Butyl Acrylate Terpolymers. *Int. J. Adhes. Adhes.* **2016**, *70*, 17–25.

(54) Bloembergen, S.; McLennan, L. J.; Cassar, S. E.; Narayan, R. Polymer Resins

Designed for Environmental Sustainability. *Adhes. Age* **1998**, *41*, 20–24.

(55) Pokeržnik, N.; Krajnc, M. Synthesis of a Glucose-Based Surfmer and Its Copolymerization with n-Butyl Acrylate for Emulsion Pressure Sensitive Adhesives. *Eur. Polym. J.* **2015**, *68*, 558–572.

(56) Ren, S.; Dubé, M. A. Modification of Latex Microstructure and Adhesive Performance Using D-Limonene as a Chain Transfer Agent. *Int. J. Adhes. Adhes.* **2017**, *75* (March), 132–138.

(57) Goldschmidh, A.; Streitberg, H.-J. *BASF Handbook on Basis of Coating Technology*, 2nd ed.; Vincentz Network: Hannover, 2007.

(58) 360researchreports. *Global Paints & Coatings Market Growth 2019-2024*; 2019.

(59) Sherman, J.; Chin, B.; Huibers, P. D. T.; Garcia-Valls, R.; Hatton, T. A. Solvent Replacement for Green Processing. *Environ. Health Perspect.* **1998**, *106*, 253–271.

(60) Goldsmith, A.; Streitberg, H.-J. *BASF Handbook on Basics of Coating Technology*, 3rd editio.; Vincentz Network: Hannover, 2018.

(61) Overbeek, A.; Bückmann, F.; Martin, E.; Steenwinkel, P.; Annable, T. New Generation Decorative Paint Technology. *Prog. Org. Coatings* **2003**, *48*, 125–139.

(62) *Waterborne Coatings Market Size, Share & Trends Analysis Report, By Resin (Acrylic, Polyurethane, Epoxy, Alkyd, Polyester, PTFE, PVDC, PVDF, Others), By Application, By Region, And Segment Forecasts, 2019 - 2025*; Grand View Research, Inc.: San Francisco, 2019.

(63) Grand View Research. *Paints And Coatings Market By Product (High Solids, Powder, Waterborne, Solvent-Borne), By Material (Acrylic, Alkyd, Polyurethane,*

Epoxy & Polyesters), By Application, And Segment Forecasts, 2018 - 2025.

(64) Stoye, D.; Freitag, W. *Paints, Coatings and Solvents*, 2 edition.; Stoye, D., Freitag, W., Eds.; Wiley-VCH: Beverly, 1998.

(65) Cordeiro, C.; Petrocelli, F. P. Vinyl Acetate Polymers. In *Encyclopedia of Polymer Science and Technology*; John Wiley & Sons, Inc, 1971; pp 146–451.

(66) Tiwari, A.; Galanis, A.; Soucek, M. D. *Biobased and Environmental Benign Coatings*, 1 edition.; Wiley-Scrivener: Beverly, 2016.

(67) Gagro, D. Bio-Based Coatings: Small Market, Full of Potential. *Eur. Coatings J.* **2019**, No. 4, 12–13.

(68) Molina-Gutiérrez, S.; Ladmiral, V.; Caillol, S.; Lacroix-desmazes, P.; Bongiovanni, R. Radical Polymerization of Biobased Monomers in Aqueous Dispersed Media. *Green Chem.* **2019**, *21*, 36–53.

(69) Nabuurs, T.; Kastelijn, M. Partially Plant-Based Polymers Evaluated in Exterior and Furniture Coatings. *Eur. Coatings 360º* **2018**, *4*, 20–24.

(70) Moreno, M.; Miranda, J. I.; Goikoetxea, M.; Barandiaran, M. J. Sustainable Polymer Latexes Based on Linoleic Acid for Coatings Applications. *Prog. Org. Coatings* **2014**, *77*, 1709–1714.

(71) Moreno, M.; Lampard, C.; Williams, N.; Lago, E.; Emmett, S.; Goikoetxea, M.; Barandiaran, M. J. Eco-Paints from Bio-Based Fatty Acid Derivative Latexes. *Prog. Org. Coatings* **2015**, *81*, 101–106.

(72) Sainz, M. F.; Souto, J.; Regentova, D.; Johansson, M. K. G.; Timhagen, S. T.; Irvine, D. J.; Buijsen, P.; Koning, C. E.; Stockman, R. A.; Howdle, S. M. A Facile and Green

Route to Terpene Derived Acrylate and Methacrylate Monomers and Simple Free Radical Polymerisation to Yield New Renewable Polymers and Coatings. *Polym. Chem.* **2016**, *7*, 2882–2887.

(73) Desport, J. S.; Mantione, D.; Moreno, M.; Sardon, H.; Barandiaran, M. J.; Mecerreyes, D. Synthesis of Three Different Galactose-Based Methacrylate Monomers for the Production of Sugar-Based Polymers. *Carbohydr. Res.* **2016**, *432*, 50–54.

(74) Desport, J. S.; Moreno, M.; Barandiaran, M. J. Fructose-Based Acrylic Copolymers by Emulsion Polymerization. *Polymers (Basel).* **2018**, *10*, 488–499.

(75) Möller, K.; Glittenber, D. TAPPI 1990 Coating Conference Proceedings. In *TAPPI: Atlanta*; 1990; pp 85–91.

(76) De Bruyn, H.; Sprong, E.; Gaborieau, M.; David, G.; Roper III, J. A.; Gilbert, R. G. Starch-Graft-Copolymer Latexes Initiated and Stabilized by Ozonolyzed Amylopectin. *J. ofPolymer Sci. Part A Polym. Chem.* **2006**, *44*, 5832–5845.

(77) De Bruyn, H.; Sprong, E.; Gaborieau, M.; Roper III, J. A.; Gilbert, R. G. Starch-Graft-(Synthetic Copolymer) Latexes Initiated with Ce 4+ and Stabilized by Amylopectin. *J. Polym. Sci. Part A Polym. Chem.* **2007**, *45*, 4185–4192.

(78) Posey-Dowty, J. D.; Seo, K. S.; Walker, K. R.; Wilson, A. K. CarboxymethylcelluJose Acetate Butyrate in Water-Based Automotive Paints. *Surf. Coatings Int. Part B Coatings Trans.* **2002**, *85*, 203–208.

(79) Poussard, L.; Lazko, J.; Mariage, J.; Raquez, J.; Dubois, P. Biobased Waterborne Polyurethanes for Coating Applications: How Fully Biobased Polyols May Improve the Coating Properties. *Prog. Org. Coatings* **2016**, *97*, 175–183.

(80) Ahmetli, G.; Deveci, H.; Altun, A.; Kurbanli, R. Corrosion and Thermal Characterization of Styrene Based Copolymers. *Prog. Org. Coatings* **2011**, *70*, 9–15.

(81) Pinheiro De Oliveira, M.; Reggiani Silva, C.; Müller Guerrini, L. Effect of Itaconic Acid on the Wet Scrub Resistance of Highly Pigmented Paints for Architectural Coatings. *J. Coatings Technol. Res.* **2011**, *8*, 439–447.

(82) Picchio, M. L.; Passeggi, M. C. G.; Barandiaran, M. J.; Gugliotta, L. M.; Minari, R. J. Waterborne Acrylic-Casein Latexes as Eco-Friendly Binders for Coatings. *Prog. Org. Coatings* **2015**, *88*, 8–16.

(83) Picchio, M. L.; Passeggi, M. C. G.; Barandiaran, M. J.; Gugliotta, L. M.; Minari, R. J. Acrylic/Casein Latexes with Controlled Degree of Grafting and Improved Coating Performance. *Prog. Org. Coatings* **2016**, *101*, 587–596.

(84) Picchio, M. L.; Minari, R. J.; Gugliotta, L. M. Enhancing the Coating Properties of Acrylic / Casein Latexes with High Protein Content. *J. Coatings Technol. Res.* **2017**, *14*, 543–553.

(85) de la Cal, J. C.; Leiza, J. R.; Asua, J. M.; Buttè, A.; Storti, G.; Morbidelli, M. Emulsion Polymerization. In *Handbook of Polymer Reaction Engineering*; Meyer, T., Keurentjes, J., Eds.; Wiley-VCH: Weinheim, 2005.

(86) Thickett, S. C.; Gilbert, R. G. Emulsion Polymerization : State of the Art in Kinetics and Mechanisms. **2007**, *48*, 6965–6991.

(87) Barandiaran, M. J.; de la Cal, J. C.; Asua, J. M. Emulsion Polymerization. In *Polymer Reaction Engineering*; Blackwell: Oxford, 2007.

(88) Smith, W. V.; Ewart, R. H. Kinetics of Emulsion Polymerization Kinetics of Emulsion

Polymerization. *J. Chem. Phys.* **1948**, *6*, 592–599.

Chapter 2

High bio-content waterborne PSAs containing 2-Octyl acrylate and isobornyl (meth)acrylate

2.1 Introduction

Vegetable oils and terpenes are considered one of the most promising renewable feedstock for the synthesis of sustainable monomers because of their abundance, low cost, and ease of separation.

The production volume of vegetable oils for 2019 exceeded 200 million metric tons worldwide, being palm oil, soybean oil and rapeseed oil the most demanded ones. In addition, the global vegetable oil market is projected to grow at a CAGR of 5.14% during the forecast period 2020-2025[1]. Vegetable oils are composed of triglycerides, i.e., saturated and unsaturated fatty acid esters of glycerol, in which the chain length of the fatty acid as well as the number and position of the double bonds strongly affect the oil properties[2]. It is well known that fatty acids are obtained by hydrolysis of the triglyceride with caustic solution (sodium hydroxide). The direct polymerization of fatty acids is considered difficult since the double bonds are not reactive enough to undergo free radical polymerization. Therefore, these molecules can be modified through the carboxylic acid group in order to promote their reactivity and incorporation[3]. In addition, the length of the aliphatic chain results of special importance since it influences to the viscous behavior in adhesive materials. Industrial production of monomers coming from fatty acids mostly involves the hydrogenation of the carboxylic acid, which yields in the primary alcohol, followed by (trans)esterification reactions (e.g. stearyl (meth)acrylate synthesis).

Terpenes, terpenoids and rosin comprise the largest single group of natural products and their remarkable structural diversity offers versatile functionalization possibilities[4–6]. These hydrocarbon-based molecules derived from isoprene (2-Methyl-1,3-butadiene) are particularly important for fine chemistry and fragrance industry. In this context, the worldwide market for terpenes is expected to grow at a CAGR of roughly 6.3% over the next five years,

reaching 730 million US$ in 2024 (from 510 million US$ in 2019)[7]. Due to the presence of double bonds, α-pinene, β-pinene, limonene and myrcene have been extensively investigated as starting building blocks for the synthesis of polymers[8]. Early attempts were carried out by cationic polymerization but limitations to achieve high monomer conversion and low molar masses have been the main issues[9]. In order to overcome these inconvenient, the synthesis of (meth)acrylate-based monomers (via oxidation and subsequent esterification of the hydroxyl groups) represent a more convenient approach, which can be directed towards the emulsion polymerization [10–12]. It is worth to mention that the cyclic and bulky structure of some terpenes could be useful for providing cohesiveness and ensure the elastic component in adhesives

The strategies mentioned above are getting more and more the attention of the industry and their implementation may provide suitable building blocks for the synthesis of environmentally friendly waterborne PSAs.

2-Octyl acrylate (2OA) and isobornyl methacrylate (IBOMA) are commercially available biobased monomers with a bio-content of 73% and 71% and whose homopolymers have a Tg of -44 ºC and 150 ºC, respectively. The glass transition temperatures of their homopolymers convert these monomers in potential candidates for the manufacturing of pressure sensitive adhesives since 2OA can act as soft monomer imparting flowability to the system, whereas IBOMA can be used as hard monomer providing rigidity.

The production of 2OA and IBOMA is industrially implanted and it implies (trans)esterification reactions of 2-Octanol and camphene/isoborneol acetate, respectively, with (meth)acrylic acid or derivative esters[13–17]. Figures 2.1 and 2.2 show the conversion steps to produce 2-Octyl acrylate and isobornyl methacrylate. 2-Octanol is produced through a cracking process of ricinoleic acid (the major component of castor oil attached to glycerol)

obtaining sebacic acid as side product, which is a diacid commonly employed in the Nylon industry[18]. On the other hand, camphene is obtained by catalytic isomerization of alpha-pinene, one of the main components of pine resin[19]. Camphene can be reacted with (meth)acrylic acid in the presence of aqueous sulfuric acid to yield in isobornyl methacrylate or can be treated with acetic acid resulting in isobornyl acetate, a flavoring and scenting agent which transesterification allows the production of the methacrylic ester. There are several industrial patents using 2-Octyl acrylate as main monomer for PSA formulations[20–24] and 3M has recently commercialized the Post-it® Greener Note and the Scotch® Magic™ Greener Tape based on plant derived adhesives (e.g. 2-Octyl acrylate).The introduction of IBOMA on PSA waterborne formulations to directly increase the binding strength between adhesive layer and adherent has also been reported[25]. However, there are no studies involving 2-Octyl acrylate together with isobornyl (meth)acrylate for the preparation of waterborne pressure sensitive adhesives.

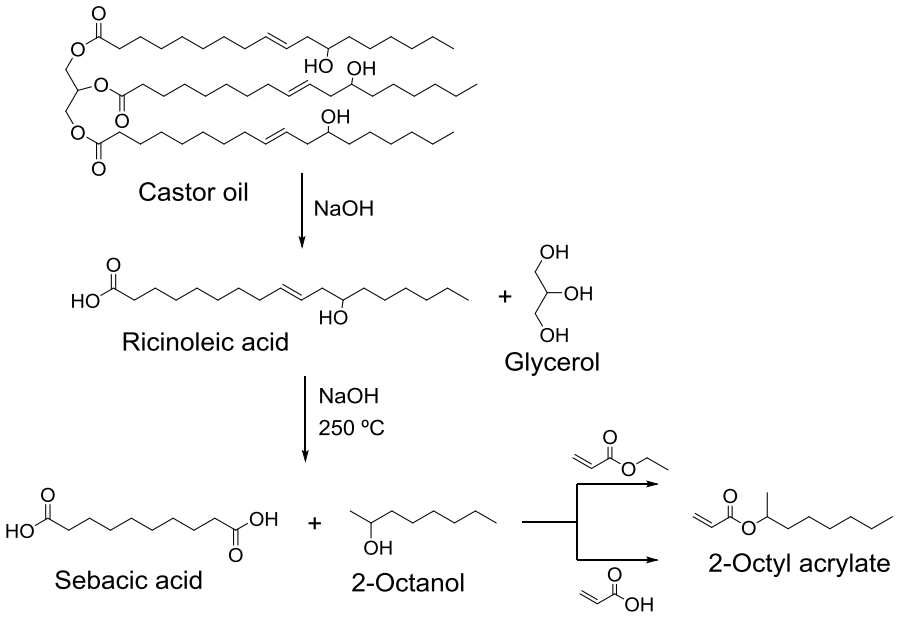

Figure 2.1. Conversion steps to produce 2-Octyl acrylate from castor oil.

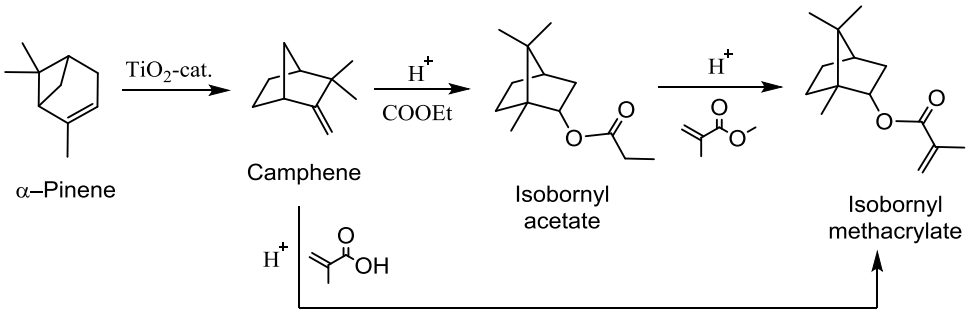

Figure 2.2. Conversion steps to produce isobornyl methacrylate from α-Pinene.

In this chapter, we explore the combination of these biobased monomers aiming to produce PSAs with high bio-content and interesting adhesive properties. Thus, latexes containing 2OA and IBOMA monomers (Scheme 2.1) were synthesized by seeded semibatch free radical emulsion polymerization and the adhesive properties were evaluated. The ratio soft/hard comonomer and the concentration of chain transfer agent (CTA) were tuned to achieve the best performance at the highest biobased content for the selected comonomer system. In addition, and with the aim of determining the proper balance between biobased content and adhesion performance, the effect of substituting partially the soft biobased monomer (2OA) by a typical soft oil-based monomer (2-Ethylhexyl acrylate) on the PSA properties was assessed.

Scheme 2.1. Commercial biobased monomers used in this chapter and their bio-content value, where the green part belongs to the carbon structure coming from the nature.

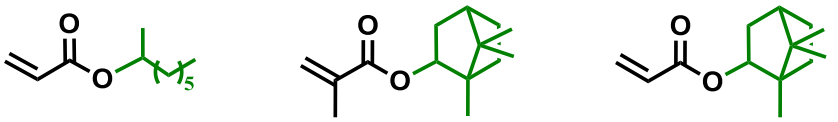

2-Octyl acrylate 2OA (73%) | **Isobornyl methacrylate IBOMA (71%)** | **Isobornyl acrylate IBOA (77%)**

2.2 Experimental

Biobased 2-Octyl acrylate (2OA) was kindly supplied by Arkema (France), and both isobornyl methacrylate (Visiomer® Terra IBOMA) and isobornyl acrylate (Visiomer® Terra IBOA) were kindly supplied by Evonik Industries (Essen, Germany). Acrylic and methacrylic acid (AA, MAA), 2-Ethylhexyl thioglycolate (2EHTG) and potassium persulfate (KPS) were purchased from Sigma-Aldrich (Saint-Louis, MO, USA). 2-Ethylhexyl acrylate (2EHA) was purchased from Quimidroga (Barcelona, Spain) and Dowfax2A1 (Alkyldiphenyloxide Disulfonate) was kindly supplied by Dow Chemical (Midland, Michigan, USA). All reagents were used without further purification.

2.2.1 Emulsion polymerization

50 wt% (weight percent) solids content acrylic latexes were synthesized by seeded semibatch emulsion polymerization. For the preparation of the seed, a coarse emulsion containing the monomers 2OA, IBOA and AA, in a relation of 88:10:2 (wt%) , emulsifier Dowfax 2A1 (2 wt% based on mononers) and deionized water (80 wt%) was created by stirring during 30 minutes at 1000 rpm at room temperature. The emulsion polymerization was carried out in a 2L glass reactor equipped with a reflux condenser, sampling device, nitrogen inlet, and a stainless steel anchor-type stirrer.

The seed was synthesized in batch. The coarse emulsion was transferred into the reactor, purged with nitrogen and heated to the reaction temperature (70ºC). Then, the initiator (KPS, 0.25 wt% based on monomers), previously dissolved in water, was added as a shot and the polymerization was carried out for 2 h at 200 rpm to obtain finally a latex with 20 % solids content and a particle size of 121 nm.

The synthesis of the desired latex was performed by seeded semibatch free radical emulsion polymerization. For that purpose, a fraction of the seed previously synthesized was charged, together with 1 wt% of monomers belonging the pre-emulsion, in a 250 mL glass reactor equipped with a reflux condenser, sampling device, nitrogen inlet, a dosing system, and a stainless steel anchor-type stirrer. This seed was purged with nitrogen and heated to the reaction temperature (70ºC). Then, an aqueous solution of KPS (0.25 wt% based on monomers) was added as a shot and a pre-emulsion containing the desired monomers, deionized water and Dowfax 2A1 (1 wt% based on monomers) was fed along 3 hours. Finally, a post-polymerization was carried out for 1 hour. The final solids content in all synthesized latexes was 50 wt% and the particle size was between 230 and 250 nm. Table 2.1 summarizes the formulations.

Table 2.1. Materials and percentages employed in the synthesis of the latexes.

Materials		**wbm %***	**Amount (g)**
Seed	2OA/IBOA/AA		24.10
Low Tg monomers	2OA 2EHA	10-88 20-74	4.64-40.82 9.28-34.32
High Tg monomer	IBOMA	5-15	2.32-6.96
Functional monomer	MAA	1	0.46
Chain transfer agent	2EHTG	0.025-0.1	0.0116-0.0464
Emulsifier	Dowfax2A1	1	1.031
Initiator	KPS	0.25	0.116
Continuous phase	Water		28.60

*weight % based on total monomer content

2.2.2 Characterization

Particle size was analyzed by dynamic light scattering (DLS) and capillary hydrodynamic fractionation (CHDF) and conversion was determined gravimetrically. For more detailed information refer to Appendix 1.

The gel fraction was measured by Soxhlet extraction, using THF as solvent. The extraction was carried out for 24 h under reflux conditions (about 70°C). The fraction of gel was calculated as the ratio between the non-extracted polymer and the initial amount of dry polymer.

The molar mass distribution of the soluble fraction in THF was determined by size exclusion chromatography (SEC) at 35°C. The samples taken out from the soxhlet were first dried, then redissolved in THF to achieve a concentration of about 0.005 g/mL and finally filtered (polyamide filter, pore size = 0.45 µm,) before injection into the SEC instrument The SEC instrument consisted of an autosampler (Waters 717 plus), a pump (LC-20, Shimadzu), three columns in series (Styragel HR2, HR4, and HR6 with a pore size from 10^2 to 10^6 Å), and a differential refractometer (Waters 2410) as detector. The flow rate of THF through the columns was 1 mL min^{-1}. The reported molar masses are referred to polystyrene standards.

The glass transition temperature (T_g) was determined by differential scanning calorimetry (DSC, Q1000, TA Instruments) of dry polymers from the final latexes using hermetic pans. The scanning cycles consisted of first cooling to -80 °C at 20 °C/min, and then heating to 150 °C at a rate of 20 °C/min, cooling again from 150 °C to -80 °C at 20 °C/min, and then heating to 150 °C at 20 °C/min under nitrogen flow.

2.2.3 Film preparation

The adhesive films were prepared by casting the latex over a flame-treated polyethylene terephthalate (PET) sheet (29 µm thick) using a gap applicator with reservoir. A gap of 30 µm was used in order to obtain films of approximately 15 µm thickness. For probe tack tests the latex films (final thickness of 100 µm to avoid the substrate effect) were directly casted on the glass plate. Films were dried at 23 °C and 50% humidity for 6h, protected from dust. For dynamic mechanical analysis, silicone templates (54cm x 26cm) were employed to form adhesive films of around 500 µm thickness (Films were dried for 7 days at the same drying conditions).

2.2.4 Evaluation as pressure sensitive adhesives

Tests were performed at 23ºC and 50% humidity. Four samples were tested for each formulation and the average values were reported. The peel, loop tack and probe tack tests were performed with a TA.HDPlus Texture Analyzer (Texture Technologies, Hamilton, MA, USA), whereas shear and SAFT test were carried out using SAFT equipment (Sneep Industries). Further information about both the tests and the conditions employed are referred in Appendix 1.

2.2.5 Dynamic Mechanical properties of PSAs

The linear viscoelastic properties of the adhesives were characterized with a rheometer Anton Paar using parallel plate geometry. Frequency sweeps (0.3-120 rad s^{-1}) with an applied strain between 0.5% and 2% were made on 500 µm thick samples of 8 mm as diameter at 23 ºC. The adhesive films were dried under controlled condition (23ºC and 55 % relative humidity).

2.3 Emulsion polymerization of commercial biobased monomers

Table 2.2 summarizes the latexes synthesized in this section as well as their main properties including gel content, the sol weight-average molar mass (Mw) and the intensity-average particle size (dp).

Table 2.2. Summary and characteristics of the synthesized PSA latexes.

PSA	Composition (%wt monomers)	dp (nm)	Gel (%)	Mw (kDa)	Đ	Tg (°C)	Bio (%)
2A	2OA:MAA (99:1)	232	81 ± 0.5	220 ± 15	3.5	-43	72
2B	2OA:IBOMA:MAA (94:5:1)	250	80 ± 0.2	220 ± 6	3.4	-39	72
2C	2OA:IBOMA:MAA (84:15:1)	245	75 ± 0.1	226 ± 4	3.4	-26	72
2B.1	2OA:IBOMA:MAA+CTA* (94:5:1 + 0.025*)	236	69 ± 0.4	250 ± 4	2.9	-39	72
2B.2	2OA:IBOMA:MAA+CTA* (94:5:1 + 0.05*)	237	52 ± 2	300 ± 1	3.5	-39	72
2B.3	2OA:IBOMA:MAA+CTA* (94:5:1 + 0.1*)	246	18 ± 0.5	320 ± 7	4.1	-40	72
2C.1	2OA:IBOMA:MAA + CTA* (84:15:1 + 0.025*)	230	59 ± 0.4	313 ± 4	3.7	-26	72
2C.2	2OA:IBOMA:MAA + CTA* (84:15:1 + 0.05*)	231	42 ± 2	375 ± 6	4.0	-26	72
2C.3	2OA:IBOMA:MAA + CTA* (84:15:1 + 0.1*)	242	19 ± 3	289 ± 9	4.0	-27	72

CTA*: Weight percent based on monomer.

In all polymerizations of this chapter, stable latexes without coagulum were obtained using relatively low surfactant concentrations. Due to the starved monomer feeding conditions used, in all reactions instantaneous conversion was higher than 90 % during the polymerization time and hence the instantaneous copolymer composition was very close to that used in the feeding stream producing homogeneous copolymer chains along the reaction and single phase particles. Full conversion was reached after a post-polymerization process of 1 hour. Figure 2.3 shows a representative evolution of both instantaneous and overall conversion as well as the particle size evolution. It can be observed that the

experimental particle size evolution followed in a properly way the theoretical one, which is indicative that secondary nucleation was not taken place.

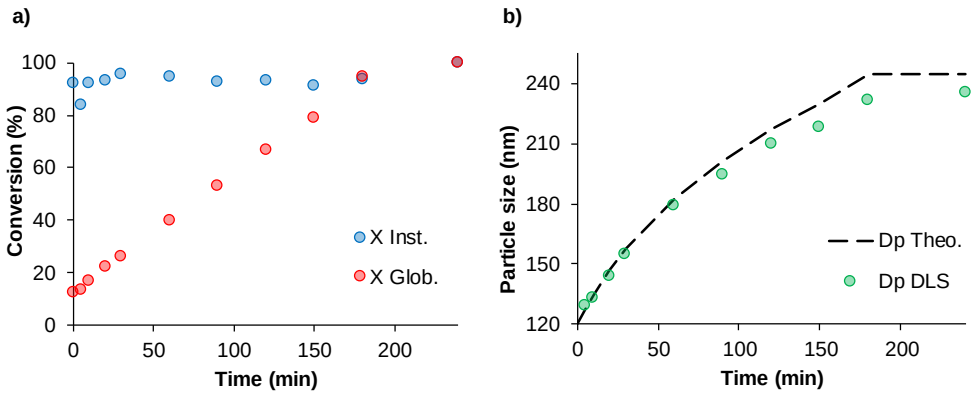

Figure 2.3. Representative evolution of (a) instantaneous and overall conversion, during the synthesis of latex **2D**, and (b) average particle size evolution measured by DLS together with the theoretical evolution.

This fact was corroborated by measuring the evolution of the particle size distribution along the reaction time. Figure 2.4 presents the CHDF chromatogram, confirming that secondary nucleation was not important. A small “tail” sited in the range of the seed particles size can be appreciated for the particle size distribution of the final latex. This small “tail” belongs to those few particles of the seed smaller than 100 nm, which have grown along the reaction.

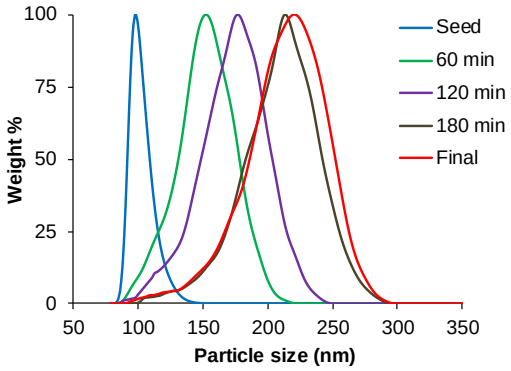

Figure 2.4. Evolution of particle size distribution along the reaction time measured by CHDF during the synthesis of latex **2D**.

2.4 Effect of the amount of isobornyl methacrylate (IBOMA)

The effect of the quantity of IBOMA, as hard monomer, on both microstructural and adhesion properties (formulations **2B** and **2C**) was compared with formulation **2A** used as reference. As expected, the incorporation of isobornyl methacrylate increased the glass transition temperature of the final polymer, reaching a value of -26 ºC for the formulation containing 15 wt% of IBOMA (**2C,** Table 2.2). The gel content was reduced when the IBOMA amount increased because of the significantly lower activity for hydrogen abstraction of the methacrylic units in the polymer chain[26]. In addition, IBOMA radicals terminate by disproportionation, which also reduces the probability of gel formation. On the other hand, similar sol molar masses were obtained.

The adhesive properties of formulations with different amounts of IBOMA are presented in Table 2.3. As it can be seen the presence of the hard monomer increased substantially the shear resistance and when 15% of this monomer was used the work of adhesion (WA, measured by the loop tack test) was also improved. Peel strength, loop tack as well as SAFT however were not much affected.

Table 2.3. Properties of PSA tapes with different amounts of IBOMA.

PSA	Composition 2OA:**IBOMA**:MAA	Peel (N/25mm)	Loop Tack (N/25mm)	WA (J/m^2)	Shear (min)	SAFT (°C)
2A	99:**0**:1	5.9 ± 0.3	4.8 ± 0.2	81 ± 3	8500	106 ± 10
2B	94:**5**:1	5.4 ± 0.2	4 ± 0.3	82 ± 12	>10080	90 ± 10
2C	84:**15**:1	6 ± 0.9	5 ± 0.5	107 ± 13	>10080	105 ± 8

Figure 2.5 shows probe tack measurements for those formulations. An increase of IBOMA (formulation **2C**: 2OA:**IBOMA**:MA (84:**15**:1)) leads to a longer and higher plateau in comparison with formulation **2B** (2OA:**IBOMA**:MA (94:**5**:1)) which exhibits a much more solid-like behaviour, which is related with a higher crosslinked polymer structure. The higher amount of IBOMA in formulation **2C** together with its slightly lower gel content makes the fibrils to be stiff enough and flexible as to detach under a greater strain; namely, the stress needed to deform fibrils is smaller than the adhesive force to the substrate. Nonetheless, all the curves present a very low adhesive energy likely because of the high amount of gel polymer content. It is worth mentioning that all PSA formulations exhibit adhesive failure, which is an indication of large cohesive forces.

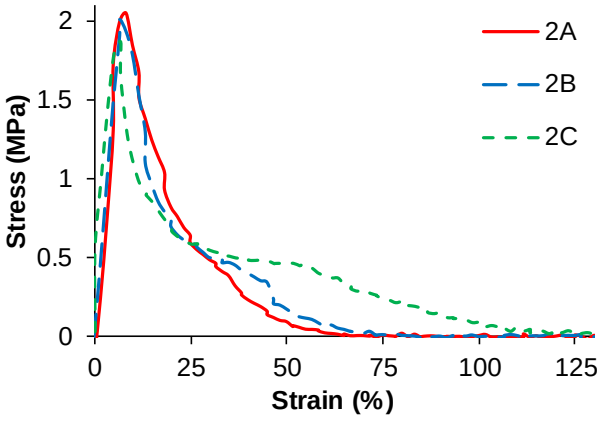

Figure 2.5. Probe tack curves for formulations containing different amounts of IBOMA.

2.5 Effect of the amount of 2-Ethylhexyl thioglycolate (2EHTG)

Chain transfer agents (CTAs) are widely employed in the adhesives field since they allow adjusting the crosslinking density of the polymer, and help controlling the sol molar mass providing good initial adhesion. These parameters allow modifying the strain hardening and control fibril extension and, therefore, the peel force. Thus, different amounts of 2-Ethylhexyl thioglycolate (2EHTG) as chain transfer agent were employed in both formulation **2B** (2OA:**IBOMA**:MAA (94:**5**:1)) and formulation **2C** (2OA:**IBOMA**:MAA (84:**15**:1)).

Figure 2.6.a shows that the higher the CTA the lower the gel content of the latex is for both series. As the amount of CTA increased, higher sol average molar masses for series **2B** were obtained (Figure 2.6.b). However, the sol molar mass evolved with a different trend for the series **2C**, reaching a maximum of 375 kDa with 0.05 wbm% of CTA. Indeed, the molar mass evolution is affected by two counteracting effects[27]. Small amounts of CTA are enough to substantially reduce the chain transfer to polymer and hence gel formation, leading to a decrease of the gel content and to an increase of the average molar mass. The effect on the decrease of the kinetic chain length is compensated by the polymer that is not transferred to gel (formulations **2C.1** and **2C.2**). At higher CTA concentrations the kinetic chain length decreases further and the average molar mass of the sol polymer decreases as well (formulation **2C.3**). The counteracting effects commented above are clearly illustrated in Figure 2.7, which shows the MMD of the latex synthesized with different amounts of CTA for the series **2C**. It is worth to point out that such phenomenon can also be appreciated for formulation **2B.3** since the highest amount of CTA resulted in a smaller increase of the sol molar mass in comparison with the tendency observed up to 0.05 wbm% CTA.

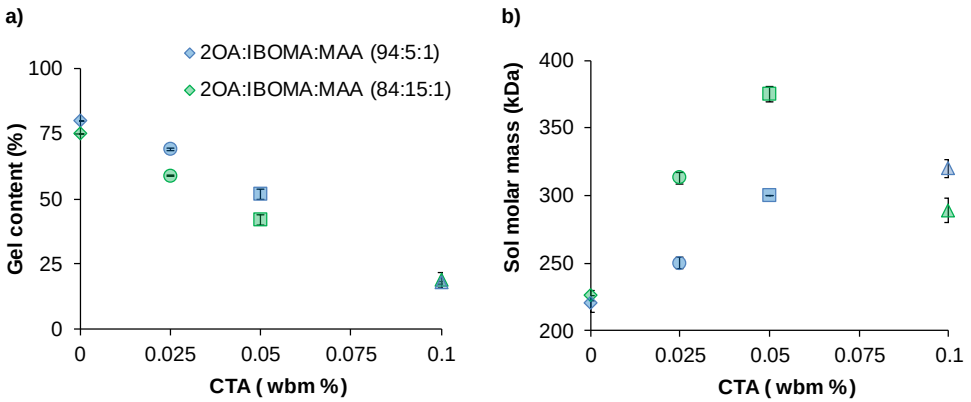

Figure 2.6. Evolution of (a) gel content and (b) sol molar mass with the amount of 2EHTG for series **2B** (2OA:IBOMA:MAA (94:5:1)) (blue marks) and **2C** (2OA:IBOMA:MAA (84:15:1)) (green marks).

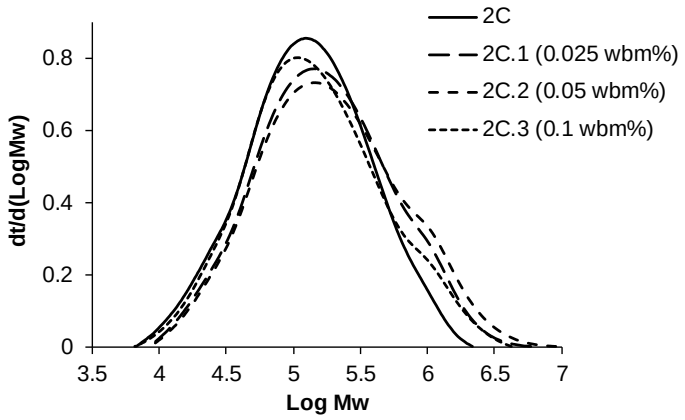

Figure 2.7. Evolution of sol molar mass distribution with the amount of 2EHTG for formulations containing 2OA:IBOMA:MAA (84:15:1). In the legend of the Figure, wbm% indicates the quantity of CTA.

2.5.1 Rheological investigations of waterborne PSAs containing 2-Ethylhexyl thioglycolate (2EHTG)

Dynamic rheological experiments are a useful tool for correlating the microstructure of an adhesive with its viscoelastic behaviour[28]. In view of this, linear viscoelasticity properties were determined aiming to gain insights about how 2EHTG affects to the adhesive nature. Figure 2.8 shows the variation with frequency of storage and loss modulus (G´ and G´´, respectively) and tanδ at 23 ºC for both series containing different amounts of CTA. It can be seen that there is a trend to decrease the storage modulus and to increase the loss modulus with the CTA content, indicating that the reduction on gel content decreases the stiffness of the PSA fibrils, namely the solid-like behaviour. Nonetheless, this tendency is not observed in the case of formulation **2C.2** because of the higher sol molar mass, which affects the viscoelastic behaviour. It is worth pointing out that series **2B** presented both lower G´ and G´´ values. This is due to the combination of a lower Tg together with a higher insoluble fraction (see Table 2.2), which influences the flowability of the polymer chains and, thereby, the viscoelastic nature of the adhesive.

According to Dahlquist criterion, high tack is achieved when G´ is smaller than 0.1 MPa meaning that a certain softness of the adhesive is needed in order to form a good contact in a short contact time[29]. The debonding process is then governed by the coupling of bulk and interfacial properties of the material. Regarding this criterion, at the relevant debonding frequency (1 Hz) all the formulations present lower values than 0.1 MPa being appropriate for their application as pressure sensitive adhesives with remarkable work of adhesion values in the tack experiments.

On the other hand, the ratio tanδ/G´ is related to the energy dissipation at the interface of adhesive-substrate, meaning that the resistance to detachment increases as the viscous

modulus to elastic modulus ratio increases. A value of tanδ/G´ > 5 MPa^{-1} has been recommended for steel substrates[30].

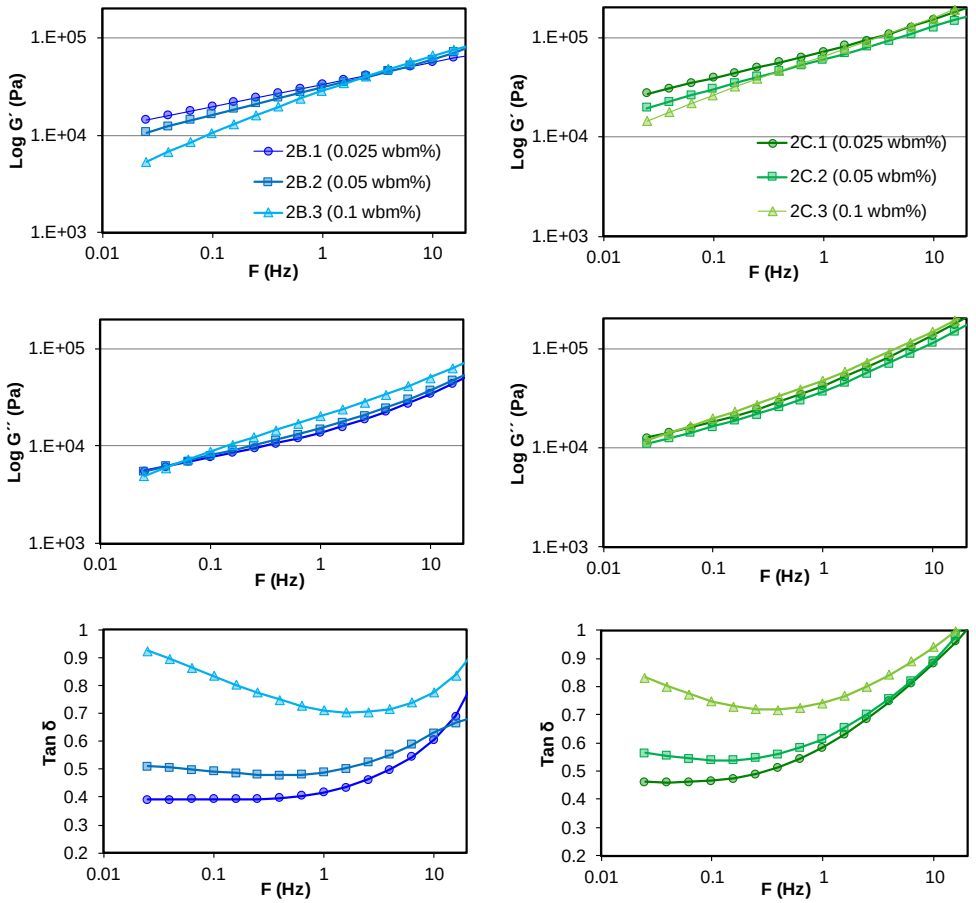

Figure 2.8. Storage modulus (G´), loss modulus (G´´) and dynamic modulus (Tanδ) for series **2B** (2OA:IBOMA:MAA (94:5:1)) (blue marks) and **2C** (2OA:IBOMA:MAA (84:15:1)) (green marks) with different amount of CTA. Measurements made at 23 ºC and 1 Hz.

Figure 2.9 presents the effect of the CTA content on tanδ/G´ for the formulations described in this section. It can be seen that the ratio increased with CTA content (the adhesive became less stiff) because of the lower elastic contribution. This increase was

more accused in the case of formulation **2B.3** because of its higher liquid-like behaviour, which is related with the low gel content together with the low Tg. However, all the formulations containing any amount of CTA presented a value of tanδ/G´ > 5 MPa^{-1} accompanied by adhesive failure, being suitable for their application as removable pressure sensitive adhesives.

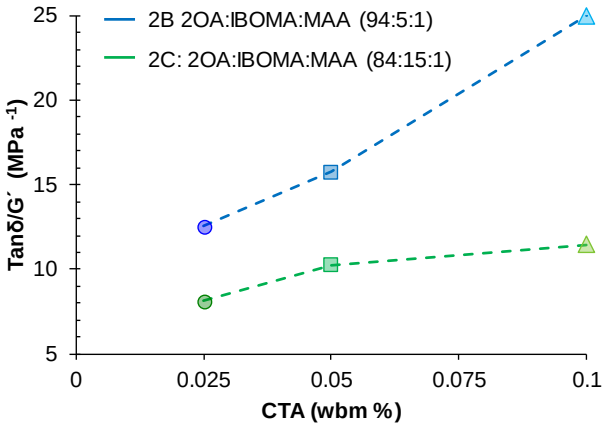

Figure 2.9. Tanδ/G´ for series **2B** (2OA:IBOMA:MAA (94:5:1)) (blue marks) and **2C** (2OA:IBOMA:MAA (84:15:1)) (green marks) with different amount of CTA. Measurements made at 23 ºC and 1 Hz.

2.5.2 Adhesive properties of waterborne PSAs containing 2-Ethylhexyl thioglycolate (2EHTG)

The adhesive properties of the latexes synthesized using different amounts of 2-Ethylhexyl thioglycolate in the formulation are plotted in Figure 2.10 as a function of the gel content.

As it can be observed, for both series, an increase in the CTA amount led to the reduction of the shear resistance since lower gel content and, thus, lower cohesive forces were obtained. This is because high shear resistance requires a solid-like response (high

creep resistance) which decreases with the increase of the chain mobility. In addition, tackiness and work of adhesion increased because of the increase of the polymer fluidity that led to an improvement of the dissipation energy during deformation, which is the response of the highly viscous liquid behavior of the adhesive. However, in series **2C**, similar results of loop tack and work of adhesion are observed in formulations in which 0.025 and 0.05 wbm% of CTA have been employed (formulations **2C.1** and **2C.2** respectively) because of the still high intermolecular forces and low chain mobility for the initial adhesion, which is more pronounced for high molar masses. This situation is completely different for series **2B** since there was a remarkable change in the mobility of the polymer chains when 0.05 wbm% of CTA was used (formulation **2B.2**), increasing loop tack value in 1.5 N/25 mm and work of adhesion in almost 40 J/m^2. The use of 0.025 wbm% of CTA in this series (formulation **2B.1**) did not produce the same substantial improvement of loop tack and work of adhesion than in formulation **2C.1** due to the greater molecular motion restrictions, namely the higher insoluble fraction.

Peel strength increases with decreasing gel contents, which could be attributed to the good relationship between the critical energy-release rate (which is the energy needed to propagate the crack between the adhesive and the substrate) and the Young´s modulus of the adhesive. Even with 0.1 wbm% of CTA (**2C.3**), adhesive failure was observed; a good indication that intermolecular forces are strong enough to allow the adhesive failure which is the one desired for the industrial application. Although formulation **2B.3** showed both the same failure and gel content, the lower Tg reduced the elastic component, not observing such good enhancement of the peel strength. Similar effects of the gel content have been reported in the literature for other waterborne PSAs[26,27,31,32].

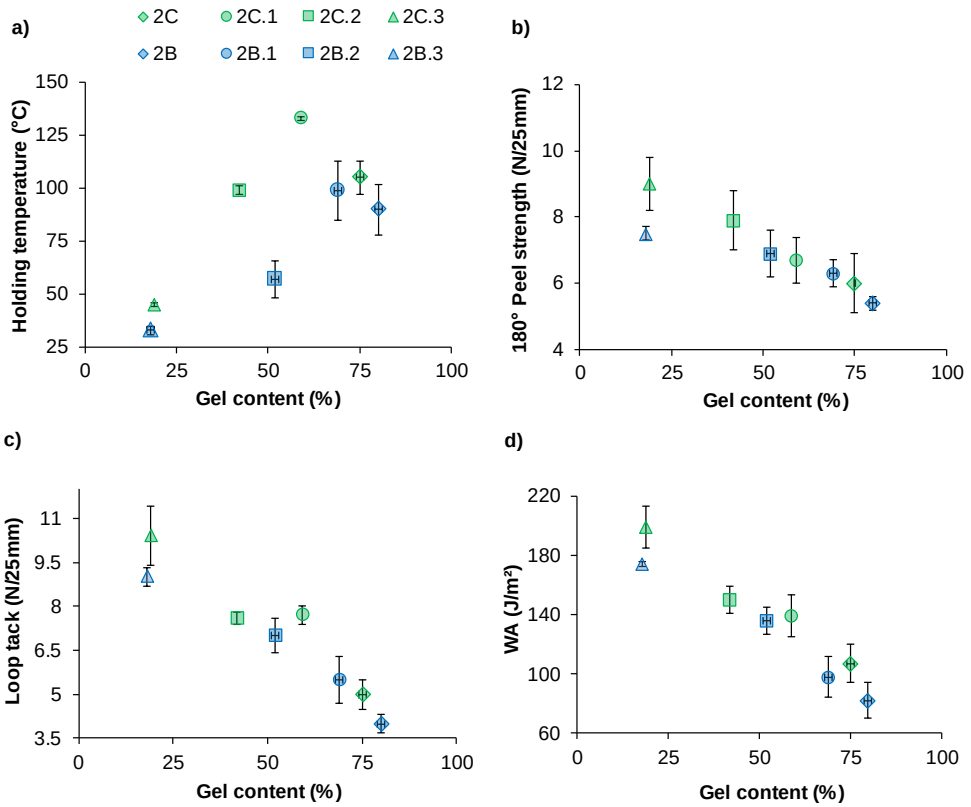

Figure 2.10. Effect of CTA percentage on the (a) SAFT tests, (b) peel strength, (c) loop tack, and (d) work of adhesion for series **2B** (2OA:IBOMA:MAA (94:5:1)) (blue marks) and **2C** (2OA:IBOMA:MAA (84:15:1)) (green marks). Note that the notation 2X.1, 2X.2 and 2X.3 make reference to 0.025, 0.05 and 0.1 wbm% of CTA respectively.

Figure 2.11 shows probe tack curves of these two series. It is worth pointing out that as gel content was reduced, a decrease of the stress at relatively low strain followed by low values of the stress until higher strain was observed. This behavior corresponds to liquid-like materials where fibrils are formed[33,34]. Formulation **2C.1** presents the highest stress value in these series. The addition of higher amounts of CTA led to weaker adhesives. This trend is more pronounced in the case of series **2B** due to the lower amount of IBOMA in the

composition, which allows better mobility of the polymer chains. Therefore, the cohesion of the fibrils was lower and both lower and longer plateaus were obtained. Note that formulation **2B.1** did not show the formation of a fibrillation plateau as consequence of the high solid-like behaviour, yielding in brittle fibrils and affecting to the initial adhesion as well. On the other hand, formulation **2B.3** showed a long and narrow fibrillation plateau as consequence of the higher liquid-like behaviour. These results are in agreement with the rheological investigations discussed above.

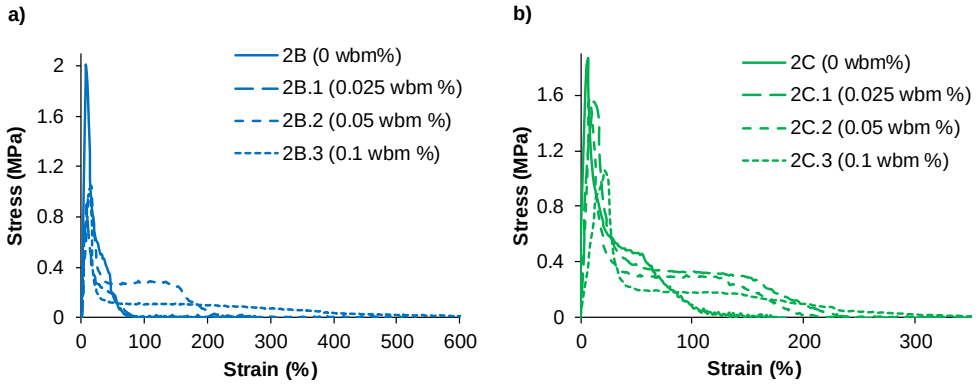

Figure 2.11. Effect of the CTA percentage on the probe tack test for series **2B** (2OA:IBOMA:MAA (94:5:1)) (blue) and **2C** (2OA:IBOMA:MAA (84:15:1)) (green).

2.6 Effect of the amount of 2-Ethylhexyl acrylate (2EHA)

In this section, PSAs with lower biobased monomer contents were investigated and their performance compared with the waterborne PSA with the highest content of biobased monomer (latex **2C.1**) that showed the best-balanced adhesive properties. The reduction of the biobased content was achieved by replacing on formulation **2C.1** fractions of the soft monomer, 2OA, by a conventional oil-based soft monomer widely used on PSA formulations like 2-Ethylhexyl acrylate (isomer of 2-Octyl acrylate). Three levels of biobased content waterborne latexes were produced as shown in Table 2.4, by using 20, 49 and 74 wbm% of

2EHA in the formulation. Moreover, data from a typical non-biobased commercial formulation containing 2EHA, MMA and AA (84:15:1) are included in order to compare its adhesion properties with the biobased content formulations[35]. The addition of 2EHA reduced the glass transition temperature because of the lower Tg of poly2EHA (Tg = -65 ºC). The microstructure of the latexes with increasing amounts of 2EHA is similar; gel contents and average molar masses are in the range of 50-60wt% and 300-390 kDa, respectively. The pure oil-based latex (100% of soft monomer being 2EHA) presents similar gel content (52%), but lower average molar mass (172 kDa).

Table 2.4. Summary and characteristics of the synthesized PSA latexes containing different 2EHA contents.

PSA	Composition	dp (nm)	Gel (%)	Mw (kDa)	Đ	Tg (ºC)	Bio (%)
	2OA:2EHA: IBOMA:MAA*						
2C.1	84:**0**:15:1	230	59 ± 0.4	313 ± 4	3.7	-26	72
2D	64:**20**:15:1	242	50 ± 1	387 ± 3	3.9	-32	60
2E	35:**49**:15:1	236	60 ± 0.5	298 ± 2	3.7	-37	40
2F	10:**74**:15:1	233	60 ± 1	303 ± 2	3.8	-43	25
	2EHA:MMA:AA						
2Ref**	84:15:1	294	52 ± 0.1	178	3.1	-49	0

* makes reference to 0.025 wbm% of 2EHTG.

Ref**: non-biobased formulation. From ref.[35]

2.6.1 Adhesive properties of waterborne PSAs containing 2-Ethylhexyl acrylate (2EHA)

As shown in Table 2.5, partially replacing 2OA by 2EHA provided similar or poorer adhesion properties when it was incorporated in a 20 wt% and 49 wt% (formulation **2D** and **2E** respectively), with a reduction of the holding temperature due to the lower Tg. Only when 74 wt% of 2OA was replaced by 2EHA (formulation **2F**) both loop tack and work of adhesion values improved. This improvement is closely related with a decrease in the glass transition

temperature and a better chain mobility. However, in the case of formulation **2Ref**, lower loop tack and shear strength (SAFT and shear resistance) values were obtained. This is likely related with the smaller molar mass of latex **2Ref** and the higher cohesion provided by the bulky IBOMA monomer as compared with MMA[25].

Table 2.5. Properties of PSAs containing different 2EHA contents.

PSA	Composition	Peel (N/25mm)	Loop tack (N/25mm)	WA (J/m^2)	Shear resistance (min)	SAFT (°C)
	2OA:2EHA: IBOMA:MAA*					
2C.1	84:**0**:15:1	6.7 ± 0.7	7.7 ± 0.3	139 ± 14	9000	133 ± 1
2D	64:**20**:15:1	6.9 ± 0.5	6.5 ± 0.2	132 ± 3	8750	110± 3
2E	35:**49**:15:1	6.5 ± 0.3	6 ± 0.2	101 ± 5	>10080	117 ± 1
2F	10:**74**:15:1	6.5 ± 0.5	8.5 ± 0.5	164 ± 15	>10080	116 ± 1
	2EHA:MMA:AA					
2Ref**	84:15:1	7.1 ± 0.3	4.2 ± 0.2	115 ± 15	200	70± 2

* makes reference to 0.025 wbm% of 2EHTG.

Ref**: non-biobased formulation. From ref.[35]

Probe tack curves, in Figure 2.12 (left), show that the addition of this oil-based monomer led, in a general way, to a decrease of the stress peak at low strain values and to longer fibrillation plateaus. This trend is in good agreement with the rheological measurements (Figure 2.12 right), since higher tanδ/G´ values but longer plateaus in comparison with formulation **2C.1** are observed for increasing amounts of 2EHA. This indicates that the detachment is produced during the fibril elongation process. It is important to note that both storage modulus and loss modulus were highly reduced when the quantity of 2EHA was above 49 wt% due to the reduction of the glass transition temperature at similar gel content and sol molar masses. Formulation **2F**, which is the one that contains the highest amount of 2EHA, presented the best probe tack curve breaking their fibrils at 350% of strain

with the same stress values than formulation **2C.1** and without leaving adhesive residue in the substrate. This implies that liquid-like behaviour was improved by the increase in chain mobility without any change in the intermolecular forces. Nonetheless, the maximum holding temperature of this PSA is circa 20ºC lower than formulation **2C.1**. Finally, if we compare these results with those obtained from a typical oil-based commercial formulation (formulation **2Ref**) a substantial decrease of the stress peak at low strain values followed by a longer fibrillation plateau at lower stress is observed, because of the low glass transition temperature (-49 ºC) together with the gel content (52%) that led to a better fluidity of the polymer chains. However, these fibrils did not present cohesion forces as strong as those adhesives containing IBOMA in their formulation, translating into a decrease in the stiffness of the fibrils and, hence, a lower plateau.

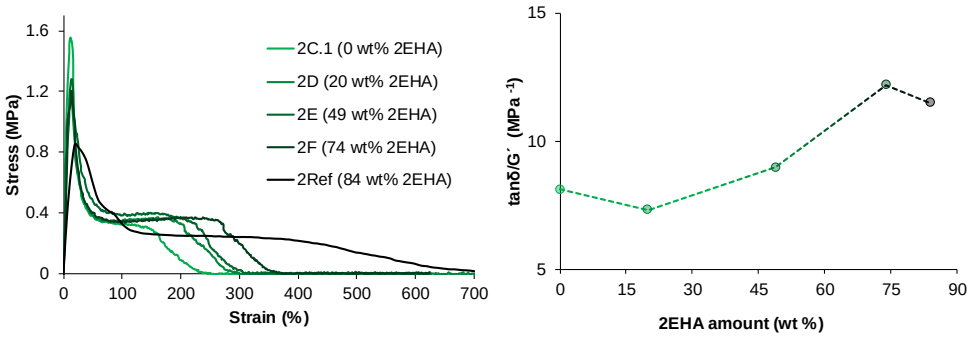

Figure 2.12. The effect of 2EHA percentage on the probe tack tests (left) and tanδ/G´ (right) for 2OA:IBOMA:MAA + CTA (84:15:1 + 0.025 wbm %) formulation and its comparison with a typical commercial formulation 2EHA:MMA:AA (84:15:1). Measurements carried out at 23 ºC and 1 Hz.

2.7 Conclusions

In this chapter, the incorporation of monomers with high biobased content like 2-Octyl acrylate (2OA, 73%) and isobornyl methacrylate (IBOMA, 71%), via emulsion polymerization, to produce high bio-content waterborne pressure sensitive adhesives was

assessed and their adhesive performance compared to traditional oil-based counterpart. The direct substitution of the oil-based monomers by the equivalent biobased monomers did not provide the same performance, namely because of the different microstructure. Thus, it was necessary to optimize the formulation of the new high biobased content waterborne PSAs to achieve a microstructure that yield similar adhesive performances. This was done by fine tuning the amount of the hard bio-based monomer, IBOMA, and the chain transfer agent. It was found that a formulation containing 15 wt% of IBOMA and gel content around 60% yielded the copolymer microstructure with similar peel resistance and loop tack, substantially better SAFT (135ºC vs 70ºC) and 45 times higher shear strength than the pure oil-based adhesive. Finally, the reduction of the bio-content as well as the glass transition temperature by the incorporation of different amounts of 2EHA provided PSAs with better liquid-like behavior, but keeping the rigidity of the adhesive fibrils because of the presence of IBOMA.

2.8 References

(1) Mordor Intelligence. *Vegetable Oil Market - Growth, Trends and Forecasts (2020 - 2025)*; 2019.

(2) Gandini, A.; Lacerda, T. M.; Carvalho, A. J. F.; Trovatti, E. Progress of Polymers from Renewable Resources : Furans , Vegetable Oils , and Polysaccharides. *Chem. Rev.* **2016**, *116*, 1637–1669.

(3) Sharmin, E.; Zafar, F.; Akram, D.; Alam, M.; Ahmad, S. Recent Advances in Vegetable Oils Based Environment Friendly Coatings : A Review. *Ind. Crop. Prod.* **2015**, *76*, 215–229.

(4) Corma, A.; Iborra, S.; Velty, A. Chemical Routes for the Transformation of Biomass into Chemicals. *Chem. Rev.* **2007**, *107*, 2411–2502.

(5) Tracy, N. I.; Chen, D.; Crunkleton, D. W.; Price, G. L. Hydrogenated Monoterpenes as Diesel Fuel Additives. *Fuel* **2009**, *88*, 2238–2240.

(6) Gershenzon, J.; Dudareva, N. The Function of Terpene Natural Products in the Natural World. *Nat. Chem. Biol.* **2007**, *3*, 408–414.

(7) 360 Research Reports. *Terpenes Market 2019 - Globally Market Size, Analysis, Share, Research, Business Growth and Forecast to 2024*; 2019.

(8) Wilbon, P. A.; Chu, F.; Tang, C. Progress in Renewable Polymers from Natural Terpenes, Terpenoids, and Rosin. *Macromol. Rapid Commun.* **2013**, *34*, 8–37.

(9) Winnacker, M.; Rieger, B. Recent Progress in Sustainable Polymers Obtained from Cyclic Terpenes : Synthesis, Properties, and Application Potential. *ChemSusChem* **2015**, *8*, 2455–2471.

(10) Sainz, M. F.; Souto, J. A.; Regentova, D.; Johansson, M. K. G.; Timhagen, S. T.; Irvine, D. J.; Buijsen, P.; Koning, C. E.; Stockman, R. A.; Howdle, S. M. Polymer Chemistry Acrylate and Methacrylate Monomers and Simple Free Tadical Polymerisation to Yield New Renewable Polymers and Coatings. *Polym. Chem.* **2016**, *7*, 2882–2887.

(11) Baek, S.; Jang, S.; Hwang, S. Construction and Adhesion Performance of Biomass Tetrahydro-Geraniol-Based Sustainable/Transparent Pressure Sensitive Adhesives. *J. Ind. Eng. Chem.* **2017**, *53*, 429–434.

(12) Li, W. S. J.; Negrell, C.; Ladmiral, V.; Lai-Kee-Him, J.; Bron, P.; Lacroix-desmazes, P.; Joly-Duhamel, C.; Caillol, S. Cardanol-Based Polymer Latex by Radical Aqueous Miniemulsion Polymerization. *Polym. Chem.* **2018**, *9*, 2468–2477.

(13) Colby, J. L.; Clem, T. A.; Spawn, T. D.; Hutt, A. E.; Teply, W. T. Selective Synthesis

of 2-Octyl Acrylate by Acid Catalyzed Esterification of 2-Octanol and Acrylic Acid . WO. Patent 2014/149669 A1, 2014.

(14) Riondel, A.; Graire, C.; Esch, M.; Linemann, R. Method for the Production of 2-Octyl Acrylate by Means of Transesterification. U.S. Patent 9018410B2, 2015.

(15) Colby, J. L.; Clem, T. A.; Spawn, T. D.; Hutt, A. E.; Teply, W. T. Selective Synthesis of 2-Octyl Acrylate by Acid Catalized Esterification of 2-Octanol and Acrylic Acid. U.S. Patent 9604902 B2, 2017.

(16) Knebel, J.; Saal, D. Method for the Synthesis and Process Inhibition of Isobornyl (Meth)Acrylate. U.S. 6479696B1, 2002.

(17) Knebel, J.; Saal, D. Process for the Synthesis of Isobornyl (Meth)Acrylate. U.S. Patent 6329543, 2001.

(18) Mubofu, E. B. Castor Oil as a Potential Renewable Resource for the Production of Functional Materials. *Sustain. Chem. Process.* **2016**, 1–12.

(19) Wisser, T.; Riedel, A.; Gscheidmeier, M.; Maginot, J. Process for the Preparation of Camphene by Isomerisation of Alpha-Pinene. EP. Patent 0539990, 1997.

(20) Anderson, K. S.; Lewandowski, K. M.; Fansler, D. D.; Gaddam, B. D.; Joseph, E. G. 2-Octyl (Meth)Acrylate Adhesive Composition. U.S. Patent 7385020 B2, 2008.

(21) Anderson, K. S.; Lewandowski, K. M.; Fansler, D.; Gaddam, B. D.; Joseph, E. G. 2-Octyl (Meth)Acrylate Adhesive Composition. U.S. 7893179 B2, 2011.

(22) Airlin L, W.; Seth, J.; Kavanagh, M. A.; Hardy, C. M.; Frank, J. W.; Tseng, C.-M. 2-Octyl (Meth)Acrylate Adhesive Composition. U.S. Patent 2012/0329898 A1, 2012.

(23) Hardy, C. M.; Frank, J. W.; Tseng, C.-M. 2-Octyl (Meth)Acrylate Adhesive

Composition. U.S. Patent 2010/0151241 A1, 2010.

(24) Kong, S.; Application, F.; Data, P. Microsphere Pressure Senstive Adhesive Composition. U.S. Patent 8318303 B2, 2011.

(25) Zhang, L.; Cao, Y.; Wang, L.; Shao, L.; Bai, Y. Polyacrylate Emulsion Containing IBOMA for Removable Pressure Sensitive Adhesives. *J. Appl. Polym. Sci.* **2016**, *133*, 1–7.

(26) Asua, M.; Degrandi-contraires, E.; Lopez, A.; Reyes, Y.; Creton, C. High-Shear-Strength Waterborne Polyurethane / Acrylic Soft Adhesives. *Macromol. Mater. Eng.* **2013**, *298*, 612–623.

(27) Plessis, C.; Arzamendi, G.; Leiza, J. R.; Alberdi, J. M.; Schoonbrood, H. A. S.; Charmot, D.; Asua, J. M. Seeded Semibatch Emulsion Polymerization of Butyl Acrylate: Effect of the Chain-Transfer Agent on the Kinetics and Structural Properties. *J. Polym. Sci. Part A Polym. Chem.* **2001**, *39* (7), 1106–1119.

(28) Benedek, I. *Pressure-Sensitive Adhesives and Applications - Second Edition , Revised and Expanded*; CRC Press, Ed.; Marcel Dekker: New York, 2004.

(29) Dahlquist, C. A. Pressure-Sensitive Adhesives. In *Treatise on Adhesion and Adhesives*; Dekker, New York, 1969; Vol. 2, pp 219–260.

(30) Deplace, F.; Carelli, C.; Mariot, S.; Retsos, H.; Chateauminois, A.; Ouzineb, K.; Creton, C. Fine Tuning the Adhesive Properties of a Soft Nanostructured Adhesive with Rheological Measurements. *J. Adhes.* **2009**, *85* (1), 18–54.

(31) Alarcia, F.; de la Cal, J. C.; Asua, J. M. Continuous Production of Specialty Waterborne Adhesives: Tuning the Adhesive Performance. *Chem. Eng. J.* **2006**, *122* (3), 117–126.

(32) Chauvet, J.; Asua, J. M.; Leiza, J. R. Independent Control of Sol Molar Mass and Gel Content in Acrylate Polymer/Latexes. *Polymer (Guildf).* **2005**, *46* (23), 9555–9561.

(33) Creton, C. Pressure-Sensitive Adhesives: An Introductory Course. *MRS Bull.* **2003**, *28* (6), 434–439.

(34) Zosel, A. The Effect of Fibrilation on the Tack of Pressure Sensitive Adhesives. *Int. J. Adhes. Adhes.* **1998**, *18* (4), 265–271.

(35) Mehravar, E.; Gross, M. A.; Agirre, A.; Reck, B.; Leiza, J. R.; Asua, J. M. Importance of Film Morphology on the Performance of Thermo-Responsive Waterborne Pressure Sensitive Adhesives. *Eur. Polym. J.* **2018**, *98*, 63–71.

Chapter 3

UV-tunable biobased waterborne PSAs containing piperonyl methacrylate

3.1 Introduction

In chapter 2 the incorporation of the commercial biobased monomers 2-Octyl acrylate and isobornyl (meth)acrylate, by emulsion polymerization, to produce waterborne PSAs with high bio-content was reported. The PSA formulation was optimized by fine-tuning the comonomer ratio and the concentration of chain transfer agent in order to achieve the best performance at 72% of bio-content. However, aiming to obtain a more similar fibrillation behavior to the petroleum-based formulation, it was necessary to use 2-Ethylhexyl acrylate for reducing the Tg. In other words, the partial reduction of the bio-content was "the necessary evil" to provide an adhesive formulation capable to compete with those ones coming from petroleum resource.

Aiming to solve the conflict between the bio-content degree and the final performance required for adhesive applications, monomers coming from renewable sources but having dual functionality are needed. In this context, benzodioxole derivatives have attracted the attention during the last years in UV-light mediated radical polymerization. Since dioxole-like structures have the ability to act as hydrogen donors, they have the potential to be functional building blocks for adhesive resins manufacturing[1–3]. One of the most abundant benzodioxole structure in the nature is piperonal. Piperonal also known as heliotropin is an aromatic aldehyde, present in fragrances and flavors, which can be obtained naturally by the oxidation of piperine, the major alkaloid present in black pepper (up to 9%)[4,5]. Traditionally, piperonal has been produced in large scale by isomerization and subsequent oxidation of safrole, which is the main constituent of sassafras oil (70-80%, *Ocotea tree*)[6–9]. The average annual production during the 2007-2012 period amounted to 1759 tons of piperonal and its reduction to yield piperonyl alcohol can be easily performed by the use of sodium borohydride, metal catalysts or even reductase enzymes[10–14]. In addition, primary alcohol offers a wide range of possibilities for its functionalization towards suitable monomers for

emulsion polymerization. Scheme 3.1 shows the most relevant synthetic pathways to produce piperonal and, hence, piperonyl alcohol from natural sources.

Scheme 3.1. Synthetic pathways to produce piperonal and piperonyl alcohol from natural sources.

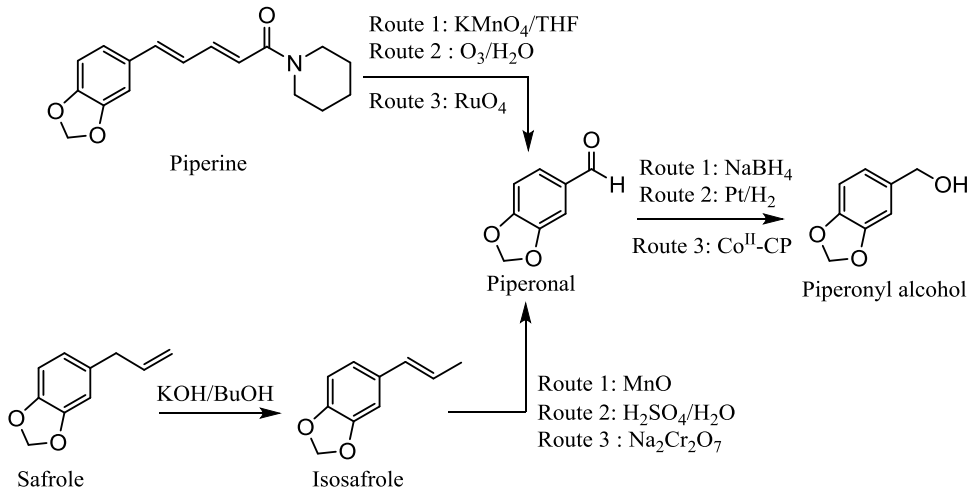

Therefore, the present chapter will be centered in the development of waterborne PSAs having the capability to be tuned under UV-light exposition. For this purpose, piperonyl methacrylate (PIPEMA) in which the piperonyl moiety comes from piperonal was synthesized. Consequently, its incorporation as hard monomer on the biobased PSA formulation was analyzed and compared in terms of polymer microstructure and adhesion properties. Finally, post-curing by UV-light was evaluated by measuring crosslinking evolution at different irradiation times and those tunable features were correlated with adhesion performance of PSAs.

3.2 Experimental

Biobased 2-Octyl acrylate (2OA) was kindly supplied by Arkema (France), and both isobornyl methacrylate (Visiomer® Terra IBOMA) and isobornyl acrylate (Visiomer® Terra IBOA) were kindly supplied by Evonik Industries (Essen, Germany). Acrylic and methacrylic acid (AA, MAA), 2-Ethylhexyl thioglycolate (2EHTG) and potassium persulfate (KPS) were purchased from Sigma-Aldrich (Saint-Louis, MO, USA). 2,2′-Azobis(2-methylpropionitrile) (AIBN, initiator), methacrylic anhydride (MAAn, 94% inhibitor 2000 ppm of topanol A), 4-(Dimethylamino)pyridine (DMAP, 99%), magnesium sulfate ($MgSO_4$) and sodium bicarbonate ($NaHCO_3$) were purchased from Sigma-Aldrich (Saint-Louis, MO, USA). Piperonyl alcohol (98%), toluene and dichloromethane (99+%) were purchased from Fisher Scientific. Dowfax2A1 (Alkyldiphenyloxide Disulfonate) was kindly supplied by Dow Chemical (Midland, Michigan, USA). All reagents were used without further purification.

3.2.1 Synthesis of pyperonyl methacrylate (PIPEMA)

Piperonyl alcohol (30 g, 0.197 mol) and DMAP (2.4g, 0.02 mol) were dissolved in 250 mL of dichloromethane in a 500 mL round bottom flask equipped with stirrer and dropping funnel. The mixture was stirred at room temperature at a rate of 500 rpm for 20 min. Then it was cooled down to 0ºC (ice-bath) and MAAn (36.3 g, 0.236 mol) was added dropwise for 1 hour. The mixture was stirred overnight. The yellowish solution was quenched with $NaHCO_3$ solution (1M, 100 mL) and then extracted with $NaHCO_3$ solution (1M, 2 x 50 mL), distilled water (3 x 50 mL) and washed with brine (3 x 50 mL). The combined organic layers were dried over $MgSO_4$, filtered and evaporated under reduced pressure yielding a yellowish oil. The product was further purified by column chromatography (SiO_2) using as eluent hexane/ethyl acetate (8:2 v/v) and yielded a colorless product. The yield for the isolated product was 89%.

3.2.2 Solution homopolymerization of piperonyl methacrylate (PIPEMA)

(Poly)piperonyl methacrylate (PolyPIPEMA) was obtained by solution polymerization for the purposes of determining the Tg of the homopolymer. For its preparation 1g of monomer was dissolved in 4g of toluene in a 25 mL volume round bottom flask equipped with a magnetic bar. The reaction was carried out at 70ºC along 5 hours under nitrogen atmosphere using AIBN (1 wbm %) as initiator. PolyPIPEMA was obtained by solvent removing under vacuum, yielding a white solid.

3.2.3 Emulsion polymerization

All the latexes were produced via starved-feed seeded semibatch emulsion polymerization using the same procedure than in chapter 2. The polymerization process included the loading of the seed and a small amount of monomers in the reactor, feeding of a pre-emulsion of monomer during 3 h and a final post-polymerization step of 1 h to fully react the remaining monomers. Reactions were performed at 70ºC and 200 rpm, being 50 wt% the final solids content. The general polymerization formulation is shown in Table 3.1.

Table 3.1. Materials and percentages employed in the synthesis of the latexes.

Materials		wbm %*	Amount (g)
Seed	2OA/IBOA/AA		24.10
Low Tg monomers	2OA	84-94	38.93-43.60
High Tg monomer	IBOMA PIPEMA	5-15	2.32-6.96
Functional monomer	MAA	1	0.46
Chain transfer agent	2EHTG	0.025	0.0116
Emulsifier	Dowfax2A1	1	1.031
Initiator	KPS	0.25	0.116
Continuous phase	Water		28.60

*weight % based on total monomer content

3.2.4 Characterization

Particle size was analyzed by dynamic light scattering (DLS) and conversion was determined gravimetrically. Gel fraction (or insoluble fraction of the copolymer in THF) was measured by Soxhlet extraction

The molar mass distribution of the polymer dispersion was determined by asymmetric flow field-flow-fractionation (AF4) (Eclipse 3) in combination with a multiangle light scattering (MALS, Dawn Heleos II) and a refractive index detector (RI, Optilab Rex). AF4 flow was controlled by Eclipse 3 AF4 Separation System controller (the whole setup from Wyatt Technology). A constant detector-flow (DF) of 1 mL/min was used. The cross-flow (XF) was linearly decreased from 3 mL/min to 0.05 mL/min during 15 min and, then, was kept constant at 0.05 mL/min for 40 min. Swelling was calculated from the weight average of the high molar mass peak and the z-average radius of gyration.

The glass transition temperature (T_g) was determined by differential scanning calorimetry (DSC, Q1000, TA Instruments) using the same conditions than in chapter 2.

The UV-vis absorption measurements were performed using a Shimadzu spectrophotometer (model UV-2550, 230V) at a wavelength ranging from 200 nm to 500 nm. Measurements were carried out in 1 cm cuvette at 25 ºC, background absorption was subtracted with deionized water and hexane.

The film preparation, the evaluation as PSA and the dynamic mechanical analysis (DMA) were performed using the same conditions and procedures than in chapter 2.

UV-light curing of the PSA films was performed by a UV-light source (Compact 4-Watt UV Lamp, 6W tube lamp of shortwave 254 nm) at room temperature in a dark chamber with a distance of 10 cm between the irradiation source and the film.

Liquid-state Proton Nuclear Magnetic Resonance (^{1}H NMR) was recorded on a Bruker 400 MHz equipment. Relaxation time experiments of the PSA films were carried out by solid-state ^{13}C NMR on a Bruker Avance III 400MHz at 310 K with a frequency of 100.6338 MHz and spinning rate of 5000 Hz. The magnetic pulse was a 90º pulse each 3.5 μs with a recycling delay of 12 s. The relaxation parameter (T_1) was calculated by fitting the decay of the intensity of the -CH_2- carbons to the equation:

$$I[t]=I[0](1-\exp(-t/T_1)) \quad \textbf{(Eq.3.1)}$$

where t is the experiment time, $I[t]$ is the signal intensity at that time, $I[0]$ is the signal intensity after the decay and T_1 is the relaxation parameter associated at such intensity decay.

The swelling degree evolution of the polymer films at different UV-irradiation times was measured using tetrahydrofuran (THF) as solvent. After the irradiation, the polymer film was submerged in a closed vial containing THF for 24 h. Then, the swollen film was carefully dried from the THF excess and weighted. The swelling degree was calculated as follows:

$$\text{Swelling degree} = \frac{w_s - w_p}{w_p} \quad \textbf{(Eq.3.2)}$$

where w_s is the weight of the swollen polymer sample (polymer + solvent) and w_p is the weight of the dry polymer sample (polymer film before the immersion).

3.3 Synthesis of piperonyl methacrylate (PIPEMA)

There are several potential ways to synthesize a methacrylate monomer coming from its corresponding alcohol, including the use of methacrylic acid, derivative esters and even boron esters [15–17]. However, in the case of piperonyl alcohol few efforts have been carried out to synthesize the methacrylate derivative. The synthesis of the benzodioxole derivative monomer was carried out following the procedure described by Shi et al[18] (Scheme 3.2,

Route 1), but changing the methacryloyl chloride reactant (very toxic, and flammable) by a safer and less toxic methacrylic anhydride (Scheme 3.2, Route 2). This common catalytic method offers a more sustainable pathway, in which 4-(Dimethylamino)pyridine catalyzes the reaction between methacrylic anhydride and piperonyl alcohol without affecting the final yield.

Scheme 3.2. Different pathways for the synthesis of PIPEMA; by method 1, using methacryloil chloride, and by method 2, using methacrylic anhydride.

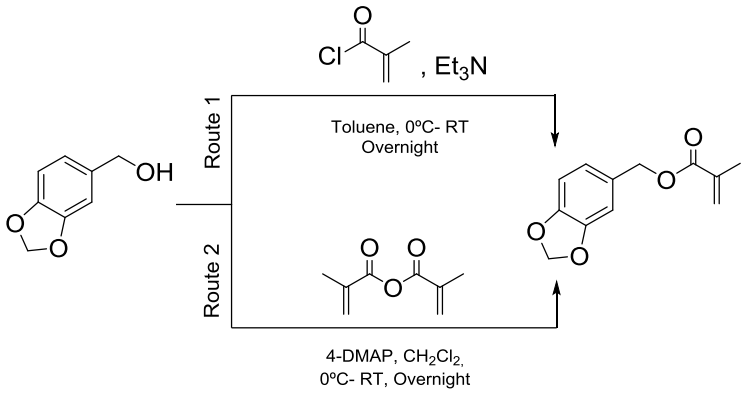

Figure 3.1 shows the ^{1}H NMR spectra and signal assignment with its corresponding integration in chloroform-*d*$_1$ of the pure pyperonyl methacrylate (PIPEMA), confirming the synthesis of this monomer. The signals between 6.74 and 6.88 ppm correspond to the three protons of the aromatic ring (4), whereas the signal at 5.95 ppm belongs to the two protons of the methylene group –O-CH_2-O– (5). The signals at 6.12 and 5.57 ppm correspond to the two protons of the methacrylic double bond (1', 1) and the signal at 5.08 ppm corresponds to the protons of the ester linkage (3). Finally, the signal belonging to the methyl group of the methacrylic group appears at 1.95 ppm

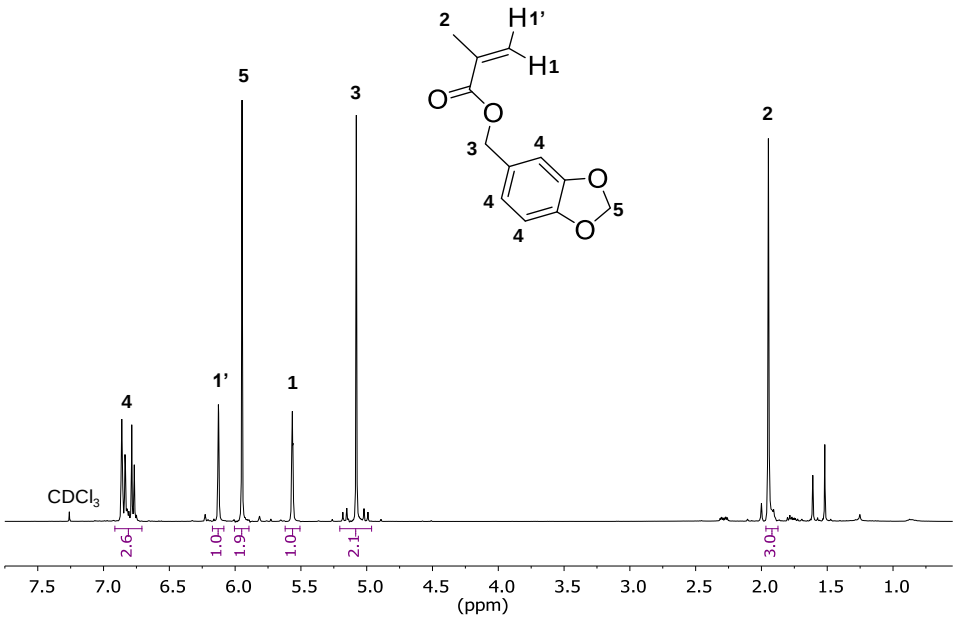

Figure 3.1. ^{1}H NMR spectra in chloroform-d_1 of piperonyl methacrylate (PIPEMA).

Thus, piperonyl methacrylate has two different functional groups: a methacrylate group, to polymerize via free radical polymerization, and 1,3-Benzodioxole moiety, which may further react by application of UV-light (see Scheme 3.3).

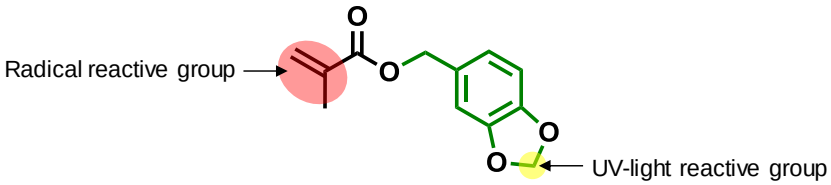

Piperonyl methacrylate
PIPEMA (67%)

Scheme 3.3. Synthetic biobased monomer used in this chapter and its bio-content, where the green part belongs to the carbon structure coming from the nature.

3.4 Solution homopolymerization of piperonyl methacrylate (PIPEMA)

Aiming to determine the glass transition temperature of the homopolymer of piperonyl methacrylate (polyPIPEMA), solution polymerization was carried out using toluene as solvent and AIBN as thermal initiator. The subsequent solvent evaporation allowed obtaining polyPIPEMA as a white solid with a yield higher than 99% (calculated by ^{1}H NMR integration). Figure 3.2 shows the ^{1}H NMR spectrum as well as the signal assignment assignation of polyPIPEMA in chloroform-*d*$_1$.

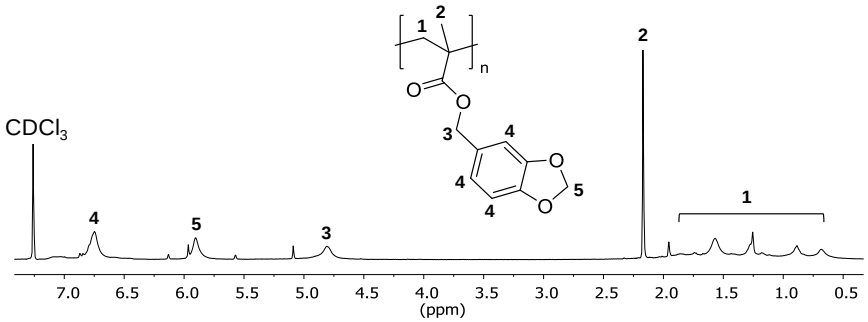

Figure 3.2. ^{1}H NMR spectrum in chloroform-*d*$_1$ of (Poly)piperonyl methacrylate (PolyPIPEMA).

The glass transition temperature of the homopolymer was determined by DSC and its corresponding curve is shown in Figure 3.3. It is worth noting that unlike isobornyl methacrylate (IBOMA, Tg = 150 ºC), PIPEMA presents a benzyl group contributing to rigidity but also allowing rotation and, hence, an increasing of the free volume when is polymerized. This results in a Tg of 70 ºC, which enables the use of PIPEMA as hard monomer for pressure sensitive adhesive formulations, but providing a better control on their viscoelastic behavior.

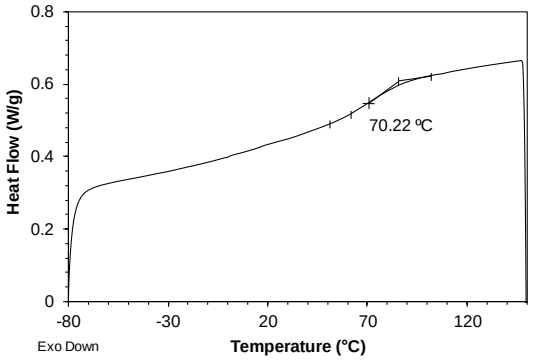

Figure 3.3. DSC curve of polyPIPEMA at a heating rate of 20 ºC/min.

3.5 Effect of the hard monomer

One of the goals of this chapter was to investigate if the incorporation of a multifunctional biobased monomer with a UV-tunable group could improve the performance of the waterborne 2OA:IBOMA biobased PSAs synthesized in chapter 2[19]. For this purpose, and because of the high Tg of IBOMA homopolymer, IBOMA was substituted by PIPEMA in the formulations **2B.1** and **2C.1** of the previous chapter. Table 3.2 summarizes the latexes synthesized as well as their main properties including average particle size (dp), gel content (measured by soxhlet extraction), swelling of the gel polymer, glass transition temperature and the biobased content.

Figure 3.4 presents the molar mass distributions determined using AF4/MALS/RI for the four latexes. The molar mass distributions were bimodal with the low molar mass peak in the range 10^5-10^6 g/mol (note that likely polymer chains in the range 10^4-10^5 g/mol were not analyzed because of the lack of light scattering signal) and a high molar mass peak in the range of 10^9 g/mol. Both systems (using IBOMA or PIPEMA as methacrylate comonomer in the formulation) presented the same trend in the MMD when varying the amount of this methacrylate monomer. Thus, the high molar mass peak appeared at higher masses and

the low molar mass peak showed lower molar masses for the lower amount of the methacrylate monomer (formulations with 5 wt% IBOMA/PIPEMA). This is in good agreement with the fact that increasing the amount of methacrylate monomer has an effect on the development of the molar mass distribution of acrylate monomer polymerizations[20,21].

Table 3.2. Properties of the PSA latexes.

PSA	Composition (%wt monomers)	dp (nm)	Gel (%)†	Swelling††	Tg (°C)	Bio (%)
2B.1	2OA:IBOMA:MAA + CTA* (94:5:1 + 0.025*)	236	69 ± 1	42.9	-36	72
2C.1	2OA:IBOMA:MAA + CTA* (84:15:1 + 0.025*)	230	59 ± 0.4	95.1	-26	72
3A.1	2OA:PIPEMA:MAA + CTA* (94:5:1 + 0.025*)	233	62 ± 1	45.9	-40	72
3B.1	2OA:PIPEMA:MAA + CTA* (84:15:1 + 0.025*)	231	53 ± 2	117	-38	71

* Weight percent of 2EHTG based on monomer.

† The fraction of the copolymer that does not dissolve in THF after 24 h of soxhlet extraction.

†† Swelling was calculated for the polymer chains in the high molar mass peak measured in the AF4/MALS/RI analysis. Swelling was calculated from the weight average molar mass and the z-average radius of gyration using $S_w = \frac{4}{3}\pi R_Z^3 \rho_{Pol} N_A / M_W$; ρ_{Pol} = 1.1 g/cm^3, N_A: Avogadro's number. The relative error of the *Mw* and R_Z measurements used to calculate Swelling is between 13% and 33% and between 5 and 15%, respectively.

The high molar mass mode, the gel polymer, is formed in the emulsion polymerization of acrylates by means of intermolecular chain transfer to polymer combined with bimolecular termination by combination[22–26]. This combined mechanism favors the incorporation of the largest chains to the gel polymer leading to bimodal molar mass distributions as shown in Figure 3.4. The addition of methacrylate comonomers reduces substantially the intermolecular chain transfer to polymer because methacrylates do not bear a labile hydrogen atom in their structure[20]. Furthermore, since the reactivity ratio of the methacrylate monomers is higher than that of acrylates (i.e. r_{MMA} = 2.12 and r_{BA} = 0.414)[27] and the tertiary

methacrylate radical is more stable than the secondary acrylate radical the overall rate of intermolecular chain transfer to polymer is reduced substantially as the amount of methacrylate monomer is increased. In addition, methacrylate radicals tend to terminate by disproportionation reactions,[28] and hence, the linking of branched chains producing polymer network decreases too.

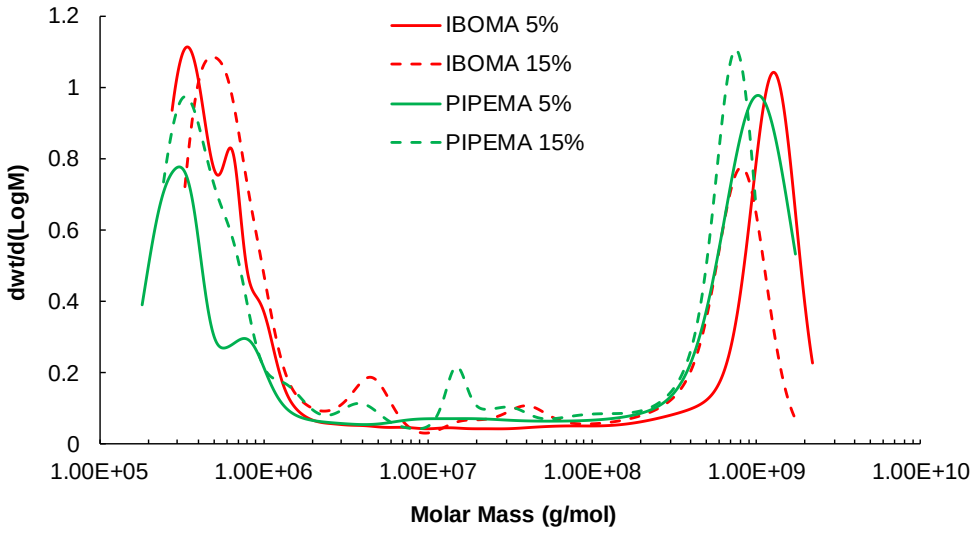

Figure 3.4. Molar mass distributions measured by AF4/MALS/RI for the four latexes of this chapter.

The gel contents and the swelling values (for the gel polymer) reported in Table 3.2 agree with the mechanistic changes occurring when either PIPEMA or IBOMA concentrations increase in the formulations. In other words, increasing the amount of PIPEMA/IBOMA decreased the amount of gel polymer, and gel polymer was less crosslinked (swelling is higher). No noticeable differences were found otherwise in the microstructure of the latexes produced with IBOMA and PIPEMA. However, the glass transition temperatures were lower when PIPEMA was used instead of IBOMA. The lower Tg of the PIPEMA homopolymer explains the differences measured in the Tg´s of the copolymer latexes.

3.5.1 Rheological investigations of waterborne PSAs containing different hard monomer

Dynamic rheological experiments were carried out in order to know the effect of the hard monomer on the viscoelastic nature of the PSAs of this chapter and its correlation with the microstructure discussed above [29–31].

Figure 3.5 shows the variation of storage and loss modulus (G´ and G´´, respectively) and tanδ with frequency at 23 ºC. As can be observed there is not much differences among formulations **2B.1**, **3A.1** and **3B.1** about G´ and/or G´´, mainly due to their close glass transition temperatures (Table 3.2). However, formulation **2C.1** presents the highest value of both moduli. The greater Tg provided by IBOMA reinforces the polymer matrix structure and the elastic nature, affecting to both the storage and loss modulus[32,33]. Its solid-like behaviour (G´) is clearly influenced by the higher Tg, whereas the viscous part (G´´) is additionally influenced by the high soluble molar mass which controls the dissipation of energy during the debonding process. A good relationship between the elastic and the viscous component can be noted in the dynamic modulus plot (tanδ). In this sense formulation **3B.1** (15 wt% of PIPEMA) exhibits a greater dampening effect, because the viscous component of the dynamic modulus dominates the material behaviour. This liquid-like behaviour is promoted as consequence of the low Tg together with a lower insoluble molar mass (Figure 3.4), resulting in an improvement of the loss energy. Despite of the lower Tg of formulation **3A.1**, the higher soluble molar mass of formulation **2C.1** influences on the loss modulus, meaning a slightly greater tanδ value. Finally 5 wt% of IBOMA (formulation **2B.1**) led to the lowest tanδ value due to the high contribution of the elastic part.

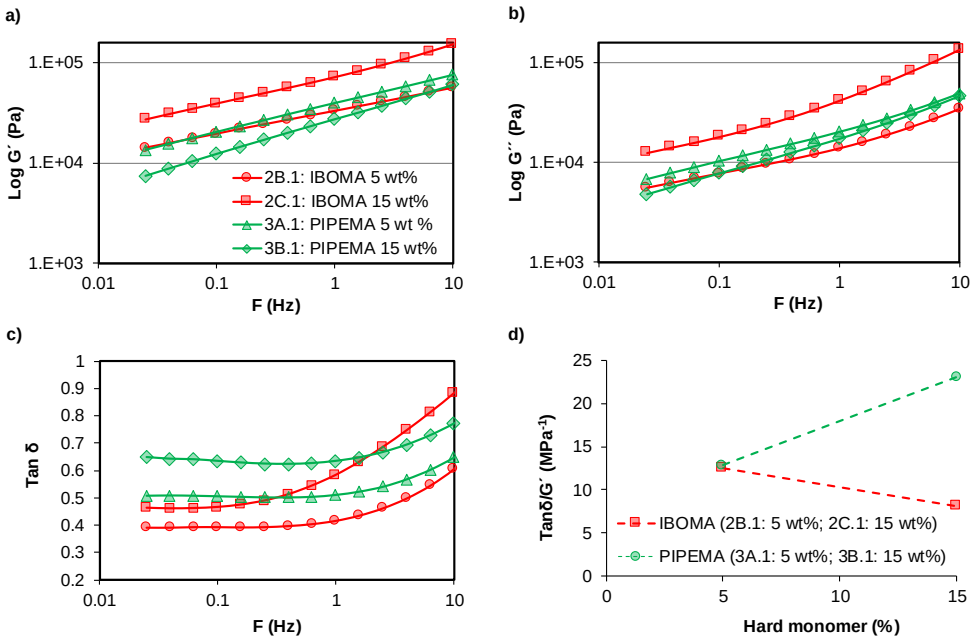

Figure 3.5. (a) Storage modulus (G´), (b) loss modulus (G´´), (c) dynamic modulus (tanδ) and (d) tanδ/G´ for 2OA:IBOMA (red marks) and 2OA: PIPEMA (green marks) formulations. Measurements made at 23 ºC and 1 Hz.

Figure 3.5.d shows the ratio tanδ/G´ as a function of the hard monomer percentage for each series of formulations. As can be noted 5 wt% of both PIPEMA and IBOMA present almost the same tanδ/G´ value because formulation **3A.1** presents a slightly greater value of G´ than formulation **2B.1** at the debonding frequency. A decrease of this ratio was produced for the formulation **2C.1** because its high contribution of G´ in comparison with G´´. On the other hand, the use of 15 wt% of PIPEMA (formulation **3B.1**) led to the greatest tanδ/G´ value, 23.1 MPa^{-1}, because its high polymer chain mobility allowed a better dissipation of the energy along the detachment process; namely, the viscous modulus had a higher contribution than the elastic part of the adhesive.

Figure 3.6 shows the corresponding viscoelastic window, according with the work of Chang[34,35], for this set of formulations. In this viscoelastic analysis, no PSA materials can be found in quadrant 1 because the high elastic nature of the material and low dissipation ability. Quadrant 2 relates to PSAs that exhibit high shear behaviour due to the high storage and loss modulus, which are compensated, resulting in a high cohesion. Quadrant 3 belongs to easily removable PSA's usually showing low peel values, whereas quadrant 4 applies to very-quick PSA's, since the low modulus/high dissipation allows a very efficient bonding at low temperatures or short contact times. Finally, the central area corresponds to the general purpose PSAs where storage and loss modulus present medium values and they are well balanced. As it can be observed, all the formulations are located in the area corresponding to perform as a well-balanced pressure sensitive adhesive. However, it is worth to mention that formulation **2C.1** is a little bit shifted towards the Q2, namely towards a high shear behaviour PSA. This fact is attributed to the high Tg of the final polymer which influences both the storage and loss modulus as it was discussed above.

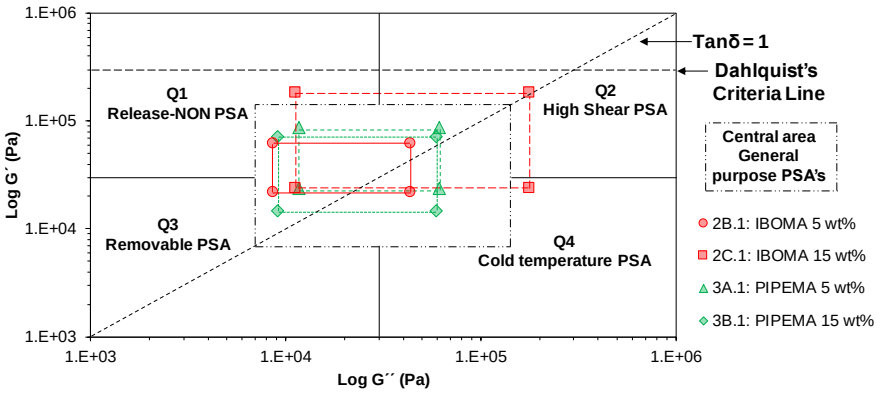

Figure 3.6. Viscoelastic window of the latexes of this chapter in the range of frequencies from 10^{-2} rad/s to 10^{2} rad/s at 23 ºC.

3.5.2 Adhesive properties of waterborne PSAs containing different hard monomer

The adhesive properties of the latexes of this chapter are presented in Figure 3.7 as a function of the hard monomer percentage. As it can be observed the direct substitution of IBOMA by PIPEMA led to an increase in tackiness and peel strength together with a high reduction of both the holding temperature and the shear resistance (from 6 days for formulations **2B.1** and **2C.1** to 58 and 90 min for formulations **3A.1** and **3B.1** respectively). The explanation for such behavior is the lower glass transition temperature provided by the use of PIPEMA as hard monomer instead of IBOMA. This reduction enhanced the polymer chains mobility improving the instantaneous adhesion as well as the dissipation of energy during the deformation process, increasing tackiness and work of adhesion respectively[31,36,37]. In addition the MMD´s measured by AF4/MALS/RI as well as the swelling degrees suggest that formulations with PIPEMA were slightly less crosslinked than those produced with IBOMA and hence the PSA´s were less cohesive. On the other hand, in latexes with the same composition but higher concentration of the hard monomer (either IBOMA or PIPEMA) the changes in the microstructure (molar mass and crosslinking density) together with the glass transition temperature have counteracting effects. For instance, when IBOMA is increased from 5 wt% to 15 wt% the gel content decreases around 10% improving chain mobility, but also the glass transition temperature increases in 10 °C reinforcing cohesion. This fact yields in a complex coupling system in which the glass transition temperature has a more remarkable effect. It is worth pointing out that no rest of adhesive was observed on the substrate surface in any of the formulations produced, indicating adhesive failure, which is the desired one for most of applications.

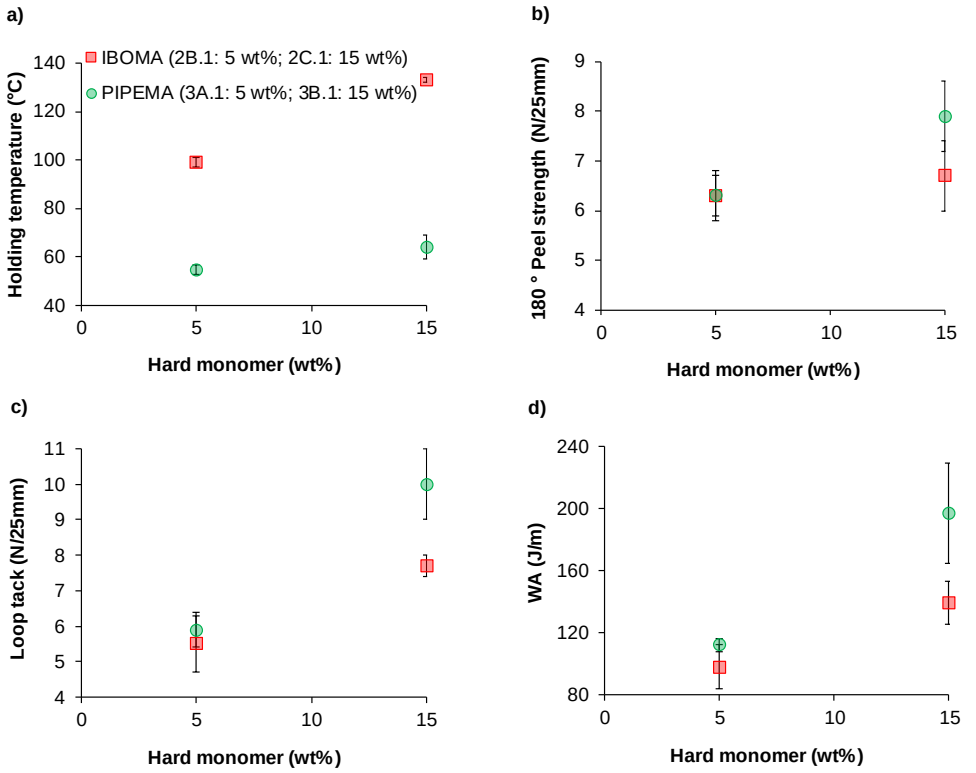

Figure 3.7. The effect of hard monomer type and percentage on the (a) SAFT tests, (b) peel strength, (c) loop tack and (d) work of adhesion of the PSA tapes for 2OA:IBOMA (red marks) and 2OA:PIPEMA formulations (green marks).

Figure 3.8 shows probe tack curves for these formulations. The incorporation of PIPEMA improves substantially the flexibility of the fibers formed during the fibrillation process maintaining enough rigidity, which means that they break at higher strain values[38]. The incorporation of 5 wt% of PIPEMA provided longer fibrillation in comparison with formulations **2B.1** (IBOMA 5 wt%) and **2C.1** (IBOMA 15 wt%). This proofs that the PIPEMA monomer contributes to a good balance between Tg and crosslinking degree, controlling the fluidity and hardness of the molecular chains. Moreover intermolecular forces should not be discarded during the fibrillation process when PIPEMA is used, since similar values of the

stress in the plateau were observed for different glass transition temperatures (formulations **2C.1** and **3A.1**). In this sense, π-π stacking of the benzyl group could contribute to the stiffness of the fibers and grants flexibility to the polymer chains[39]. A more liquid-like behavior is noted for formulation **3B.1** (PIPEMA 15 wt%) because of the lower gel content, leading to a decrease of the stress peak at low strain values, in comparison with formulation **2C.1**, and to longer fibrillation plateau without affecting to the fibers cohesiveness.

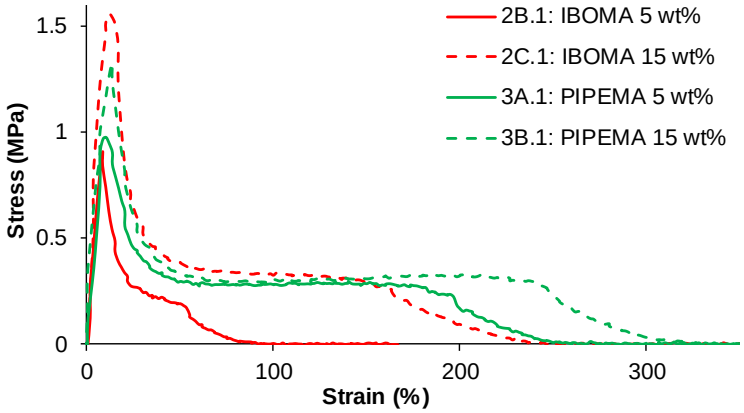

Figure 3.8. Probe tack tests for 2OA:IBOMA (red lines) and 2OA: PIPEMA (green lines) formulations.

These results are in agreement with the rheological investigations presented above. Furthermore, a good relationship between the shape of the probe tack curve and the dynamic modulus and the ratio tanδ/G´ can be stablished.

3.6 Effect of the UV-light irradiation time

Benzodioxole derivatives are widely used as coinitiators in radical polymerizations via UV-light through hydrogen donation[1–3]. Moreover, it is also well known that the active hydrogen between two alkoxyl groups in cyclic acetals can be abstracted as a radical under photolytic conditions[40–42]. Those cyclic acetal radicals generated are rearranged rapidly by *β*-scission forming the corresponding ester radicals, which are able to initiate the polymerization of vinyl compounds as well as to react each other. Scheme 3.4 shows the photochemical rearrangement mechanism, proposed by Elad and Youssefyeh, for 1,3-Dioxolane compounds[43].

Scheme 3.4. Photochemical rearrangement mechanism of 1,3-Dioxolane compounds, proposed by Elad and Youssefyeh, and their corresponding reactions

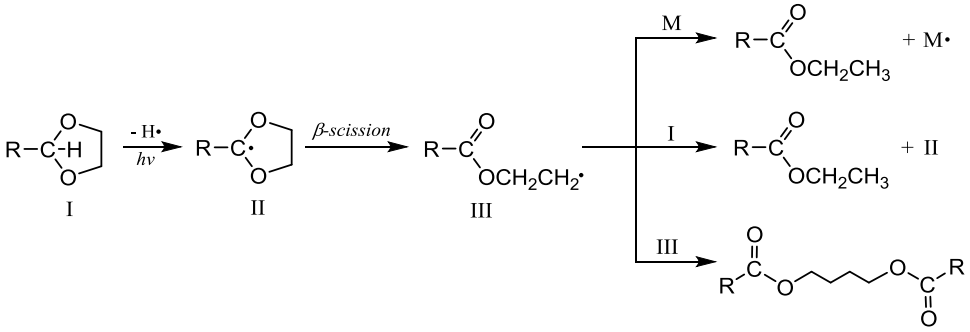

Therefore, it could be assumed that in the copolymers containing piperonyl derivatives, a crosslinking reaction may be promoted after UV treatment as shown in Scheme 3.5.

Scheme 3.5. Proposed photoreaction mechanism for adhesive films containing PIPEMA

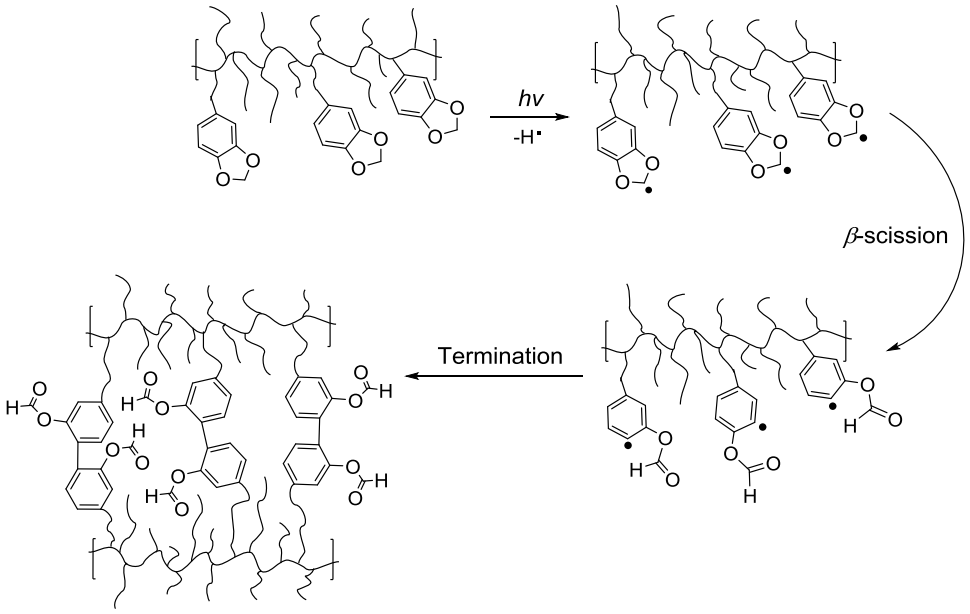

To corroborate this hypothesis, first, the UV absorption spectra of both PIPEMA and latex with formulation **3B.1** (containing 15 wt% of PIPEMA) were analyzed, confirming that the latex absorbed UV in the same range than PIPEMA, at about 254 nm. Figure 3.9 presents the absorption spectra of pure PIPEMA monomer and the absorption of formulation **3B.1**. Next, adhesive films were irradiated with UV-light at 254 nm over time, and the ability to crosslink the PSA film was determined by swelling measurements. Figure 3.10 shows that swelling decreased as irradiation time increased for formulation **3B.1**, whereas it was maintained constant when formulation **2C.1** (without PIPEMA) was irradiated. This clearly indicates the formation of a more crosslinked polymer film.

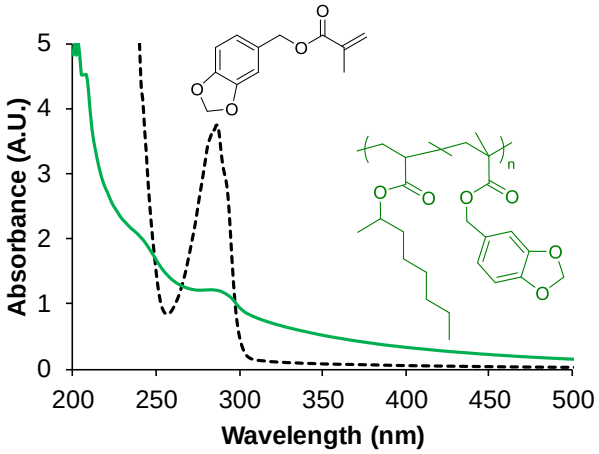

Figure 3.9. UV spectra of PIPEMA (5 x 10^{-5} g/L, dashed line) and latex **3B.1** (4 x 10^{-6} g/L, continuous line) in hexane and water, respectively.

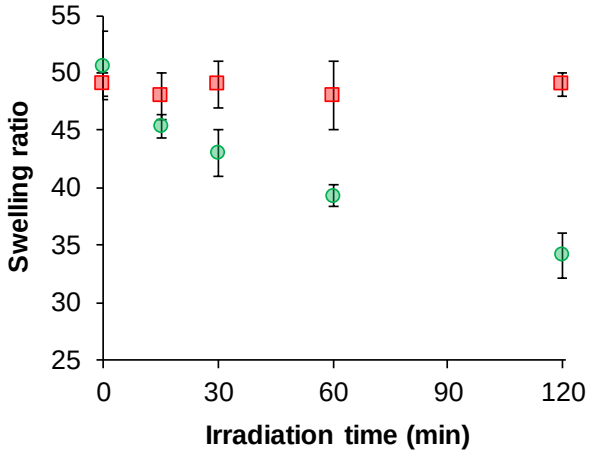

Figure 3.10. Evolution of swelling ratio (measured in THF) for formulation **3B.1** (2OA:PIPEMA 84:15; green circles) and formulation **2C.1** (2OA:IBOMA 84:15; red squares) cured at different irradiation times using a UV-light at 254 nm of wavelength.

To shed light on the crosslinking process, solid state ^{13}C NMR measurements of the cured samples were performed. Figure 3.11 shows, as representative example, the ^{13}C NMR spectra of the PSA film (formulation **3B.1**) at irradiation times of 30, 60 and 120 minutes. As

it can be seen, increasing the irradiation time the intensity of the peak at about 173 ppm (corresponding to the carbonyl of the ester produced after the *β*-scission; see Scheme 3.4) increased. Note that the reference peak around 70 ppm corresponds to the -O-CH_2- group of the alkyl chains. This observation of the changes on the chemical structure together with the decrease of the swelling of the films (increasing crosslinking density) proofs the crosslinking reactions occurring in the film under UV irradiation as proposed in Scheme 3.5.

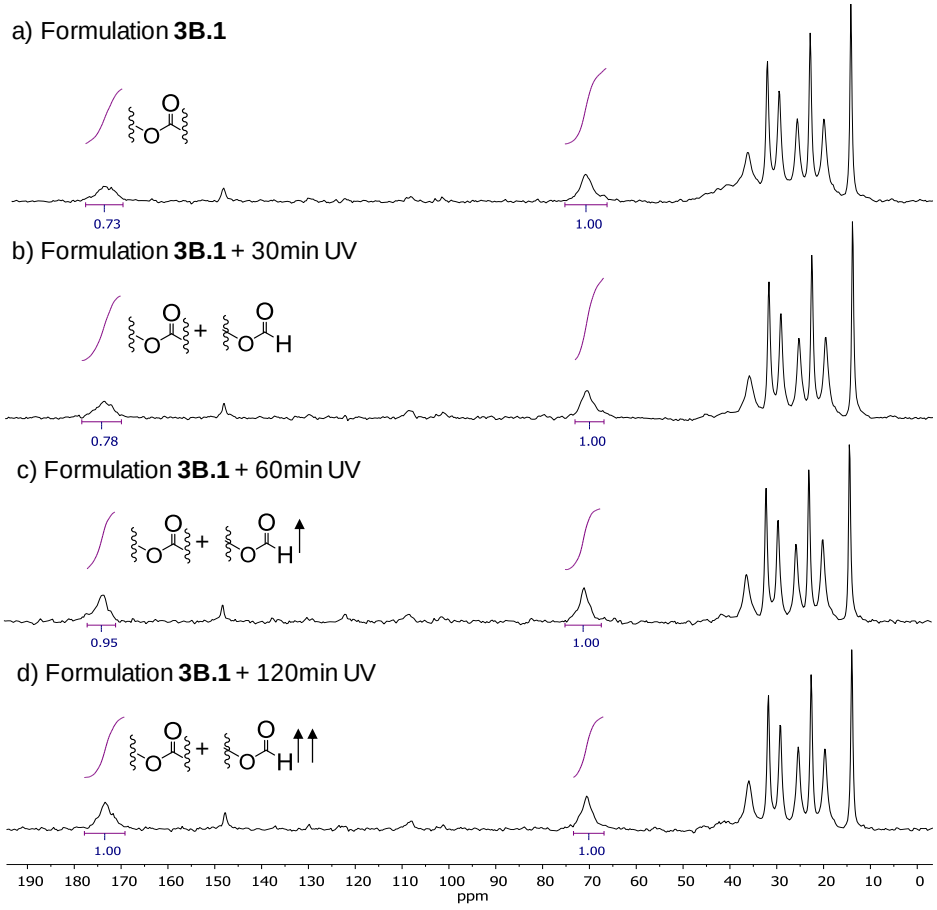

Figure 3.11. Solid state ^{13}C NMR spectra of formulation **3B.1** (2OA:PIPEMA 84:15) at different UV exposure times: a) no exposure, b) 30 min, c) 60 min and d) 120 min. Measurements were carried out at 310K.

The creation of covalent crosslinking points among molecular chains can also be detected by the NMR spin-lattice relaxation measurements, T_1. In this regard, the evolution of T_1 for the carbons corresponding to the backbone chain (CH_2) was monitored by solid state ^{13}C NMR. Figure 3.12 shows the evolution of T_1, for formulation **3B.1** cured at different irradiation times. The higher T_1 values with increasing irradiation indicated the formation of more crosslinked structures that reduced the motion of the polymer chains. This result further proofs the mechanism proposed in Scheme 3.5.

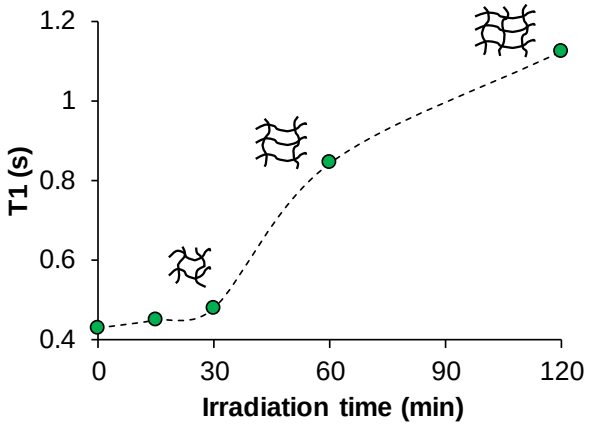

Figure 3.12. ^{13}C NMR T_1 relaxation parameter as a function of the irradiation time for formulation **3B.1** (2OA:PIPEMA 84:15). T_1 was calculated by fitting the decay of the intensity of the -CH_2- carbons to I[t]=I[0](1-exp(-t/T1)).

3.6.1 Rheological investigations of UV-tunable waterborne PSA containing PIPEMA

Once the ability of the PIPEMA containing PSA films to cure under UV-light was demonstrated, linear rheological measurements of films of latex **3B.1** irradiated at 254 nm during 15, 30, 60 and 120 min were performed. It is worthy pointing out that, above 60 min of irradiation, films become yellowish likely due to the high generation of conjugate structures between the phenolic rings during the photoreaction process[44].

The augmentation of the crosslinking degree via UV-light led to an increase of the storage modulus (G´), which enhanced the elastic part of the adhesive and reduced its energy dissipation capability[45]. Figure 3.14 shows the evolution of both the storage modulus and tanδ/G´ value at the debonding frequency during the irradiation time. There was a slight increase of G´ for those films cured at 15 and 30 min, not showing relevant differences between them due to the short period of irradiation. As consequence, the energy dissipation at the interface suffered a small decrease. However, for those films cured at 60 and 120 min the storage modulus stepped up in a more accused way, which yielded a more constrained polymer network as it was previously observed in the evolution of the swelling ratio (Figure 3.10) and the T_1 (Figure 3.12). This promoted the capability to absorb energy, namely the solid-like behavior of the adhesive and, hence, the reduction of the tanδ/G´ value.

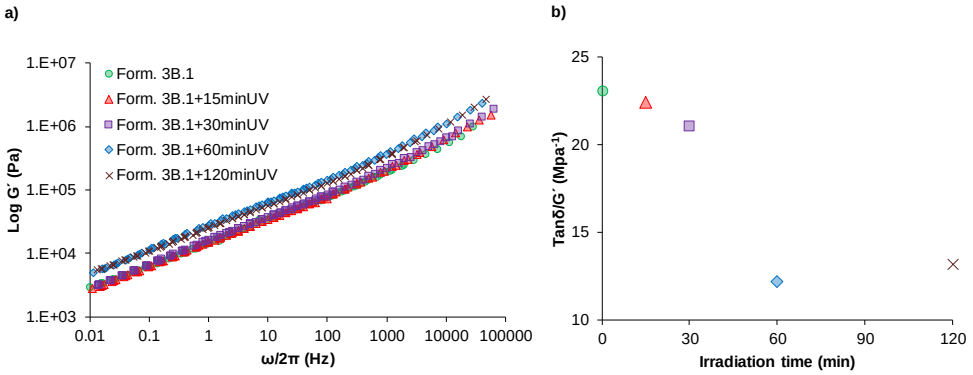

Figure 3.14. Evolution of (a) storage modulus (G´) and (b) tanδ/G´ value and for formulation **3B.1** (2OA:PIPEMA 88:15) cured at different irradiation times using 254 nm of wavelength.

3.6.2 Adhesive properties of UV-tunable waterborne PSA containing PIPEMA

Table 3.3 summarizes the adhesion properties of those films at different irradiation times. Increasing irradiation time peel strength and loop tack decreased while both shear

resistance and SAFT increased substantially, which can be considered as a typical behaviour of a PSA when the crosslinking density increases. However, it is important to remark that 15 min of curing did not noticeable reduce peel and loop tack, but it was enough to increase more than 50 times the shear resistance and around 40 ºC the holding temperature.

Table 3. Properties of PSA tapes with the formulation **3B.1** (2OA:PIPEMA 88:15) cured at different irradiation times at 254 nm of wavelength.

PSA	Peel (N/25mm)	Loop tack (N/25mm)	WA (J/m^2)	Shear resistance (min)	SAFT (°C)
3B.1	7.9 ± 0.7	10 ± 1	197 ± 32	90 ± 10	64 ± 5
3B.1+15minUV	6.9 ± 0.2	10.4 ± 0.4	156 ± 19	5000 ± 200	105 ± 6
3B.1+30minUV	5.8 ± 0.4	7.1 ± 0.5	125 ± 9	29000 ± 500	136 ± 3
3B.1+60minUV	4.5 ± 0.5	4.5 ± 0.4	72 ± 9	> 35000	140 ± 5
3B.1+120minUV	4.6 ± 0.9	3.9 ± 0.7	67 ± 15	> 35000	145 ± 3

More information about the evolution of the adhesive performance with irradiation time is given by the probe tack curves (Figure 3.15). Only 15 min of UV-light promoted a major resistance of the polymer fibers, yielding a higher fibrillation plateau, but also a broader stress peak at low strain values. This behavior in which both the stress of the plateau and the strain before breaking the fibrils increased corresponds to an increased degree of crosslinking of the polymer chains that enhanced cohesiveness of the polymer fibrils (stiffness). 30 min of irradiation time did not produce changes in the length of the fibrillation plateau, but led to an increase of the broadness of the stress peak as well as its maximum value in comparison with the untreated film. The increase of the rigidity of the formed fibers after the cavitation process is closely related with the observed reduction of tackiness and, furthermore, the improved shear resistance. By irradiating for longer times, the fibrillation

plateau decreased substantially as a consequence of the higher crosslinked network, which is in agreement with the rheological results presented in Figure 3.14.

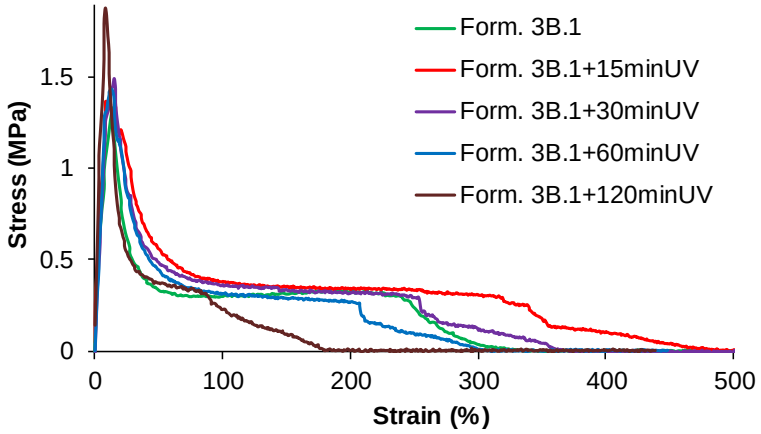

Figure 3.15. Probe tack tests for formulation **3B.1** (2OA:PIPEMA 88:15) cured at different irradiation times using 254 nm of wavelength.

3.7 Comparison of microstructure and adhesive performance with an oil-based waterborne PSA.

Keeping in mind the conflict of interest of this chapter and considering the potential viscoelastic properties of the biobased composition containing the highest amount of PIPEMA (formulation **3B.1**), a comparison with the oil-based waterborne PSA (**2Ref**), which was showed in the previous chapter, was carried out. As shown in Table 3.4, the pure oil-based latex provided a lower glass transition temperature because of the presence of 2-Ethylhexyl acrylate (2EHA) but similar gel content than formulation **3B.1**.

The adhesive properties of the biobased PSA **3B.1** irradiated during 15 min, which showed a well-balanced viscoelastic behaviour, were compared with the pure oil-based PSA. As it can be observed both compositions showed similar 180º peel strength values

(Figure 3.16.a). Nevertheless, the biobased PSA presented two times higher initial adhesion and a greater work of adhesion, likely because benzodioxole units allow the separation among polymer chains and, thereby, an increasing of the dissipation energy along the debonding process. In addition, the creation of few conjugated structures due to the short UV-light irradiation time made possible to overcome in 35ºC the holding temperature and reaching a 25 times higher shear resistance value in comparison with petroleum-based formulation (Figure 3.16.b).

Table 3.4. Characteristics of the latexes synthesized with oil-based monomers (**2Ref**)[46] and that obtained by substitution of the oil-based monomers by the biobased monomers of this chapter (**3B.1**).

PSA	Composition	dp (nm)	Gel (%)	Tg (°C)	Bio (%)
2Ref**	2EHA:MMA:AA (84:15:1)	294	52 ± 0.1	-49	0
3B.1	2OA:PIPEMA:MAA + CTA* (84:15:1 + 0.025*)	231	53 ± 2	-38	72

CTA*: Weight percent based on monomer.

Ref**: non-biobased formulation. From ref.[46]

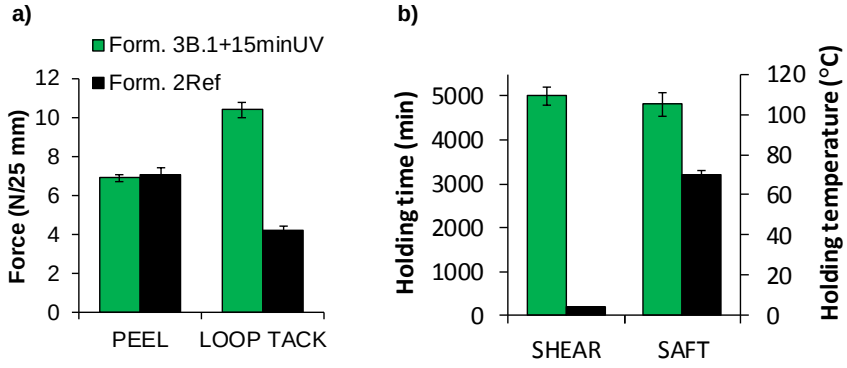

Figure 3.16. Comparison of (a) 180º Peel strength and loop tack and (b) Shear resistance and holding temperature between formulation **3B.1**+15minUV (in green) and formulation **2Ref** (in black).

Probe tack curves revealed that the use of 2EHA in the commercial tape (**2Ref**) provided a higher viscous behavior as it is showed in Figure 3.17.a. Nonetheless, its fibrils support less stress than those belonging to the biobased formulation (**3B.1**+15minUV). In this context, the use of benzodioxole moieties together with a slightly crosslinked polymer network promoted the energy storage of the material, but also ensured its good release, which is an indication of flexible and enough stiff adhesive fibers. Proof of this, is the energy dissipation at the interface adhesive-substrate (tanδ/G´), which was two times higher for the PSA with 71% of bio-content polymer (Figure 3.17.b).

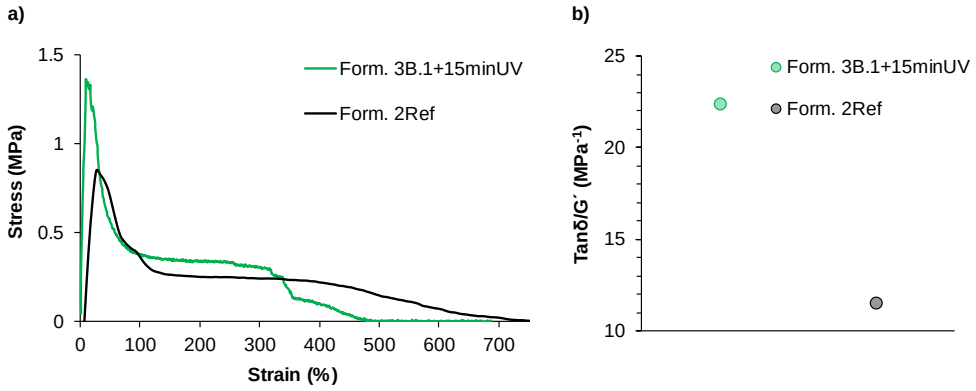

Figure 3.17. Comparison of (a) probe tack curves and (b) tanδ/G´ values between formulation **3B.1**+15minUV (green line and circle) and formulation **2Ref** (black line and circle).

3.8 Conclusions

In this chapter, the synthesis and incorporation of biobased monomer pyperonyl methacrylate (PIPEMA) into waterborne high biobased monomer containing PSA formulations was explored. The influence of the hard monomer nature (PIPEMA vs IBOMA) in its incorporation was evaluated in terms of the polymer microstructure and the final adhesive performance. It was found that the incorporation of PIPEMA, specifically 15 wt%,

provided a better viscous behavior of the adhesive fibers, maintaining enough stiffness and yielding the maximum dissipation energy value. Furthermore, the benzodioxol structures present in the piperonyl functionality allowed tuning the adhesive performance (increasing shear resistance and SAFT without substantially damaging adhesion) when the adhesives are UV irradiated. Both rheological studies and nuclear magnetic resonance studies corroborated the photocrosslinking reaction mechanism proposed and, hence, the formation of a crosslinked network via generation of conjugated structures. Notably, 15 min of UV-light curing provided the best balance of adhesive properties, overcoming the performance of a pure oil-based PSA and, therefore, solving the conflict between bio-content degree and adhesive efficiency.

3.9 References

(1) Shi, S.; Xiao, P.; Wang, K.; Gong, Y.; Nie, J. Influence of Chemical Structures of Benzodioxole-Based Coinitiators on the Properties of the Unfilled Dental Resin. *Acta Biomater.* **2010**, *6* (8), 3067–3071.

(2) Da Silveira Lima, G.; Ogliari, F. A.; Souza E Silva, M. G.; Münchow, E. A.; Petzhold, C. L.; Piva, E. Benzodioxoles as Alternative Coinitiators for Radical Polymerization in a Model-Dental Adhesive Resin. *J. Appl. Polym. Sci.* **2013**, *127* (5), 4160–4167.

(3) Yang, J.; Xu, F.; Shi, S.; Nie, J. Influence of Structure of Benzodioxole Derivatives on Photoinitiation Efficiency of Benzophenone. *Photochem. Photobiol. Sci.* **2012**, *11* (8), 1377–1382.

(4) Gorgani, L.; Mohammadi, M.; Najafpour, G. D.; Nikzad, M. Piperine — The Bioactive Compound of Black Pepper : From Isolation to Medicinal Formulations. *Compr. Rev.*

Food Sci. Food Saf. **2017**, *16*, 124–140.

(5) Plummer, C. M.; Breadon, T. W.; Pearson, J. R.; Jones, O. A. H. The Synthesis and Characterisation of MDMA Derived from a Catalytic Oxidation of Material Isolated from Black Pepper Reveals Potential Route Specific Impurities Science and Justice. *Sci. Justice* **2016**, *56*, 223–230.

(6) Salmoria, G. V; Oglio, E. L. D. Synthetic Communications : An International Journal for Rapid Communication of Synthetic Organic Chemistry Isomerization of Safrole and Eugenol Under Microwave Irradiation. *Synth. Commun.* **1997**, *27* (24), 4335–4340.

(7) Kishore, D.; Kannan, S. Isomerization of Eugenol and Safrole over MgAl Hydrotalcite, a Solid Base Catalyst. *Green Chem.* **2002**, *4*, 607–610.

(8) Grimsiuw, J.; Hua, C. The Conversion of Isosafrole to Piperonal and Anethole to Anisaldehyde: Electrochemical Active Manganese Dioxide. *Electrochim. Acta* **1994**, *39* (4), 497–499.

(9) Blair, E. A.; Hill, D. Process for Producing Aromatic Carbonyl Compounds and Peroxide Compounds. U.S. Patent 2916499, 1959.

(10) UNODC. Precursor Control. In *Worl Drug Report*; Vienna, 2013; pp 55–93.

(11) Young Jang, H.; Jin Park, H.; Damodar, K.; Kim, J.; Jun, J. Dihydrostilbenes and Diarylpropanes : Synthesis and in Vitro Pharmacological Evaluation as Potent Nitric Oxide Production Inhibition Agents. *Bioorg. Med. Chem. Lett.* **2016**, *26*, 5438–5443.

(12) Wu, J.; Zeng, H.; Cheng, J.; Zheng, S.; Golen, J. A.; Manke, D. R.; Zhang, G.; Zhang,

G. Cobalt(II) Coordination Polymer as a Precatalyst for Selective Hydroboration of Aldehydes, Ketones, and Imines. *J. Org. Chem.* **2018**, *83*, 9442–9448.

(13) Osako, T.; Torii, K.; Hirata, S.; Uozumi, Y. Chemoselective Continuous-Flow Hydrogenation of Aldehydes Catalyzed by Platinum Nanoparticles Dispersed in an Amphiphilic Resin. *ACS Catal.* **2017**, *7*, 7371–7377.

(14) Schwendenwein, D.; Fiume, G.; Weber, H.; Rudroff, F.; Winkler, M. Selective Enzymatic Transformation to Aldehydes in Vivo by Fungal Carboxylate Reductase from Neurospora Crassa. *Adv. Synth. Catal.* **2016**, *358*, 3414–3421.

(15) Dubois, D. A. Preparation of Alkyl Methacrylate Monomers for Anionic Polymerization. U.S. Patent 4889900, 1989.

(16) Evans, S. B.; Mulvaney, J. E.; Hall, H. K. On the Synthesis of Pure (Meth) Acrylate Esters and Their Corresponding Homopolymers. *J. Polym. Sci. Part A Polym. Chem.* **1990**, *28* (5), 1073–1078.

(17) Gunes, D.; Karagoz, B.; Bicak, N. Synthesis of Methacrylate-Based Functional Monomers via Boron Ester Acidolysis and Their Polymerization. *Des. Monomers Polym.* **2009**, *12* (5), 445–454.

(18) Suqing, S.; Nie, J. Investigation of 3,4-Methylenedioxybenzene Methoxyl Methacrylate as Coinitiator and Comonomer for Dental Application. *J. Biomed. Mater. Res. B. Appl. Biomater.* **2007**, *83* (2), 340–344.

(19) Badía, A.; Movellan, J.; Barandiaran, M. J.; Leiza, J. R. High Biobased Content Latexes for Development of Sustainable Pressure Sensitive Adhesives. *Ind. Eng. Chem. Res.* **2018**, *57*, 14509–14516.

(20) González, I.; Asua, J. M.; Leiza, J. R. The Role of Methyl Methacrylate on Branching and Gel Formation in the Emulsion Copolymerization of BA/MMA. *Polymer (Guildf).* **2007**, *48* (9), 2542–2547.

(21) Hamzehlou, S.; Reyes, Y.; Leiza, J. R. Detailed Microstructure Investigation of Acrylate / Methacrylate Functional Copolymers by Kinetic Monte Carlo Simulation. *Macromol. React. Eng.* **2012**, *6*, 319–329.

(22) Plessis, C.; Arzamendi, G.; Leiza, J. R.; Schoonbrood, H. A. S.; Charmot, D.; Asua, J. M. Seeded Semibatch Emulsion Polymerization of N-Butyl Acrylate. Kinetics and Structural Properties. *Macromolecules* **2000**, *33* (14), 5041–5047.

(23) Plessis, C.; Arzamendi, G.; Leiza, R.; Schoonbrood, H. A. S.; Charmot, D.; Asua, M. Modeling of Seeded Semibatch Emulsion Polymerization of N-BA. *Ind. Eng. Chem. Res.* **2001**, *40*, 3883–3894.

(24) Ballard, N.; Hamzehlou, S.; Asua, J. M. Intermolecular Transfer to Polymer in the Radical Polymerization of N‐Butyl Acrylate. *Macromolecules* **2016**, *49*, 5418–5426.

(25) Arzamendi, G.; Asua, J. M. Modeling Gelation and Sol Molecular Weight Distribution in Emulsion Polymerization. *Macromolecules* **1995**, *28* (vii), 7479–7490.

(26) Arzamendi, G.; Leiza, J. R. Molecular Weight Distribution (Soluble and Insoluble Fraction) in Emulsion Polymerization of Acrylate Monomers by Monte Carlo Simulations. *Ind. Eng. Chem. Res.* **2008**, *47*, 5934–5947.

(27) Hutchinson, R. A.; Mcminn, J. H.; Paquet, D. A.; Beuermann, S.; Jackson, C. A Pulsed-Laser Study of Penultimate Copolymerization Propagation Kinetics for

Methyl Methacrylate / n-Butyl Acrylate. *Ind. Eng. Chem. Res.* **1997**, *36*, 1103–1113.

(28) Ballard, N.; Hamzehlou, S.; Ruipérez, F.; Asua, J. M. On the Termination Mechanism in the Radical Polymerization of Acrylates. *Macromol. Rapid Commun.* **2016**, *37*, 1364–1368.

(29) Lakrout, H.; Creton, C.; Ahn, D.; Shull, K. R. Influence of Molecular Features on the Tackiness of Acrylic Polymer Melts. *Macromolecules* **2001**, *34* (21), 7448–7458.

(30) Dahlquist, C. A. Pressure-Sensitive Adhesives. In *L.R. Patrick (Ed.), Treatise on Adhesion and Adhesives*; Dekker, New York, 1969; pp 219–260.

(31) Deplace, F.; Carelli, C.; Mariot, S.; Retsos, H.; Chateauminois, A.; Ouzineb, K.; Creton, C. Fine Tuning the Adhesive Properties of a Soft Nanostructured Adhesive with Rheological Measurements. *J. Adhes.* **2009**, *85* (1), 18–54.

(32) Zhang, X.; Ding, Y.; Zhang, G.; Li, L.; Yan, Y. Preparation and Rheological Studies on the Solvent Based Acrylic Pressure Sensitive Adhesives with Different Crosslinking Density. *Int. J. Adhes. Adhes.* **2011**, *31* (7), 760–766.

(33) Kajtna, J.; Ali, B.; Krajnc, M.; Š, U. Influence of Hydrogen Bond on Rheological Properties of Solventless UV Crosslinkable Pressure Sensitive Acrylic Adhesive Prepolymers. *Int. J. Adhes. Adhes.* **2014**, *49*, 103–108.

(34) Chang, E. P. Viscoelastic Windows of Pressure- Sensitive Adhesives. *J. Adhes.* **1991**, *34*, 189–200.

(35) Chang, E. P. Viscoelastic Properties of Pressure-Sensitive Adhesives. *J. Adhes.* **1997**, *60*, 233–248.

(36) Tobing, S. D.; Klein, A.; Sperling, L. H.; Petrasko, B. Effect of Network Morphology on Adhesive Performance. *J. Appl. Polym. Sci.* **2001**, *81*, 2109–2117.

(37) Lee, J. H.; Lee, T. H.; Shim, K. S.; Park, J. W.; Kim, H. J.; Kim, Y.; Jung, S. Effect of Crosslinking Density on Adhesion Performance and Flexibility Properties of Acrylic Pressure Sensitive Adhesives for Flexible Display Applications. *Int. J. Adhes. Adhes.* **2017**, *74*, 137–143.

(38) Lakrout, H.; Sergot, P.; Creton, C. Direct Observation of Cavitation and Fibrillation in a Probe Tack Experiment on Model Acrylic Pressure-Sensitive-Adhesives. *J. Adhes.* **1999**, *69* (3–4), 307–359.

(39) Stupp, S. I.; Lebonheur, V.; Walker, K.; Li, L. S.; Huggins, K. E.; Keser, M.; Amstutz, A. Supramolecular Materials : Self-Organized Nanostructures. *Science (80-.).* **1997**, *276* (5311), 384–389.

(40) Ouchi, T.; Nagaya, K.; Oiwa, M. Cyclic Acetal-Photosensitized Polymerization. III. Photopolymerization of Styrene in the Presence of 2,4,8,10- Tetra Oxaspiro[5,5]Undecane Compounds. *Polym. Sci.* **1976**, *14*, 2835–2839.

(41) Ouchi, T.; Hamada, M. Cyclic Acetal-Photosensitized Polymerization. II. Photopolymerization of Styrene in the Presence of Various Monocyclic Acetals. *J. Polym. Sci.* **1976**, *14* (8), 2527–2533.

(42) Ouchi, T.; Nakamura, S.; Hamada, M.; Oiwa, M. Cyclic Acetal-Photosensitized Polymerization. I. Photopolymerization of Styrene in the Presence of 1,3-Dioxolanes. *Polym. Sci.* **1975**, *13*, 455–466.

(43) Elad, D.; Yousseffyeh, R. D. The Photochemical Conversion of Acetals to Carboxylic

Esters. *Tetrahedron Lett.* **1963**, No. 30, 2189–2191.

(44) Yang, J.; Shi, S.; Nie, J. Reasons for the Yellowness of Photocured Samples by the Benzophenone/1,3-Benzodioxole Photoinitiating System. *New J. Chem.* **2015**, *39* (7), 5453–5458.

(45) Taghizadeh, S. M.; Diba, G. Rheological and Adhesion Properties of Acrylic Pressure-Sensitive Adhesives. *J. Appl. Polym. Sci.* **2011**, *120*, 411–418.

(46) Mehravar, E.; Gross, M. A.; Agirre, A.; Reck, B.; Leiza, J. R.; Asua, J. M. Importance of Film Morphology on the Performance of Thermo-Responsive Waterborne Pressure Sensitive Adhesives. *Eur. Polym. J.* **2018**, *98*, 63–71.

Chapter 4

Removable biobased waterborne PSAs containing mixtures of isosorbide methacrylate monomers

4.1 Introduction

In Chapter 1, waterborne pressure sensitive adhesives (PSAs) were introduced as materials forming part of our daily consuming goods such as tapes, note pads and labels for paper derivative products, stainless steel, glass, PP and PET bottles or even skin[1,2]. However, due to the growing environmental concerns, recycling processes of those materials containing even small amounts of this kind of adhesives is becoming more and more important[3]. In this context, the development of pressure-sensitive adhesives that would easily remove under mild conditions when applied in recyclable substrates (e.g., glass bottles) would make this process more sustainable than the current technologies that required high temperatures, aggressive solutions and in some applications solvents or harsh reagents[4–6]. This need has made academia and industry to seek for clean adhesion-switching-off technologies, while ensuring a good performance of the waterborne PSA.

A commonly employed chemical strategy is the use of water/alkali-soluble tackifiers. They are low molar mass polymers mainly composed by ethoxylated alkyl phenols and linear glycols or (meth)acrylate copolymers containing elevated amounts of carboxyl groups. These resins are added to the adhesive formulation making it removable under water (cold or hot) and/or alkali conditions[7–14]. However, large amounts (20-70 wt%) are needed and, under high humidity conditions, tackifier is able to migrate from the adhesive to the adjacent substrate[15]. Among the different kind of resins, a synthetic hygroscopic family based on Polyethyloxazoline has been commercialized with the name of Aquazol[16]. When between 50 wt% and 70 wt% of this type of resin is incorporated in adhesive formulations for paper applications a quick removability has been claimed[17].

Another alternative to alkali soluble resins (tackifiers) is the use of water-soluble polymers such as polyvinyl alcohol, polyvinyl methyl ether, polyethyleneamine, polyethyleneimine, polyvinyl pirrolidone, polyacrylamide derivatives, hydroxyl ethyl cellulose

or carboxymethyl cellulose derivatives[18–23]. These polymers act as stabilizers during the emulsion polymerization process, using at different quantities depending on the ratio performance/water sensitivity desired. As example, polyvinyl methyl ether has been used in the range 0.5% to 95%, or carboxymethyl cellulose from about 0.1% to 30%. It is worth to mention that cellulose derivatives has been mostly employed on skin adhesive applications because of their chemical affinity as well as their biocompatibility.

In the context of solventborne PSAs, 3M Company has patented water-soluble pressure sensitive adhesives containing N-Vinyl caprolactam homopolymers (NVC), N-Vinyl pyrrolidone copolymers (NVP) and mixtures thereof for their application in skin bandages[24,25]. Water-removable PSAs have been also produced by the use of hydrophilic macromonomers based on hydroxyalkyl structures (e.g., HEMA derivatives), but it requires a minimum of 15 wt% of these macromonomers and the presence of solvents such as ethyl acetate or isopropyl alcohol for the polymerization process[15,26].

In the previous chapters, the production of biobased waterborne PSAs using both commercial and synthetic monomers was explored, assessed and modified aiming to ensure a good performance at the maximum bio-content degree. Nevertheless, considering the recyclability issues, renewable building blocks having the potential to increase both performance and removability in the final formulation are needed in order to provide products capable to be industrially implemented.

One of the most promising renewable building blocks because of its simple structure and easy functionalization is isosorbide (1,4:3,6-Dianhydrohexitol). Isosorbide is a chiral renewable diol industrially produced from de double dehydratation of D-Sorbitol, which comes from the catalytic hydrogenation of D-Glucose (Scheme 4.1). It is noteworthy that glucose is an easily accessible starting material mostly obtained from the hydrolysis of starch, as feedstock source[27]. The global isosorbide market is expected to reach USD 703.1 million by 2025, exhibiting a compound annual growth rate (CAGR) of 8.5% over the forecast period

(2014-2025)[28]. In this context, Roquette is the largest producer of isosorbide, which is present across the value chain and is engaged in the production of starch, isosorbide, as well as biopolymers (Polysorb®). This V-shaped bicyclic structure presenting two non-equivalent secondary hydroxyl groups has been widely used and modified as building block in the last few years for thermoset[29–31], thermoplastic[32], adhesive[33–35] or dental restorative[36] applications.

Accordingly, the present chapter will be focused in the development of high performance adhesives with the capability to be removed in water at short times. To reach this goal, a non-explored synthetic pathway for the production of a mixture of isosorbide methacrylate derivatives and its purification is presented. Next the analysis of its homopolymer is studied. Furthermore, its use as hard monomer in waterborne PSAs was evaluated in terms of microstructure, adhesion properties and removability by water treatment. Finally, its incorporation in small amounts (1 wt%) as (un)purified monomer on two biobased PSA systems was deeply investigated as well as their adhesion switching-off (or easy removability) in water.

Scheme 4.1. Main synthetic pathway for the isosorbide production and its polymer derivatives.

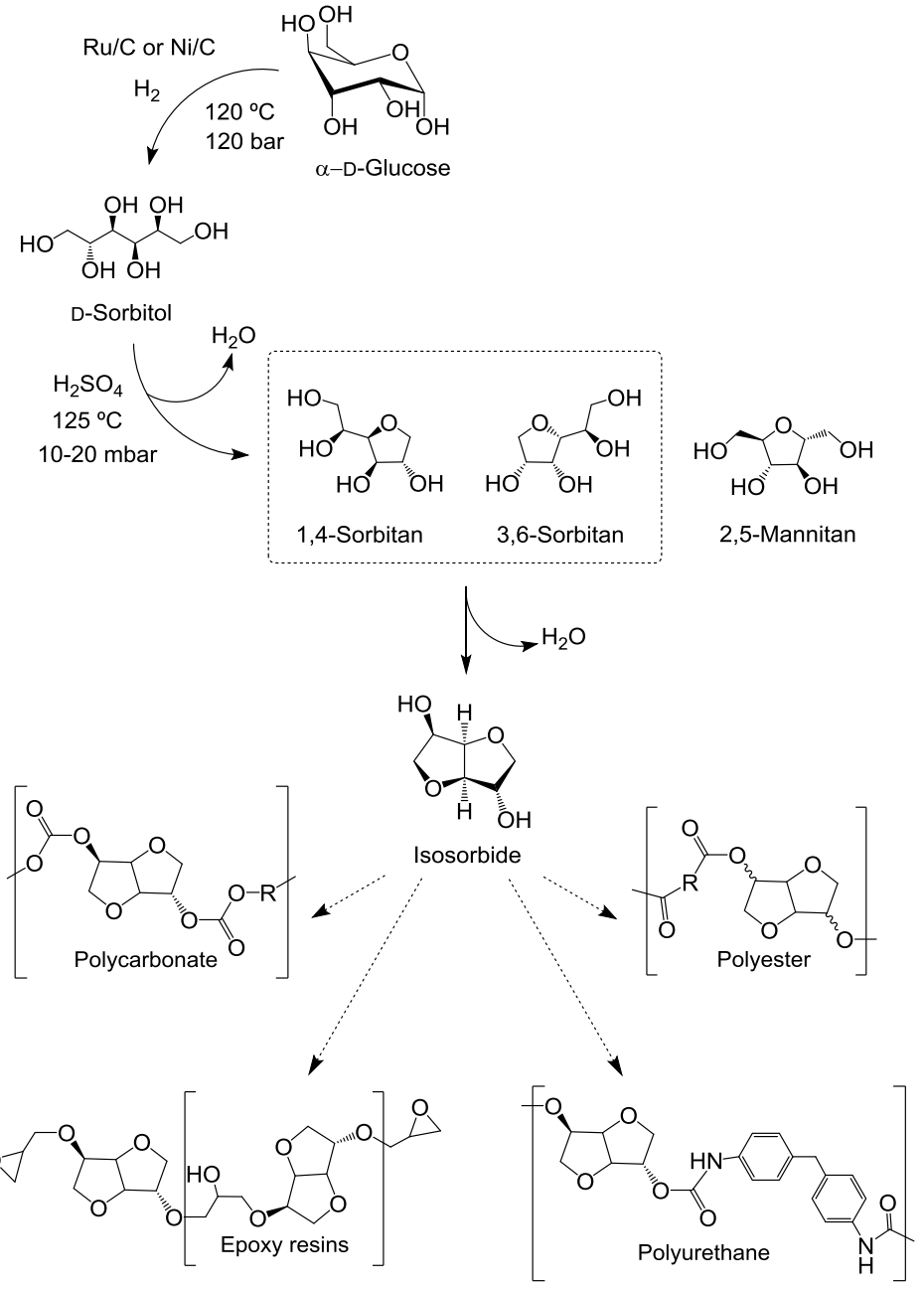

4.2 Experimental

Biobased 2-Octyl acrylate (2OA) was kindly supplied by Arkema (France), and both isobornyl methacrylate (Visiomer® Terra IBOMA) and isobornyl acrylate (Visiomer® Terra IBOA) were kindly supplied by Evonik Industries (Essen, Germany). Acrylic and methacrylic acid (AA, MAA), 2-Ethylhexyl thioglycolate (2EHTG), 1-Butanethiol (1BuSH) and potassium persulfate (KPS) were purchased from Sigma-Aldrich (Saint-Louis, MO, USA). 2,2´-Azobis(2-methylpropionitrile) (AIBN,initiator), methacrylic anhydride (MAAn, 94% inhibitor 2000 ppm of topanol A), 4-(Dimethylamino)pyridine (DMAP, 99%), magnesium sulfate ($MgSO_4$) and sodium bicarbonate ($NaHCO_3$) were purchased from Sigma-Aldrich (Saint-Louis, MO, USA). Isosorbide (98%), toluene, dichloromethane, hexane and ethyl acetate (99+%) were purchased from Fisher Scientific. Dowfax2A1 (Alkyldiphenyloxide Disulfonate) was kindly provided by Dow Chemical (Midland, Michigan, USA). All reagents were used without further purification.

4.2.1 Synthesis of isosorbide methacrylate derivatives (ISOMAraw) and its purification (ISOMA)

Isosorbide (30 g, 0.205 mol) and DMAP (2.51g, 0.021 mol) were partially dissolved in 250 mL of dichloromethane in a 500 mL round bottom flask equipped with stirrer and dropping funnel. The mixture was stirred at room temperature at a rate of 500 rpm for 20 min. Then it was cooled down to 0ºC (ice-bath) and MAAn (21.1 g, 0.137 mol) was added dropwise for 1 hour. The mixture was stirred overnight. The yellowish solution was quenched with $NaHCO_3$ solution (1M, 100 mL) and then extracted with $NaHCO_3$ solution (1M, 2 x 50 mL), distilled water (3 x 50 mL) and washed with brine (3 x 50 mL). The combined organic layers were dried over $MgSO_4$, filtered and evaporated under reduced pressure yielding in a yellowish oil (ISOMAraw). ISOMAraw is the mixture of both monomethacrylic and dimethacrylic isosorbide

in a molar ratio 4:1. The further purification by column chromatography (SiO_2) using as eluent hexane/ethyl acetate (6:4 v/v) allows the isolation of the monomethacrylic monomer (ISOMA) as a colorless oil. The yields were 56% (ISOMAraw) and 35% (ISOMA), respectively.

4.2.2 Solution homopolymerization of isosorbide 5-methacrylate (ISOMA)

(Poly)isosorbide methacrylate (PolyISOMA) was obtained by solution polymerization. For its preparation, 1g of monomer was dissolved in 4g of toluene in a 25 mL volume round bottom flask equipped with a magnetic bar. The reaction was carried out at 70ºC along 5 hours under nitrogen atmosphere using AIBN (1 wbm %) as initiator. Along the reaction, a white insoluble solid in toluene was obtained. The solid was filtered off, washed with toluene and dried under reduced pressure.

4.2.3 Emulsion polymerization

All the latexes were produced via starved-feed seeded semibatch emulsion polymerization using the same procedure than in chapter 2. The polymerization process included the loading of the seed and a small amount of monomers in the reactor, feeding of a pre-emulsion of monomer during 3 h and a final post-polymerization step of 1 h to fully react the remaining monomers. Reactions were performed at 70ºC and 200 rpm, being 50 wt% the final solids content. The general polymerization formulation is shown in Table 4.1.

Table 4.1. Materials and percentages employed in the synthesis of the latexes.

Materials		wbm %*	Amount (g)
Seed	2OA/IBOA/AA		24.10
Low Tg monomer	2OA	84	38.96
High Tg monomers	IBOMA PIPEMA ISOMAraw	14-15	6.50-6.96
Functional monomers	MAA ISOMAraw ISOMA	1	0.46
Chain transfer agent	2EHTG 1BuSH	0.025-0.05 0.075	0.0116-0.0232 0.0348
Emulsifier	Dowfax2A1	1	1.031
Initiator	KPS	0.25	0.116
Continuous phase	Water		28.60

*weight % based on total monomer content.

4.2.3 Characterization

Particle size was analyzed by dynamic light scattering (DLS) and conversion was determined gravimetrically. Gel fraction (or insoluble fraction of the copolymer in THF) was measured by Soxhlet extraction.

The molar mass distribution of the soluble fraction in THF was determined by both size exclusion chromatography (SEC) at 35°C and asymmetric flow field-flow-fractionation (AF4) (Eclipse 3) in combination with a multiangle light scattering (MALS, Dawn Heleos II) and a refractive index detector (RI, Optilab Rex). AF4 flow was controlled by Eclipse 3 AF4 Separation System controller (the whole setup from Wyatt Technology). During the separation along the channel in the AF4, the detector-flow was kept constant at 1 mL/min. On the other hand the cross-flow was exponentially decreased from 3 mL/min to 0.05 mL/min except for the Latex **2C.1** where the cross-flow was decreased in a linear mode from 3 mL/min to 0.05 mL/min

The glass transition temperature (T_g) was determined by differential scanning calorimetry (DSC, Q1000, TA Instruments) using the same conditions than in chapter 2.

The film preparation, the evaluation as PSA and the dynamic mechanical analysis (DMA) were performed using the same conditions and procedures than in chapter 2.

Liquid-state Proton Nuclear Magnetic Resonance (^{1}H NMR) was recorded on a Bruker 400 MHz equipment.

4.2.4 Removability studies

The removability studies were performed at room temperature and at 65 ºC in water. For that purpose, peel test was carried out using glass as substrate. The adhesive tapes were attached to the substrate and they were submerged into water. Four samples were tested for each formulation and the average values were reported before and after being submerged in water.

4.3 Synthesis of isosorbide methacrylate derivatives (ISOMAraw) and its purification (ISOMA)

Isosorbide is a chiral bicyclic structure presenting two secondary hydroxyl groups at C2 and C5 sites, usually called *exo* and *endo* positions, respectively[37,38]. This chirality together with the V-shaped like structure gives reactivity differences depending on the material used for its functionalization, since *endo*-OH and *exo*-OH have different molecular environments[29,31,39,40]. Although *endo*-OH is more sterically hindered due to the bicyclic conformation, it is also more nucleophilic because of the intramolecular hydrogen bonding with the oxygen of the opposite tetrahydrofuran ring (Figure 4.1). In addition, numerous studies have been carried out about the reactivity of this alcohol, which can be promoted with the use of catalysts[30,32,35,36]. There are only few works describing the monomethacrylation of

isosorbide in the *endo* position. In the open literature, both a five-step method and an enzymatic method for the synthesis of isosorbide 5-methacrylate have been reported[41,42], while there are patents in which regioisomeric mixtures of monomethacrylates have been synthesized[43,44].

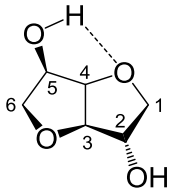

Isosorbide

Figure 4.1. Structure of isosorbide.

For the synthesis of isosorbide 5-methacrylate, methacrylic anhydride together with small amounts of a nucleophilic catalyst were used in order to promote the electrophilicity of the carbonyl group of the anhydride and thus the attack by the *endo*-alcohol. The use of dichloromethane as solvent could prevent the undesired cleavage of the anhydride yielding methacrylic acid[31]. Scheme 4.2 shows the reaction pathway to produce isosorbide 5-methacrylate (ISOMA).

Scheme 4.2. Synthesis of ISOMAraw and ISOMA from isosorbide and MAAn.

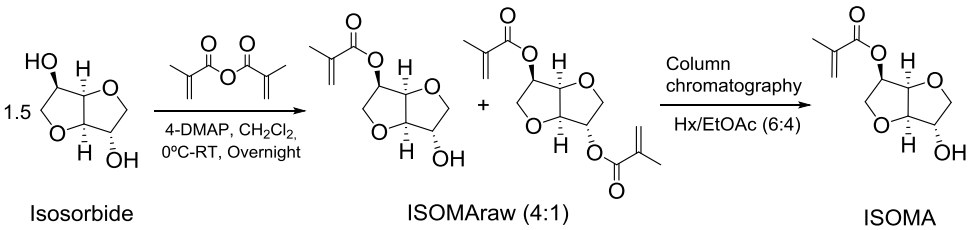

Isosorbide ISOMAraw (4:1) ISOMA

As described in the experimental section, 1.5 equivalents of this sugar were used in order to minimize the dimethacrylate counterpart, which is produced in the later stage of the

reaction by the alcohol at C2 position (*exo*-OH). After this first stage a yellowish oil (ISOMAraw) was obtained with a yield of 56%, being the mixture of both monomethacrylate and dimethacrylate isosorbide in a molar relation 4:1, calculated by ^{1}H NMR. This product can be used as raw material in adhesive formulations or could be purified by column chromatography using a mixture of hexane and ethyl acetate (6:4) as eluent. Figure 4.2 (a) shows the ^{1}H NMR spectrum of ISOMAraw in chloroform-d_1, observing the monomethacrylate isosorbide as major product. Proof of this is the multiplet at 4.3 ppm corresponding to the proton at the position C2 of the bicyclic, this is the one next to the free OH group.

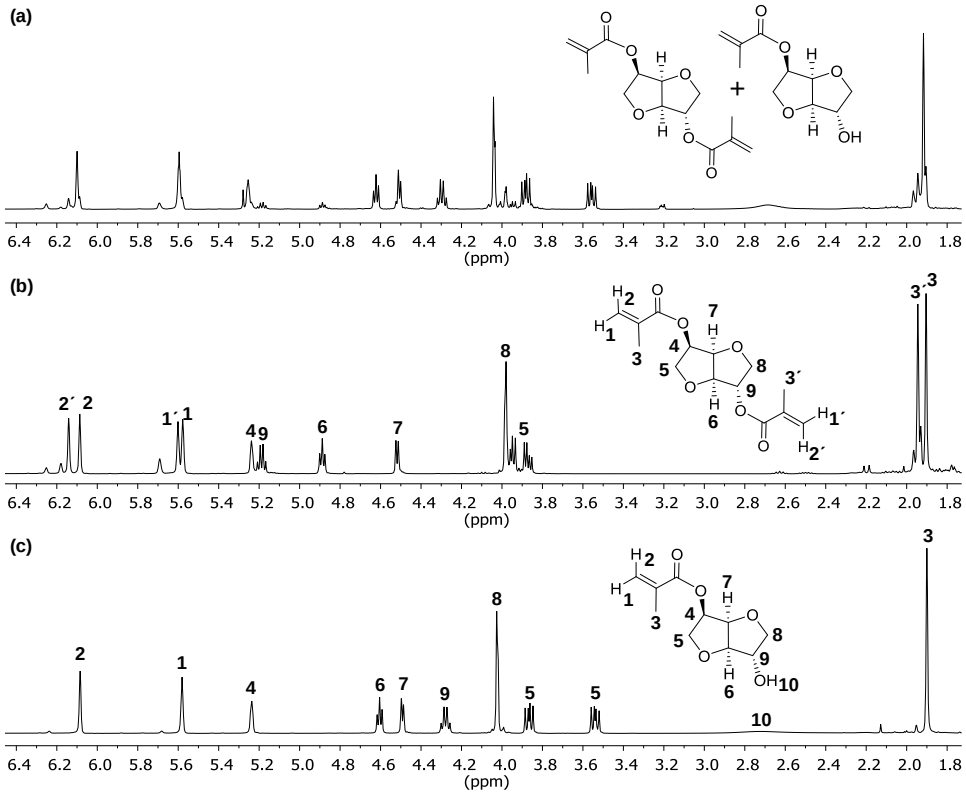

Figure 4.2. ^{1}H NMR spectra in chloroform-d_1 of (a) ISOMAraw, (b) isosorbide dimethacrylate and (c) isosorbide 5-methacrylate. Note that the spectra are showed in order of the chromatographic column elution time.

The subsequent purification allowed to separate the dimethacrylate product (Figure 4.2.b) and then the monomethacrylate one (Figure 4.2.c) as a colorless oil (ISOMA) with a final yield of 35% and a bio-content of 60%. However, small signals were detected around 5.7 and 6.3 ppm in both fractions, corresponding to the (meth)acrylic units chemical shift. This is indicative of the formation, in a small quantity, of the *exo*-methacrylate (Isosorbide 2-methacrylate) which has a lower presence (<1%) in the final product.

The monomer mixture based on mono and dimethacrylate isosorbide has two different functional groups: a methacrylic group, susceptible to be polymerized via free radical and a hydroxyl group giving cohesion and water-affinity (Scheme 4.3).

Scheme 4.3. Synthetic biobased monomer mixture used in this chapter and its bio-content, where the green part belongs to the carbon structure coming from the nature.

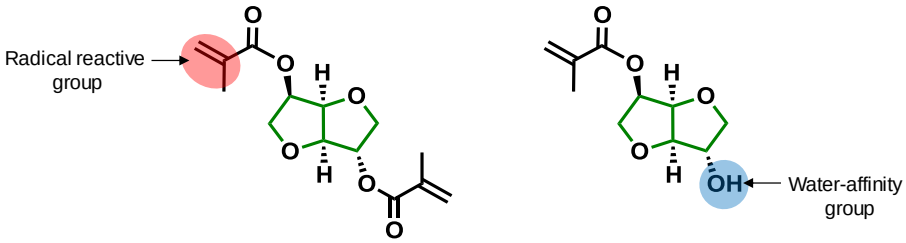

Isosorbide dimethacrylate (43%) **Isosorbide 5-methacrylate ISOMA (60%)**

4.4 Solution homopolymerization of isosorbide 5-methacrylate (ISOMA)

Solution homopolymerization of the synthetic biobased monomer isosorbide 5-methacrylate was performed using toluene as solvent and AIBN as thermal initiator. A white crystalline solid was obtained (polyISOMA) as the reaction advanced as consequence of the insolubility of the homopolymer in the reaction medium, reaching a conversion higher than 99% (calculated by ^{1}H NMR integration).

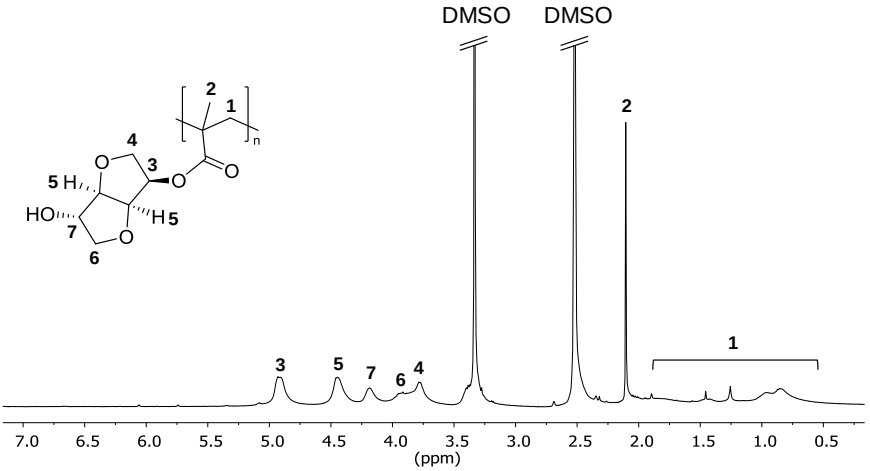

Figure 4.3. ^{1}H NMR spectra in DMSO-d_6 of (Poly)isosorbide 5-methacrylate (PolyISOMA).

Differential scanning calorimetry provided the thermal transition of polyISOMA (Figure 4.4), which presents a glass transition temperature around 80 ºC because of the pendant hetero-bicyclic structure, being able to play the role of hard monomer in PSA formulations. It is worthy to mention that a Tg of 140 ºC has been reported for the homopolymer of isosorbide dimethacrylate[31]. This value is related with both the absence of flexibility of the molecule and the high crosslinking density limiting the molecular motions[45].

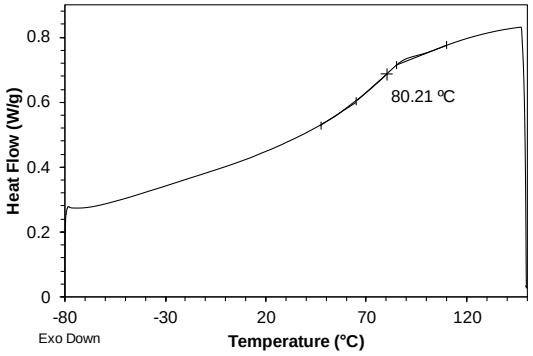

Figure 4.4. DSC curve of polyISOMA at a heating rate of 20 ºC/min.

4.5 Waterborne PSAs using ISOMAraw and ISOMA as hard monomer: Comparison with IBOMA and PIPEMA

Aiming to investigate the effect of the hard monomer nature on the performance of the waterborne biobased PSAs, a comparison study of PSAs produced from latex formulations having IBOMA (**2C.1** from Chapter 2), PIPEMA (**3B.1** from Chapter 3) and ISOMAraw was carried out. Table 4.2 summarizes the compositions of the latexes synthesized as well as their main properties including average particle size (dp), gel content, the soluble weight average molar mass (Mw), dispersity index (Đ) and Tg of the copolymer.

Table 4.2. Summary and characteristic of PSA latexes containing different kind of hard monomer.

PSA	Composition (%wt monomers)	Dp (nm)	Gel (%)	Mw (kDa)	Đ	Tg (°C)	Bio (%)
2C.1	2OA:IBOMA:MAA + CTA* (84:15:1 + 0.025*)	230	59 ± 0.4	313 ± 4	3.7	-26	72
3B.1	2OA:PIPEMA:MAA + CTA* (84:15:1 + 0.025*)	231	53 ± 2	300 ± 1	3.9	-38	71
4A.1	2OA:ISOMAraw:MAA + CTA* (84:15:1 + 0.025*)	230	83 ± 0.1	191 ± 1	4	-34	71

*Weight percent of 2EHTG based on monomer.

It is worth to mention that a formulation with 15 wt% of ISOMA (isosorbide 5-methacrylate) was also attempted, but the system started to be unstable at 30-60 min of reaction (aggregation of particles) yielding a large amount of coagulum at the end of the process. Figure 4.5 shows the average particle size evolution during the synthesis of the latexes containing ISOMA or ISOMAraw in their formulation. The higher water solubility of ISOMA led to the formation of aqueous soluble polymer chains at the beginning of the feeding process. Those species, in addition to increasing the viscosity of the aqueous phase, promote inter particle interactions (by hydrogen bonding) leading to bridging flocculation and coagulation[46–50]. This scenario was not observed for ISOMAraw since the presence of dimethacrylate units provide enough hydrophobicity to avoid water-soluble polymer species

and, hence, the coagulation. A remarkable difference in the microstructure of the formulation **4A.1** (with ISOMAraw) is the substantially higher gel content produced (83% vs 53-59%). This was expected because of the presence of around 3 wt% (with respect to the whole monomer in the formulation) of the dimethacrylate species in the ISOMAraw.

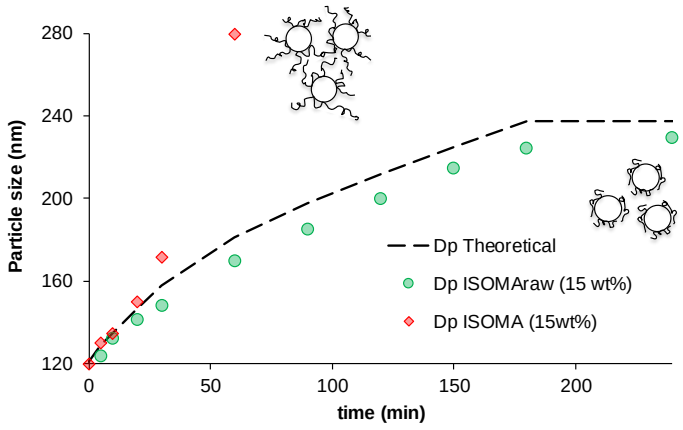

Figure 4.5. Theoretical and experimental average particle size evolution measured by DLS in the synthesis of latexes contaning 15 wt% of either ISOMA (red diamonds) or ISOMAraw (green circles) as hard monomer.

The adhesive properties of these formulations are presented in Table 4.3. As it was described in the previous chapter, when PIPEMA was used in the formulation a lower gel content copolymer with a lower glass transition temperature was produced, which enhanced the polymer fluidity and thus increased tackiness and peel strength and reduced both shear resistance and holding temperature. The use of ISOMAraw in formulation **4A.1** led to a material with poor tack presenting very low values of both peel strength and loop tack. The explanation for such elastic behavior is the high crosslinking density, which reduced the polymer chain motion, affecting the work of adhesion and increasing both the holding temperature (200 ºC) and shear resistance (>7 days).

Table 4.3. Adhesive properties of PSA tapes with the formulation 2OA: Hard monomer: MAA + CTA* (84:15:1 + 0.025 wbm%).

PSA	Peel (N/25mm)	Loop tack (N/25mm)	WA (J/m^2)	Shear resistance (min)	SAFT (°C)
2C.1 (IBOMA)	6.7 ± 0.7	7.7 ± 0.3	139 ± 14	8640	133 ± 1
3B.1 (PIPEMA)	7.9 ± 0.7	10 ± 1	197 ± 32	90 ± 10	64 ± 5
4A.1 (ISOMAraw)	3 ± 1	0.6 ± 0.2	8 ± 2	>10080	200

CTA*: 2EHTG

The lack of tackiness of formulation **4A.1** is well reflected in the probe tack curve shape presented in Figure 4.6, which corresponds to a material with a remarkable solid-like behavior. This highly crosslinked polymer network led to an increase of the stress peak at low strain values followed by a fast breakage without the observation of fibrillation process, yielding in a "brittle" fracture[51–53]. On the other hand, the increase of the viscous behavior because of the gel content reduction in formulations **2C.1** and **3B.1** promoted the fibrils formation and, hence, the release of energy through them during the debonding process. This was deeply discussed in the previous chapters.

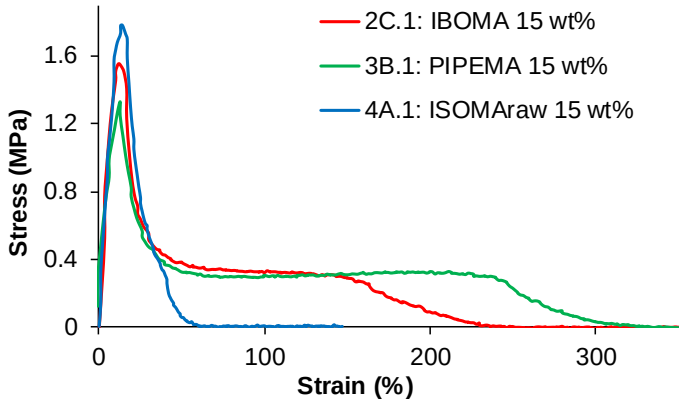

Figure 4.6. Probe tack curves for formulations containing different kind of hard monomer.

4.6 Removability studies in water

It is well known that the hydrophilicity of a monomer can promote its incorporation on the surface of the polymer particles in emulsion polymerization processes[54,55]. Concerning this, the free hydroxyl group of the isosorbide derivative monomer could allow its incorporation on the surface of the growing particles. This strategy could improve the adhesion properties of the tape on glass substrates as well as its removability in water.

Scheme 4.4 illustrates this process, in which part of the OH groups of the particle would be directed towards the outside (air-adhesive interlayer) after the drying process, during the film formation. Those free hydroxyl groups may interact with silanol groups via hydrogen bonding improving mechanical properties, but it could also increase the sensitivity to water (interaction with water could lead to this non-covalent bond breakage). In order to proof this, 180º peel strength measurements on glass substrates before and after water treatment were performed. For that, the attached adhesive tapes were submerged into water at room temperature and the force needed to detach them was measured at different immersion times.

Scheme 4.4. Disposition of the OH groups of the particles surface after the drying process and their interaction with the glass substrate.

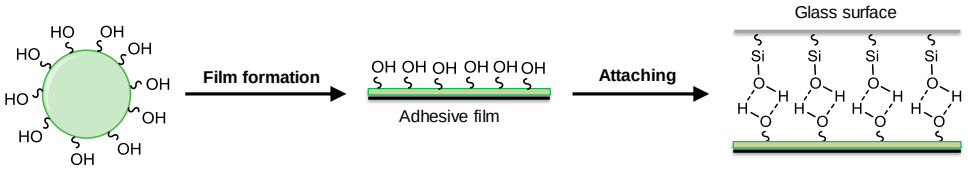

Figure 4.7 shows the peel test results for the formulations of this section. As it can be observed the adhesion properties of those tapes containing IBOMA or PIPEMA in their formulation did not suffer a relevant change after 1 hour of water treatment, but the peel

resistance substantially reduced after 3 hours of immersion. In addition, formulation **2C.1** displays higher force values than formulation **3B.1** on glass substrates, which was not the case on stainless steel (Table 4.3). These results are related with the hydrophilic/hydrophobic nature of the adhesive but also with the differences in the surface energy between the adhesive layer and the substrate and how polymer chains can be adapted to the surface imperfections (cracks and holes)[1,56]. On one hand, it is well know that the pendant isobornyl group of IBOMA increases the space among the polymer chains leading to an increase of their flexibility, enhancing the penetration through the cracks and holes and, thus, improving the adhesion[57], which is more pronounced for glass because of its higher surface energy. On the other hand, aromatic interactions of PIPEMA (formulation **3B.1**) would have a great effect for stainless steel substrates, due to the chemical affinity in hydrophobic systems[58], but not on glass surfaces, where polar moieties such as carboxylic, hydroxyl, or amino groups would be needed. This situation was observed for formulation **4A.1**, that showed a remarkable increase of peel strength (from 3 ± 1 in steel to 7.6 ± 0.2 N/25 mm in glass). The free hydroxyl groups of ISOMA interact via hydrogen bonding with the silanol groups of the glass (Scheme 4.4) enhancing the adhesiveness and, therefore, the force needed for the detachment. Moreover, the hydrophilicity of this adhesive film promoted its removability in water, reducing the peel strength in almost three times after 10 min and getting a complete removal in 20 min.

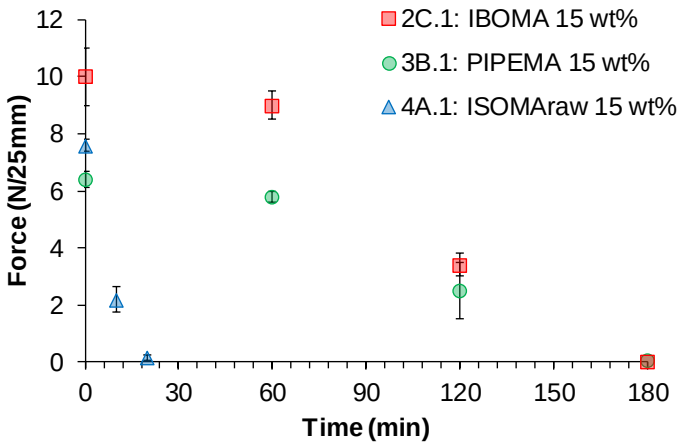

Figure 4.7. Evaluation of 180º peel strength at different times of water treatment at room temperature on glass of PSA tapes with the formulation 2OA: **Hard monomer**: MAA + CTA* (84:**15**:1 + 0.025 wbm%).

4.7 Incorporation of ISOMAraw/ISOMA as functional monomer in waterborne PSAs with IBOMA as hard monomer

In view of the effects of ISOMA (monomethacrylate) and ISOMAraw (mixture of mono and dimethacrylate) on the polymerization and the performance of the adhesives and its removability in water, it was considered to use them in the formulation of waterborne adhesives at lower percentages, namely, as functional monomer rather than as hard monomer. Thus, ISOMAraw or ISOMA monomers were incorporated in compositions **2C.1** and **3B.1** (see below) with the goal to enhance both the removability of the adhesive tapes and their performance.

Table 4.4 summarizes the latexes synthesized for this purpose as well as their main properties including particle size (dp), gel content (measured by soxhlet extraction), swelling of the gel polymer (measured from the AF4/MALS/RI analysis) and the glass transition temperature.

Table 4.4. Properties of the PSA latexes containing 2OA:IBOMA as main formulation, and ISOMA and ISOMAraw as functional monomer.

PSA	Composition (%wt monomers)	dp (nm)	Gel (%)†	Tg (°C)	Bio (%)
	2OA:IBOMA: ISOMAraw:MAA				
2C.1*	84:15:0:1	230	59 ± 0.4	-26	72
4C.1*	84:14:1:1	236	65 ± 0.5	-27	72
4C.2**	84:14:1:1	235	55 ± 1	-27	72
	2OA:IBOMA: ISOMA:MAA				
4C.3**	84:14:1:1	235	50 ± 1	-29	72

* and ** make reference to 0.025 wbm% and 0.05 wbm% of 2EHTG, respectively.

† The fraction of the copolymer that does not dissolve in THF after 24 h of soxhlet extraction.

Figure 4.8 presents the molar mass distributions determined using AF4/MALS/RI. As in the previous chapter, bimodal molar mass distributions were obtained with the high molar mass peak centred at around 10^9 Da and the low molar peak at around 10^5-10^6 Da. The incorporation of ISOMAraw in formulation **4C.1**, using the same amount of CTA than the reference formulation **2C.1**, increased the insoluble polymer fraction (gel polymer) and this was more crosslinked as reflected in the MMD that showed a slight shift of the high molar mass mode. At the same time the low molar mass mode shifts to lower masses because of the preferential incorporation of the high molar masses to the gel polymer (the high molar mass mode). When the CTA amount was increased (formulation **4C.2**) the gel content decreased and the high molar mass peak slightly shifted to lower values, indicating a less crosslinked polymer network due to the reduced efficiency of the isosorbide dimethacrylate crosslinker at higher chain transfer agent concentrations. Furthermore, the low molar mass mode was shifted to even lower values than formulation **4C.1** due to the combined effect of less crosslinking reactions and shorter kinetic chain lengths.

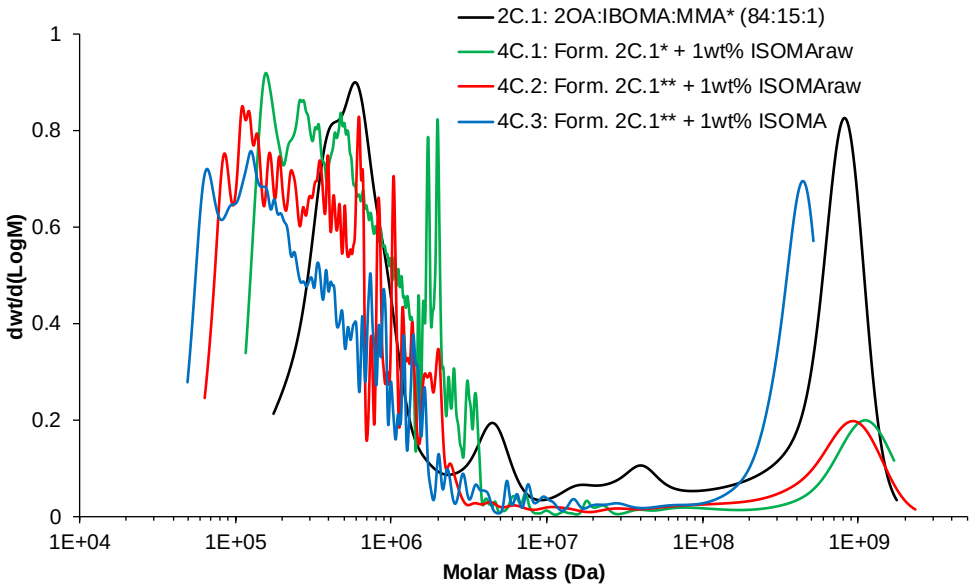

Figure 4.8. Molar mass distributions measured by AF4/MALS/RI for the latexes containing 2OA:IBOMA as main formulation and ISOMA or ISOMAraw as functional monomer.

The substitution of ISOMAraw by ISOMA, namely, the elimination of isosorbide dimethacrylate in formulation **4C.3** led to the lowest gel content (measured by soxhlet extraction). Both, the high molar mass and low molar mass modes of the MMD distribution were shifted to lower molar masses in good agreement with the lack of dimethacrylate monomer and the highest concentration of CTA used.

In conclusion, all the formulations of the 2OA/IBOMA system presented bimodal molar mass distributions and the incorporation of ISOMAraw (1 wt%) slightly increased the molar mass and the crosslinking density of the high molar mass mode. The addition of further CTA was necessary to maintain the insoluble polymer fraction below 60%.

4.7.1 Rheological investigations of waterborne PSAs containing IBOMA as hard monomer and ISOMAraw/ISOMA as functional monomer

Dynamic rheological experiments were carried out aiming to correlate the microstructure of the adhesives together with their viscoelastic properties. Figure 4.9 shows the variation of storage and loss modulus and the damping factor with the frequency at 23 ºC. All formulations presented storage modulus values below 0.1 MPa and a value of tanδ/G´ > 5 MPa^{-1}, forming a good contact in a short time[59,60].

It can be observed that formulation **4C.1** showed the lowest value of both G´ and G´´ at the debonding frequency (1 Hz). The result for the loss modulus was because of the higher gel content (higher crosslinking density of the high molar mass fraction), which reduced the viscous behavior of the material. Nonetheless, the elastic component of the material (related with G´) is not consistent with this microstructure. This could be related with the presence of molecular chains with lower molar masses (see Figure 4.8, green line), which reduced the capability for storing energy but increased the dissipation of energy. Higher moduli (G' and G'') values were observed for formulations **4C.2** and **4C.3**, not showing relevant differences regarding the viscous component. At this point, it seems that the enhancement of the chain mobility, because of the higher amount of CTA, promotes supramolecular interactions (hydrogen bonding between isosorbide moieties), which contribute to the absorption (elastic component), but also to the dissipation (viscous component) of energy. The increase in the solid-like behavior was also reflected in the energy dissipation capability at the interphase adhesive-substrate (tanδ/G´), whose value fell off.

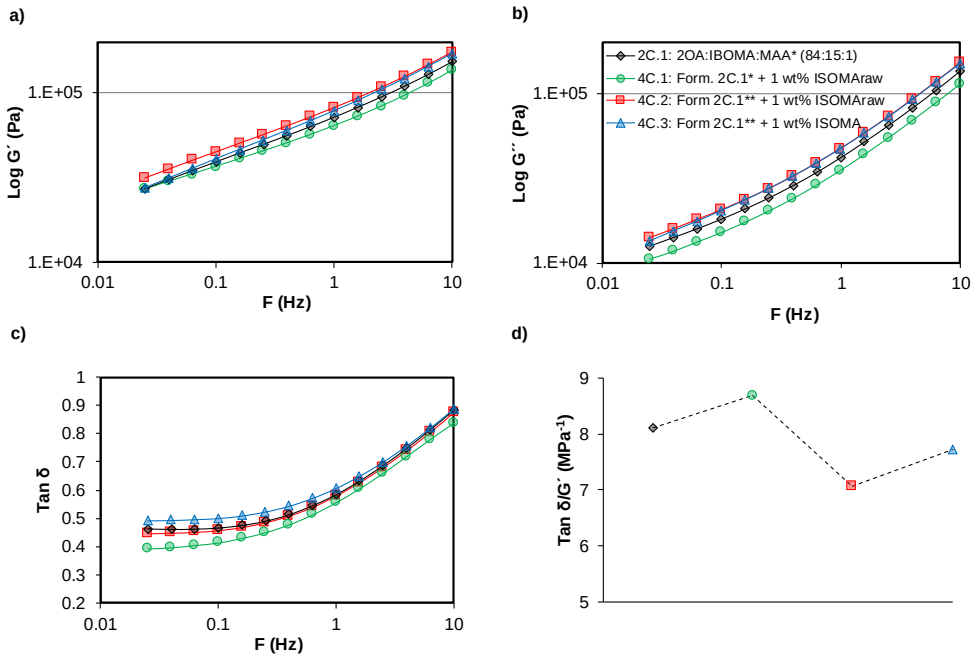

Figure 4.9. (a) Storage modulus (G´), (b) loss modulus (G´´), c) dynamic modulus (tanδ) and (d) tanδ/G´ for 2OA:IBOMA formulations containing ISOMA or ISOMAraw as functional monomer. Measurements made at 23 ºC and 1 Hz.

4.7.2 Adhesive properties of waterborne PSAs containing IBOMA as hard monomer and ISOMAraw/ISOMA as functional monomer

The adhesive properties of these four latexes are shown in Table 4.5. The presence of ISOMAraw in formulation **4C.1** reduced a little bit the peel strength without affecting tackiness and work of adhesion. This lightly crosslinked polymer network resulted in a higher holding temperature, but lower shear resistance, likely because the presence of low molar mass polymer chains reduced the cohesiveness of the adhesive along time. The decrease of the gel content in formulation **4C.2** enhanced the polymer chain mobility, namely, the liquid-like behavior, improving both peel strength and loop tack, but affecting shear resistance and SAFT. Formulation **4C.3** used ISOMA and as shown in Figure 4.8 (blue line) the high molar

mass peak shifted to lower values and gel content decreased. This was translated into an increase of the instantaneous adhesion as well as the work of adhesion. However, due to reduction in the cohesiveness both peel strength and shear resistance were decreased. It is noteworthy that an adhesive failure was observed for all the formulations.

Table 4.5. Adhesive properties of the PSA tapes containing 2OA:IBOMA as main formulation.

PSA	Composition	Peel (N/25mm)	Loop tack (N/25mm)	WA (J/m^2)	Shear resistance (min)	SAFT (°C)
	2OA:IBOMA: ISOMAraw:MAA					
2C.1*	84:15:0:1	6.7 ± 0.7	7.7 ± 0.3	139 ± 14	8640	133 ± 1
4C.1*	84:14:1:1	5.5 ± 0.4	7.2 ± 0.2	128 ± 10	1530 ± 60	157 ± 5
4C.2**	84:14:1:1	8.9 ± 0.5	8.3 ± 0.3	144 ± 10	1110 ± 60	130 ± 5
	2OA:IBOMA: ISOMA:MAA					
4C.3**	84:14:1:1	7.2 ± 0.6	9.4 ± 0.5	176 ± 20	510 ± 3	120 ± 2

* and ** makes reference to 0.025 wbm% and 0.05 wbm% of 2EHTG, respectively.

Figure 4.10 shows the probe tack curves for these formulations. At first view, the incorporation of ISOMAraw provided stronger but also more flexible adhesive fibrils. Regarding this, the presence of a substantial fraction of the polymer (the high molar mass mode) forming a covalent crosslinked network enhanced the solid-like behaviour, but the low molar mass fraction also promoted the motion of the polymer chains, yielding stiff and flexible fibers. As consequence, a broader stress peak at lower strain values followed by a longer fibrillation plateau at higher stress was observed for formulation **4C.1**. There is a reduction of the rate at which the cracks, formed by the cavitation process, propagate to the interface resulting in a greater elongation of the fibrils formed[61]. Formulation **4C.2** showed even a longer elongation at break with a little reduction of the plateau height because of the greater

viscous behaviour. The decrease in tanδ/G´ value is in agreement with the broader initial stress peak in the probe tack curve, which is related with a greater contribution of G´.

The use of ISOMA in formulation **4C.3** yielded an interesting shape of the probe tack curve obtained. The stress plateau suggests a reinforcement of the adhesive fibrils during the dissipation of energy, showing a slight shoulder which breaks around 420% of strain. This reinforcement could be attributed to supramolecular interactions (hydrogen bonding interactions) which promote the ability for storing energy during the elongation and releasing it in a sharply way. In this context, there is an interfacial contribution of supramolecular bonds among the polymer chains, namely, the motions within the walls of the cavities[62,63]. Moreover, the less-constricted polymeric structure provides a greater movement promoting the hydrogen bonding and hence the alignment of the polymer chains.

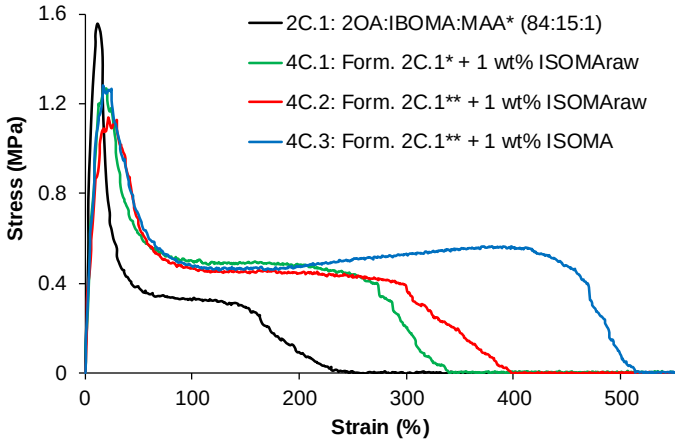

Figure 4.10. Probe tack tests for 2OA:IBOMA formulations.

The form of the probe tack curve of the formulation containing ISOMA (**4C.3**) is in accordance with the rheological results, since the hydrogen bonding interactions benefit the solid-like behavior, namely, the storage modulus (G´), affecting to the tanδ/G´ value.

4.7.3 Removability studies of waterborne PSAs containing IBOMA as hard monomer and ISOMAraw/ISOMA as functional monomer

In order to know the impact of small fractions of this sugar derivative monomer in the water sensitivity of the adhesive tapes, removability studies were performed. The peel strength of adhesive films adhered on glass and immersed in water (at room temperature as well as at 65 ºC). The results are shown in Figure 4.11. The incorporation of only 1 wt% of ISOMAraw in the case of the formulations **4C.1** and **4C.2** promoted their complete detachment after 40 min without letting any noticeable adhesive residue on the glass surface. On the other hand, the use of ISOMA in formulation **4C.3** increased the peel strength on the glass surface before the water treatment and promoted even faster the posterior detachment, reaching the complete removal in almost 30 min. Finally, Figure 4.11.b shows that the water treatment at 65 ºC sped up the process, achieving complete removal of the adhesive tapes in 10 min for those formulations containing the isosorbide derivative monomer.

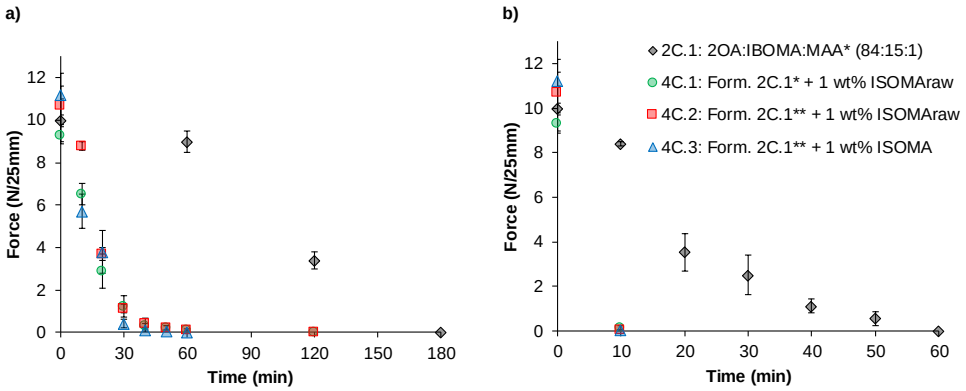

Figure 4.11. Evaluation of 180º peel strength at different times of water treatment at room temperature (a) and at 65 ºC (b) on glass for PSA tapes containing 2OA:IBOMA as main formulation and ISOMA or ISOMAraw as functional monomer.

4.8 Incorporation of ISOMAraw/ISOMA as functional monomer in waterborne PSAs with PIPEMA as hard monomer

Following the line of the last section, 1 wt% of ISOMAraw/ISOMA was incorporated in formulation **3B.1**. Table 4.6 summarizes the latexes synthesized together with their main properties.

Table 4.6. Properties of the PSA latexes containing 2OA:PIPEMA as main formulation.

PSA	Composition (%wt monomers)	dp (nm)	Gel (%)†	Tg (°C)	Bio (%)
	2OA:PIPEMA: ISOMAraw:MAA				
3B.1*	84:15:0:1	231	53 ± 2	-38	71
4B.1*	84:14:1:1	234	58 ± 0.1	-36	71
4B.2**	84:14:1:1	232	50 ± 1	-36	71
	2OA:PIPEMA: ISOMA:MAA				
4B.3**	84:14:1:1	231	32 ± 0.5	-36	71

* and ** make reference to 0.025 wbm% and 0.075 wbm% of 2EHTG and 1BuSH, respectively.

† The fraction of the copolymer that does not dissolve in THF after 24 h of soxhlet extraction.

Figure 4.12 shows the molar mass distributions determined using AF4/MALS/RI. As shown in Chapter 3 the molar mass distribution for the 2OA/PIPEMA formulations were also bimodal, the high molar mass peak in the range 10^8-10^9 Da (although lower values than for the 2OA/IBOMA system) and the low molar mass peak between 10^4-10^6 Da. The addition of ISOMAraw (at two different concentrations of CTA, formulation **4B.1** and **4B.2**) and of ISOMA (formulation **4B.3**) affected the MMD in a similar manner than for 2OA/IBOMA formulations. Adding ISOMAraw at the same CTA concentration clearly shifted the high molar mass peak at higher values (green line) decreasing the molar mass of the low mode at the same time. The gel content, in agreement with this trend, increased to 58%. The increase of CTA for the

same concentration decreased the molar mass of the high molar mass mode (making it smaller than for the pure 2OA/PIPEMA) and the low molar mass mode also shifted to slightly lower values.

The addition of ISOMA affected the MMD of the latex in a similar manner, both, the high molar mass mode and the low molar mass mode shifted to lower molar masses in agreement with the substantially lower insoluble polymer measured in the soxhlet (30% as compared with values above 50% for the other formulations). The low molar mass mode also shifted to lower masses. These effects were not as pronounced for the 2OA/IBOMA formulations.

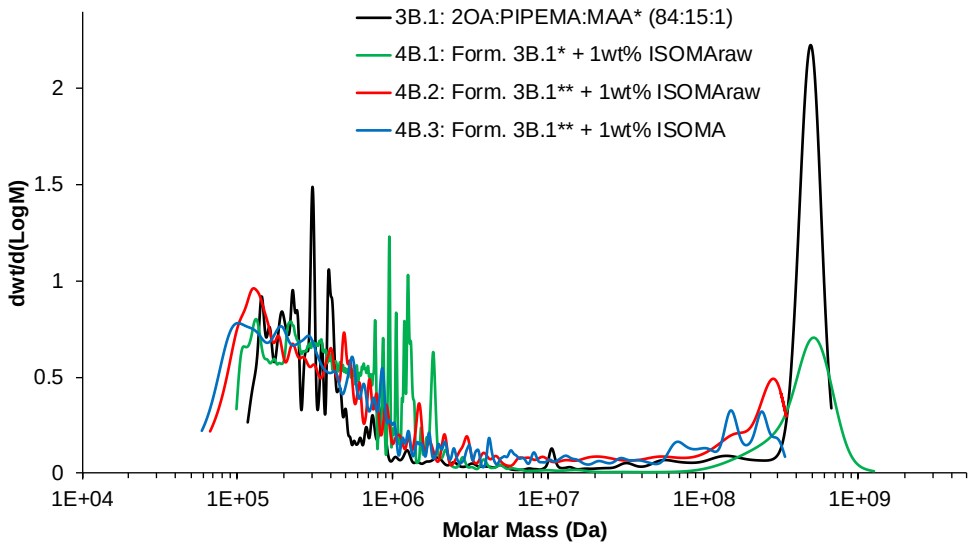

Figure 4.12. Molar mass distributions measured by AF4/MALS/RI for the latexes containing 2OA:PIPEMA as main formulation.

4.8.1 Rheological investigations of waterborne PSAs containing PIPEMA as hard monomer and ISOMAraw/ISOMA as functional monomer

Concerning the dynamic viscoelastic measurements, all formulations of **4B** series presented higher values of both G´ and G´´ than those ones for formulation **3B.1** (Figure 4.13). Nevertheless, this formulation showed the best relationship between elastic and viscous behavior, yielding the best energy dissipation. The storage modulus was especially high in formulation **4B.1** because of the high molar mass of the insoluble fraction (see Figure 4.12, green line), which affected to the motion of the polymer chains and, therefore, to the energy dissipation. The solid-like behavior of the adhesive decreased in formulation **4B.2**, providing a lower value for the storage modulus and, consequently, higher tanδ/G´. Although similar values of storage modulus (G´), in the whole range of frequencies, were obtained for formulations **4B.2** and **4B.3**, the damping factor (Tanδ) was higher for the later. This might be related with the presence of several low molar mass polymer chains (Figure 4.12, range $4x10^4$-10^6 Da, blue line) promoting the liquid-like behavior. However, similar values of tanδ/G´ at the debonding frequency were obtained for these formulations (Figure 4.13.d) because of the compensation between G´´ and G´. It is worth to mention that formulations containing PIPEMA present a higher dissipation of energy at the interface adhesive-substrate than those ones containing IBOMA. This is due to the greater viscous behavior that piperonyl methacrylate comonomer provides to the polymer network, as it was discussed in Chapter 3.

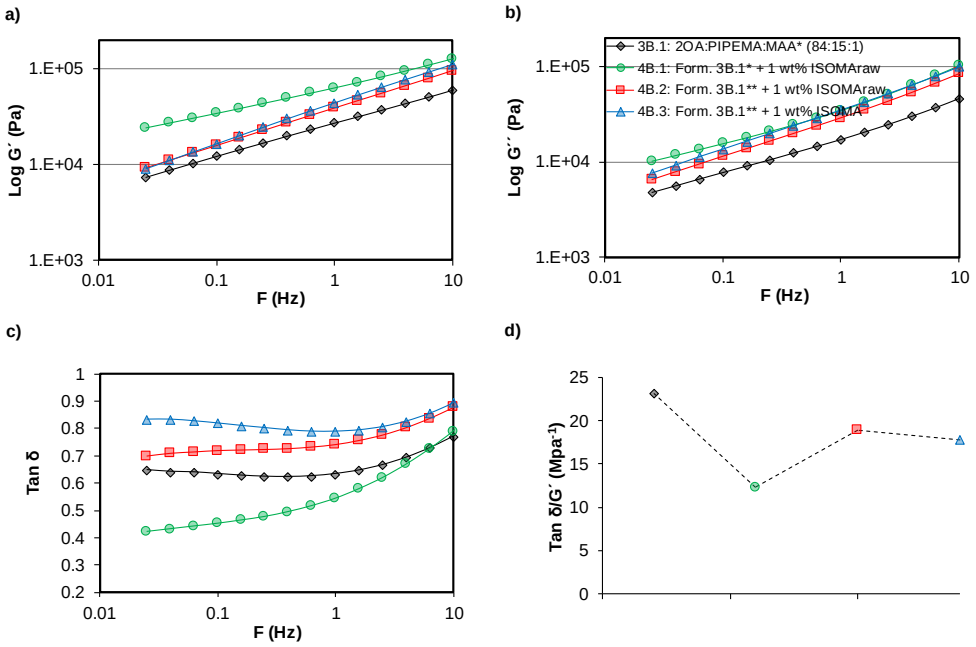

Figure 4.13. (a) Storage modulus (G´), (b) loss modulus (G´´), (c) dynamic modulus (tanδ) and (d) tanδ/G´2OA:PIPEMA formulations containing ISOMA or ISOMAraw as functional monomer. Measurements made at 23 ºC and 1 Hz.

4.8.2 Adhesive properties of waterborne PSAs containing PIPEMA as hard monomer and ISOMAraw/ISOMA as functional monomer

Table 4.7 shows the adhesive properties of these formulations observing a similar effect as those seen for the 2OA/IBOMA system. It is worth to remind that, as it was discussed in Chapter 3, the 2OA/PIPEMA system showed better adhesiveness (peel strength and work of adhesion), but substantially worst cohesiveness (shear resistance and SAFT) than the 2OA/IBOMA system (**3B.1** vs **2C.1**).

The presence of ISOMAraw in formulation **4B.1** reduced the peel strength but increased loop tack and work of adhesion because of the lower mass of the low molar mass peak. In formulation **4B.2**, the peel force increased to 8.8 N/25mm as consequence of the

good balance between the chains motion and the cohesion among them, keeping good values of both loop tack and work of adhesion. Formulation **4B.3** (with only ISOMA monomer) led to a remarkable increase of the tackiness as well as the work of adhesion, reaching a value of 282 J/m^2 without leading rest of adhesive on the substrate surface. Peel strength also increased, getting a force value close to 10 N/25mm, which means that cohesiveness among the polymer entanglements is still enough during the debonding process, getting a similar holding temperature but affecting shear resistance[64].

Table 4.7. Adhesive properties of the PSA tapes containing 2OA:PIPEMA as main formulation.

PSA	Composition	Peel (N/25mm)	Loop tack (N/25mm)	WA (J/m^2)	Shear resistance (min)	SAFT (°C)
	2OA:PIPEMA: ISOMAraw:MAA					
3B.1*	84:15:0:1	7.9 ± 0.7	10 ± 0.1	197 ± 32	90 ± 10	64 ± 5
4B.1*	84:14:1:1	6 ± 0.8	11.8 ± 1.4	222 ± 23	75 ± 15	88 ± 1
4B.2**	84:14:1:1	8.8 ± 0.2	10.9 ± 1.3	202 ± 24	150 ± 30	52 ± 1
	2OA:PIPEMA: ISOMA:MAA					
4B.3**	84:14:1:1	9.6 ± 1	15.4 ± 2	282 ± 29	35 ± 5	48 ± 1

* and ** makes reference to 0.025 wbm% and 0.075 wbm% of 2EHTG and 1BuSH, respectively.

The probe tack curves in Figure 4.14 show that ISOMAraw provided a similar behavior than the one of the previous section, namely, adhesive fibers with higher elongation at break capable to hold greater stress in comparison with formulation **3B.1**. As it was expected, the lower Tg of this system did not lead to fibrillation plateaus as high as those ones coming from formulations containing IBOMA. Moreover, the viscous component remarkably increased when 1 wt% of ISOMA was used. The changes observed in the molar mass distribution in Figure 4.12 are responsible for this behavior. The decrease in the molar mass of the high

molar mass peak as well as the fraction of this polymer (gel content) favor the high reduction of the polymeric network cohesiveness that did not allow the alignment of the polymer chains, resulting in a progressive diminution of the stress supporting by the fibers along the strain.

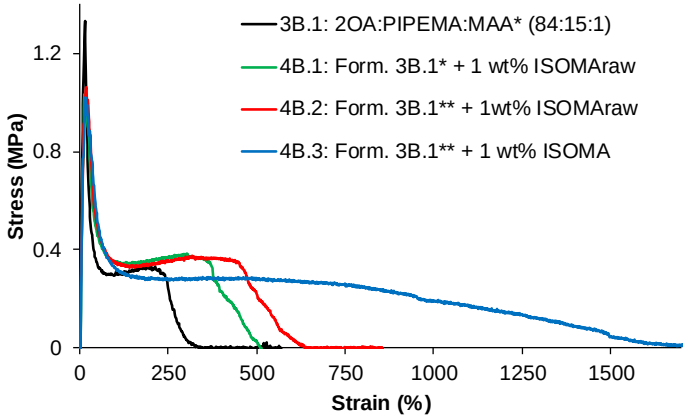

Figure 4.14. Probe tack tests for 2OA:PIPEMA formulations.

4.8.3 Removability studies of waterborne PSAs containing PIPEMA as hard monomer and ISOMAraw/ISOMA as functional monomer

Figure 4.15 shows the removability studies in water for this set of formulations containing PIPEMA as hard monomer. As the previous section, 1 wt% of ISOMAraw/ISOMA allowed the complete detachment of the adhesive tape from the glass in less than 40 min at room temperature and around 10 min at 65 ºC. Furthermore, formulations **4B.2** and **4B.3** showed the highest values of peel strength with a similar removability rate in water without letting residues on the substrate surface.

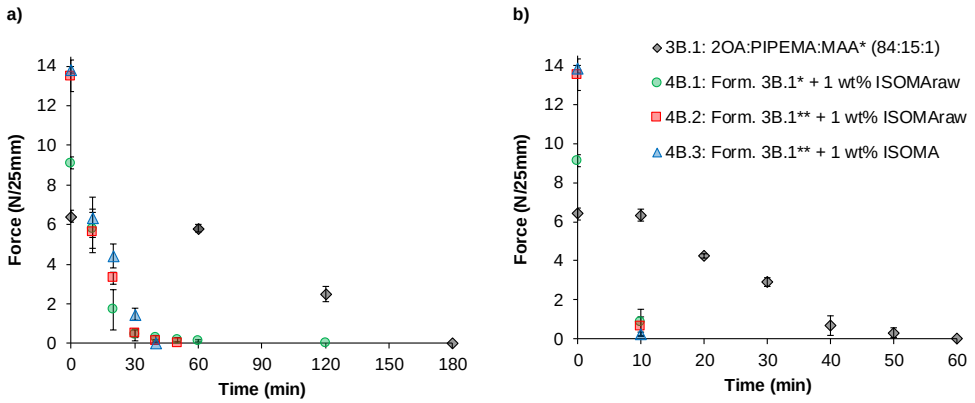

Figure 4.15. Evaluation of 180º peel strength at different times of water treatment at room temperature (a) and at 65 ºC (b) on glass for PSA tapes containing 2OA:PIPEMA as main formulation.

4.9 Conclusions

In this chapter, the synthesis of a dual functional monomer derived from isosorbide, more specifically isosorbide dimethacrylate, isosorbide 5-methacrylate and mixtures thereof, and its incorporation into the biobased PSA formulations of Chapter 2 and Chapter 3 was investigated. The nature of the monomer mixture ISOMAraw was assessed and compared as hard component in the PSA formulation. Regarding this, the polymer microstructure resulted in a highly crosslinked net that affected the adhesive performance, but getting a removability in water at 20 min. Nevertheless, it was found that the incorporation of 1 wt% of ISOMAraw/ISOMA in PSA formulations, containing either IBOMA or PIPEMA, enhanced both the flexibility and the cohesiveness of the adhesive fibrils. In addition, the low percentage of this sugar derivative monomer promoted the removability in water of the PSA tapes in less than 40 min at room temperature, and it was increased in almost 4 times at 65 ºC. It is worthy pointing out that the molar relation 4:1 of monomethacrylate:dimethacrylate isosorbide obtained in the synthesis of ISOMAraw may be modified, but this ratio results in a good commitment of crosslinker incorporation into the formulation.

4.10 References

(1) Benedek, I. *Pressure-Sensitive Adhesives and Applications - Second Edition , Revised and Expanded*; CRC Press, Ed.; Marcel Dekker: New York, 2004.

(2) Jovanović, R.; Dubé, M. A. Emulsion-Based Pressure-Sensitive Adhesives: A Review. *J. Macromol. Sci. - Polym. Rev.* **2004**, *44* (1), 1–51.

(3) Onusseit, H. The Influence of Adhesives on Recycling. *Resour. Conserv. Recycl.* **2006**, *46* (2), 168–181.

(4) Schneck, T.; Grossmann, C.; Hackenberger, S. Process for Cleaning and Label Removal for Bottles. WO. Patent 2012062372A1, 2012.

(5) Nair, P. J.; Hire, H. R.; Heederik, S. Process for the Removel of Labels from Materials. WO. Patent 2015058184A1, 2015.

(6) Hunt, M.; Chen, C. J. Solvent Application in Bottle Wash Using Amidine Based Formulas. WO. Patent. 2017143009A1, 2017.

(7) Frazee, G. R. Aqueous Pressure Sensitive Adhesive Compositions. U.S. Patent 4879333, 1989.

(8) Frazee, G. R. Pressure Sensitive Adhesive Compositions. U.S. Patent 4923919, 1990.

(9) Griffith, W. B. Primerless Removable Adhesive Systems. U.S. Patent 9163465 B2, 2015.

(10) Guo, J.; Severson, S. J. Optimizing the Monomer Composition of Acrylic Water-Based Pressure-Sensitive Adhesives To Minimize Their Impact on Recycling Operations. *Ind. Eng. Chem. Res.* **2007**, *46*, 2753–2759.

(11) Guo, J.; Severtson, S. J. Effect of Amphiphilic Additives on the Behavior of Water-Based Acrylic Pressure-Sensitive Adhesives during Paper Recycling. *Ind. Eng. Chem. Res.* **2008**, *47*, 2612–2617.

(12) Ko, K.; Lee, J. Y.; Shim, J. K.; Lee, J. Formulation of Emulsion Adhesives with Removal Properties by Using Alkali Soluble Resins. *J. Nanosci. Nanotechnol.* **2013**, *13*, 7467–7471.

(13) Rosenski, J. M.; Arora, A. Redispersable Waterborne Pressure Sensitive Adhesive Polymer. U.S. Patent 5319020, 1994.

(14) Therriault, D. .; Workinger, J. . Water-Inactivatable Pressure Sensitive Adhesive. U.S. Patent 5032637 A, 1991.

(15) Zajaczkoxski, M. J. Water-Soluble Pressure Sensitive Adhesive. U.S. Patent 5395907, 1995.

(16) Chiu, T. . Poly(2-Ethyl-2-Oxazoline): A New Water- -and Organic-Soluble Adhesive. *Adv. Chem.* **1986**, 425–433.

(17) Hanrot, A. Water Soluble Adhesive. U.S Patent 8119732B2, 2012.

(18) Kuramoto, K.; Maejima, N. Polyvinylmethyl Ether Acrylic Polymer Containing Pressure-Sensitive Adhesive Compositions. U.S. Patent 3657396, 1972.

(19) DeHullu, J. G. Pressure Sensitive Adhesives. U.S. Patent 5834538, 1998.

(20) Liu, W.-F. Pressure-Sensitive Adhesives of Polyvinyl Methyl Ether. U.S. Patent 5330832.

(21) Davis, I. J.; Sirota, J. Water Soluble Pressure Sensitive Adhesives. U.S. Patent 3249572, 1966.

(22) Fei, C.; Danuta, C. Pressure Sensitive Adhesive Composition for Medical Use. EP. Patent 2221067 A1, 2010.

(23) Martin, J. B. Release Coating for Pressure Sensitive Adhesive Sheet Material and Process of Maing a Sheet Coated with the Same. U.S. Patent 2803557, 1957.

(24) Kantner, S. S. Water-Soluble Pressure Sensitive Adhesives. U.S. Patent 8968772 B2, 2015.

(25) Kantner, S. S. Water-Soluble Pressure Sensitive Adhesives. U.S. Patent 0143991 A1, 2013.

(26) Zajaczkoxski, M. J. Water-Soluble Pressure Sensitive Adhesive. U.S. Patent 5508367, 1996.

(27) Dussenne, C.; Delaunay, T.; Wiatz, V.; Wyart, H.; Suisse, I.; Sauthier, M. Synthesis of Isosorbide : An Overview of Challenging Reactions. *Green Chem.* **2017**, *19*, 5332–5344.

(28) *Isosorbide Market Size, Share & Trends Analysis Report By Application (Polycarbonate, PEIT, Polyurethane), By End Use (Resins & Polymers, Additives), By Region, And Segment Forecasts, 2019 - 2025*; Grand View Research, Inc.: San Francisco, 2019.

(29) Gallagher, J. J.; Hillmyer, M. A.; Reineke, T. M. Isosorbide-Based Polymethacrylates. *ACS Sustain. Chem. Eng.* **2015**, *3* (4), 662–667.

(30) Sadler, J. M.; Nguyen, A. P. T.; Toulan, F. R.; Szabo, J. P.; Palmese, G. R.; Scheck, C.; Lutgen, S.; La Scala, J. J. Isosorbide-Methacrylate as a Bio-Based Low Viscosity Resin for High Performance Thermosetting Applications. *J. Mater. Chem. A* **2013**, *1* (40), 12579–12586.

(31) Shin, S.; Kim, B. C.; Chang, E.; Cho, J. K.; Suh, D. H. A Biobased Photocurable Binder for Composites with Transparency and Thermal Stability from Biomass-Derived Isosorbide. *RSC Adv.* **2014**, *4* (12), 6226–6231.

(32) Zhang, M.; Lai, W.; Su, L.; Wu, G. Effect of Catalyst on the Molecular Structure and Thermal Properties of Isosorbide Polycarbonates. *Ind. Eng. Chem. Res.* **2018**, *57*, 4824–4831.

(33) Baek, S. S.; Jang, S. H.; Hwang, S. H. Sustainable Isosorbide-Based Transparent Pressure-Sensitive Adhesives for Optically Clear Adhesive and Their Adhesion Performance. *Polym. Int.* **2017**, *66* (12), 1834–1840.

(34) Gallagher, J. J.; Hillmyer, M. A.; Reineke, T. M. Acrylic Triblock Copolymers Incorporating Isosorbide for Pressure Sensitive Adhesives. *ACS Sustain. Chem. Eng.* **2016**, *4* (6), 3379–3387.

(35) Vendamme, R.; Eevers, W. Sticky Degradable Bioelastomers. *Chem. Mater.* **2017**, *29* (12), 5353–5363.

(36) Berlanga Duarte, M. L.; Reyna Medina, L. A.; Reyes, P. T.; González Pérez, S. E.; Herrera González, A. M. Biobased Isosorbide Methacrylate Monomer as an Alternative to Bisphenol A Glycerolate Dimethacrylate for Dental Restorative Applications. *J. Appl. Polym. Sci.* **2017**, *134* (11), 1–8.

(37) Cecutti, C.; Mouloungui, Z.; Gaset, A.; Ensct, I.-; Agro-Industrielle, L. D. C.; Narbonne, R. De. Synthesis of New Diesters of With Fatty Acid Chlorides. *Bioresour. Technol.* **1998**, *66*, 63–67.

(38) Zhu, Y.; Durand, M.; Molinier, V.; Aubry, J. M. Isosorbide as a Novel Polar Head Derived from Renewable Resources. Application to the Design of Short-Chain

Amphiphiles with Hydrotropic Properties. *Green Chem.* **2008**, *10* (5), 532–540.

(39) Liu, W.; Xie, T.; Qiu, R. Biobased Thermosets Prepared from Rigid Isosorbide and Flexible Soybean Oil Derivatives. *ACS Sustain. Chem. Eng.* **2017**, *5* (1), 774–783.

(40) Feng, X.; East, A. J.; Hammond, W. B.; Zhang, Y.; Jaffe, M. Overview of Advances in Sugar-Based Polymers. *Polym. Adv. Technol.* **2011**, *22* (1), 139–150.

(41) Mansoori, Y.; Hemmati, S.; Eghbali, P.; Zamanloo, M. R.; Imanzadeh, G. Nanocomposite Materials Based on Isosorbide Methacrylate / Cloisite 20A. *Polym. Int.* **2012**, *62*, 280–288.

(42) Matt, L.; Parve, J.; Parve, O.; Pehk, T.; Pham, T. H.; Liblikas, I.; Vares, L.; Jannasch, P. Enzymatic Synthesis and Polymerization of Isosorbide-Based Monomethacrylates for High‐Tg Plastics. *ACS Sustain. Chem. Eng.* **2018**, *6*, 17382–17390.

(43) Veregin, R. P. N.; Sacripante, G. G. Bio-Based Acrylate and Methacrylate Resins. U.S. Patent 0082936 A1, 2017.

(44) Yu, D.; Huang, H.; Wang, Y.; Liu, T.; Feng, T.; Han, H. Synthetic Method for Isosorbide Acrylic Ester and Application of Isosorbide Acrylic Ester in Improving Thermal Performance of Polymer. CN Patent 105198892 A, 2015.

(45) Mays, J. W.; Siakali-Kioulafa, E.; Hadjichristidis, N. Glass Transition Temperatures of Polymethacrylates with Alicyclic Side Groups. *Macromolecules* **1990**, *23(14)*, 3530–3531.

(46) Healy, T. W.; La Mer, V. K. The Adsorption-Flocculation Reactions of a Polymer with an Aqueous Colloidal Dispersion. *J. Phys. Chem.* **1962**, *66* (10), 1835–1838.

(47) Fellows, C. M.; Doherty, W. O. S. Insights into Bridging Flocculation. *Macromol.*

Symp. **2006**, *231*, 1–10.

(48) Hogg, R. Bridging Flocculation by Polymers. *KONA Powder Part. J.* **2012**, *30* (30), 3–14.

(49) Gregory, J.; Barany, S. Adsorption and Flocculation by Polymers and Polymer Mixtures. *Adv. Colloid Interface Sci.* **2011**, *169* (1), 1–12.

(50) Dickinson, E.; Goller, M. I.; Wedlock, D. J. Creaming and Rheology of Emulsions Containing Polysaccharide and Non-Ionic or Anionic Surfactants. *Colloids Surfaces A Physicochem. Eng. Asp.* **1993**, *75* (C), 195–201.

(51) Lakrout, H.; Sergot, P.; Creton, C. Direct Observation of Cavitation and Fibrillation in a Probe Tack Experiment on Model Acrylic Pressure-Sensitive-Adhesives. *J. Adhes.* **1999**, *69* (3–4), 307–359.

(52) Lee, J. H.; Lee, T. H.; Shim, K. S.; Park, J. W.; Kim, H. J.; Kim, Y.; Jung, S. Effect of Crosslinking Density on Adhesion Performance and Flexibility Properties of Acrylic Pressure Sensitive Adhesives for Flexible Display Applications. *Int. J. Adhes. Adhes.* **2017**, *74*, 137–143.

(53) Zosel, A. The Effect of Fibrilation on the Tack of Pressure Sensitive Adhesives. *Int. J. Adhes. Adhes.* **1998**, *18* (4), 265–271.

(54) Blackley, D. . *Polymer Latices: Science And Technology Volume 1: Fundamental Principles*, 2nd ed.; Chapman and Hall: London, 1997; Vol. 1.

(55) Lovell, P. A.; El-Aasser, M. S. *Emulsion Polymerization and Emulsion Polymers*; John Wiley & Sons L&d: Chichester, 1997.

(56) Satas & Associates. *Handbook of Pressure Sensitive Adhesive Technology.*, 3rd

editio.; Satas, D., Ed.; Warwick, 1999.

(57) Zhang, L.; Cao, Y.; Wang, L.; Shao, L.; Bai, Y. Polyacrylate Emulsion Containing IBOMA for Removable Pressure Sensitive Adhesives. *J. Appl. Polym. Sci.* **2016**, *133*, 1–7.

(58) Hofman, A. H.; van Hees, I. A.; Yang, J.; Kamperman, M. Bioinspired Underwater Adhesives by Using the Supramolecular Toolbox. *Adv. Mater.* **2018**, *30* (19).

(59) Dahlquist, C. A. Pressure-Sensitive Adhesives. In *Treatise on Adhesion and Adhesives*; Dekker, New York, 1969; Vol. 2, pp 219–260.

(60) Deplace, F.; Carelli, C.; Mariot, S.; Retsos, H.; Chateauminois, A.; Ouzineb, K.; Creton, C. Fine Tuning the Adhesive Properties of a Soft Nanostructured Adhesive with Rheological Measurements. *J. Adhes.* **2009**, *85* (1), 18–54.

(61) Roos, A.; Creton, C. Styrenic Block Copolymers as Hot-Melt PSA's : Role of Molecular Architecture on Properties. In *Proceedings of Euradh*; Freiburg am Breisgau, 2004.

(62) Crosby, A. J.; Shull, K. R.; Lakrout, H.; Creton, C. Deformation and Failure Modes of Adhesively Bonded Elastic Layers. *J. Appl. Phys.* **2000**, *88*, 2956–2966.

(63) Callies, X.; Fonteneau, C.; Pensec, S.; Bouteiller, L.; Ducouret, G.; Creton, C. Adhesion and Non-Linear Rheology of Adhesives with Supramolecular Crosslinking Points. *Soft Matter* **2016**, *12*, 7174–7185.

(64) Zosel, A. Effect of Cross-Linking on Tack and Peel Strength of Polymers. *J. Adhes.* **1991**, *34* (1–4), 201–209.

Chapter 5

Synthesis of electrosterically stabilized latexes using biobased ASRs for PSAs: High performance and removability

5.1 Introduction

It has been shown in chapter 4, that the incorporation of small amounts of an isosorbide derivative monomer in waterborne biobased PSA formulations enhanced the performance of the adhesive material as well as its removability in water at short times. These isosorbide based PSAs provide an environmentally friendly and economical method that could be implemented in materials using tapes and labels (for example, glass bottles or in packaging), in which the adhesion-switching-off constitute an important step during the recycling process. Nevertheless, from an industrial point of view, excellent adhesion properties at the minimum film thickness are desired for PSA tapes. To address this challenging requirements, different types of alkali soluble resins (ASRs) have been employed over the past 60 years, replacing conventional surfactants in emulsion polymerization[1,2].

ASRs are a special type of polymeric emulsifiers, specifically, hydrophobically modified anionic polyelectrolytes, which can improve the stability of colloidal dispersions[3–5]. They are random copolymers containing a large amount of carboxylic groups and having a molecular weight usually ranging between 500 and 20000 Da[4]. Above the pKa of the carboxylic groups, the polymer chains become negatively charged and, thereby, soluble in water, being able to provide electrosteric stabilization[6]. These amphiphilic random copolymers have the ability to self-organize in aggregates in water as consequence of the intermolecular and/or intramolecular hydrophobic interactions[7–9]. The particle nucleation mechanism in emulsion polymerization using ASRs as polymeric stabilizers has been described as micellar-like, where the aggregates of ASRs behaves similar to micelles of conventional surfactants. Once the particles have been formed the mechanisms about radical entry and exit are expected to be similar in both processes[8,10,11].

Scheme 5.1. Mechanism for emulsion polymerization by ASRs-stabilized systems.

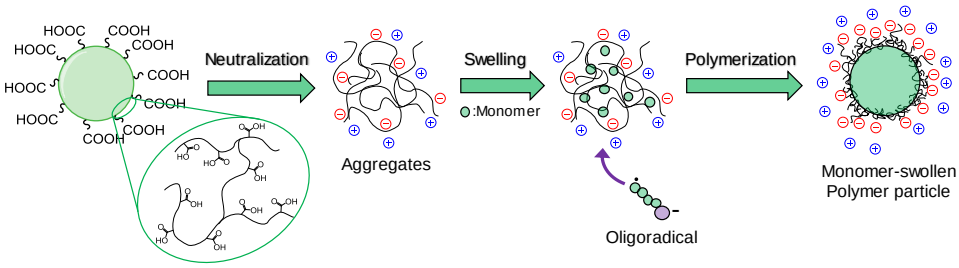

It is worthy to mention that there is a reduction of the radical entry as a consequence of the high density of negative charges provided by the polymeric hairy layer of the resin once it is absorbed on the particle surface. In this context, three mechanisms have been proposed to justify the decrease of the radical entry rate[12]: (1) The hairy layer offers a resistance to the diffusion of the entering oligoradicals[13]. (2) The anionic oligoradicals are repelled by the negative charges in the hairy layer[11]. (3) The entering oligoradical is able to abstract hydrogens from the ASR monomer units leading to tertiary radicals[14]. These tertiary radicals have low reactivity (low propagation rate), the monomer concentration is also very low and, hence, the probability of termination between them is high in the hairy layer that can be considered a radical sink[15,16]. In addition, the tertiary radicals might suffer β-scission reactions yielding unsaturated water-soluble species.

As advantages, ASR-fortified emulsion polymers impart Newtonian-like rheological properties, excellent pigment dispersity, wetting and mechanical properties and freeze-thaw stabilities[15,16]. Furthermore, their solubility in alkali solution facilitates the PSA tape/label separation during the recycling process[17]. There are few works in both open and patent literature about the synthesis of biobased alkali soluble resins making use of monomers coming from renewable sources[18–20]. However, there are not studies that report the synthesis of waterborne PSAs presenting competitive commercial performances and having both high bio-content and solids content using biobased ASRs as stabilizers. Among the

main disadvantages, the resin may be able to migrate from the adhesive to the adjacent substrate under high humidity conditions, affecting the final properties[21]. In order to avoid these kind of problems, as well as those ones coming during storage, the resin must be sufficiently grafted to the final polymer.

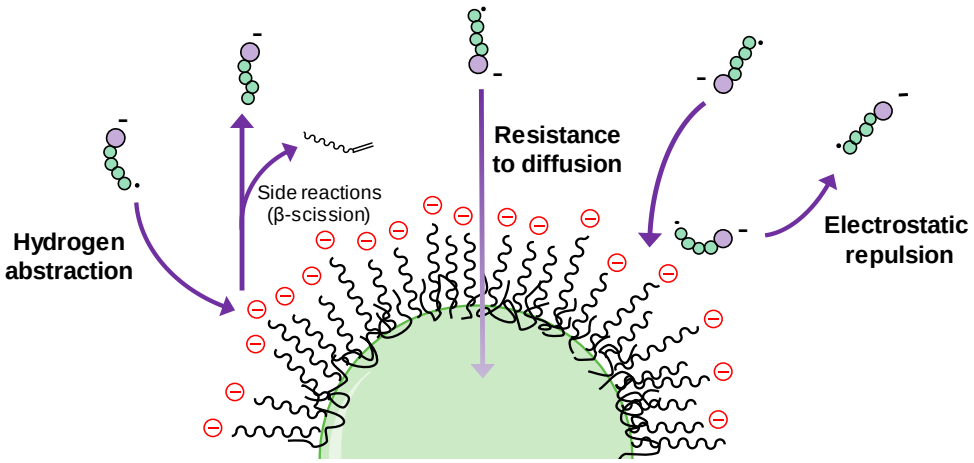

Figure 5.1. General mechanisms for the decreasing of the radical entry in polymerization by ASRs-stabilized systems.

Therefore, this chapter will be focused on the one-pot approach synthesis of high solids content waterborne pressure sensitive adhesives having bio-contents (up to 71%) stabilized with ASR-type electrosteric stabilizers with excellent adhesive performance and removable properties. For this purpose, the already studied biobased monomers 2-Octyl acrylate (2OA, Arkema) and isobornyl methacrylate (IBOMA, Evonik) together with the isosorbide mixture and the isosorbide 5-methacrylate (ISOMAraw/ISOMA) synthesized in this work (Chapter 4) will be employed.

In the present chapter, two ASRs with similar acid value (AV), but with different renewable methacrylic monomer were synthesized and used as stabilizers in the synthesis of PSA formulations. The study aimed to know how the resin nature affects to the adhesive

microstructure and its properties. For that, rheological investigations were carried out to shed light about the relationship between the adhesive behavior and supramolecular interactions, which were confirmed by VT-FTIR. Finally, removability studies of the PSA tapes in alkaline medium were also assessed.

5.2 Experimental

Biobased 2-Octyl acrylate (2OA) was kindly supplied by Arkema (France), isobornyl methacrylate (Visiomer® Terra IBOMA) was kindly supplied by Evonik Industries (Essen, Germany). The isosorbide monomer mixture (ISOMAraw) formed by isosorbide dimethacrylate: isosorbide 5-methacrylate (4:1) was synthesized and further purified to obtain ISOMA (isosorbide 5-methacrylate) following the procedure of Chapter 4. Methacrylic acid (MAA), 2-Ethylhexyl thioglycolate (2EHTG), isopropanol, sodium persulfate (NaPS), sodium dodecyl sulfate (SDS) and sodium hydroxide (NaOH) were purchased from Sigma-Aldrich. Ammonium hydroxide solution (25%) was purchased from Fisher Scientific. All reagents were used without further purification.

5.2.1 Synthesis of biobased alkali soluble resins ASRs

Biobased ASRs were produced using 2EHTG as chain transfer agent to get a weight-average molar mass around 10000 Da, following a formulation previously reported in our group[16]. Table 5.1 presents the composition of these two resins as well as their bio-content.

Table 5.1. Formulations used for the synthesis of the ASRs.

RESIN	2OA (% w/w)	IBOMA (% w/w)	ISOMAraw (% w/w)	MAA (% w/w)	Bio-content (%)
R1	75	10	-	15	62
R2	75	-	10	15	61

The reactions were carried out in a 250 mL jacketed glass reactor equipped with reflux condenser, nitrogen and feeding inlet, sample outlet and anchor type stainless steel stirrer at 200 rpm. For the synthesis of the resin, the reactor was charged with the initial charge (see Table 5.2). The system was purged and the temperature increased to 80 ºC. Once the temperature was reached an aqueous solution of initiator was added as a shot and the feeding of the comonomer pre-emulsion was started and completed in 40 min. After the feeding process, a post polymerization process was carried out for 30 min. The general resin formulation is shown in Table 5.2 and a representative scheme of the process is presented in Figure 5.2.

Table 5.2. Materials and percentages employed in the synthesis of the ASRs.

		Amount (g)
Initial charge	Water	85
	SDS solution 15 wt%	1.33
Initiator solution (1.7 wbm%*)	Water	6.64
	NaPS	0.5
Pre-emulsion	Water	20
	SDS solution 15 wt%	1.13
	Monomers	30
	2EHTG	1.1

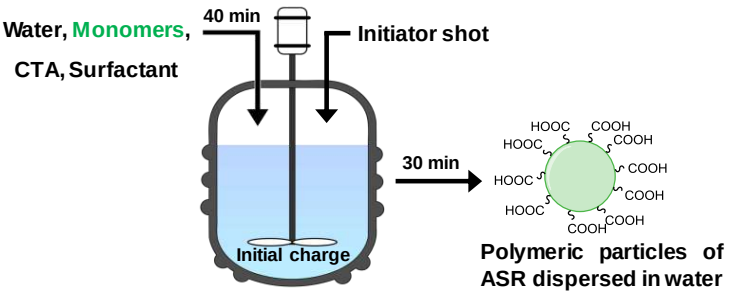

Figure 5.2. Scheme of reaction for the synthesis of the ASRs.

5.2.2 Synthesis of biobased waterborne PSAs stabilized with biobased ASRs

For the synthesis of waterborne PSAs, a known quantity of the obtained resin was charged in the reactor. The temperature was raised to 80 ºC under moderate nitrogen flux. After that, a shot of ammonia was added, followed by other 10 min of agitation at 200 rpm. Then, a shot of initiator solution was added and the pre-emulsion of comonomers (second-stage) was fed over 120 min. A post-polymerization process was performed for additional 60 min at 80 ºC before cooling to room temperature. The ratio ASR:monomer was set to 20:80 and the final solids content of the dispersions was 50 wt%. An example of the formulation is given in Table 5.3 and a representative scheme of the process is presented in Figure 5.3. In addition, Table 5.4 summarizes the monomers employed in the pre-emulsion for the synthesis of waterborne PSAs as well as the ASRs used as stabilizers.

Table 5.3. Representative formulation used for the synthesis of waterborne PSAs by semibatch emulsion polymerizations stabilized by biobased ASRs.

		Amount (g)
Initial charge	ASR	28.6
Base	Ammonia solution 25 wt%	0.77
Initiator solution (0.05 wbm%*)	Water NaPS	3 0.226
Second stage Pre-emulsion	Water SDS solution 15 wt% Monomers	23.86 1.02 45.14

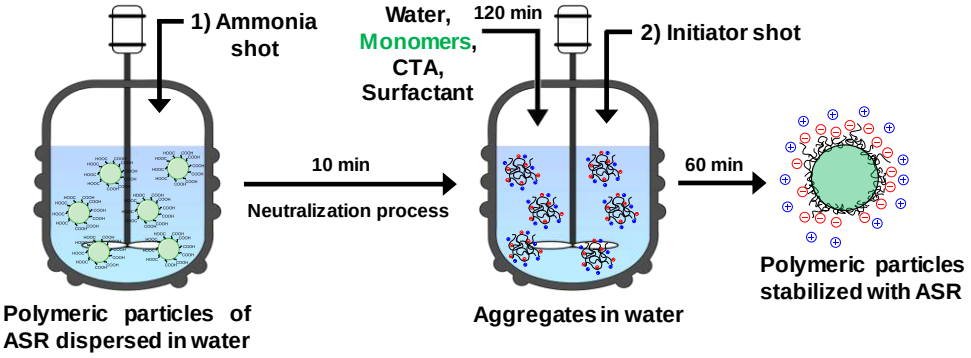

Figure 5.3. Scheme of reaction for the synthesis of waterborne PSAs stabilized with biobased ASRs.

Table 5.4. Comonomer composition of the pre-emulsions used for the synthesis of the waterborne PSAs stabilized with biobased ASRs.

PSA run	2OA (% w/w)	IBOMA (% w/w)	ISOMA (% w/w)	2EHTG (wbm %)
R1.1	100	-	-	-
R1.2	85	15	-	-
R1.3	85	15	-	0.025
R2.1	85	15	-	-
R2.2	85	15	-	0.025
R2.3	85	10	5	0.025

5.2.3 Characterization

Particle size was analyzed by dynamic light scattering (DLS) and conversion was determined gravimetrically. Gel fraction (or insoluble fraction of the copolymer in THF) was measured by Soxhlet extraction.

The acid value was measured by conductometric titration to determine the amount of free-carboxylic acid groups in the resin. The resin was dissolved in isopropanol and the

solution was then titrated with NaOH solution (1.0 M). The amount of acidic groups is given by the acid number:

$$AV = \frac{mg\ KOH}{g\ ASR} \quad \textbf{(Eq.5.1)}$$

Where *AV* is the amount in milligrams of potassium hydroxide that is required to neutralize one gram of ASR. The theoretical acid value of the ASRs was 98 mg KOH/g ASR.

Due the insolubility of the polymer dispersion in both THF and DMF, the whole molar mass distribution could not be analyzed by AF4. Therefore, the molar mass distribution of the soluble fraction in THF was determined by size exclusion chromatography (SEC/RI) at 35°C using the same conditions and procedure than in chapter 2. The glass transition temperature (T_g) was determined by differential scanning calorimetry (DSC, Q1000, TA Instruments) using the same conditions than in chapter 2. Thermogravimetric analysis were performed with a ramp of 10 ºC/min from 40 ºC to 600 ºC under nitrogen atmosphere (TGA, Q500 device, TA analysis).

The film preparation and the evaluation of the PSA performance was carried out using the same conditions and procedures than in chapters 2-4. Dynamic mechanical analysis (DMA) was performed in a rheometer Anton Paar using parallel plate geometry. Frequency sweeps (0.3-120 rad s^{-1}) with an applied strain between 0.5% and 2% were made on 500 µm round thick samples of 8 mm of diameter at a temperature range from -20 ºC to 90 ºC 23 ºC.

Variable temperature Fourier-transform infrared spectroscopy (VT-FTIR) was performed in a spectrometer Nicolet 6700 FTIR (transmission mode) using a heating cell Specac. For the sample preparation, few drops of latex were dried over a KBr tablet at room temperature.

Liquid-state Proton Nuclear Magnetic Resonance (^{1}H NMR) was recorded on a Bruker 400 MHz equipment.

5.2.4 Removability studies

The studies were performed at room temperature in aqueous basic media, using an ammonium hydroxide solution. For that purpose peel tests were carried out using glass as substrate. The adhesive tape was attached to the substrate and it was submerged into water at pH 10. Four samples were tested for each formulation and the average values were reported before and after being submerged in basic media.

5.3 Synthesis of ASRs

The two synthesized biobased ASRs were obtained as stable dispersions with full conversion and solids content around 25% and similar particle size (100-125 nm). Table 5.5 shows the two resin compositions together with their main properties including intensity-average particle size (dp), molar mass (Mw), dispersity index (Đ), glass transition temperature (Tg) and experimental acid value (AV). Both formulations had similar molar masses and circa the targeted value of 10000 Da, which is in agreement with the formulations reported by Bandiera et al.[16] that were used as reference to adjust the CTA amount (2-Ethylhexylthioglycolate). As it was expected the use of ISOMAraw yielded lower Tg in comparison with the formulation containing IBOMA.

Table 5.5. Summary and characteristics of the synthesized biobased alkali soluble resins. Note that ISOMAraw is the mixture of both monomethacrylate and dimethacrylate isosorbide in a molar ratio 4:1.

ASR	Composition (%wt monomers)	Dp (nm)	Mw (kDa)	Đ	Tg (°C)	AV (mg/g)
R1	2OA:IBOMA:MAA (75:10:15)	125	9.3 ± 0.2	1.9	-30	88
R2	2OA:ISOMAraw:MAA (75:10:15)	104	9.5 ± 0.2	2	-40	89

It is worth to point out that the presence 2 wt% of isosorbide dimethacrylate in the formulation **R2** provided pendant double bonds in the polymer structure. Figure 5.4 shows the selected region of the ^{1}H NMR spectra in $CDCl_3$ of this resin, in which those peaks belonging to the pendant methacrylic groups can be clearly appreciated.

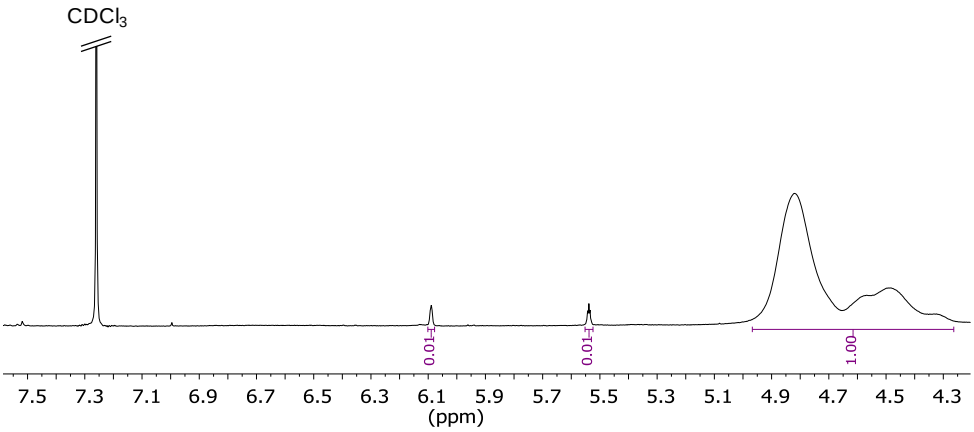

Figure 5.4. ^{1}H NMR spectra in chloroform-d_1 of the resin **R2** (2OA:ISOMAraw:MAA (75:10:15)).

5.4 Biobased waterborne PSAs using ASRs as polymeric stabilizers

The ASRs presented above were used as polymeric stabilizers in the synthesis of biobased latexes with final solids content of 50% and particle sizes between 210 and 230 nm via semicontinuous emulsion polymerization. The main properties of these latexes are summarized in Table 5.6. Starved-feed conditions (i.e., instantaneous conversions close to 100% were achieved) were reached for all the formulations using both resins. All latexes were stable. A representative example of the evolution of instantaneous and overall conversion is shown in Figure 5.5 for ASR **R1**

Table 5.6. Summary and characteristics of the synthesized PSA latexes using **R1** and **R2** as polymeric stabilizers.

PSA	Compostion (%wt monomers)	Dp (nm)	Gel (%)	Mw (kDa)	Đ	Tg (°C)	Bio (%)
R1.1	2OA (100)	230	66 ± 1	63± 5	4.1	-43	71
R1.2	2OA:IBOMA (85:15)	229	61.5 ± 0.2	89± 0.3	6.2	-28	71
R1.3	2OA:IBOMA+CTA* (85:15)	210	50.3 ± 0.2	111± 0.3	5.9	-28	71
R2.1	2OA:IBOMA (85:15)	215	56.2 ± 0.2	104± 1.3	6.2	-28	70
R2.2	2OA:IBOMA+CTA* (85:15)	210	51.3 ± 1	122± 19.6	8.2	-28	70
R2.3	2OA:IBOMA:ISOMA+CTA* (85:10:5)	220	47 ± 2	151± 4.3	9.6	-29	70

CTA*: 0.025 weight percent of 2EHTG based on monomer composition.

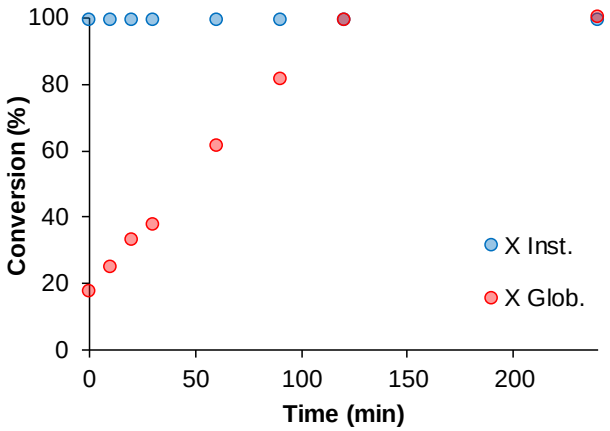

Figure 5.5. Instantaneous (blue circles) and overall (red circles) conversions for the emulsion copolymerization of 2OA and IBOMA using ASR **R1** (**R1.2**).

The soluble molar mass distributions of the synthesized latexes using the ASR **R1** as polymeric stabilizer is showed in Figure 5.6. As it can be observed the use of **R1** as stabilizer led to distributions in which the resin contributed in an important way to the soluble molar mass, particularly in the region between 10^3 to $5*10^4$ Da. This contribution was notable for

the formulation **R1.1** and it was reduced when 15 wt% of IBOMA was used (formulation **R1.2**). The incorporation of this methacrylate monomer led to a decreasing of the gel content[22] and, hence, to an increase of the average molar mass (see Table 5.6). This resulted in a lower contribution of the resin to the whole soluble molar mass because a higher amount of longer soluble polymer chains with a molar mass between $5*10^4$ and 10^6 Da were present in the sol fraction. Logically, this contribution was even lower when a chain transfer agent was used (formulation **R1.3**) due to the lower gel content and, thus, the higher amount of soluble polymer chains.

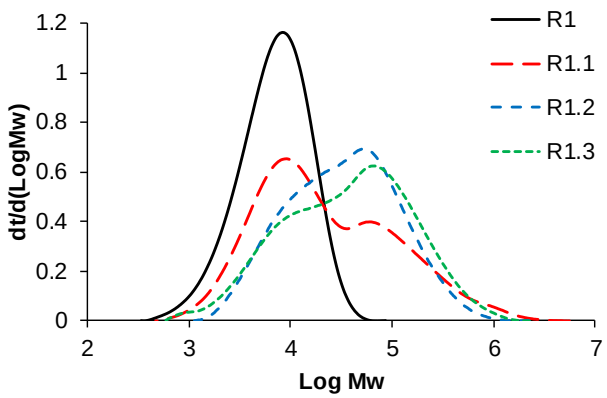

Figure 5.6. Soluble molar mass distributions for the PSA latexes synthesized using ASR **R1**.

Nevertheless, when the resin **R2** was employed, formulations with similar breath of the soluble molar mass distributions and lower resin contribution were obtained (see Figure 5.7). This is because of the presence of pendant double bonds, coming from the isosorbide dimethacrylate, in ASR **R2**, which are able to promote grafting reactions between the resin and the polymer chains produced in the semibatch stage.

The grafting in the ASR pendant double bonds resulted in a lower fraction of the free ASR in the soluble polymer, that is, a smaller area under the curve in the corresponding

region of the resin molar mass. It is worthy pointing out that there was an increasing of both the sol molar mass and the dispersity index for those formulations coming from **R2**, likely because of this grafting process.

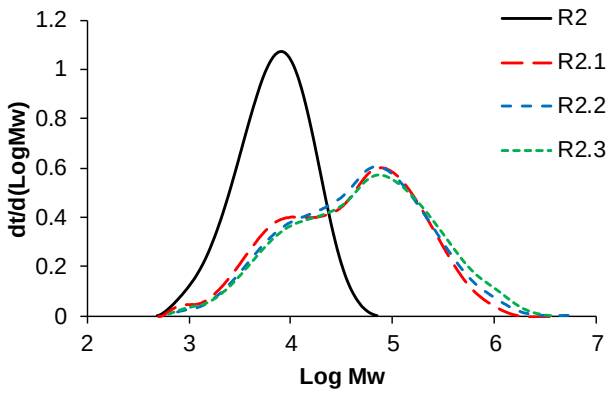

Figure 5.7. Soluble molar mass distributions for the PSA latexes synthesized using ASR **R2**.

Figure 5.8 shows the deconvoluted molar mass distributions (assuming two populations of chains; one corresponding to the pure ASR resin and the other due to copolymer formed in the second stage) of the PSA latexes with the same composition of the comonomers but different ASR resin (**R1.2** vs **R2.1** and **R1.3** vs **R2.2**). The amount of non-grafted ASR resin was lower in both comonomer compositions for ASR **R2**, likely due to the pendant double bonds in its structure that favor the incorporation of the ASR resin in the polymer particle.

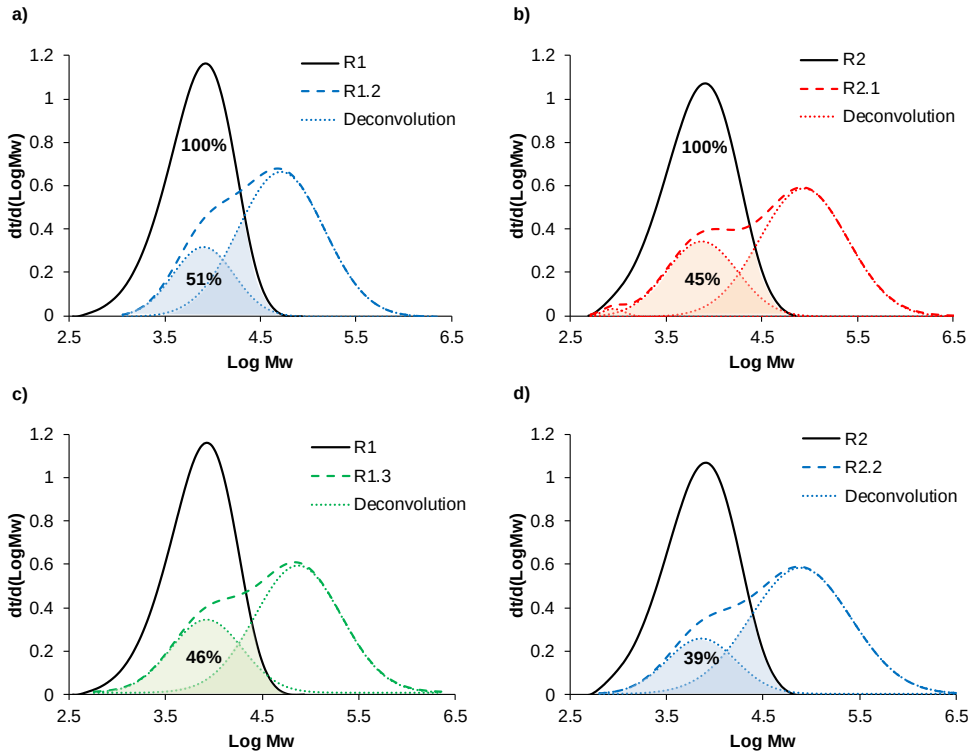

Figure 5.8. Deconvolution analysis of the MMD´s of formulations **R1.2** (a), **R2.1** (b), **R1.3** (c) and **R2.2** (d), and percentage of resin contributing to the sol molar mass.

5.5 Rheological analysis of PSA films containing ASRs as stabilizers

Dynamic rheological experiments shed light about the viscoelastic properties of the PSA films as well as their correlation with the chemical composition and the microstructure. At this point it is important to note that the composition ASR **R2** contains, aside the methacrylic acid, free OH groups coming from ISOMA, which can interact among them and/or with the acid groups by hydrogen bonding. Figures 5.9 and 5.10 present the variation of storage (G´) and loss modulus (G´´) over a range of frequencies at 23 ºC for the PSA formulations synthesized with ASR **R1** and ASR **R2**, respectively. For all adhesive films, G´

remained higher than G´´, which means a rheological response as a soft elastic solid before the transition regime (G´~ G´´).

For the adhesives synthesized with ASR **R1**, the highest storage modulus corresponded to formulation **R1.2,** since its microstructure (harder polymer with a substantial fraction of gel) promoted the solid-like behavior and, thus, the enhancement of the energy storage. Formulations **R1.1** and **R1.3** have smaller G´ and G´´ than **R1.2**. Formulation **R1.3** that only differs in the gel fraction (lower due to the CTA added in the reaction) have lower G´ and G´´ at low frequencies, but at high frequencies they behaved very similar (**R1.2** vs **R1.3**). On the contrary, formulation **R1.1** is governed by the softness of the 2OA polymer and presents two times smaller G´ and G´´ values than the other two formulations despite of having larger gel fraction.

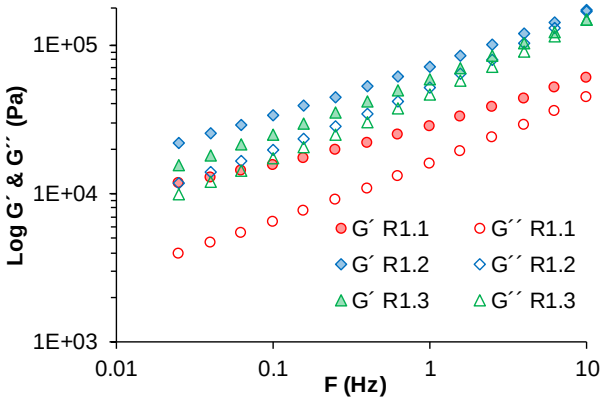

Figure 5.9. Linear rheology curves at 23 ºC for PSA series films with ASR **R1**. The storage modulus **G´** is represented by solid markers while the loss modulus **G´´** is represented by hollow markers.

For the adhesive formulations synthesized with ASR **R2**, differences in the G´ and G´´ are not as pronounced as for series with ASR **R1**, likely because the composition of the three formulations contain IBOMA monomer. Nevertheless, slightly higher values of G´ (and

more clearly higher values for G´´) were measured for the formulation containing ISOMA monomer (**R2.3**). This can be linked to the formation of hydrogen bonding interactions, which reinforce the viscoelastic character of the polymer network improving elasticity, but also energy dissipation.

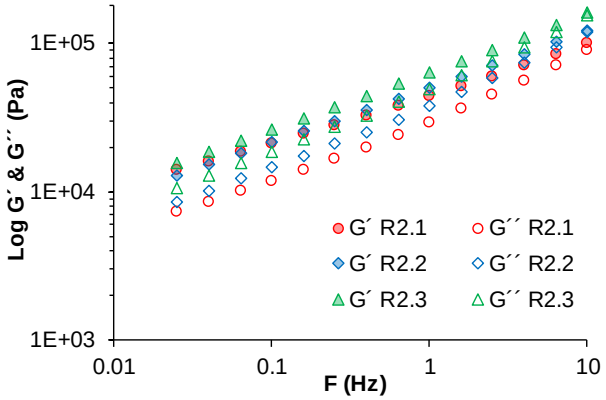

Figure 5.10. Linear rheology curves at 23 ºC for PSA series films with ASR **R2**. The storage modulus **G´** is represented by solid markers while the loss modulus **G´´** is represented by hollow markers.

It is worth to mention that the greater the hydrogen bonding density, the more the elastic nature prevails over the viscous one. Complex viscosity (η*) is defined as a frequency-dependent viscosity, specifically as the difference between the dynamic viscosity and the imaginary out-of-phase viscosity[23]. This rheological property represents the material resistance to flow, which increases as the supramolecular interactions do[24]. In order to clarify whether the presence of supramolecular interactions were acting over the viscoelastic nature of the PSAs, complex viscosity was measured.

Figure 5.11 shows the variation of η* over a broader range of frequencies at 23 ºC for both series of PSA formulations. An increase of η* from formulation **R2.1** to formulation **R2.2** was observed despite the gel content reduction in the later (see Figure 5.11.b).

Concerning this, the increase in the chain mobility promoted the hydrogen bonding interaction and, thereby, the resistance of the material to flow. When ISOMA monomer was used in formulation **R2.3** (yielding similar gel contents as controlled by the CTA concentration) η* increased as consequence of the higher hydrogen bonding density, enhancing the elastic nature. A different situation was observed for the series with ASR **R1** (see Figure 5.11.a), in which first an increase of the complex viscosity was detected when IBOMA was used (**R1.1** vs **R1.2**). However, η* decreased when the gel content was reduced in formulation **R1.3** because of the enhancement of the liquid-like behavior together with the lack of supramolecular interactions.

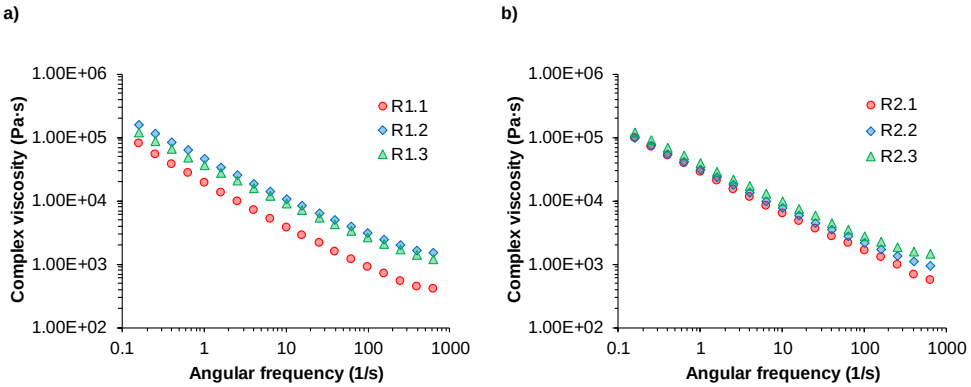

Figure 5.11. Complex viscosity (η*) at 23 ºC for PSA series films with ASR **R1** (a) and with ASR **R2** (b).

Hydrogen bonding formation among polymer chains can also explain the lower differences found between G´ and G´´ for series with ASR **R2**. Regarding this, intermolecular interactions provide a better stability of the polymer structure, namely, a better equilibrium between the solid-like and the liquid-like behavior of the PSA[25]. Those differences are specially noticed at frequencies below the transition regime (G´~ G´´), becoming more pronounced in the solid regime (G´ >> G´´) and having small differences along the dissipative

regime (G´ < G´´). The construction of master curves using the time-temperature superposition (TTS) principle provides an effective vision of the PSA viscoelasticity over a wide range of frequencies. Figure 5.12 shows the master curves for the PSA compositions of this chapter at the reference temperature (23 ºC) as well as the value of the frequency at which G´ and G´´ cross each other (ω_e).

Formulations coming from resin **R1** led to different master curves to each other with a higher separation between G´ and G´´ at the beginning of the solid regime. Those differences in the shape of TTS master curves are attributed to the change in the viscoelastic behavior when IBOMA is incorporated. Nonetheless, superposed-like master curves having similar shape were obtained for those PSAs containing the resin **R2**. Moreover, slightly closer moduli values were observed when ISOMA was incorporated (**R2.3**).

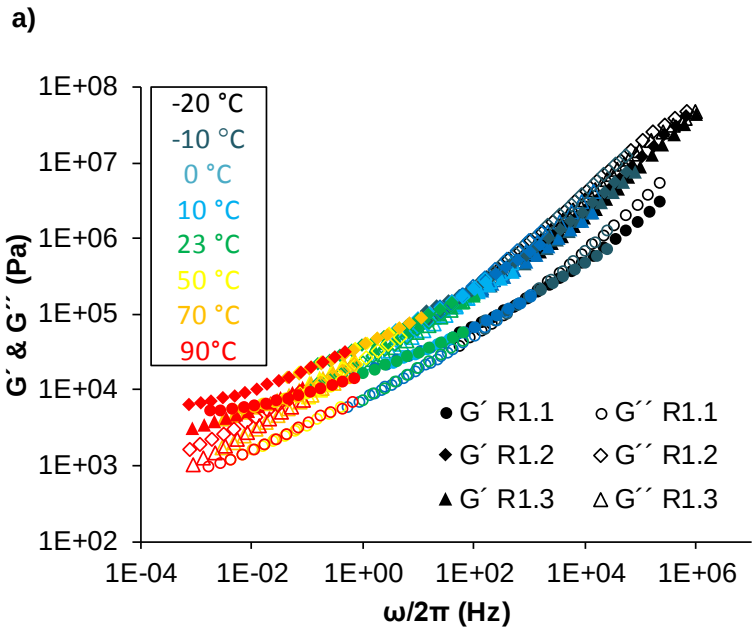

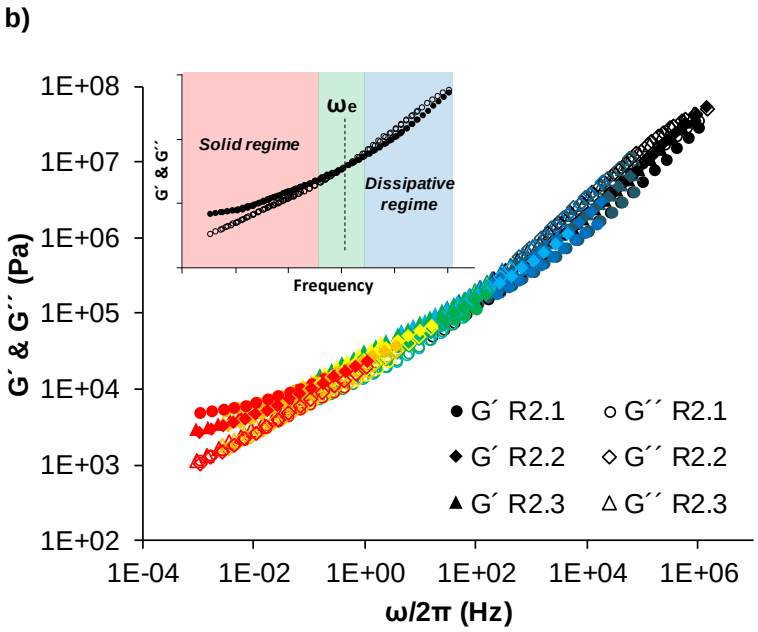

	ω_e (Hz)		ω_e (Hz)
R1.1	872	**R2.1**	173
R1.2	173	**R2.2**	151
R1.3	204	**R2.3**	125

Figure 5.12. G´ and G´´ master curves for PSA series films with ASR **R1** (a) and with ASR **R2** (b) at T_{ref} = 23 ºC, and frequency ω_e for each composition. The color of the markers indicates the temperature at which the frequency sweeps were performed.

The ω_e value sheds light about the correlation between the resin nature and the composition and its influence in the final viscoelasticity. The cross-over frequency occurs at lower frequencies (more elastic behavior) when IBOMA was incorporated in **R1** series. The slight increase in the cross-point, ω_e (from 173 to 204 Hz) for **R1.3** (as compared to **R1.2**) was likely because of the lower gel content that enhanced polymer fluidity, which is in agreement with a more viscous-like material. Despite of the similarities in the TTS master

curves of **R2** series, a progressive reduction of ω_e was detected corroborating that supramolecular interactions influence the relaxation of molecular chains towards a more solid-like behavior. However, aside of this elastic component improvement, the dissipative properties of formulations **R2.2** and **R2.3** resulted especially interesting for its application as high performance PSAs.

The damping factor (Tan δ) of these PSAs (**R2.2** and **R2.3**) was greater than 0.7 over four decades until it reached the specific frequency ω_e. This corroborates that hydrogen bonding interactions improved the adhesive dissipative behavior, but also extended the frequency range of these supramolecular interactions[24] (see Figure 5.13.b). Furthermore, Tan δ values nearly unit over broad frequency ranges are an indicative proof of a good balance of the polymer network viscoelasticity[26].

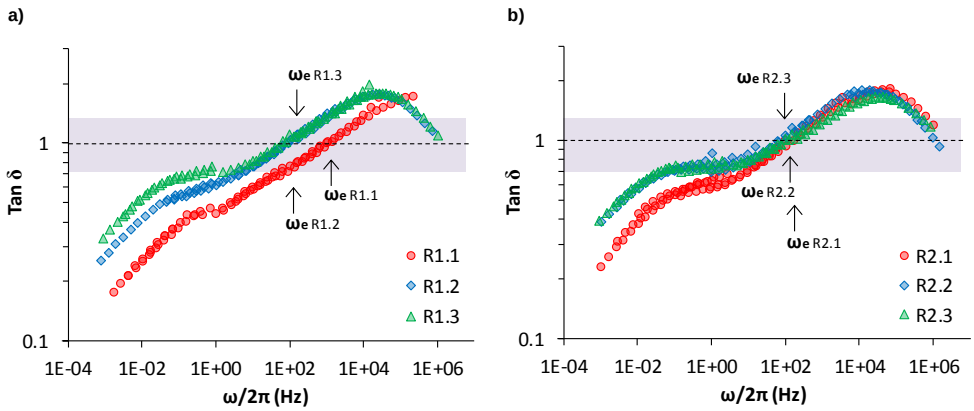

Figure 5.13. Tan δ master curves for PSA series films with ASR **R1** (a) and with ASR **R2** (b) at T_{ref} = 23 ºC. The arrows indicate the frequency ω_e for the different compositions and the purple window shows the Tan δ range from 0.7 to 1.3.

5.6 Adhesive properties of PSAs containing ASRs as stabilizers

The adhesive properties of the synthesized PSAs containing ASRs as stabilizers are presented in Table 5.7. Independently of the type of ASR used, the incorporation of IBOMA was necessary in order to enhance the cohesiveness among the polymer chains during the (de)bonding process as well as to ensure the adhesive failure kind[27]. The high liquid-like behavior of formulation **R1.1** (Tg = -43 ºC), mainly composed by 2OA, together with the too high gel content resulted in poor adhesive properties.

As can be observed, the ASR resin composition played an important role in the polymer microstructure and, thereby, in the material adhesion performance. In order to understand the role of the ASR resin, PSAs with the same comonomer composition, but having different ASRs as stabilizers have to be compared (**R1.2** vs **R2.1** and **R1.3** s **R2.2**).

Table 5.7. Properties of the synthesized PSA measured on stainless steel.

PSA	Composition (%wt monomers)	Peel (N/25mm)	Loop tack (N/25mm)	WA (J/m^2)	Shear resistance (min)	SAFT (°C)
R1.1	2OA (100)	3.5 ± 0.8	3.1 ± 0.6	43 ± 6	393 ± 35	70 ± 1
R1.2	2OA:IBOMA (85:15)	6.6 ± 0.4	6.6 ± 0.1	132 ± 8	15047 ± 439	94 ± 1
R1.3	2OA:IBOMA+CTA* (85:15)	7.3 ± 0.8	6.2 ± 0.5	119 ± 15	1659 ± 73	82 ± 1
R2.1	2OA:IBOMA (85:15)	6 ± 0.5	5.1 ± 0.4	79 ± 2	5273 ± 40	100 ± 1
R2.2	2OA:IBOMA+CTA* (85:15)	6.9 ± 0.5	10 ± 1	179 ± 24	2137 ± 130	90 ± 1
R2.3	2OA:IBOMA:ISOMA+ CTA* (85:10:5)	5.8 ± 0.4	5.4 ± 0.4	102 ± 5	4334 ± 180	85 ± 1

CTA*: 0.025 weight percent of 2EHTG based on monomer composition

For the first pair, although formulation **R1.2** tripled the shear resistance value of formulation **R2.1** because its higher gel content, it also showed greater adhesiveness, namely higher loop tack and work of adhesion. This can be explained by the higher amount of free ASR resin present in formulation **R1.2** than in **R2.1** (see MMD in Figure 5.6 and discussion above) that favored instantaneous adhesion[28].

For the second pair of PSAs (**R1.3** vs **R2.2)**, the addition of CTA controlled the formation of the gel polymer and, therefore, similar soluble molar masses were obtained (Table 5.6). Nonetheless, greater values of loop tack, work of adhesion, shear resistance and SAFT were detected for the last one. The explanation for such material behavior was the formation of OH···OH and C=O···HO hydrogen bonds among the polymer chains which had a better mobility to interact each other because of the reduction of the crosslinking density. These supramolecular interactions formed a reversible physical network which reinforces the polymer matrix but also allows molecular motion and, thus, improves the adhesion strength[29,30]. The dynamic network enhances the initial adhesion and the energy release during the detachment process as well as the solid-like behavior of the material, which augments when the hydrogen bonds density is higher[25]. This is the case of formulation **R2.3**, in which the incorporation of 5 wt% of ISOMA provided a two times greater shear resistance value than for formulation **R2.2** because of the increase of the adhesive elasticity, which also reduced peel strength and loop tack.

The efficiency of the hydrogen bond interactions commented above in formulations **R2.1** and **R2.2** comes from the grafting capability of the ASR resin. This covalent incorporation leads to polymer chains with pendant carboxylic and hydroxyl groups suitable for the adhesion and cohesion, being the last property more remarkable in formulation **R2.3**.

Probe tack test is a useful tool to further understand how supramolecular interactions and viscoelastic nature of a PSA link each other, and hence, their effect in the final performance[30]. Figure 5.14 shows the stress-strain curves for the synthesized PSA series using ASR **R1** (left) and ASR **R2** (right) as stabilizers. As it was discussed above, IBOMA strengthens the cohesion of the adhesive. This was reflected during the cavitation process of formulation **R1.2**, showing a broad stress peak above 1.7 MPa followed by a lower propagation rate of the cracks along the fibrillation process, which yielded a higher

elongation at break than formulation **R1.1**. When the gel content was reduced in formulation **R1.3**, longer but weaker adhesive fibrils were observed as consequence of the enhancement of the viscous component.

On the other hand, it is remarkable the shapes of the stress-strain curves obtained for compositions containing ASR resin **R2**. A constant increase of the stress during the fibrillation (after the relaxation process) up to large strain values are observed which can be considered as a reinforcement of the material fibers. This behavior is more prominent when the concentration of ISOMA moieties increases in the adhesive formulation (formulation **R2.3**). It also increases when the viscoelasticity of the adhesive increases for the same concentration of ISOMA moieties (**R2.2** vs **R2.1**). This kind of behavior is due to the interfacial contributions of supramolecular bonds among the molecular chains, particularly to those interactions within the cavity walls[31,32].

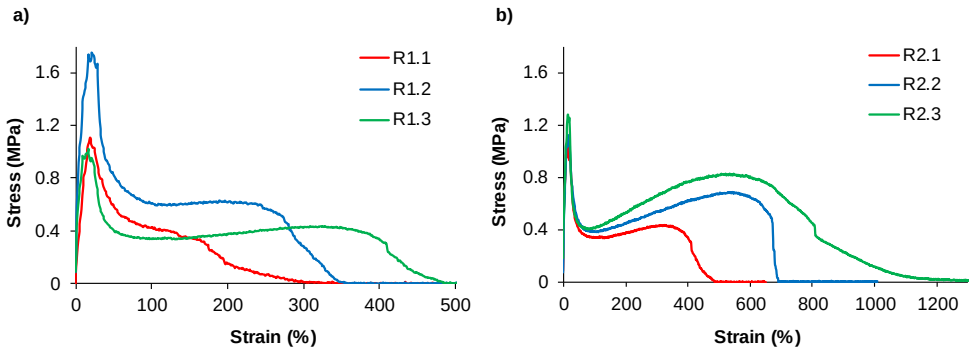

Figure 5.14. Probe tack curves for the PSA formulations coming from both resin **R1** (a) and resin **R2** (b).

Finally, a sharp decrease of the nominal stress at the maximum strain value was observed for formulations **R2.1** and **R2.2** indicating a total breakage of the adhesive fibrils and, hence, a fast energy release. Nevertheless, in formulation **R2.3** the stress decreased progressively from 700% to 800% strain, dropping to 0.35 MPa and reaching later a larger

strain value without letting any noticeable adhesive residue in the probe. In this case there was not a total breakage of the fibrils, but those residual ones continued to stretch.

These results are in agreement with the rheological analysis discussed in section 5.5. The promotion of hydrogen bonding formation improved both storage and dissipative energy properties (enhancement of G´ and G´´ and η*), being reflected in higher and longer shoulder-like shapes in the probe tack curves.

5.7 Variable temperature Fourier-transform infrared spectroscopy (VT-FTIR)

VT-FTIR is a useful technique to investigate the hydrogen bonding and debonding in a physical polymer network as a function of the temperature[33–36]. Figure 5.15 displays the FTIR absorbance spectra of composition **R2.3**, which contains the highest hydrogen bonding density, over a broad temperature range (23 ºC - 180 ºC). It is important to mention that very low intensity O-H stretching band near 3500 cm^{-1} was detected, not observing any noticeable shift towards high frequencies as the temperature was increased. Moreover, the wavenumber of the C=O stretching vibration band remained constant at 1730 cm^{-1} meaning that the most carbonyl groups did not suffer hydrogen bond association and, therefore, the band did not shift toward the blue region. However, the absorption band at 1082 cm^{-1} corresponding to the C-O stretching of secondary alcohol shifted to 1090 cm^{-1}, showing the appearance of a shoulder above 120 ºC due to the C-O bond reinforcement after the hydrogen debonding. This absorption band was not observed in FTIR absorbance spectra of composition **R1.3** because of the absence of alcohol groups (Figure 5.14.b, black dashed line). Although slight differences were found among the VT-FTIR spectra, isosorbide moieties provided those secondary alcohols and, therefore, contributed to a greater extent to hydrogen bond formation. At this point, it could be hypothesized that those hydroxyl

groups mainly interact with the carbonyl groups, which did not show any noticeable shift because of the high free number of this carbonyl species.

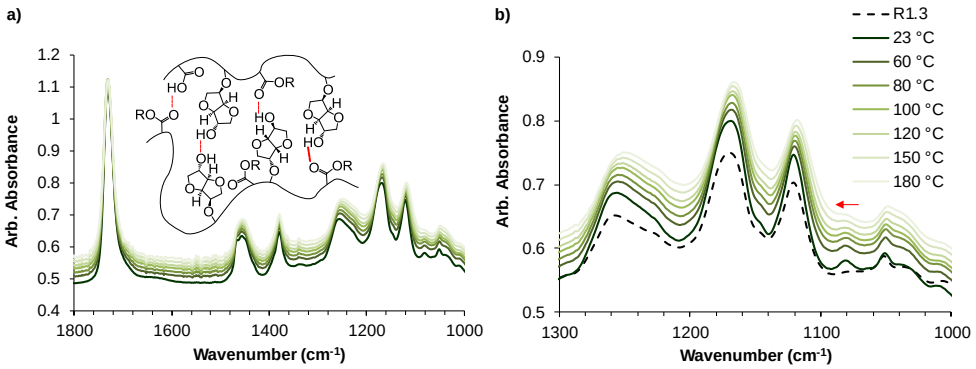

Figure 5.15. VT-FTIR spectra of formulation **R2.3** in the 1800-1000 cm^{-1} region (a) and in the 1300-1000 cm^{-1} region (b) at varying temperatures. Note that the dashed line corresponds to FTIR spectrum at 23 ºC of formulation **R1.3**.

5.8 Removability studies of PSAs containing ASRs as stabilizers

In order to study the potential removability for industrial applications, the synthesized PSAs using ASRs as polymeric stabilizers were subjected to basic conditions. For that purpose, the adhesive tapes were attached to glass substrates (mimicking glass bottles) and then they were submerged into an ammonium hydroxide solution adjusted at pH 10 (Scheme 5.2). The force needed to detach the adhesive tape from the substrate was measured at different soaking times. The test was carried out at room temperature using a static soaking procedure.

Scheme 5.2. Separation mechanism of PSAs in alkali solution

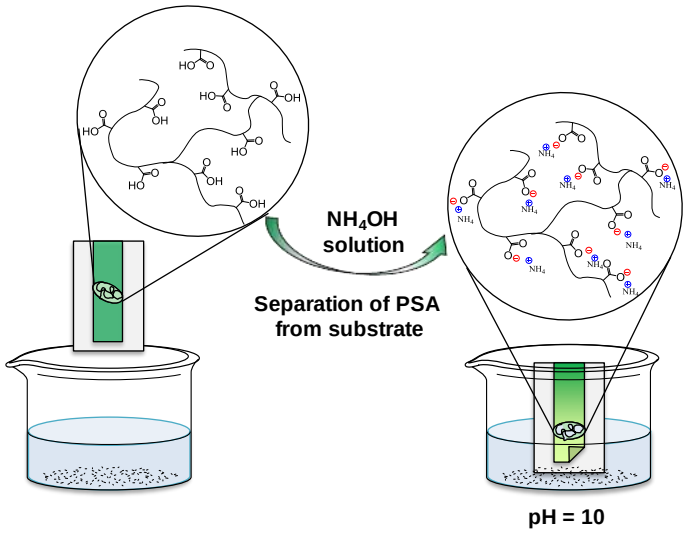

PSA compositions contain a large number of carboxylic acid groups (both ASRs contain acid groups) that allow their reaction with NH_4^+ ion in alkali solution and form the corresponding salt. As result of this reaction the adhesion of the tape to the substrate is weakened and hence the adhesive tape easily detached. Figure 5.16 shows the removability results obtained for the two PSAs series. All compositions showed a similar trend, getting a complete separation before 20 min not letting any rest of adhesive on the glass surface. Surprisingly, composition **R2.3** showed a higher peel strength value than the rest of formulations at 10 min of soaking. This was attributed to the greater quantity of ISOMA in the formulation, which provided a stronger interaction with the glass and, hence, reinforced the adhesive strength.

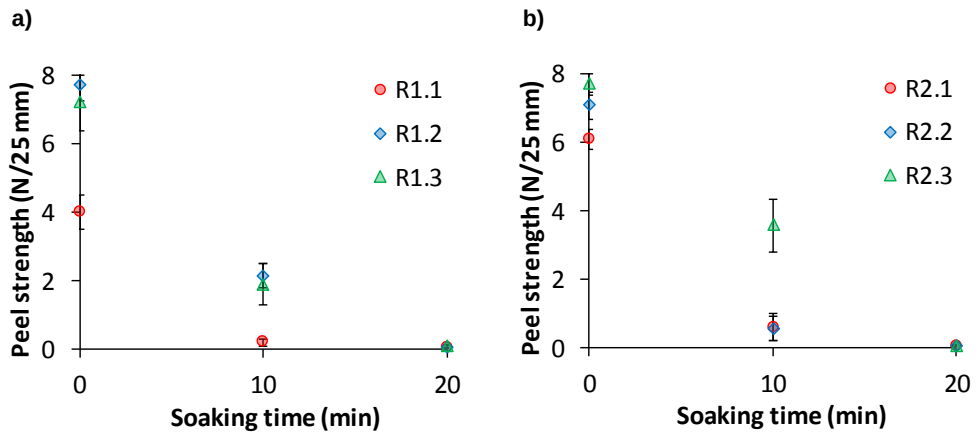

Figure 5.16. Evaluation of 180º peel strength in glass at different soaking times for PSA series films with ASR **R1** (a) and with ASR **R2** (b) at room temperature.

5.9 Conclusions

In this chapter, the synthesis of biobased alkali soluble resins (ASRs) and its use as stabilizers in emulsion polymerization aiming to obtain high performance and easy removable PSA formulations was investigated. The influence of the resin nature was evaluated and compared in terms of polymer microstructure and adhesive properties. It was found that the use of ISOMAraw in the resin composition provided pendant double bonds to the structure and, thereby, allowed the grafting of the resin to the polymer. This resulted in lower free ASR resin in the PSA latex that notably influenced in the viscoelasticity of the adhesive tapes. In addition, supramolecular interactions associated with the isosorbide groups enhanced the mechanical properties of the PSA tapes, which increased as the hydrogen bonding density did. This adhesive behavior was supported by a deep rheological assessment of the PSA films and by VT-FTIR studies, which allowed to link the hydrogen bonds formation with the viscoelastic behavior. In this context, the grafting capability of the resin containing ISOMAraw together with the existence of a physical crosslinking provided a good relationship between adhesion and cohesion, namely, a good balance of the polymer

network viscoelasticity. Finally, removability studies in alkali solution of the PSA tapes promoted their complete detachment in less than 20 min. These results provide high performance adhesive formulations ready to be industrially implemented in consumer goods and suitable for their subsequent recycling process.

5.10 References

(1) Frazee, G. R. Aqueous Pressure Sensitive Adhesive Compositions. U.S. Patent 4879333, 1989.

(2) Frazee, G. R. Pressure Sensitive Adhesive Compositions. U.S. Patent 4923919, 1990.

(3) Wu, W.; Severtson, S.; Miller, C. Alkali-Soluble Resins (ASR) and Acrylic Blends : Influence of ASR Distribution on Latex Film and Paint Properties. *J. Coatings Technol. Res.* **2016**, *13* (4), 655–665.

(4) Tsaur, S.-L. Resin-Fortified Emulsion Polymers and Methods of Preparing The Same. U.S. Patent 4820762, 1989.

(5) Siddiq, M.; Tam, K. C.; Jenkins, R. D. Dissolution Behaviour of Model Alkali-Soluble Emulsion Polymers : Effects of Molecular Weights and Ionic Strength. *Colloid Polym. Sci.* **1999**, *277*, 1172–1178.

(6) Fritz, G.; Scha, V.; Willenbacher, N.; Wagner, N. J. Electrosteric Stabilization of Colloidal Dispersions. *Langmuir* **2002**, *18*, 6381–6390.

(7) Kuo, P.; Chen, C. Functional Polymers for Colloidal Applications. V. Novel Behavior of Polymeric Emulsifiers in Emulsion Polymerization. *J. Polym. Sci. Part A Polym.*

Chem. **1993**, *31*, 99–111.

(8) Lee, D.; Kim, J.; Min, T. Role of Alkali-Soluble Random Copolymer in Emulsion Polymerization. *Colloids Surfaces A Physiochemical Eng. Asp.* **1999**, *153*, 89–97.

(9) Kato, S.; Suzuki, K.; Nomura, M. Kinetic Investigation of Styrene Emulsion Polymerization with Surface-Active Polyelectrolytes as Emulsifier , 1 Kinetic Study. *e-Polymers* **2005**, No. 33, 1–15.

(10) Lee, D.; Kim, J. Preparation of Small-Sized Carboxylated Latexes by Emulsion Polymerization Using Alkali-Soluble Random Copolymer. *J. Appl. Polym. Sci.* **1997**, *69*, 543–550.

(11) Lee, D. Y.; Kim, J. H. Emulsion Polymerization of Styrene Using an Alkali-Soluble Random Copolymer as Polymeric Emulsifier. *J. Polym. Sci. Part A Polym. Chem.* **1998**, *36*, 2865–2872.

(12) Caballero, S.; de la Cal, J. C.; Asua, J. M. Radical Entry Mechanisms in Alkali-Soluble-Resin-Stabilized Latexes. *Macromolecules* **2009**, *42*, 1913–1919.

(13) Leemans, L.; Jérome, R.; Teyssié, P. Diffusive Radical Entry as the Rate-Determining Step in Amphiphilic Block Polyelectrolyte Mediated Emulsion Polymerization. *Macromolecules* **1998**, *31*, 5565–5571.

(14) Thickett, S. C.; Gilbert, R. G. Mechanism of Radical Entry in Electrosterically Stabilized Emulsion Polymerization Systems. *Macromolecules* **2006**, *39*, 6495–6504.

(15) Bandiera, M.; Balk, R.; Barandiaran, M. J. Grafting in Polymeric Dispersions

Stabilized with Alkali-Soluble Resins : Towards the Production of Leaching-Free Waterborne Coatings. *Eur. Polym. J.* **2017**, *97*, 77–83.

(16) Bandiera, M.; Balk, R.; Barandiaran, M. J. One-Pot Synthesis of Waterborne Polymeric Dispersions Stabilized with Alkali-Soluble Resins. *Polymers (Basel).* **2018**, *10* (88), 1–14.

(17) Ko, K.; Lee, J. Y.; Shim, J. K.; Lee, J. Formulation of Emulsion Adhesives with Removal Properties by Using Alkali Soluble Resins. *J. Nanosci. Nanotechnol.* **2013**, *13*, 7467–7471.

(18) Ma, S.; Liu, X.; Fan, L.; Jiang, Y.; Cao, L.; Tang, Z.; Zhu, J. Synthesis and Properties of a Bio-Based Epoxy Resin with High Epoxy Value and Low Viscosity. *ChemSusChem* **2014**, *7*, 555–562.

(19) Wosnick, J. Bio-Based Polyester Resins. U.S. Patent 0171589 A1, 2014.

(20) Veregein, R. P. . Bio-Based Acrylate and Methacrylate Resins. U.S. Patent 0082936 A1, 2017.

(21) Zajaczkoxski, M. J. Water-Soluble Pressure Sensitive Adhesive. U.S. Patent 5395907, 1995.

(22) González, I.; Asua, J. M.; Leiza, J. R. The Role of Methyl Methacrylate on Branching and Gel Formation in the Emulsion Copolymerization of BA/MMA. *Polymer (Guildf).* **2007**, *48* (9), 2542–2547.

(23) Barnes, H. A. *Handbook of Elementary Rheology*; Institute of Non-Newtonian FluidMechanics, University of Wales, 2000.

(24) Callies, X.; Fonteneau, C.; Pensec, S.; Chazeau, L.; Bouteiller, L.; Ducouret, G.; Creton, C. Linear Rheology of Supramolecular Polymers Center-Functionalized with Strong Stickers. *Macromolecules* **2015**, *48*, 7320–7326.

(25) Kajtna, J.; Ali, B.; Krajnc, M.; Š, U. Influence of Hydrogen Bond on Rheological Properties of Solventless UV Crosslinkable Pressure Sensitive Acrylic Adhesive Prepolymers. *Int. J. Adhes. Adhes.* **2014**, *49*, 103–108.

(26) Croisier, E.; Liang, S.; Scheweizer, T.; Balog, S.; Mionic, M.; Snellings, R.; Cugnoni, J.; Michaud, V.; Frauenrath, H. A Toolbox of Oligopeptide-Modified Polymers for Tailored Elastomers. *Nat. Commun* **2014**, *5*, 4728.

(27) Zhang, L.; Cao, Y.; Wang, L.; Shao, L.; Bai, Y. Polyacrylate Emulsion Containing IBOMA for Removable Pressure Sensitive Adhesives. *J. Appl. Polym. Sci.* **2016**, *133*, 1–7.

(28) Kajtna, J.; Golob, J.; Krajnc, M. The Effect of Polymer Molecular Weight and Crosslinking Reactions on the Adhesion Properties of Microsphere Water-Based Acrylic Pressure-Sensitive Adhesives. *Int. J. Adhes. Adhes.* **2009**, *29*, 186–194.

(29) Feldstein, M. M.; Dormidontova, E. E.; Khokhlov, A. R. Pressure Sensitive Adhesives Based on Interpolymer Complexes. *Prog. Polym. Sci.* **2015**, *42*, 79–153.

(30) Heinzmann, C.; Weder, C.; De Espinosa, L. M. Supramolecular Polymer Adhesives: Advanced Materials Inspired by Nature. *Chem. Soc. Rev.* **2016**, *45*, 342–358.

(31) Callies, X.; Fonteneau, C.; Pensec, S.; Bouteiller, L.; Ducouret, G.; Creton, C. Adhesion and Non-Linear Rheology of Adhesives with Supramolecular Crosslinking Points. *Soft Matter* **2016**, *12*, 7174–7185.

(32) Crosby, A. J.; Shull, K. R.; Lakrout, H.; Creton, C. Deformation and Failure Modes of Adhesively Bonded Elastic Layers. *J. Appl. Phys.* **2000**, *88*, 2956–2966.

(33) Zhang, K.; Fahs, G. B.; Margaretta, E.; Hudson, A. G.; Robert, B.; Long, T. E. Acetyl-Protected Cytosine and Guanine Containing Acrylics as Supramolecular Adhesives as Supramolecular Adhesives. *J. Adhes.* **2019**, *95*, 146–167.

(34) Morita, S. Hydrogen-Bonds Structure in Poly (2-Hydroxyethyl Methacrylate) Studied by Temperature-Dependent Infrared Spectroscopy. *Front. Chem.* **2014**, *2*, 1–5.

(35) Zhang, K.; Chen, M.; Drummey, K. J.; Talley, S. J.; Anderson, L. J.; Moore, R. B.; Long, T. E. Ureido Cytosine and Cytosine-Containing Acrylic Copolymers. *Polym. Chem.* **2016**, *7*, 6671–6681.

(36) Bhadra, J.; Al-thani, N. Advances in Blends Preparation Based on Electrically Conducting Polymer. *Emergent Mater.* **2019**, *2*, 67–77.

Chapter 6

Development of biobased waterborne coatings containing Ecomer® monomer

6.1 Introduction

So far, all the chapters have been focused in the development of sustainable waterborne PSAs with high bio-content as potential consumer goods for future applications. Nonetheless, waterborne coating compositions coming from renewable feedstock represent a growing and promising market for the paint & coating industry. Among the most important renewable sources, carbohydrates-derived products are attracting more and more interest since they represent 75% of the annually renewable biomass, i.e. 200 billion tons[1]. The main research in the emulsion polymerization field has been focused on the synthesis and incorporation of vinyl starch macromonomers, (un)protected monosaccharide derived (meth)acrylates or even modified starch nanoparticles for their application as biodegradable coatings, resins, inks or paints[2–9]. However, the hydrophilic nature of such kind of monomers induce colloidal stability problems above a certain concentration, being necessary to attach a hydrophobic group to the carbohydrate skeleton to produce stable latexes[10,11]. In this regard, a sugar-based monomer has been developed by Ecosynthetix with the name of Ecomer®, an alkyl polyglucoside (APG) maleic acid ester coming mainly from dextrose with an average oligomerization degree between 1.3 and 2 and having a hydrophobic tail (Scheme 6.1)[12]. Few patents have reported recently the use of this kind of macromonomer to produce repulpable and biodegradable pressure sensitive adhesives[13–15]. Nevertheless, there are no studies involving this APG derived monomer together with other monomers coming from renewable sources for the preparation of waterborne coatings.

Accordingly, this chapter will be focused in the development of waterborne coatings by the combination of Ecomer® together with the already studied commercial biobased monomers 2-Octyl acrylate (2OA) and isobornyl methacrylate (IBOMA). For this purpose, Ecomer® was firstly characterized to better know its composition (degree of oligomerization and substitution degree) and hence its potential impact in the emulsion polymerization.

Secondly, its copolymerization with different hard monomers was studied aiming to understand its incorporation in the preformed polymer particles. Then, biobased waterborne coatings containing 2OA and IBOMA as main comonomers were developed and fully characterized. The caramelization process allowed to incorporate the free Ecomer® content as well as to improve both mechanical and coating properties. IR, TGA and DMTA analysis shed light about this process and its correlation with the final properties. Finally, biodegradability studies of the coatings films were carried out.

This work was carried out during the internship in the R&D department (Acrylics team) of DSM Coating Resins (Netherlands).

Scheme 6.1. Commercial biobased monomer used in this chapter and its bio-content, where the green part belongs to the carbon structure coming from the nature.

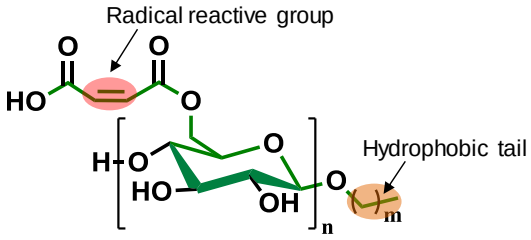

Ecomer® (100%)
n = 1.3-2 ; m = 2-7

6.2 Experimental

Biobased monomer isobornyl methacrylate (IBOMA, 71% bio-content) was purchased from Evonik Industries (Germany), while 2-Octyl acrylate (2OA, 73% bio-content) was purchased from Arkema (France). Ecomer® was supplied from Ecosynthetix (Ontario, Canada) as a mixture Ecomer:Butyl acrylate 50 wt:50 wt. Styrene (ST) was purchased from BASF (Germany), whereas methyl methacrylate, (MMA) and methacrylic acid (MAA) were purchased from Lucite International (Germany). Calcium bicarbonate ($CaCO_3$) was acquired

from Brenntag (Germany), whereas potassium persulfate (KPS), ascorbic acid (AsA) and methylethyl ketone (MEK) were purchased from Nexeo Solutions (Germany) and tert-butyl hydroperoxide (TBHP) was purchased from AkzoNobel (Netherlands). Dowfax2A1 (Alkyldiphenyloxide Disulfonate, emulsifier) was purchased from Dow Chemical (Midland, Michigan, USA), ammonium hydroxide solution (25 wt%) was purchased from sigma Aldrich (Germany) and the biocide Proxel Ultra 10 was purchased from Vink Chemicals (Germany). Butyl diglycol (BDG) and N-Methyl-2-pyrrolidone (NMP) together with deuterated solvents such as chloroform ($CDCl_3$) and dimethyl sulfoxide (DMSO-d6) were purchased from VWR International (Netherlands). Deuterated pyridine (C_5D_5N) was acquired from Merck (Netherlands). BYK 346 (wetting agent) was kindly supplied by BYK Additives & Instruments (Abelstrasse, Germany). All reagents were used without further purification.

6.2.1 Emulsion polymerization

All the latexes were synthesized via starved-feed seeded semibatch emulsion polymerization, being 45 wt% the final solids content. The polymerization process included the loading of the seed in the reactor and the feeding of an Ecomer containing pre-emulsion of monomer during 210 min. Upon finishing the pre-emulsion feeding, the reactor content was post-polymerized for 1 h. After the post-polymerization process, a biocide solution was added and the final pH adjusted to 7 with an ammonium hydroxide solution. Emulsion polymerizations were performed at 80ºC and 150 rpm in a 2L glass reactor equipped with a reflux condenser, sampling device, nitrogen inlet and a stainless steel anchor-type stirrer. Table 6.1 summarizes the formulations.

Table 6.1. Materials and percentages employed in the synthesis of the latexes

	Materials	wbm %*	Amount (g)
Seed	BA/MMA/MAA (49.5/49.5/1)		294.04
Second stage pre-emulsion			
Low Tg monomers	2OA BA	0-27 15-42	0-110.17 61.21-171.38
High Tg monomers	IBOMA ST MMA	42	171.38
Functional monomers	MAA Ecomer®	1 15	4 61.21
Emulsifier	Dowfax2A1	1	9.06
Initiator	KPS	0.5	2.04
Continuous phase	Water		292.52

*weight % based on total monomer content fed

The seed was synthesized in semibatch having a solids content 15 wt% and a composition BA/MMA/MAA:49.5/49.5/1 by weight (see Table 6.1). A pre-charge formed by deionized water, Dowfax 2A1, and calcium bicarbonate was introduced into a reactor. The mixture was srirred at 175 rpm for 30 min under nitrogen and the temperature was increased to 75°C. Then, a shot of KPS (0.5 wbm%) was added and the monomers mixture was fed along 2 h. When the feeding process was completed a post-polymerization process was carried out for 1h at 175 rpm and 75°C. After the post-polymerization step a killing process was performed at 60 °C using a redox pair Ascorbic acid/TBHP (0.1 wbm%/0.1 wbm%).

6.2.2 Characterization

Particle size was analyzed by dynamic light scattering (DLS) and conversion was determined gravimetrically. The gel fraction (or insoluble fraction of the copolymer in MEK) was measured by static extraction.

The molar mass distribution of the soluble fraction as well as Ecomer® conversion were determined by size exclusion chromatography (SEC) at 70°C, using N-Methylpyrrolidone (NMP)/ methylethylketone (MEK) (80/20) and 10 mmol lithiumbromide (LiBr) as eluent and referred to polystyrene standards.

Ecomer® conversion was corroborated by thermogravimetric analysis of the supernatant of the binder after the centrifugation process at 20 ºC for 24 h with a relative centrifugal force (RCF) of 20000 x g (Sigma 3-30KS).

Ecomer® characterization was carried out by high pressure liquid chromatography (HPLC) using gradient elution of H_2O/acetonitrile/THF and PDA/ELSD/ESI-TOF-MS (Photodiode Array/Evaporative Light Scattering Detector/Electrospray Ionization-Time Of Flight-Mass Spectrometry) detection. Nuclear magnetic resonance (NMR) spectra were recorded on a Bruker 400 MHz equipment.

The glass transition temperature (Tg) was determined by differential scanning calorimetry (DSC250, TA Instruments) of dry polymers from the final latexes using hermetic pans. The scanning cycles consisted of first cooling to -85 °C at 20 °C/min, and then heating to 160 °C at a rate of 10 °C/min, cooling again from 160 °C to -85 °C at 20 °C/min, and then heating to 160 °C at 10 °C/min. Isotherm thermogravimetric analysis (TGA) were performed at 120 ºC under oxygen atmosphere using a Q500 device (TA analysis). The minimum film formation temperature (MFFT) was determined by a MFFT-60 equipment (Rhopoint instrument) using a gap applicator of 100 µm under air conditions. Dynamic-Mechanical Thermal Analysis (DMTA) were carried out using a dynamic mechanical thermal analyzer (Triton 2000 DMA, Triton Technology, Ltd) with single cantilever tension geometry.

Fourier transform infrared spectroscopy (FTIR) was used in order to follow the condensation reaction of hydroxyl groups during the caramelization process. The IR spectra was obtained using Alpha FT-IR spectrometer Platinum ATR operated with OPUS software.

6.2.3 Film preparation and coating properties

***Water uptake*.** The coating films were prepared by the addition of a known quantity of latex into a silicone template in order to obtain films of approximately 500 µm thickness. The films were dried at 22 ºC and 50 % humidity for 4h and then at 50 ºC overnight. 2 dry films of 2 cm^2 area per formulation were weighted (m_o) and submerged into 25 mL of deionized water for 24h and then were carefully dried and weighted again (m_t).

$$Water\ uptake = \frac{m_t - m_o}{m_o} \times 100 \qquad \textbf{(Eq.6.1)}$$

In what follows, for the film preparation, wetting agent (0.5 wt%) was used in all formulations and BDG for the formulations: **6Ref**, **6A**, (2 wt%) and **6B** (4 wt%).

Hardness. The coating films were prepared by casting the latex over a glass panel (10 cm x 20 cm) using a gap applicator of 100 µm in order to obtain films of approximately 45 µm thickness. The films were dried at 22 ºC and 50 % humidity for 4h and then at 50 ºC overnight. The hardness of the coating films was measured by Persoz pendulum hardness at 22 ºC and 50 %. At least three measurements of each film were performed, and the results were averaged.

Blocking. Films were cast on black and white sealed chart from Leneta (form 8B) using a roll applicator of 100 µm. The films were dried at 22 ºC and 50 % humidity for 24 h. Then the Leneta chart was cut in strips (3.3 cm x 9.7 cm) and stacked in a cross-like way. The stacked strips were subjected to 1 kg of pressure for 4h at 50 ºC. The visual evaluation

was carried out following the standard method ASTM D4946. Grades were attributed to each coating ranging from 0 for a bad film separation (adhesion, film damages) to 5 for an easy and damage-free separation of the strips.

***Contact angle*.** Water contact angles were measured in a OCA 20 Instrument (Dataphysics). The coating films were prepared by casting the latex over glass substrates using a gap applicator of 100 µm in order to obtain films of approximately 45 µm thickness The films were dried for two days at 23^0C and 55% relative humidity. The measurement of the contact angle was done by placing 10 µl droplets of distilled water on the surface of the films. The values given are an average of twenty measurements per film.

Tensile test. The coating films were prepared by casting the latex over a release paper using a gap applicator of 425 µm. Films were dried under the same conditions than the hardness test ones. Afterwards, films were cut in order to obtain probes with approximately 190 µm thickness, 4 mm width and 30 mm of effective length. Tensile tests were performed at 22 ºC and 50 % humidity in a Zwick Roell Z010 10kN tensile testing machine applying a crosshead speed of 100 mm/min. At least five specimens of each film were tested, and the results were averaged.

Chemical resistance. Waterborne dispersions were applied on sanded melamine panels by a roll applicator, obtaining a final coating thickness of 45 µm and 54 µm, respectively (the films were dried at 22 ºC and 50 % humidity for 4h and then at 50 ºC overnight). Chemical resistance to coffee, ethanol (48%), red wine, mustard and water was evaluated by “spot test”. Circular filter papers (25 mm diameter) were submerged into the substance for 30 seconds and then placed on the coating during a period of time, covering the testing area with a small glass vessel. The filter paper was placed during 1 hour for coffee and ethanol, 6 hours for mustard and wine and 16 hours for water and coffee. After these

given times, liquid spots were carefully wiped off with absorbent paper. After 24 hours, the dry spots were cleaned up with soap using a sponge and films damage was evaluated visually, grading from 0 (extremely damaged) to 5 (intact films).

6.2.4 Caramelization process

Caramelization reaction of the final coatings was perfomed at 120 ºC. For that purpose glass panels, melamine panels and leneta chart, which contained the coating as well as tensile test probes, were introduced in the oven overnight. Thereafter, mechanical and coating properties such as tensile test, hardness, blocking, and chemical resistance were evaluated.

6.2.5 Biodegradability assessment

Biodegradability of dry polymer materials was evaluated in agreement with OECD 301 (biodegradation in water/activated sludge) by measuring the Biochemical Oxygen Demand (BOD) in a closed system, i.e. the amount of O_2 consumed by the decomposition of organic matter in a biochemical process, for 29 days at 25 ºC. Where TOD is the Theoretical Oxygen Demand

$$Biodegradation = \frac{BOD\ measured}{TOD} \times 100 \qquad \textbf{(Eq.6.2)}$$

The TOD (Theoretical Oxygen Demand) of a substance $C_cH_hCl_{cl}N_nNa_{na}O_oP_pS_s$ of molecular weight MW is calculated as:

$$TOD\ \left(\frac{mg\ O_2}{mg\ test\ substance}\right) = \frac{16[2c+0.5(h-cl-3n)+3s+2.5p+0.5na-o]}{MW} \qquad \textbf{(Eq. 6.3)}$$

This calculation implies that C is mineralized to CO_2, H to H_2O, P to P_2O_5 and Na to Na_2O. Halogen is eliminated as hydrogen halide and nitrogen as NH_3.

6.3 Ecomer® characterization

Ecomer® is a family of alkyl polyglucoside (APG) maleic acid esters coming mainly from dextrose (α-D-Glucose) and having an average oligomerization degree ranging from 1.3 to 2. In addition, the hydrophobic tail length, which is composed by an aliphatic chain, can range from 1 to 30 carbons or a mixture thereof, being more preferably a C3 to C8 alkyl chain as it was described in the patent literature[13]. The Ecomer® used in this chapter was fully characterized before its incorporation to emulsion polymerization formulations.

Figure 6.1 shows both ^{1}H NMR (up) and ^{13}C NMR (down) spectra of Ecomer® in dimethyl sulfoxide-*d6*. As it can be observed, the ^{1}H NMR spectra shows the alkyl chain protons about 0.7-1.7 ppm. The C-H groups signals from the glucose ring appear between 3.0 and 5.5 ppm intercalated with the signals corresponding to the $O\text{-}CH_2$ group of the aliphatic chain (3.33-3.38 ppm), while a broad variety of the H-C=C-H signals are placed between 6.0 and 6.5 ppm. In addition, traces of p-toluene sulfonic acid were detected (less than 1 mol%) likely because is used as catalyst in the first step of the synthetic pathway of Ecomer®. ^{13}C NMR allowed to identify all the significant signals that confirm the length of the alkyl group, concluding that Ecomer® was a hexyl polyglucoside maleic acid ester. Regarding this, five signals corresponding to the alkyl chain are placed between 10 and 35 ppm, while the $O\text{-}CH_2$ group of the chain together the sugar CH groups are between 60 and 80 ppm. The C=C group from the maleic anhydride moiety is in the region between 110 and 130 ppm and the C=O bonds from the ester groups appear around 165 ppm. Furthermore, the ^{1}H NMR signals integration revealed that each glucose unit contained 0.52-0.6 of hexyl and 0.58-0.66 of maleic ester substituents (lowest number for a polymer and the highest number based upon one glucose unit).

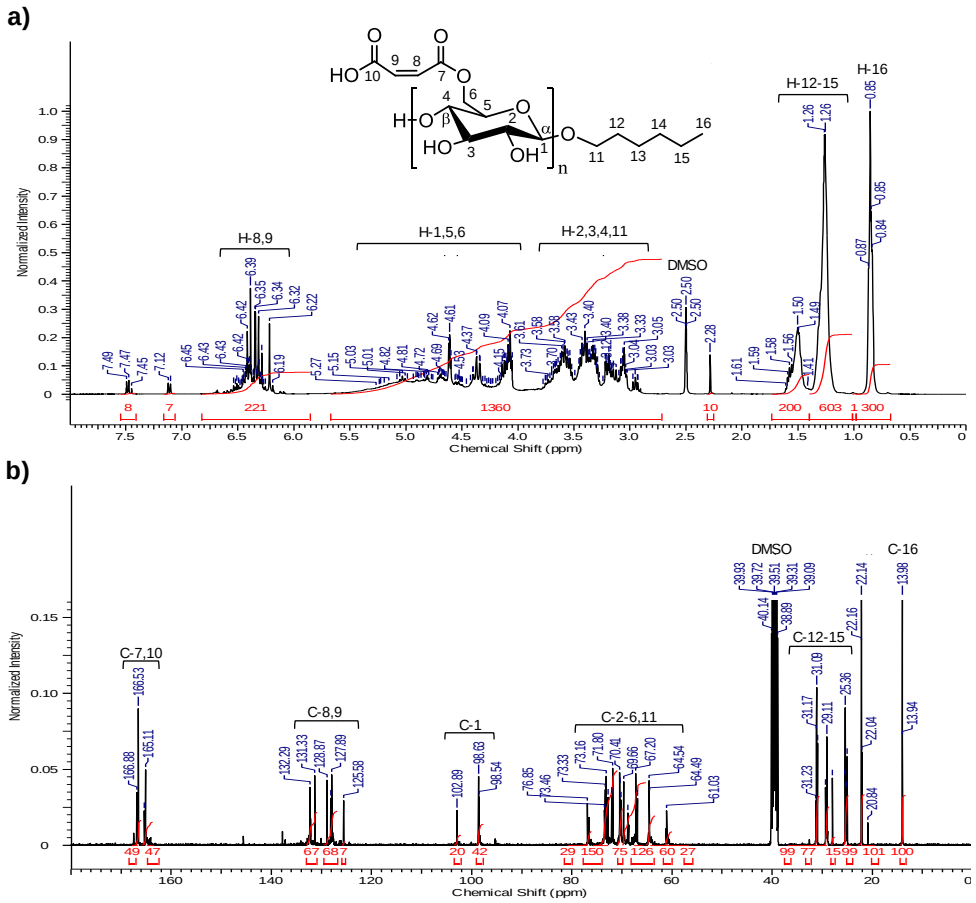

Figure 6.1. ^{1}H NMR (a) and ^{13}C NMR (b) spectra of Ecomer® in dimethyl sulfoxide-d6.

The mass spectroscopy analysis of Ecomer® (Figure 6.2) revealed several peaks corresponding to different glucose derivative species. The base peak at *m/z* = 385.15 is associated with the presence of a single charge sodium adduct of a glucose ring containing a maleic anhydride skeleton and a hexyl chain tail, whereas the peak at *m/z* = 483.15 corresponds to a triple charged sodium and dilithium adduct of the hexyl monoglucoside disubstituted maleic acid ester. Moreover, other ions with diglucose groups, which arise from the first step of the reaction pathway, were also detected. The peaks at *m/z* 547.20 and

747.30 correspond to a singly charged sodium adduct diglucose maleic acid ester and a doubly charged sodium and ammonium adduct diglucose dimaleic acid ester, respectively. However, a single charged sodium adduct of hexyl diglucoside not containing polymerizable double bonds was also observed (*m/z* 449.20). This non-polymerizable species could come from the breakage of the maleic anhydride moiety during the ionization process or, most likely, being a side product of the synthetic route to produce Ecomer®.

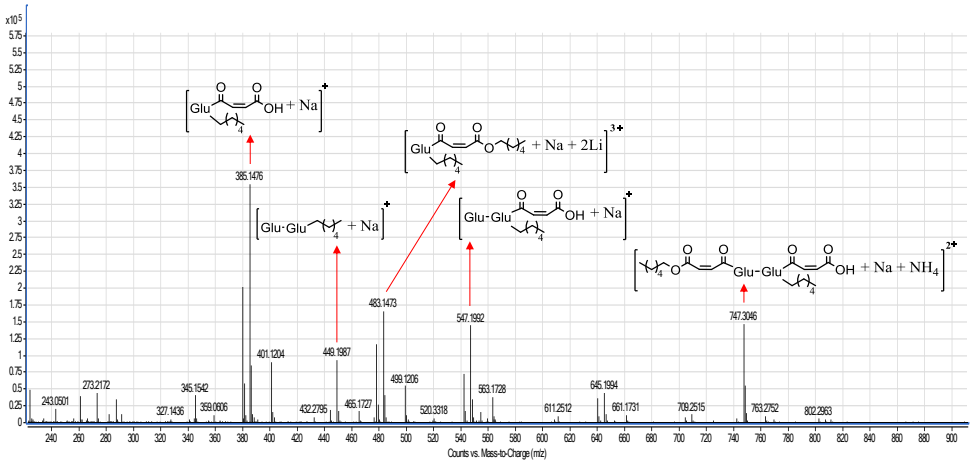

Figure 6.2. HPLC-ESI-TOF mass spectrum of Ecomer®.

Ecomer® was also characterized using DSC analysis (see Figure 6.3.a) detecting a glass transition temperature of -3 ºC in the first heating cycling. Nevertheless, as the number of heating cycles increased the glass transition temperature did too, reaching a value around 34 ºC in the last one because its homopolymerization or even caramelization reactions. Finally, SEC analysis (see Figure 6.3.b) revealed a broad molecular weight distribution for this sugar based vinyl monomer (SBV) having an average molar mass (Mw) of 737 g/mol and a polydispersity index (PDI) of 1.24.

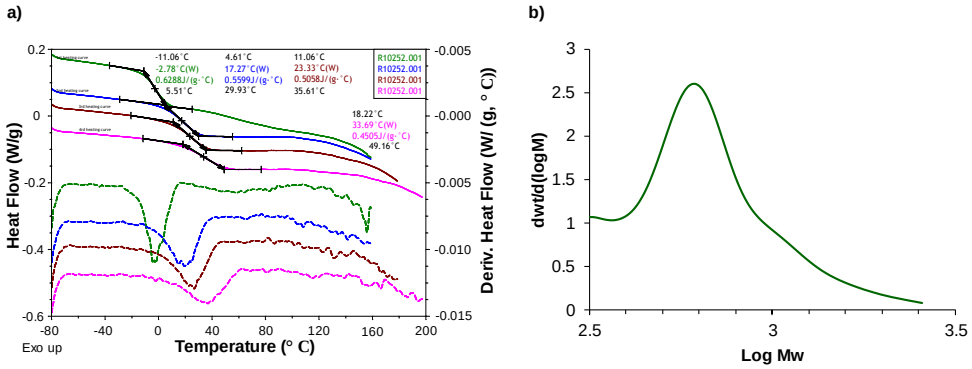

Figure 6.3. DSC curves of Ecomer® at a heating rate of 10 ºC/min (a) and selected molecular weight distribution from the GPC chromatogram (b). Note that in the case of DSC analysis 4 heating cycles were performed.

6.4 Effect of the hard monomer in the copolymerization of Ecomer®

One of the goals of this work was to investigate the incorporation of Ecomer® in coating compositions containing different kind of hard monomer. It is worth noting that above 15 wt% of Ecomer® in the composition caused the coagulation of the latexes, likely because of the high amount of water soluble species formed. Therefore, latexes with the composition: BA:Hard monomer:SBV:MAA (42:42:15:1) were explored.

For this purpose, methyl methacrylate (MMA), isobornyl methacrylate (IBOMA) and styrene (ST) were used as hard monomers. It was found that the nature of the hard monomer influenced the quantity of Ecomer® incorporated into the polymer particles, namely the SBV monomer content copolymerized. Figure 6.4 shows the ^{1}H NMR spectra in chloroform-d_1 of the binder composition: BA:MMA:SBV:MAA (42:42:15:1), observing free double bonds in the region between 6.0 and 6.5 ppm coming from the non-incorporated SBV. In addition, Ecomer® species not containing polymerizable double bonds contribute to the low incorporation of Ecomer® (peak at *m/z* = 449.19 in the mass spectrum).

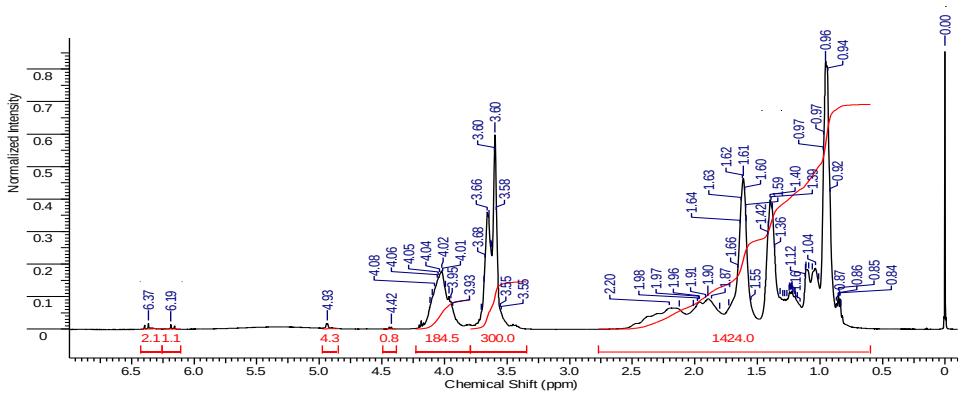

Figure 6.4. ^{1}H NMR spectra in chloroform-d_1 of the latex composition BA:MMA:SBV:MAA (42:42:15:1). Tetramethyl silane was used as internal standard.

SEC analysis revealed that the free Ecomer® content remaining in the water phase per kg of binder was around 20-23 g for MMA, 17-18g for IBOMA and between 9.7 and 14g when ST was used (Scheme 6.2). These values were corroborated by measuring the solids content of the latex supernatant after the centrifugation process. This limited incorporation is likely due to the lower reactivity ratio of the maleic double bonds of the Ecomer monomer with respect to the (meth)acrylate ones used in the formulation and the high water solubility of Ecomer that favors its partition to the aqueous phase and hence its difficulty to be incorporated into the copolymer in the polymer particles[16,17].

Scheme 6.2. Ecomer incorporation yield and free content as a function of the kind of hard monomer used.

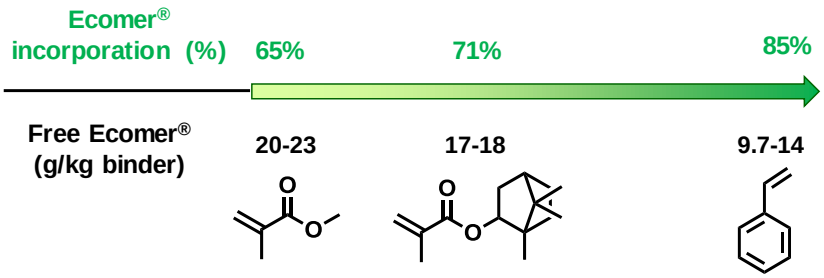

In what follows only the latexes synthesized with IBOMA as hard monomer are discussed (those synthesized with MMA and ST can be found in the Appendix 2) since this monomer yields the latexes with the higher bio-content.

6.5 Synthesis of acrylic latexes containing IBOMA/Ecomer®

Table 6.2 summarizes the latexes synthesized as well as their main properties including gel content, sol weight-average molar mass (Mw), glass transition temperature (Tg), Minimum Film Formation Temperature (MFFT), bio-content and the free Ecomer® content (SBV). Figure 6.5 shows a representative evolution of both instantaneous and overall conversion as well as the particle size evolution along the reaction time. In all reactions instantaneous conversions higher than 90% were achieved because of the starved monomer feeding conditions, reaching full conversion (measured by gravimetry) after a post-polymerization process of one hour. In addition, the experimental particle size evolution was similar to the predicted one meaning that either secondary nucleation or coagulations were minimized during the process.

Table 6.2. Summary and characteristics of the synthesized latexes by two-stage process.

COMP	2nd Stage (%wt monomers)	Gel (%)	Mw (kDa)	Tg (°C)	MFFT (°C)	Bio (%)	SBV (g/kg)*
6Ref	BA:IBOMA:MAA (49.5:49.5:1)	52 ± 0.1	301	33	19.5	33	-
6A	BA:IBOMA:SBV:MAA (42:42:15:1)	65 ± 1	112	29.3	21	41	17
6B	2OA:BA:IBOMA:SBV:MAA (27:15:42:15:1)	67 ± 0.1	89.9	34.5	25	63	18

* Makes reference to the quantity of free Ecomer® in 1 kg of binder.

As it can be observed, the incorporation of Ecomer® in composition **6A** reduced the glass transition temperature and increased the insoluble fraction (gel content) due to the existence of sugar based divinyl species acting as crosslinkers. As a consequence, the diffusion of the polymer chains across the particle interface was affected yielding higher

MFFT values. When a fraction of butyl acrylate was substituted by 2-Octyl acrylate in composition **6B**, the Tg of the final polymer increased around 5 ºC, which also affected to the MFFT value without observing any relevant change in the soluble molar mass and gel content.

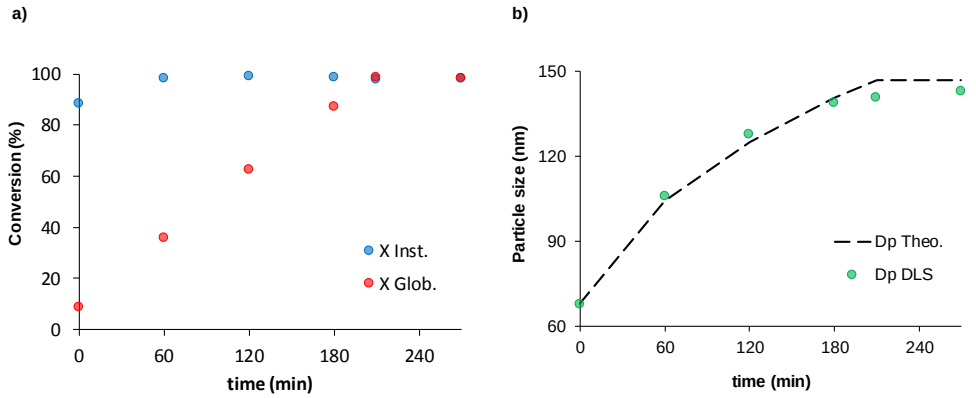

Figure 6.5. Representative evolution of (a) the instantaneous and overall conversion, during the synthesis of latex **6A**, and (b) average particle size evolution measured by DLS together with the theoretical evolution.

6.6 Caramelization process

Caramelization and Maillard reactions are complex oligomerization processes taking place when carbohydrates are exposed to high temperatures, yielding both volatile (degradation process) and nonvolatile components (~95%), which complete chemical structure remains unknown[18–20]. Both processes involve a group of reactions which are clearly influenced by temperature, time, pH, sugar concentration and the presence of amino compounds, being this last one the case of the Maillard reaction[21,22]. In general terms, the caramelization reaction is preceded by sugar isomerization and degradation reactions (most of them dehydration processes) producing mostly organic acids such as formic, acetic, lactic or glycolic acid and other furan compounds like 2-Hydroxyacetylfurane (HAF), with special

preponderance to the thermodynamically stable 5-Hydroxymethylfurfural (HMF), which is one of the main responsibles of the brownish colour and flavor in the caramel[23–26]. These degradation reactions are accelerated at temperatures above 120 ºC and are catalyzed by acids and bases[27].

On the other hand, glucose oligomerization by condensation reactions forms strongly colored nonvolatile components of relatively high molar mass, which are classified into three classes: caramelans, tetramers of hexoses ($C_{24}H_{36}O_{18}$); caramelens, hexamers of glucose ($C_{36}H_{50}O_{25}$); and caramelins, polymers of glucose ($C_{125}H_{188}O_{80}$)[28]. It is worth to point out that the molecular formula of these structures depends on the type of carbohydrate used and, furthermore, intermediate products composed by dimers or trimers are also formed[29]. Moreover, as the caramelization time increases, and hence dehydration reactions, the formed furan compounds HMF, furfural and HAF may act as precursors of coloring polymeric products[19].

Keeping in mind this oligomerization process and in order to reduce the free Ecomer® content in the final product caramelization reactions of the final coatings were performed aiming to incorporate the remaining Ecomer® by condensation reactions. In order to minimize degradation reactions the caramelization process was carried out overnight at 120 ºC[22]. Figure 6.6 shows a coating film containing Ecomer® before and after the caramelization process together with a schematic view about the hypothetical chemical structure of the polymer. It can be noted the brownish color of the film after the caramelization due to the presence of furan derivative moieties and to the condensation reactions, which increased both the hardness and brittleness of the final coating.

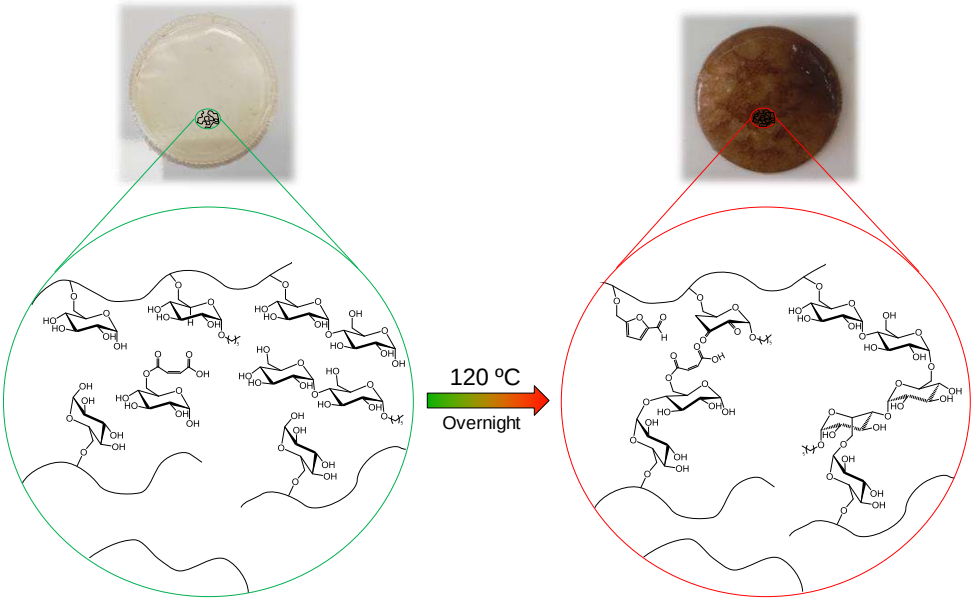

Figure 6.6. Coating films containing Ecomer® with schematic view about the hypothetical chemical structure of the polymer before and after caramelization process.

Figure 6.7 shows the evolution of the soluble molar mass distribution for compositions **6A** and **6B** as well as the gel content before and after the caramelization. As it can be observed the oligomerization process allowed to incorporate the remaining SBV molecules, observing the disappearance of the peak close to 10^3 g/mol, which corresponds to the free Ecomer®. In addition, sol molar masses were shifted towards lower masses because of the formation of both intra and intermolecular glycosidic linkages as well as the possibility of interconnected furan derivative structures, which increased the insoluble fraction. Concerning this, the gel content shifted from 65% to 72% for composition **6A** and from 67% to 75% in the case of composition **6B**.

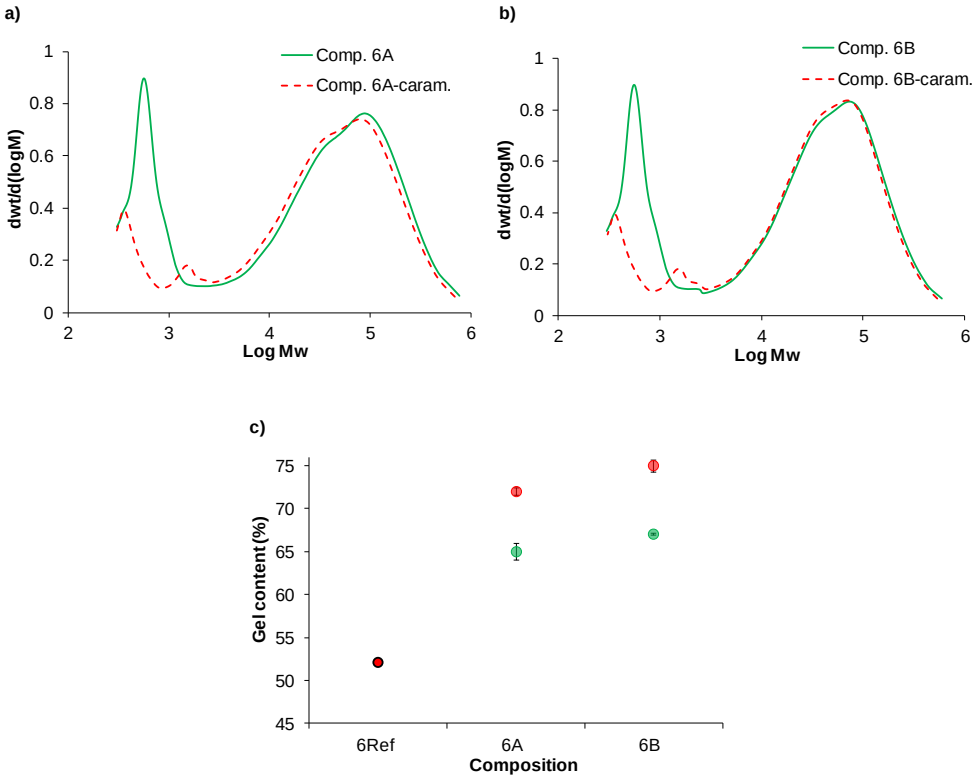

Figure 6.7. Soluble molar mass distribution of compositions **6A** (a) and **6B** (b); and gel content evolution (c) before (green circles) and after (red circles) caramelization process.

Infrared spectroscopy (see Figure 6.8) confirmed the condensation reactions due to reduction of the O-H stretching vibration band at 3240 cm^{-1} together with a strong diminution of the band at 616 cm^{-1}, which is associated to the out-of-plane O-H bending vibration (O-H δ oop). Furthermore, the in-plane O-H bending vibration band appearing around 1450 cm^{-1} shifted towards lower wavelengths, unfolding into two bands, which is typical for acetals and ketals. The HC-OH stretching band at 1112 cm^{-1} shifted towards higher wavelengths, concretely to 1160 cm^{-1}, which is the stretching vibration for the ether linkage (HC-O-CH) corroborating the glycosidic bond formation.

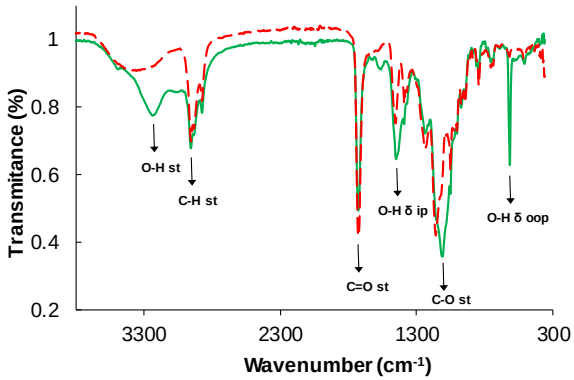

Figure 6.8. Infrared spectra before (green continuous line) and after (red dashed line) caramelization process.

Isothermal thermogravimetric analysis was carried out emulating the caramelization conditions to determine the percentage weight loss during the process. For that, polymers from compositions **6A** and **6B** were subjected at 120 ºC for 14 h under oxygen atmosphere. Figure 6.9 shows the isothermal TGA curves of the corresponding compositions. It was found a loss of 0.85 wt% and 0.65 wt% for compositions **6A** and **6B**, respectively before reaching 110 ºC, which belongs to the loss of water absorbed by the material. An effective weight loss of 2.79% and 3.14% was detected during the caramelization time meaning that not only carbohydrate oligocondensation products were formed, but also dehydration products coming from the glucose itself, which is able to lose up to three molecules of water, yielding furan derivative compounds. Despite of the low caramelization temperature, the generation of unexpected volatile molecules should not be discarded.

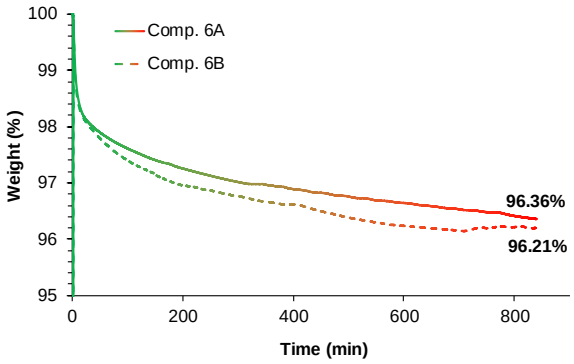

Figure 6.9. Isothermal TGA curves at 120 ºC of compositions **6A** and **6B** under oxygen atmosphere for 840 min.

6.7 DMTA analysis of acrylic dispersions containing IBOMA/Ecomer®

In order to understand how the solid-like behavior of the materials is affected by the caramelization process, the coatings cast at ambient temperature were analyzed using dynamical thermal analysis (DMTA). Figure 6.10 shows the storage modulus (G') and tanδ vs temperature curves before (green) and after (red) the caramelization for the compositions **6A** and **6B** together with the reference one.

As it can be observed, the use of Ecomer® decreased the storage modulus in the final coating due to the increasing of the space among the polymeric chains and, hence, the mobility of them. In addition, the incorporation of Ecomer® in composition **6A** led to a lower glass transition temperature than the one corresponding to the reference composition. The use of 2OA in composition **6B** counteracted the effect produced by Ecomer®, resulting in a higher Tg in comparison with the reference one. All the coatings (the reference and the coatings containing Ecomer monomer before and after caramelization) presented a liquid-like behavior at temperatures above 80ºC (G' decreases sharply), which is an indication of lightly or non-crosslinked polymers. After the caramelization process, a similar tanδ transition change was detected for both compositions, indicating a reinforcement of the polymer

network. Nevertheless, composition **6A** presented more clear differences of G´ (before and after the caramelization) than composition **6B**, which means a small enhancement of the crosslinking density. Surprisingly, above 80 ºC, G´ for the caramelized polymers decreased faster than for non-caramelized polymers, without observing any rubbery plateau. This suggests changes in the solid-like behavior which are appreciated at room temperature, but not in the solid regime because the high liquid-like behavior of the caramelized system.

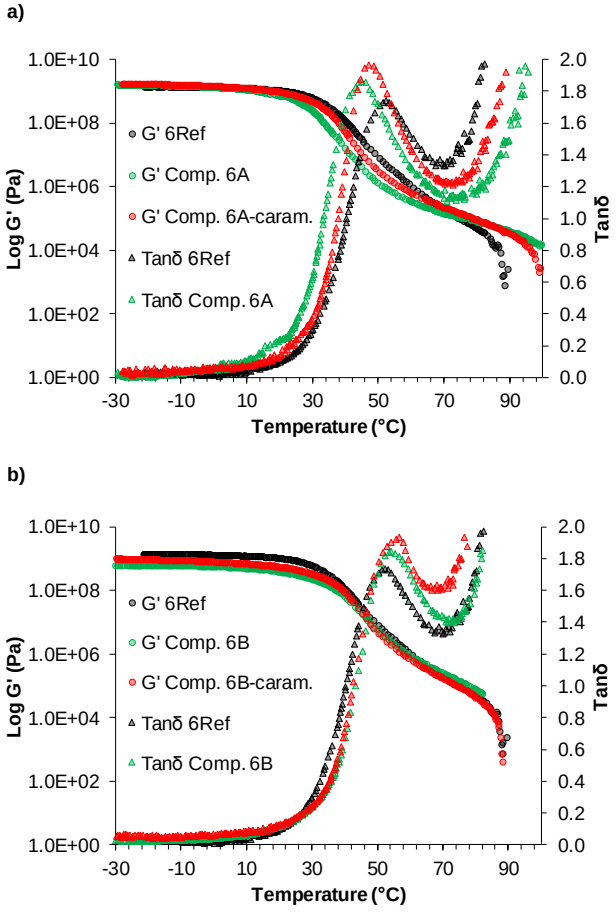

Figure 6.10. Dynamic mechanical thermal analysis of the coatings of the compositions **6A** (a) and **6B** (b) before (green) and after (red) the caramelization together with the reference composition (black).

6.8 Evaluation of the performance of acrylic dispersions containing IBOMA/Ecomer® for melamine coating application

Mechanical properties

Table 6.3 summarizes the mechanical properties obtained in the tensile test for both the caramelized and non-caramelized coatings, whereas figure 6.11 shows the corresponding stress-strain curves. Overall, the coating films containing Ecomer® (green lines) were softer in comparison with the reference composition, showing a lower Young's modulus (slope of the elastic region), yield stress (stress at the beginning of the plastic region) and ultimate strength (stress at break). This mechanical performance is in agreement with the results obtained in the DMTA analysis, since Ecomer® reduces the solid-like behavior and, thereby, the stiffness of the final coating.

The elongation at break was increased in composition **6A** because of the lower glass transition temperature and, thus, the increasing in the material plasticity. On the other hand, the incorporation of 2-Octyl acrylate in composition **6B** reduced the extensibility of the probe, reaching a similar value than the reference one, which is attributed to the minor Tg differences among them. The small increment of the crosslinking degree, after the caramelization process, promoted both the elastic behavior and the brittleness of the coating, showing an increase of the strength and stiffness together with a great reduction of the elongation at break (red lines), which was more pronounced in the case of composition **6B**.

Table 6.3. Mechanical properties of the coatings cast at ambient temperature before and after the caramelization process.

COMP	2nd Stage (%wt monomers)	Young's Modulus (MPa)	Yield Stress (MPa)	Elongation at break (%/100)	Ultimate Strength (MPa)
6Ref	BA:IBOMA:MAA (49.5:49.5:1)	154.3 ± 7.9	10.6 ± 0.6	3.2 ± 0.1	11.8 ± 1.7
6A	BA:IBOMA:SBV:MAA (42:42:15:1)	15.5 ± 1.9	3.2 ± 0.4	4.7 ± 0.02	6.6 ± 0.2
6A-caram.		750.3 ± 70.7	20.4 ± 1.1	0.5 ± 0.1	21.3 ± 1.3
6B	2OA:BA:IBOMA:SBV:MAA (27:15:42:15:1)	62.5 ± 22.44	5.9 ± 1.1	2.7 ± 0.4	6.1 ± 0.9
6B-caram.		784.5 ± 30.2	22.9 ± 1.3	0.09 ± 0.01	23.3 ± 0.5

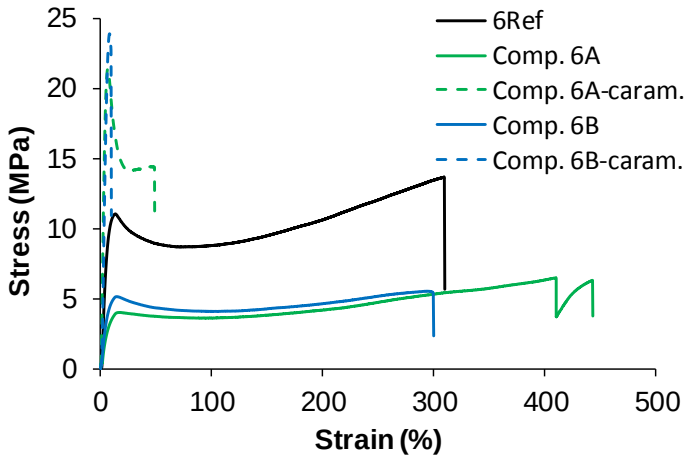

Figure 6.11. Stress-strain curves of compositions **6A** (green line) and **6B** (blue line) before (solid line) and after (dashed line) the caramelization together with the reference composition (black solid line).

In view of the mechanical behavior, the non-caramelized coatings could be useful for their application as architectural coatings (wall and trim paints). As representative example, polyurethane dispersions (with low crosslinking density) showing a yield stress: 2-15 MPa; ultimate strength: 4-20 MPa and elongation at break: 200-1100% have been described[30]. On the other hand, the harder caramelized coatings could find their place as protective coating

for industrial applications (furniture, joinery) since they present high crosslinking density. In this concern, industrial UV cured coatings presenting a yield stress: 2-4 MPa; ultimate strength: 5-8 MPa and elongation at break: 5-50% have been reported[31].

Water uptake

The water uptake of the caramelized and non-caramelized polymer films is shown in Figure 6.12. The incorporation of the sugar based vinyl monomer in composition **6A** and, thereby, the existence of hydrophilic glucose rings provided higher water uptake in comparison with the reference composition. However, the addition of 2OA in composition **6B** had a strong effect in the hydrophobicity of the coating that was below 10% after 21 days and reached the plateau from the seventh day. A decrease of water uptake was caused by the increasing of the crosslinking density after the caramelization process, which also reduced the number of hydroxyl groups.

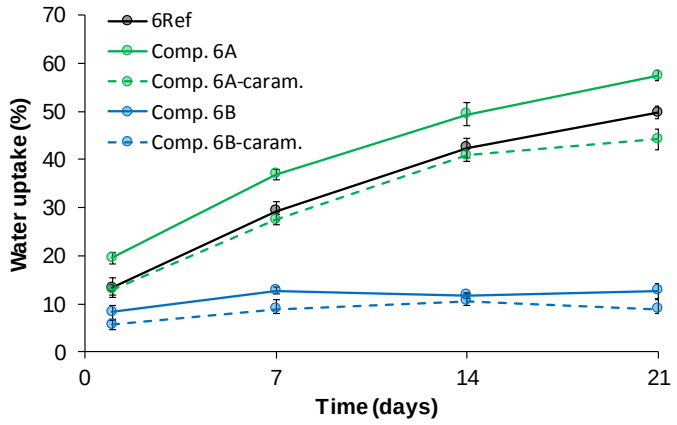

Figure 6.12. Water uptake measurement of compositions **6A** (green line) and **6B** (blue line) before (solid line) and after (dashed line) the caramelization together with the reference composition (black solid line)

Hardness and blocking resistance

Hardness and blocking resistance are important properties for waterborne decorative coatings, which evaluate the resistance of a coating to a mechanical force (such as pressure, rubbing or scratching) and the adhesion between two coating surfaces, respectively. Figure 6.13 presents the pendulum hardness as well as the blocking resistances of the coating films before (blue bars) and after (red bars) the caramelization process. As it can be appreciated, the hardness of the coatings (Figure 6.13.a) displayed the same trend than the previously discussed mechanical properties, correlating a higher Young's modulus with a higher hardness, as it was proposed by Sato[32]. An increase in the pendulum hardness after the caramelization was attributed to a more crosslinked polymer network, which reduced the molecular motions and, thus, reinforced the elastic part of the coating film.

Concerning the resistance of the coating to blocking (Figure 6.13.b), a slight improvement was observed after the Ecomer® incorporation since the higher gel content reduced tackiness, counteracting the glass transition temperature effect and, thereby, increasing the antiblocking ability. This adhesion reduction raised after the caramelization. It is worthy pointing out that, unexpectedly, the blocking resistance of reference composition (which is zero before caramelization indicating the worse blocking) increased as well after the caramelization process. A possible explanation for such behavior could be related with a reorganization of the polymer chains after the treatment at 120 ºC. This reorganization could oriented the IBOMA groups towards the coating-air interface, reducing the surface free energy and leading to poorer inter-coating adhesion, namely, a better anti-blocking.

In order to corroborate this, contact angle measurements of the reference composition were carried out before and after the caramelization process. It was observed an increase of the contact angle, which shifted from 81.5 º to 88 º, after the treatment at 120

ºC, being indicative of an increasing of the coating hydrophobicity and, hence, a reorganization of the methacrylate groups within the polymer chains (see Figure 6.14).

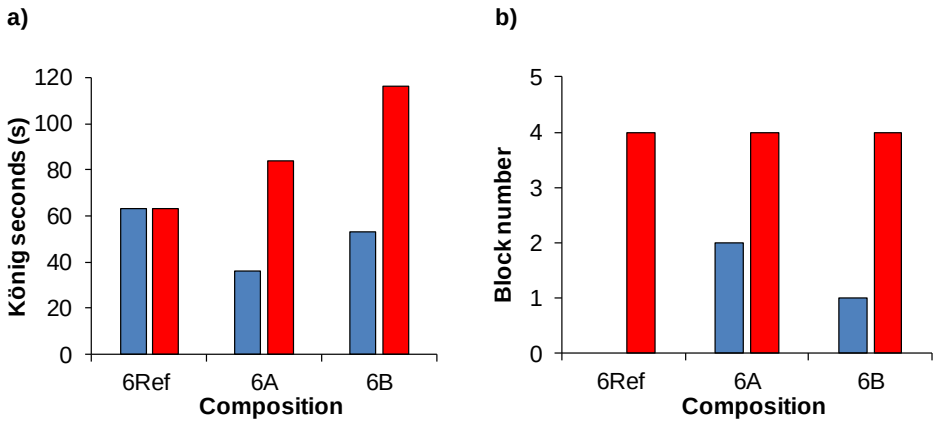

Figure 6.13. Pendulum hardness (a) and blocking resistance (b) for the coating films before (blue bars) and after (red bars) the caramelization process.

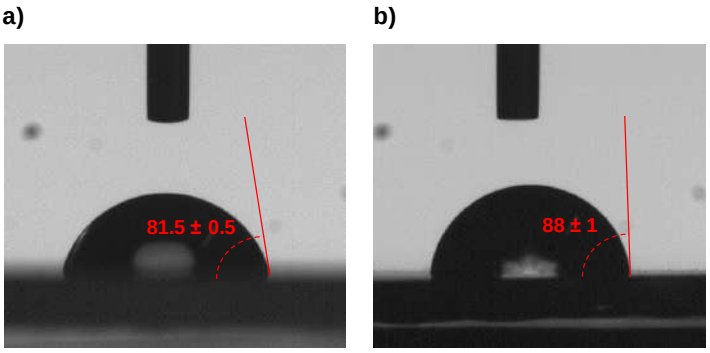

Figure 6.14. Contact for reference composition before (a) and after (b) the caramelization process.

Chemical resistance

The resistance of the coatings cast on melamine manufactured-wood substrates, either before or after the caramelization process, against common chemicals is showed in

Figure 6.15. As general observation, the introduction of Ecomer® in composition **6A** reduced the chemical resistance against coffee, ethanol and water due to the incorporation of polar moieties such as hydroxyl groups coming from the glucose rings, which increase the chemical affinity to polar substances and, therefore, cause the damage of the coating. A slight resistance improvement was observed in composition **6B** when a percentage of butyl acrylate was substituted by 2-Octyl acrylate, which raised the hydrophobicity of the film.

The caramelization of the melamine-wood panel containing the coating with the composition **6A** provided the same chemical resistance values than those ones observed for the reference composition. This is because of the glycosidic bond formation and the increasing of the crosslinking degree, which decreased the hydrophilicity of the coating and the permeation speed as well as enhanced its rigidity[33–35]. A better impact of the caramelization can be appreciated in composition **6B**, overcoming the reference values, except for ethanol and mustard, and not observing any kind of visual remark for water and coffee on the panel.

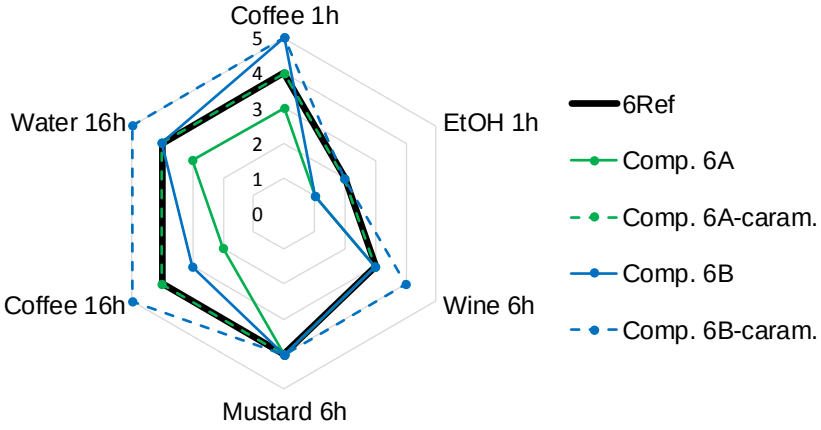

Figure 6.15. Chemical resistance of the coatings cast on melamine-wood substrate before (green) and after (red) the caramelization. 5 = no visible change, 1 = strong marks visible.

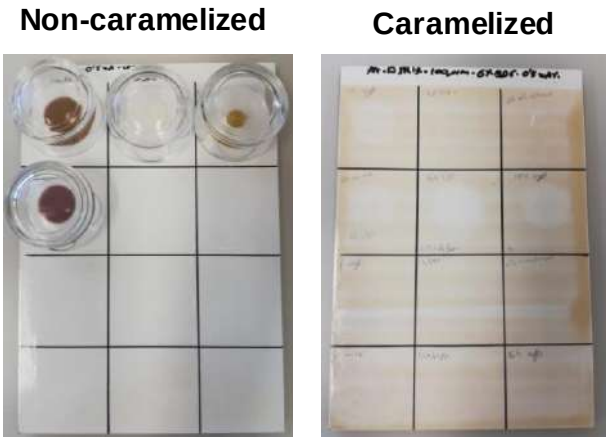

Figure 6.16. The coated melamine substrate with the coatings before (left) and after (right) the caramelization process.

6.9 Biodegradability assessment

Biodegradation of polymers involves the attachment of microorganism to the surface of the material followed by their growth employing the polymer as carbon source. This process occurs either under aerobic or anaerobic conditions, generating CO_2, H_2O or CH_4 as end products[36]. Moreover, the closer the similarity of a polymeric structure to a natural one, the easier its degradation by microorganisms[37].

Taking advantage of the existence of glucose derivative moieties in the coating compositions, biodegradation studies in activated sludge were monitored by measuring the biochemical oxygen demand (BOD) along the time. Figure 6.17 presents the biodegradation profile of the polymer film having the composition **6A** before and after the caramelization treatment. It was observed a 7.4% of biodegradation of the polymer film, which is almost the complete conversion of every glucose ring into CO_2. However, a final biodegradation around 4.6% was found for the caramelized film. This is because the increasing in the crosslinking density constrains the polymer network, namely minimizes the network voids, resulting in a

reduction of the water absorption and, hence, in the efficiency of the biodegradation[38,39]. As it was expected, no relevant changes in the biochemical oxygen demand for the reference composition were observed.

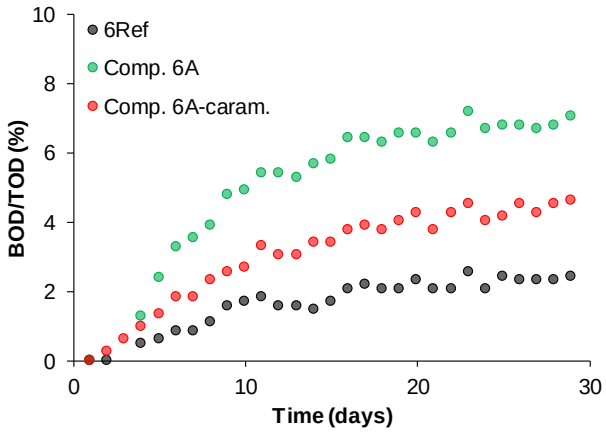

Figure 6.17. Changes of biochemical oxygen demand (BOD) in an activated sludge as a function of the degradation time of dry polymer films of composition **6A** before (green) and after (red) the caramelization process together with the reference composition (black).

6.10 Conclusions

In this chapter, the incorporation of the commercial functional monomer Ecomer® into waterborne coating compositions containing 2OA and IBOMA as main comonomers was explored.

The characterization of the commercial sugar based vinyl monomer revealed that it was a mixture of hexyl polyglucoside maleic acid esters with an oligomerization degree between 1.3 and 2. Ecomer® incorporated better in compositions that use styrene as hard monomer than methacrylates, likely to closer reactivity ratios of the comonomers. It was found that caramelization reactions of the final coatings helped to incorporate the remaining glucose based vinyl molecules, which resulted in stiffer materials with improved mechanical

and coating properties. The impact of the caramelization on the final properties was studied by DMTA analysis and the process itself was corroborated by IR spectroscopy, changes in both the molar mass and gel content and TGA. In addition, the partial biodegradation degree of the coating was affected by the caramelization, resulting in a lower CO_2 production as consequence of the greater crosslinked network.

These results provide the first insights about the incorporation of a commercial glucose-derivative monomer for the development of partially biodegradable waterborne coatings with a bio-content ranging from 30% to 63%.

6.11 References

(1) Lichtenthaler, F. W.; Peters, S. Carbohydrates as Green Raw Materials for the Chemical Industry. *Comptes Rendus Chim.* **2004**, *7* (2), 65–90.

(2) Heinze, T.; Liebert, T.; Koschella, A. *Esterification on Polysaccharides*; Springer-Verlag: Berlin/Heidelberg, 2006.

(3) Brune, D.; Von Eben-worlée, R. Starch-Based Graft Polymer, Process for Its Preparation, and Use Thereof in Printing Inks and Overprint Varnishes. U.S. Patent 6423775 B1, 2002.

(4) Abeylath, S. C.; Turos, E. Glycosylated Polyacrylate Nanoparticles by Emulsion Polymerization. *Carbohydr. Polym.* **2007**, *70*, 32–37.

(5) Neqal, M.; Voisin, A.; Neto, V.; Coma, V.; Héroguez, V. New Active Supported Antifungal Systems for Potential Aeronautical Application. *Eur. Polym. J.* **2018**, *105*, 304–312.

(6) Desport, J. S.; Mantione, D.; Moreno, M.; Sardon, H.; Barandiaran, M. J.; Mecerreyes, D. Synthesis of Three Different Galactose-Based Methacrylate Monomers for the Production of Sugar-Based Polymers. *Carbohydr. Res.* **2016**, *432*, 50–54.

(7) Desport, J. S.; Moreno, M.; Barandiaran, M. J. Fructose-Based Acrylic Copolymers by Emulsion Polymerization. *Polymers (Basel).* **2018**, *10*, 488–499.

(8) Smeets, N. M. B.; Imbrogno, S.; Bloembergen, S. Carbohydrate Functionalized Hybrid Latex Particles. *Carbohydr. Polym.* **2017**, *173*, 233–252.

(9) Cummings, S.; Cunningham, M.; Dubé, M. A. The Use of Amylose-Rich Starch Nanoparticles in Emulsion Polymerization. *J. Appl. Polym. Sci.* **2018**, *46485*, 1–8.

(10) Al-bagoury, M.; Yaacoub, E. Semicontinuous Emulsion Copolymerization of 3-O-Methacryloyl-1,2:5,6-Di-O -Isopropylidene-α-D-Glucofuranose (3-MDG) and Butyl Acrylate (BA). Monomer Feed Addition. *J. Appl. Polym. Sci.* **2003**, *90*, 2091–2102.

(11) Al-bagoury, M.; Yaacoub, E. Semicontinuous Emulsion Copolymerization of 3-O-Methacryloyl-1,2:5,6-Di-O-Isopropylidene-α-D-Glucofuranose (3-MDG) and Butyl Acrylate (BA) by Pre-Emulsion Addition Technique. *Eur. Polym. J.* **2004**, *40*, 2617–2627.

(12) Mansfield, R. C. Process for Preparation of Alkyl Glucosides and Alkyl Oligosaccharides. U.S. Patent 3839318, 1974.

(13) Bloembergen, S.; McLennan, I. J.; Narayan, R. Enviromentally Friendly Sugar-Based Vinyl Monomers Useful in Repulpable Adhesives and Other Applications. U.S. Patent 6242593, 2001.

(14) Cassar, S. E.; Fishman, D. H.; McLennan, I. J.; Bloembergen, S. Resin-Fortified Sugar-Based Vinyl Emulsion Copolymers and Methods of Preparing the Same. U.S. Patent 6355734 B1, 2002.

(15) Bloembergen, S.; Van Leeuwen, J.; Mathieu, N.; Smeets, B.; Noeei Ancheh, V.; Mesnager, J. F.; Lee, D. I. Bio-Based Polymer Nanoparticle and Composite Materials Derived Therefrom. U.S. Patent 2017/0029549 A1, 2017.

(16) Schoonbrood, H. A. S.; Unzué, M. J.; Amalvy, J. I.; Asua, J. M. Reactive Surfactants in Heterophase Polymerization . VIII . Emulsion Polymerization of Alkyl Sulfopropyl Maleate Polymerizable Surfactants (Surfmers) with Styrene. *J. Polym. Sci. Part A Polym. Chem.* **1997**, *35*, 2561–2568.

(17) Shaffei, K. A.; Moustafa, A. B.; Hamed, A. I. The Emulsion Polymerization of Each of Vinyl Acetate and Butyl Acrylate Monomers Using Bis (2-Ethylhexyl) Maleate for Improving the Physicomechanical Properties of Paints and Adhesive Films. *Int. J. Polym. Sci.* **2009**, *2009*, 1–6.

(18) Queneau, Y.; Jarosz, S.; Lewandowski, B.; Fitremann, J. Sucrose Chemistry and Applications of Sucrochemicals. In *Advances in Carbohydrate Chemistry and Biochemistry*; 2007; Vol. 61, pp 218–271.

(19) Kroh, L. W. Caramelisation in Food and Beverages. *Food Chem.* **1994**, *51*, 373–379.

(20) Payet, B.; Shum Cheon Sing, A.; Smadja, J. Assessment of Antioxidant Activity of Cane Brown Sugars by ABTS and DPPH Radical Scavenging Assays : Determination of Their Polyphenolic and Volatile Constituents. *J. Agric. Food Chem.*

2005, *53*, 10074–10079.

(21) Brands, C. M. J.; Van Boekel, M. A. J. S. Reactions of Monosaccharides during Heating of Sugar - Casein Systems : Building of a Reaction Network Model. *J. Agric. Food Chem.* **2001**, *49*, 4667–4675.

(22) Woo, K. S.; Kim, H. Y.; Hwang, I. G.; Lee, S. H.; Jeong, H. S. Characteristics of the Thermal Degradation of Glucose and Maltose Solutions. *Prev. Nutr. Food Sci.* **2015**, *20* (2), 102–109.

(23) Quintas, M. A. C.; Branda, T. R. S.; Silva, C. L. M. Modelling Colour Changes during the Caramelisation Reaction. *J. Food Eng.* **2007**, *83* (4), 483–491.

(24) García Fernández, J. M.; Gadelle, A.; Defaye, J. Difructose Dianhydrides from Sucrose and Fructo- Oligosaccharides and Their Use as Building Blocks for the Preparation of Amphiphiles , Liquid Crystals , and Polymers. *Carbohydr. Res.* **1994**, *6215*, 249–269.

(25) Ratsimba, V.; García Fernández, J. M.; Defaye, J.; Nigay, H.; Voilley, A. Qualitative and Quantitative Evaluation of Mono- and Disaccharides in D -Fructose , D -Glucose and Sucrose Caramels by Gas – Liquid Chromatography – Mass Spectrometry Di-D -Fructose Dianhydrides as Tracers of Caramel Authenticity. *J. Chromatogr. A* **1999**, *844*, 283–293.

(26) Defaye, J.; Gracía Fernández, J. M. Protonic and Thermal Activation of Sucrose and the Oligosaccharide Composition of Caramel. *Carbohydr. Res.* **1994**, *256*, 8–11.

(27) Sengar, G.; Sharma, H. K. Food Caramels : A Review. **2014**, *51* (9), 1686–1696.

(28) Kitaoka, S.; Suzuki, K. Caramels and Caramelization Part 1 . The Nature of Caramelan. *Agric. Biol. Chem.* **1967**, *31* (6), 753–755.

(29) Golon, A.; Kuhnert, N. Unraveling the Chemical Composition of Caramel. *J. Agric. Food Chem.* **2012**, *60*, 3266–3274.

(30) Liu, M.; Zhong, J.; Li, Z.; Rong, J.; Yang, K.; Zhou, J. A High Stiffness and Self-Healable Polyurethane Based on Disulfide Bonds and Hydrogen Bonding. *Eur. Polym. J.* **2020**, *124*, 109475.

(31) Fu, J.; Yu, H.; Wang, L.; Lin, L.; Ullah Khan, R. Preparation and Properties of UV-Curable Hyperbranched Polyurethane Acrylate Hard Coatings. *Prog. Org. Coatings* **2020**, *144*, 105635.

(32) Sato, K. The Hardness of Coating Films. *Prog. Org. Coatings* **1980**, *8*, 1–18.

(33) Feng, J.; Berger, K. R.; Douglas, E. P. Water Vapor Transport in Liquid Crystalline and Non-Liquid Crystalline Epoxies. *J. Mater. Sci.* **2004**, *39*, 3413–3423.

(34) Wang, Z.; Han, E.; Lio, F.; Ke, W. Effect of Different Curing Agents on Cure Reaction and Exposure Resistance of Phenolic-Epoxy Resins in Hot Acid Solutions. *Corrosion* **2010**, *66* (7), 750011–750019.

(35) Liu, M.; Mao, X.; Zhu, H.; Lin, A.; Wang, D. Water and Corrosion Resistance of Epoxy – Acrylic – Amine Waterborne Coatings : Effects of Resin Molecular Weight , Polar Group and Hydrophobic Segment. *Corros. Sci.* **2013**, *75*, 106–113.

(36) Kyrikou, I.; Briassoulis, D. Biodegradation of Agricultural Plastic Films : A Critical Review. *J. Polym. Environ.* **2007**, *15*, 125–150.

(37) Gu, J.-D. Microbial Degradation of Polymeric Materials. *Int. Biodeterior. Biodegradation* **2000**, *52*, 69–91.

(38) Wang, W.; Wang, A. Nanocomposite of Carboxymethyl Cellulose and Attapulgite as a Novel PH-Sensitive Superabsorbent : Synthesis, Characterization and Properties. *Carbohydr. Polym.* **2010**, *82* (1), 83–91.

(39) Jena, D. K.; Sahoo, P. K. Development of Biodegradable Cellulose-g-Poly (Butyl Acrylate)/Kaolin Nanocomposite with Improved Fire Retardancy and Mechanical Properties. *J. Appl. Polym. Sci.* **2018**, *45968*, 1–8.

Chapter 7

Conclusions and future perspectives

The main objective of this thesis was to develop high bio-content waterborne polymeric dispersions with competitive performance for their application as pressure sensitive adhesives (PSAs) and coatings. For this purpose, both commercial and non-commercial biobased monomers having special features were employed.

As first attempt, 72% bio-content waterborne PSAs containing the commercial biobased monomers 2-Octyl acrylate (2OA, coming from castor oil) and isorbornyl methacrylate (IBOMA, coming from pine tree resin) were produced. It was observed that the direct substitution of the oil-based monomers by the renewable counterparts did not provide the same adhesive performance. Consequently, the fine tuning of the microstructure by adjusting the amount of hard biobased monomer (IBOMA at 15 wt%) and gel content (~60%) yielded a copolymer with similar peel resistance and loop tack, better SAFT (135ºC vs 70ºC) and 45 times higher shear strength than the pure oil-based PSA. The reduction of the bio-content as well as the glass transition temperature by the incorporation of different amounts of 2-Ethylhexyl acrylate (2EHA) was the necessary evil for extending the elongation at break of the adhesive fibrils.

Aiming to solve the conflict between the bio-content degree and the final performance required for adhesive applications, piperonyl methacrylate (PIPEMA, coming from sassafras oil and black pepper) was synthesized and incorporated by emulsion polymerization in PSA compositions, replacing hard comonomer IBOMA. It was found that 15 wt% of PIPEMA provided a better viscous behavior of the adhesive fibrils, maintaining enough stiffness and yielding the maximum dissipation energy value. In addition, benzodioxol structures present in the piperonyl functionality allowed tuning the adhesive performance (increasing cohesion without substantially damaging adhesion) when the adhesive was irradiated with UV-light. Solid state ^{13}C NMR and rheological studies confirmed the formation of a crosslinked network via generation of conjugated structures that increased the solid-like behavior. It was

found that 15 min of UV-light curing provided the best balance of adhesives properties, overcoming the performance of an oil-based PSA and keeping a bio-content of 71%.

In an attempt to improve the adhesion and promote the removability of the adhesive tape in water, an isosorbide based methacrylate mixture (ISOMAraw, coming from glucose) was synthesized and incorporated into the already studied biobased PSA formulations. The monomer mixture consisted in isosorbide dimethacrylate and isosorbide 5-methacrylate (ISOMA)in a 4/1 ratio.The later one can be isolated by purification of the mixture. It was found that low percentages (1 wt%) of ISOMAraw/ISOMA enhanced both the flexibility and the cohesiveness of the adhesive fibrils because of the presence of crosslinking species and supramolecular interactions (hydrogen bonding). Furthermore, the low percentage of this sugar derivative monomer promoted the removability in water of the adhesive tapes in less than 40 min at room temperature, reducing this time in almost 4 times if temperature is increased to 65 ºC.

In view of the results provided by the isosorbide derivative monomers, and aiming to obtain an excellent adhesion and switching-off at the minimum film thickness, biobased alkali soluble resins (ASRs) were synthesized and used as electrosteric stabilizers for the production of high solids content waterborne PSAs. The use of ISOMAraw in the resin composition not only allowed the grafting to the polymer chains in the polymer particle, but also the enhancement of the mechanical properties as the hydrogen bonding density increased. Regarding this, the existence of a dynamic physical crosslinking provided a good balance of the polymer network viscoelasticity, which was deeply studied by rheological analysis. The nature of the ASR-fortified waterborne PSAs promoted the complete detachment of the adhesive tapes from the glass substrate in basic media in less than 20 min at room temperature.

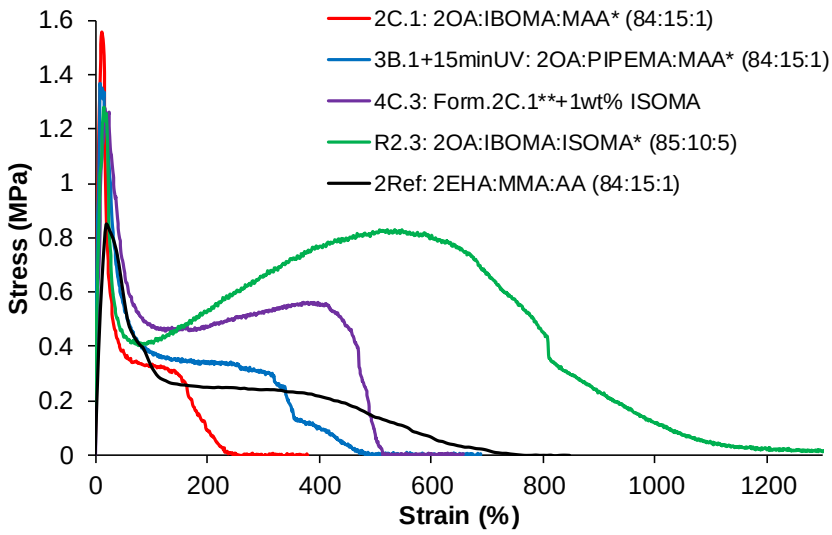

Figure 7.1. Most relevant probe tack curves of biobased waterborne PSA formulations together with the one coming from petroleum-based composition (2Ref). Note that * and ** make reference to 0.025 wbm% and 0.05 wbm% of 2EHTG, respectively.

Finally, the development of waterborne coatings by the combination of the commercial glucose-derivative monomer Ecomer® (an alkyl polyglucoside maleic acid ester coming from glucose) together with the already studied 2OA and IBOMA was explored. Ecomer® was incorporated better in compositions that use styrene as hard monomer than methacrylates, likely because of the closer reactivity ratios of the comonomers. Nonetheless, it was found that caramelization reaction of the final coating helped to incorporate the remaining Ecomer®, yielding stiffer materials with improved mechanical and coating properties. Moreover, the presence of glucose moieties in the polymer network promoted the partial biodegradation of the coating, being lower when it was caramelized.

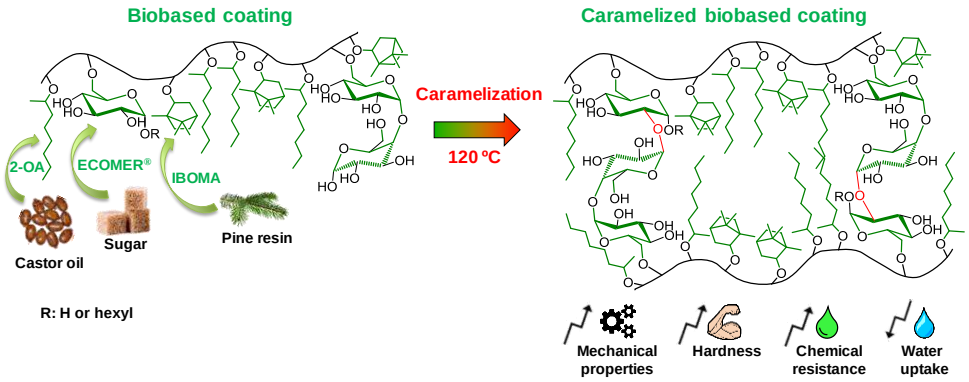

Figure 7.2. Representative scheme of Chapter 6: Development of biobased waterborne coatings containing Ecomer® monomer.

As future perspectives of this thesis, the synthesis of potential monomers coming from fatty acids and lignin, and their incorporation by (mini)emulsion polymerization could be further explored. The production of waterborne PSAs and coatings containing these new components could bring a broader variety of features and performances. In this context, we explored the use of the commercial biobased monomer Visiomer C13, which is composed by a mixture of methacrylate monomers having an alkyl length chain ranging from 14 to 16 carbon atoms. However, reproducibility problems because of the varied nature of different batches did not allow to produce reliable neither competitive PSAs compositions.

As alternative, tetradecanol, which comes from the hydrogenation of myristic acid, could be a promising candidate for the production of a methacrylate monomer with a long alkyl chain. This non-exploited biobased monomer (myristyl methacrylate) could be useful as soft monomer in waterborne PSA formulations produced by miniemulsion polymerization. Because of its long aliphatic chain, small amounts of this monomer would increase the liquid-like behavior of the adhesive, promoting its fibrillation.

Lignin fragmentation can also provide interesting and versatile molecules such as eugenol or vanillin. Eugenol is a phenol which can be easily transformed into a methacrylate monomer by direct esterification reaction. Its incorporation by emulsion polymerization could promote the elastic behavior in adhesives and coating formulations, enhancing cohesion and hardness. Furthermore, demethylation reaction of eugenol leads to a catechol group, which results on special interest for the creation of water-resistant adhesives. Nevertheless, it is well known that catechol groups may act as radical scavengers, reducing the polymerization rate and, hence, the incorporation by means of free radical polymerization might be challenging. As solution, the remaining double bond of this catechol-based molecule could be epoxidized for allowing its fast incorporation in the shell of polymer particles by reaction with hydroxyl groups. This post-functionalization reaction would lead to the production of biobased pressure sensitive adhesives suitable for its use under water.

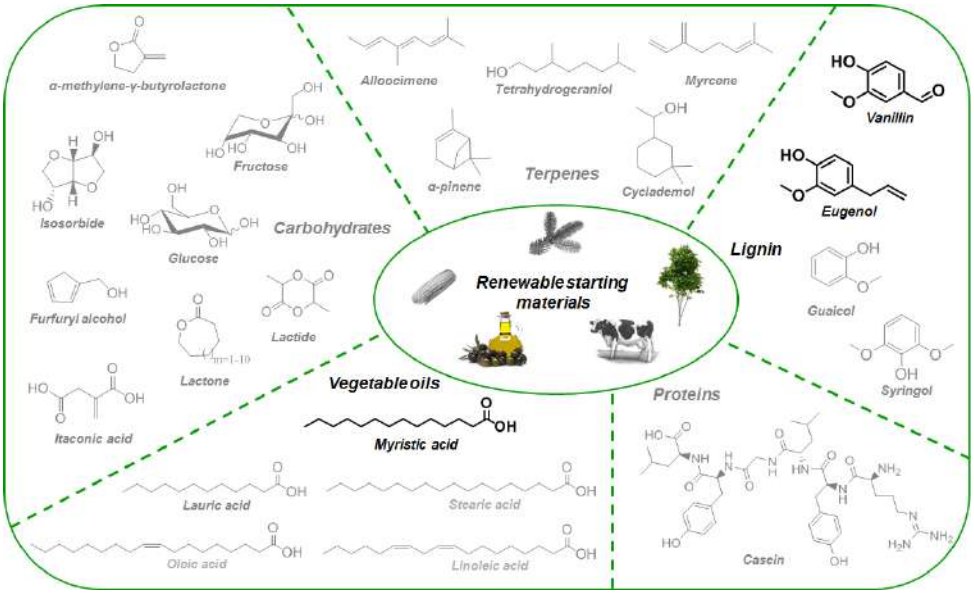

Figure 7.3. Chemical structures of renewable molecules for the preparation of future potential biobased monomers suitable for (mini)emulsion polymerization.

Appendix I

Polymer characterization and adhesion properties

I.1 Polymer characterization

Monomer conversion. Monomer conversion was determined by gravimetry. The instantaneous conversion, X_{Inst}, was defined as the amount of polymer in the reactor divided by the total amount of monomer and polymer in the reactor. The overall conversion, X_{Glob}, was the amount of polymer in the reactor divided by the amount of monomer plus the amount of polymer in the formulation.

Particle size and particle size distribution. Particle size was measured by dynamic light scattering (DLS) using a Zetasizer Nano Z (Malvern Instruments), whereas particle size distribution was determined by capillary hydrodynamic fractionation (CHDF 3000, Matec instruments). The samples were prepared by dilution of the latex in distilled water. CHDF measurements were carried with samples at 1 % of solid content using a flow rate of 1.4 mL/min and a wavelength of 220 nm for the detection. Polystyrene particles between 86 and 790 nm were used as calibration patterns.

The theoretical evolution of the particle size (dp) was calculated assuming that the number of particles of the seed is maintained constant during the reaction, through the following equation:

$$dp = \sqrt[3]{\frac{6*[m_{seed}+x_{ins}F_M t]}{\pi N_p \rho_{pol}}} * 10^7 (\text{nm}) \qquad \textbf{(Eq.I1)}$$

where m_{seed} (g) is the mass of polymer in the seed, x_{inst} is the instantaneous monomer conversion, F_M is the monomer feeding rate (g/min), t is the feeding time (min), ρ_{pol} is the polymer density (g cm^{-3}) and Np is the number of particles (-) of the seed.

Gel fraction and swelling degree. The gel fraction is defined as the fraction of the polymer that is not soluble in a good solvent (tetrahydrofuran, THF, in this case). The gel

fraction was measured by Soxhlet extraction, using THF as solvent. A glass fiber squad pad was impregnated with latex (a few drops) and dried overnight (w_p). The extraction was carried out for 24 h under reflux conditions (about 70°C). The gel remained in the glass fiber and it was dried in the oven at 60°C (w_g), whereas the sol polymer was recovered from the THF solution. The swelling degree was calculated as the ratio between the weight of the swollen gel after 24 hours extraction (w_s) and the weight of dried gel (w_g).

$$\text{Gel Content } (\%) = \frac{w_g}{w_p} \times 100 \qquad \textbf{(Eq. I2)}$$

$$\text{Swelling } (\%) = \frac{w_s}{w_g} \times 100 \qquad \textbf{(Eq. I3)}$$

Where w_g is the weight of insoluble fraction of sample (dried sample), w_s is the weight of the swollen gel and w_p is the weight of whole polymer sample.

Sol molar masses. The molar mass distribution of the soluble fraction in THF was determined by size exclusion chromatography (SEC) at 35°C. The samples taken out from the soxhlet were first dried, then redissolved in THF to achieve a concentration of about 0.005 g/mL and finally filtered (polyamide filter, pore size = 0.45 µm,) before injection into the SEC instrument The SEC instrument consisted of an autosampler (Waters 717 plus), a pump (LC-20, Shimadzu), three columns in series (Styragel HR2, HR4, and HR6 with a pore size from 102 to 106 Å), and a differential refractometer (Waters 2410) as detector. The flow rate of THF through the columns was 1 mL.min^{-1}. The reported molar masses are referred to polystyrene standards.

I.2 Adhesion properties

180° Peel strength. The 180° peel strength test was performed on both stainless steel and glass panels in accordance with ASTM-D3330. PSA tape specimens with a width of 25 mm were applied to the panel with the adhesive contacting the panel and pressed 4 times with a 2kg rubber-coated roller. The tapes applied were allowed to dwell for 10 min. The tapes were then peeled off at a crosshead speed of 5 mm/s. The average value of peel strength in newtons per centimeter was obtained for peeling 6 cm of the tape specimens.

Loop tack. Loop tack test was performed on a 25 mm wide stainless steel plate in accordance with ASTM-D6195. 10 cm long PSA tape specimens with a width of 25 mm were attached in as loop to the upper grip of the equipment. The loop was allowed to move downward at a speed of 0.1 mm/s until it was brought in full contact with the plate (25 mm x 25 mm). It was left 0.1 s in contact before moving upward at 0.055 mm/s. The force required to peel off the loop was measured in N/25mm and the average was reported. The area under the curve represents the work of adhesion of the loop (WA) and was reported in J/m^2.

Probe tack. The probe tack tests were performed on glass plates. Latex films (final thickness of 100 µm to avoid the substrate effect) were directly casted on the glass plate and dried for 6 hours before carrying the test. Then a stainless steel ball probe was allowed to move downward at a speed of 0.1 mm/s until it was brought into contact to the adhesive test panel surface with a compressive force of 4.5 N. Immediately after the contact (1 s), the crosshead was allowed to move upward at a speed of 0.055 mm/s until the probe was completely separated from the adhesive.

Shear resistance and SAFT. Shear tests were performed on stainless steel panels using SAFT equipment (Sneep Industries) in accordance with ASTM-D3654. The PSA tape

specimens were applied to the panel with a contact area of 25 mm × 25 mm and pressed 4 times with a 1kg rubber-coated roller. After the tapes applied were dwelled for 10 min, the free ends of the tapes were attached to a mass of 1000 g. The test panel (and the tapes applied) was held by the test stand at an angle of about 1° relative to the vertical. The time to failure, i.e., the time from the attachment of the mass until the complete separation of the tape from the test panel, was recorded and used as an indication of the shear strength of the PSA tapes. The test was performed at room temperature (23°C). SAFT test was prepared similarly as shear test in accordance with ASTM-D4498. Once the weights placed, the temperature was increased from 23°C to 200°C at 1°C/min rate. For this test, the temperature of failure is reported.

Appendix II

Supporting Information Chapter 6. Acrylic latexes containing MMA/Ecomer® and ST/Ecomer®

II.1 Acrylic latexes containing MMA/Ecomer®

Table II.1 summarizes the latexes synthesized containing MMA/Ecomer® in their formulation, as well as their main properties including gel content, sol weight-average molar mass (Mw), glass transition temperature (Tg), Minimum Film Formation Temperature (MFFT), bio-content and the free Ecomer® content (SBV).

Table II.1. Summary and characteristics of the synthesized latexes containing MMA by two-stage process.

COMP	2nd Stage (%wt monomers)	Gel (%)	Mw (kDa)	Tg (°C)	MFFT (°C)	Bio (%)	SBV (g/kg)*
6Ref.2	BA:MMA:MAA (49.5:49.5:1)	35 ± 0.5	350	18.2	10	0	-
6C	BA:MMA:SBV:MAA (42:42:15:1)	57 ± 1	184	11.7	7.5	14	20
6D	2OA:BA:MMA:SBV:MAA (27:15:42:15:1)	53 ± 0.2	208	17	8.5	33	23

* Makes reference to the quantity of free Ecomer® in 1 kg of binder.

Figure II.1 shows the evolution of the gel content for compositions **6Ref.2**, **6C** and **6D** before and after the caramelization.

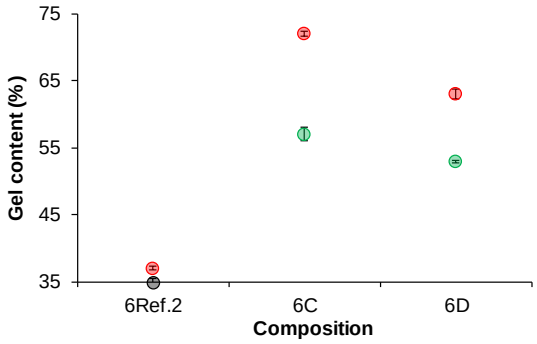

Figure II.1. Gel content evolution of compositions, **6C** and **6D** together with the reference composition **6Ref.2** before (green circles) and after (red circles) caramelization process.

Evaluation of the performance of acrylic dispersions containing MMA/Ecomer® for melamine coating application

Table II.2 summarizes the mechanical properties obtained in the tensile test for both the caramelized and non-caramelized coatings, whereas Figure II.2 shows the corresponding stress-strain curves.

Table II.2. Mechanical properties of the coatings cast at ambient temperature before and after the caramelization process.

COMP	2nd Stage (%wt monomers)	Young's Modulus (MPa)	Yield Stress (MPa)	Elongation at break (%/100)	Ultimate Strength (MPa)
6Ref.2	BA:MMA:MAA (49.5:49.5:1)	6.3 ± 0.1	1.9 ± 0.1	6.4 ± 0.8	10.9 ± 1.6
6C	BA:MMA:SBV:MAA (42:42:15:1)	1.5 ± 1	0.9 ± 0.1	9.3 ± 0.7	7.5 ± 0.3
6C-caram.		9.7 ± 0.4	1.5 ± 0.1	8.1 ± 0.4	9 ± 0.3
6D	2OA:BA:MMA:SBV:MAA (27:15:42:15:1)	4.8 ± 0.3	1.5 ± 0.1	5.6 ± 0.6	5 ± 0.5
6D-caram.		13.6 ± 4	2.9 ± 0.1	6.3 ± 0.5	9.5 ± 1

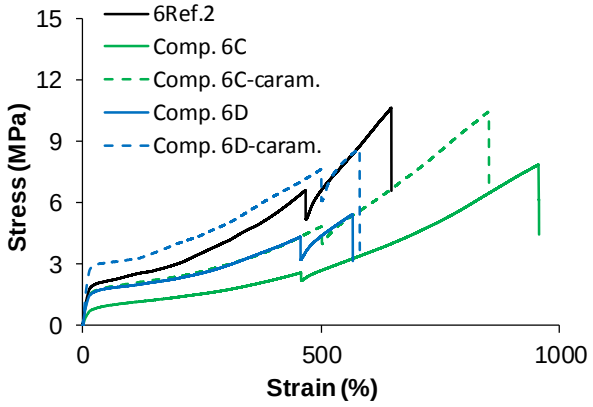

Figure II.2. Stress-strain curves of compositions **6C** (green line) and **6D** (blue line) before (solid line) and after (dashed line) the caramelization together with the reference composition **6Ref.2** (black solid line).

Figure II.3 presents the pendulum hardness as well as the blocking resistances of the coating films before (blue bars) and after (red bars) the caramelization process.

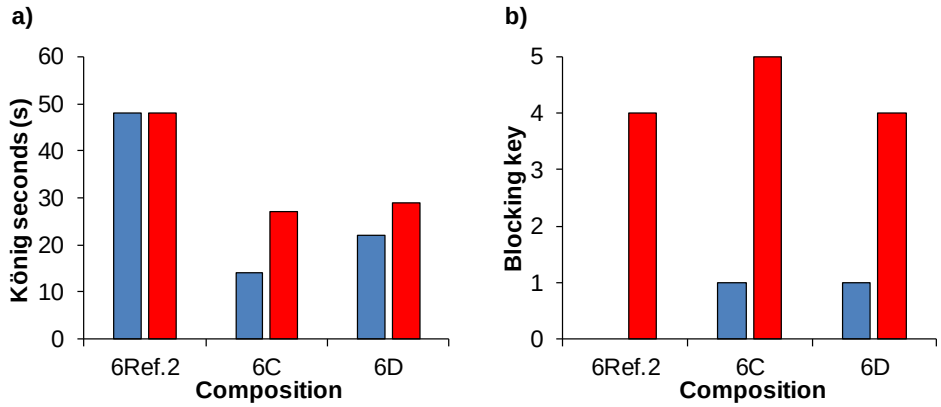

Figure II.3. Pendulum hardness (a) and blocking resistance (b) for the coating films before (blue bars) and after (red bars) the caramelization process.

The chemical resistance of the coatings cast on melamine manufactured-wood substrates, either before or after the caramelization process, against common chemicals is showed in Figure II.4.

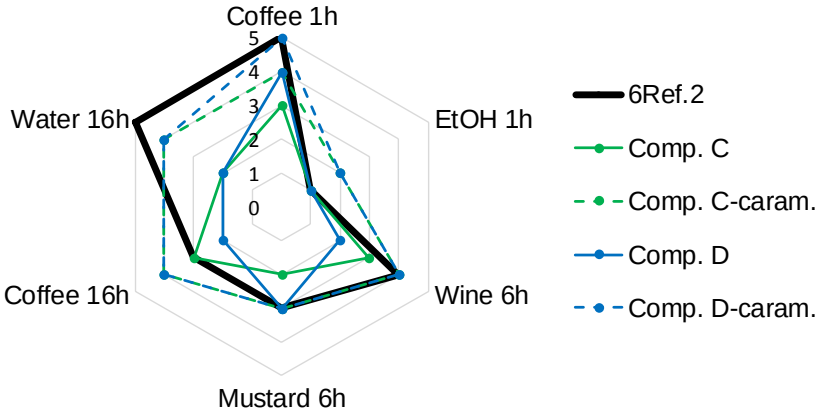

Figure II.4. Chemical resistance of the coatings cast on melamine-wood substrate before (green) and after (red) the caramelization. 5 = no visible change, 1 = strong marks visible.

II.2 Acrylic latexes containing ST/Ecomer®

Table II.3 summarizes the latexes synthesized containing ST/Ecomer® in their formulation, as well as their main properties including gel content, sol weight-average molar mass (Mw), glass transition temperature (Tg), Minimum Film Formation Temperature (MFFT), bio-content and the free Ecomer® content (SBV).

Table II.3. Summary and characteristics of the synthesized latexes containing ST by two-stage process.

COMP	2nd Stage (%wt monomers)	Gel (%)	Mw (kDa)	Tg (°C)	MFFT (°C)	Bio (%)	SBV (g/kg)*
6Ref.3	BA:ST:MAA (49.5:49.5:1)	2 ± 0.1	517	9	17	0	-
6E	BA:ST:SBV:MAA (42:42:15:1)	57 ± 1	175	8	15	14	20
6F	2OA:BA:ST:SBV:MAA (27:15:42:15:1)	62 ± 0.1	188	23.4	12	33	9.7

* Makes reference to the quantity of free Ecomer® in 1 kg of binder.

Figure II.5 shows the evolution of the gel content for compositions **6Ref.3**, **6E** and **6F** before and after the caramelization.

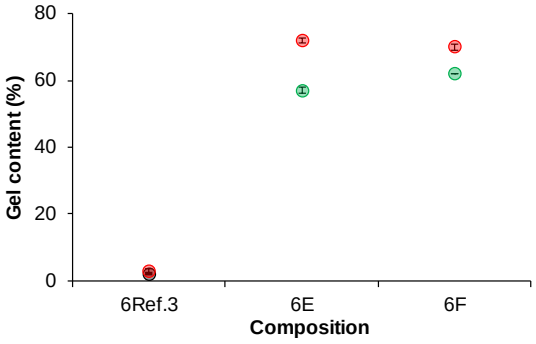

Figure II.5. Gel content evolution of compositions **6E** and **6F** together with the reference **6Ref.3** before (green circles) and after (red circles) caramelization process.

Evaluation of the performance of acrylic dispersions containing ST/Ecomer® for melamine coating application

Table II.4 summarizes the mechanical properties obtained in the tensile test for both the caramelized and non-caramelized coatings, whereas Figure II.6 shows the corresponding stress-strain curves.

Table II.4. Mechanical properties of the coatings cast at ambient temperature before and after the caramelization process.

COMP	2nd Stage (%wt monomers)	Young's Modulus (MPa)	Yield Stress (MPa)	Elongation at break (%/100)	Ultimate Strength (MPa)
6Ref.3	BA:ST:MAA (49.5:49.5:1)	13.2 ± 2.6	3.9 ± 0.5	6.9 ± 0.8	8 ± 0.3
6E	BA:ST:SBV:MAA (42:42:15:1)	8.8 ± 0.4	2.9 ± 0.4	6.4 ± 0.4	6.1 ± 1
6E-caram.		128.3 ± 6.7	10.8 ± 1.1	3.8 ± 0.5	12.2 ± 0.3
6F	2OA:BA:ST:SBV:MAA (27:15:42:15:1)	11.1 ± 1.4	3.5 ± 0.5	5.1 ± 0.1	5.8 ± 1.4
6F-caram.		66.5 ± 10.2	9.1 ± 0.1	4.3 ± 1	10.3 ± 2.2

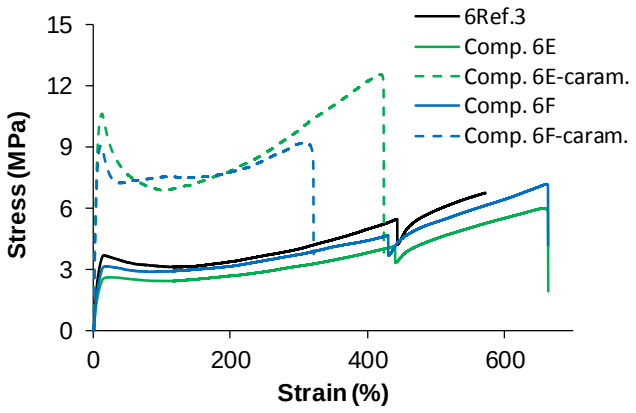

Figure II.6. Stress-strain curves of compositions **6E** (green line) and **6F**(blue line) before (solid line) and after (dashed line) the caramelization together with the reference composition **6Ref.3** (black solid line).

Figure II.7 presents the pendulum hardness as well as the blocking resistances of the coating films before (blue bars) and after (red bars) the caramelization process.

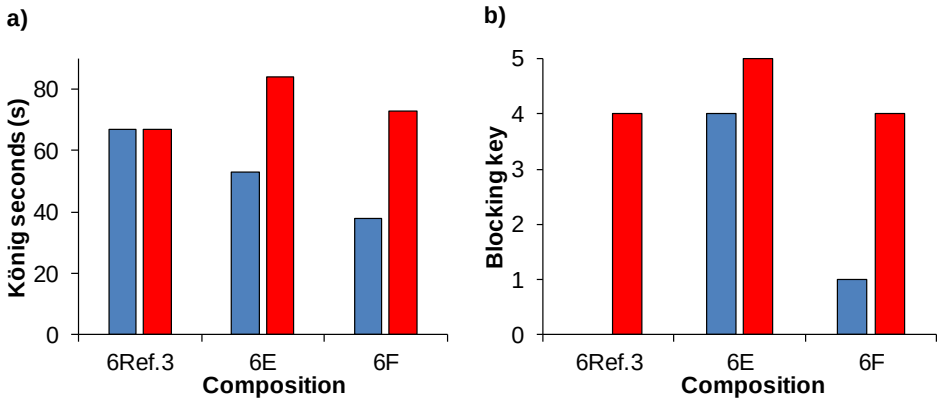

Figure II.7. Pendulum hardness (a) and blocking resistance (b) for the coating films before (blue bars) and after (red bars) the caramelization process.

The chemical resistance of the coatings cast on melamine manufactured-wood substrates, either before or after the caramelization process, against common chemicals is showed in Figure II.8.

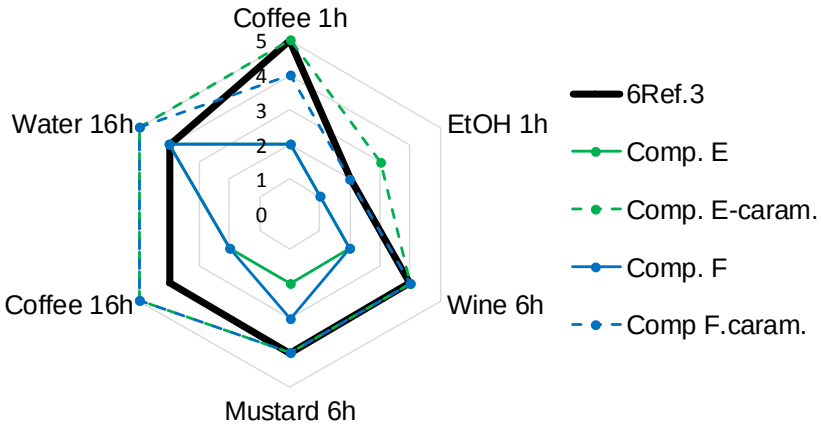

Figure II.8. Chemical resistance of the coatings cast on melamine-wood substrate before (green) and after (red) the caramelization. 5 = no visible change, 1 = strong marks visible.

Appendix III

List of acronyms and abbreviations

$[M]_p$	Monomer concentration in the particles
PSA	Pressure sensitive adhesive
AA	Acrylic acid
AsA	Ascorbic acid
AF4	Asymmetric flow-field-flow fractionation
AIBN	2,2'-Azobisisobutyronitrile
ASR	Alkali soluble resin
APG	Alkyl polyglucoside
AV	Acid Value
BA	Butyl acrylate
BDG	Butyl diglycol
BOD	Biochemical oxygen demand
1BuSH	1-Butanethiol

CAGR	Compound annual growth rate
CDMA	Cyclademol acrylate
CHDF	Capillary hydrodynamic fractionation
CMC	Critical micellar concentration
CTA	Chain transfer agent
^{13}C NMR	Carbon nuclear magnetic resonance
Đ	Polydispersity
Dp	Particle size
DF	Detector flow
DLS	Dynamic light scattering
DMA	Dynamic mechanical analysis
DMAP	4-(Dimethylamino)pyridine
DMSO	Dimethyl sulfoxide
DMTA	Dynamic mechanical thermal analysis
EGDMA	Ethylene glycol dimethacrylate
2EHA	2-Ethylhexyl acrylate
2EHTG	2-Ethylhexyl thioglycolate
ELSD	Evaporative light scattering detector
EtOAc	Ethyl acetate

ESI-TOF-MS	Electrospray ionization - time of flight – mass spectrometry
G´	Storage modulus
G´´	Loss modulus
Hx	Hexane
HAD	Hazardous air pollutant
HAF	2-Hydroxy acetyl furane
HEMA	Hydroxyethyl methacrylate
HMF	5-Hydroxymethyl furfural
HPLC	High pressure liquid chromatography
^{1}H NMR	Proton nuclear magnetic resonance
IBOA	Isorbornyl acrylate
IBOMA	Isorbonyl methacrylate
ISOMA	Isosorbide 5-methacrylate
k_p	Propagation rate constant
KPS	Potassium persulfate
M_w	Weight-average molar mass
MAA	Methacrylic acid
MAAn	Methacrylic anhydride
MALS	Multiangle light scattering

MEK	Methylethyl ketone
MFFT	Minimum film formation temperature
MMA	Methyl methacrylate
MMD	Molar mass distribution
MOA	Methacrylate oleic acid
N_A	Avogadro's number
N_p	Number of particles
NaPS	Sodium persulfate
NMP	N-Methyl-2-pyrrolidone
NVC	N-Vinyl caprolactam
NVP	N-Vinyl pyrrolidone
$\bar{n}$	Average number of radicals per particle
2OA	2-Octyl acrylate
PDI	Polydispersity index
PDA	Photodiode array
PET	Polyethylene terephthalate
PIPEMA	Piperonyl methacrylate
PP	Polypropylene

PVC	Polyvinyl chloride
R	Ideal gas constant
R_p	Rate of polymerization
R_x	Reactivity ratio of monomer X
R_z	z-Average radius of gyration
RCF	Relative centrifugal force
RI	Refractive index
SAFT	Shear adhesion failure time
SBV	Sugar based vinyl monomer
SDS	Sodium dodecyl sulfate
SEC	Size exclusion chromatography
ST	Styrene
T_1	Relaxation parameter
T_g	Glass transition temperature
Tanδ	Damping factor
TBHP	Terc-butyl hydroperoxide
TGA	Thermogravimetric analysis
THF	Tetrahydrofuran
THGA	Tetrahydrogeraniol acrylate

TOD	Theoretical oxygen demand
TTS	Time temperature superposition
UV	Ultraviolet
V_m	Partial molar volume of the monomer
VOC	Volatile organic compound
VT-FTIR	Variable temperature-Fourier transform infrared
WA	Work of adhesion
wt%	Weight percent
wbm%	Weight percent based on monomer
X_n	Number average degree of polymerization
XF	Cross flow

Greek symbols

γ	Polymer/water interfacial tension
η*	Complex viscosity
μ	Flory-Huggins interaction parameter
ρ	Density
Φ_P	Volume fraction of polymer in the particle
ω_e	Cross frequency

List of publications and conference presentations

Part of this Thesis has been published or will be published soon. The list of papers that would be issued from this work is as follows (variation in the authors list and/or paper title might be possible).

"High Biobased Content Latexes for Development of Sustainable Pressure Sensitive Adhesives". Adrián Badía, Julie Movellan, María Jesús Barandiaran, and Jose Ramon Leiza. *Industrial & Engineering Chemistry Research.* **2018**, 57, 14509-14516.

"UV-Tunable Biobased Pressure-Sensitive Adhesives Containing Piperonyl Methacrylate". Adrián Badía, José I. Santos, Amaia Agirre, María J. Barandiaran, and Jose R. Leiza. *ACS Sustainable Chemistry & Engineering*. **2019**, 7, 19122-19130.

"Self-stick adhesive made with black pepper derivative adjusts to many tastes". Fernando Gomollón-Bel. *ACS Chemical & Engineering News*. **2020**.

PCT/EP 2020/061586. International patent application entitled **"Method for producing a removable pressure-sensitive adhesive (PSA) and pressure-sensitive adhesive thus produced"** Adrián Badía , María Jesús Barandiaran, and Jose Ramon Leiza (25-Mar-2020).

"Development of biobased waterborne coatings containing Ecomer®: An alkyl polyglucoside maleic acid ester monomer". Adrián Badía, Maud Kastelijn, Jurgen Scheerder, and Jose R. Leiza. *Progress in Organic Coatings*. **2020**. DOI: 10.1016/j.porgcoat.2020.105708

"Removable biobased waterborne Pressure-Sensitive Adhesives containing mixtures of isosorbide methacrylate monomers". Adrián Badía, Amaia Agirre, María Jesús Barandiaran, and Jose Ramon Leiza. *Biomacromolecules*. **2020**. DOI: 10.1021/acs.biomac.0c00474

"Towards strong and easy removable biobased waterborne pressure sensitive adhesives". Adrián Badía, María Jesús Barandiaran, and Jose Ramon Leiza. To be submitted to *ACS Sustainable Chemistry & Engineering*.

Part of this work have been presented in national and International conferences, as well as in internal meetings from the Industrial Liason Program (ILP).

Oral presentations

"Waterborne polymer latexes based on renewable monomers for pressure sensitive adhesive applications". J. Movellan, A. Badía, M.J. Barandiaran, J.R. Leiza. International*. Conference on Biobased Materials and Composites ICBMC*, Nantes, France 2017.

"Development of waterborne adhesives with reduced environmental impact". A. Badía, J. Movellan, J.R. Leiza, M.J. Barandiaran. *National Conference of Young Researchers of Polymers*, La Pineda, Spain 2017.

"Development of water-based pressure sensitive adhesive from biomass derived monomers". A. Badía, J. Movellan, J.R. Leiza, M.J. Barandiaran. *ILP Meeting*, 2017.

"Development of water-based pressure sensitive adhesive from biomass derived monomers". A. Badía, J. Movellan, J.R. Leiza, M.J. Barandiaran. *European Polymer Federation EPF*, Lyon, France 2017.

"Development of water-based pressure sensitive adhesive from biomass derived monomers". A. Badía, J.R. Leiza, M.J. Barandiaran. *ILP Meeting*, 2018.

"Bio-based pressure sensitive adhesives with UV-light tunability and easy removability". A. Badía, M.J. Barandiaran, J.R. Leiza. *Graduate Research Seminar GRS*, Sentosa, Singapore 2019.

"Biobased waterborne coatings containing Ecomer®: a glucose modified monomer". Adrián Badía, Maud Kastelijn, Jurgen Scheerder, and J. R. Leiza*. ILP Meeting*, 2019.

"High performance, tunable and easy removable bio-based waterborne pressure sensitive adhesives". A. Badía, M.J. Barandiaran, J.R. Leiza. *Conference on*

Green Chemistry and Nanotechnologies in Polymeric Materials GCNPM, Riga, Letonia 2019.

"Towards UV-tunable and easy removable biobased waterborne pressure sensitive adhesives". A. Badía, M.J. Barandiaran, J.R. Leiza. V *Young Researchers in Colloids and Interfaces Meeting, Zaragoza, España 2020*.

Poster presentations

"Bio-based latexes for development of sustainable pressure sensitive adhesives". A. Badía, J.R. Leiza, M.J. Barandiaran. *Bordeaux Polymer Conference BPC*, Bordeaux, France 2018.

"Bio-based pressure sensitive adhesives with UV-light tunability and easy removability". A. Badía, M.J. Barandiaran, J.R. Leiza. *International Polymer Colloids Group Conference IPCG*, Sentosa, Singapore 2019.

Resumen y Conclusiones

Durante los últimos años, las preocupaciones medioambientales junto con las demandas de los consumidores y las estrictas regulaciones acerca de la emisión de gases de efecto invernadero (particularmente CO_2) han propiciado el desarrollo de materiales sostenibles y/o respetuosos con el medio ambiente. El interés en reducir el impacto de la huella de carbono en materiales poliméricos de uso diario, tales como adhesivos o recubrimientos, ha llevado a la búsqueda de componentes procedentes de fuentes renovables, monómeros, capaces de reemplazar a aquellos provenientes de la industria petroquímica. Sin embargo, debido al bajo coste del petróleo y a la gran demanda de los sectores de adhesivos, recubrimientos y pinturas, estos monómeros, procedentes de la naturaleza, necesitan ofrecer mejores prestaciones mecánicas y/o ventajas adicionales. En este escenario, los monómeros derivados de aceites vegetales, lignina, terpenos, proteínas o carbohidratos se encuentran entre los principales precursores para el desarrollo de este tipo de productos.

La polimerización en emulsión, que usa agua como fase continua, garantiza la producción de materiales de alta calidad de una forma consistente, segura y respetuosa con el medio ambiente. Se espera que el mercado global de las dispersiones poliméricas aumente su valor de 7,6 billones de dólares, en 2019, a 11,8 billones de dólares, en 2027, y se estima que más del 60% de las dispersiones son utilizadas en su aplicación como adhesivos y recubrimientos, siendo las formulaciones acrílicas aquellas más versátiles. En este sentido, los poliacrilatos ofrecen altas prestaciones, así como la posibilidad de controlar la temperatura de transición vítrea (Tg) y la hidrofobicidad del material, gracias a la amplia gama de ésteres acrílicos y combinaciones existentes.

Dentro de la gran familia de los adhesivos, los adhesivos sensibles a la presión (del inglés Pressure Sensitive Adhesives, PSAs) resultan de especial interés para aplicación tanto permanente como removible. Ejemplos incluyen etiquetas de seguridad para equipos

de energía, películas de amortiguación de sonido/vibración, cintas adhesivas, notas adhesivas, materiales gráficos y vendajes y electrodos para su contacto con la piel entre otros. La formulación típica de un PSA acrílico consiste mayoritariamente en un monómero "blando", de baja Tg, capaz de otorgar fluidez y pegajosidad al sistema, pequeños porcentajes de un monómero "duro", de alta Tg, cuya finalidad en proporcionar cohesión y comportamiento elástico, junto con monómeros derivados de ácidos carboxílicos capaces de impartir humectabilidad y aumentar la resistencia al pelado.

Por otro lado, los recubrimientos tales como barnices, tintas y pinturas son considerados materiales necesarios en nuestra sociedad, puesto que toda superficie necesita ser protegida y/o decorada por algún motivo. Así como los recubrimientos decorativos tienen como finalidad mejorar el aspecto del producto final de cara al consumidor, los recubrimientos protectores son económicamente más importantes, ya que su objetivo consiste en alargar el ciclo de vida útil de productos y maquinaria (generalmente empleados en superficies de acero y madera). La formulación básica de un recubrimiento consiste principalmente en un aglutinante, rellenos, pigmentos y aditivos. El aglutinante es el polímero que forma la matriz del recubrimiento y proporciona propiedades mecánicas y de barrera (el brillo del recubrimiento). Mientras que los rellenos (o extensores) son partículas inorgánicas que mejoran la resistencia mecánica y reducen el costo, los pigmentos (partículas orgánicas o inorgánicas) son los componentes más caros y aseguran la opacidad y el color del recubrimiento. Finalmente, se agregan aditivos en pequeñas cantidades para modificar las propiedades del recubrimiento (por ejemplo, biocidas e inhibidores de corrosión). Los recubrimientos que presentan monómeros acrílicos en su formulación son utilizados en gran medida para su aplicación en exteriores gracias a su excelente resistencia al agua y a la luz ultravioleta.

Tanto los adhesivos sensibles a la presión como los recubrimientos están experimentando un aumento creciente de su producción en emulsión, asegurando así la obtención de un material de fácil aplicación, inodoro y sin disolventes tóxicos. No obstante, el aumento en la demanda de formulaciones sostenibles hace necesario un estudio profundo acerca de la incorporación de nuevos monómeros renovables y su desempeño en las prestaciones del material final. Así, el principal objetivo de esta tesis ha sido el desarrollo de dispersiones poliméricas con alto contenido biológico y prestaciones competitivas para su aplicación como PSAs y recubrimientos en base agua. Para ello se han empleado tanto monómeros comerciales como nuevos monómeros procedentes de fuentes renovables con características especiales.

El primer paso fue producir PSAs en base agua con un contenido biológico del 72% que intentaran mimetizar a aquellas formulaciones procedentes del petróleo. Para este propósito se emplearon los monómeros renovables comercial acrilato de 2-Octilo (2OA, procedente del aceite de castor y cuyo homopolímero presenta una Tg = -44ºC) y metacrilato de isobornilo (IBOMA, procedente de la resina de pino y cuyo homopolímero presenta una Tg = 150 ºC). Se observó que la sustitución directa de los monómeros procedentes del petróleo por sus análogos de base biológica resultó en peores prestaciones adhesivas. Consecuentemente, la microestructura del adhesivo tuvo que ser modificada mediante el ajuste de la cantidad de monómero duro, IBOMA (15% en peso), y el contenido en gel (alrededor de un 60%). De esta forma se consiguieron valores similares en la pegajosidad y resistencia al pelado, mejor SAFT (135ºC vs 70ºC) y 45 veces mayor resistencia al corte que la formulación PSA procedente del petróleo. La incorporación de diferentes porcentajes de acrilato de 2-Etilhexilo fue el “mal necesario” para mejorar la elongación de las fibras del adhesivo a costa de reducir su contenido biológico.

En aras de resolver el conflicto entre la sostenibilidad de la formulación y las prestaciones adhesivas requeridas, se sintetizó e incorporó metacrilato de piperonilo (PIPEMA, procedente del aceite de sassafras y la pimienta negra, y cuyo homopolímero presenta una Tg= 70ºC) en las composiciones PSA, reemplazando a IBOMA. Se observó que un 15% en peso de PIPEMA mejoraba el comportamiento viscoso de las fibras adhesivas, manteniendo suficiente rigidez y proveyendo una alta disipación de energía. Además, el grupo benzodioxol, presente en PIPEMA, permitía el modulado de las prestaciones adhesivas (aumentando la cohesión sin dañar sustancialmente la adhesión) cuando el adhesivo era irradiado con luz ultravioleta. La espectroscopía magnética nuclear en estado sólido de ^{13}C junto con estudios reológicos confirmaron la creación de una red reticulada mediante la formación de estructuras conjugadas que aumentaban el comportamiento elástico del material. Se observó que 15 minutos de curado de luz ultravioleta proporcionaban el mejor balance en las propiedades adhesivas, superando a aquellas de la formulación PSA procedente del petróleo y manteniendo un contenido biológico del 71%.

En un intento por mejorar la adhesión de las formulaciones estudiadas y promover la removabilidad de las cintas adhesivas en agua, se sintetizó e incorporó una mezcla de monómeros metacrílicos derivado de isosorbida (ISOMAraw, procedente de la glucosa). La mezcla consistía en dimetacrilato de isosorbida y metacrilato de 5-isosorbida, el cual se obtuvo tras posterior purificación (ISOMA). La incorporación de pequeños porcentajes (1% en peso) de ISOMAraw/ISOMA mejoró tanto la flexibilidad como la cohesión de las fibras adhesivas. Ello fue posible debido a la presencia de especies reticulantes en la formulación y a la existencia de interacciones supramoleculares (puentes de hidrógeno). Además, se observó que un pequeño porcentaje de este monómero era más que suficiente para

promover la removabilidad de las cintas en agua en menos de 40 minutos, a temperatura ambiente, y en alrededor de 10 minutos a 65ºC.

En vista de los resultados obtenidos con los monómeros derivados de isosorbida, se sintetizaron resinas solubles en alkali (ASRs) renovables y se usaron como estabilizantes electrostéricos en la producción de PSAs. El objetivo era lograr una excelente adhesión y desunión al mínimo espesor de película adhesiva. El uso de ISOMAraw en la composición de la resina permitió su anclaje a la partícula de polímero y aumentó las propiedades mecánicas a medida que aumentaba la densidad de puentes de hidrógeno. La existencia de un entrecruzamiento físico proporcionó un buen equilibrio de la viscoelasticidad de la red polimérica, lo cual se confirmó mediante estudios reológicos. La naturaleza de las ASRs promovió la completa desunión de las cintas adhesivas en medio básico (pH=10) en menos de 20 minutos.

Finalmente, se llevó a cabo el desarrollo de recubrimientos en base agua mediante la combinación del monómero comercial procedente de la glucosa Ecomer® (una familia de ésteres de alquil poliglucósidos del ácido maleico) junto con los ya explorados 2OA y IBOMA. Se observó que Ecomer® se incorporaba mejor en aquellas formulaciones que usaban estireno como monómero duro en vez de metacrilatos, probablemente debido a las próximas relaciones de reactividad de los comonómeros. No obstante, el proceso de caramelización del recubrimiento final fomentó la incorporación de Ecomer® libre, dando lugar a un material más duro con propiedades mecánicas y de recubrimiento mejoradas. Así mismo, la presencia de grupos derivados de glucosa en la estructura del polímero fomentó la biodegradación parcial del recubrimiento, siendo menos acusada para aquellos caramelizados.